University of Kentucky
UKnowledge

Theses and Dissertations--Chemistry | Chemistry

2011

OPIOID CODRUGS FOR PAIN MANAGEMENT

Ujjwal Chakraborty
University of Kentucky, ujjwalcc@aol.com

Right click to open a feedback form in a new tab to let us know how this document benefits you.

Recommended Citation
Chakraborty, Ujjwal, "OPIOID CODRUGS FOR PAIN MANAGEMENT" (2011). *Theses and Dissertations--Chemistry*. 2.
https://uknowledge.uky.edu/chemistry_etds/2

This Doctoral Dissertation is brought to you for free and open access by the Chemistry at UKnowledge. It has been accepted for inclusion in Theses and Dissertations--Chemistry by an authorized administrator of UKnowledge. For more information, please contact UKnowledge@lsv.uky.edu.

STUDENT AGREEMENT:

I represent that my thesis or dissertation and abstract are my original work. Proper attribution has been given to all outside sources. I understand that I am solely responsible for obtaining any needed copyright permissions. I have obtained and attached hereto needed written permission statements(s) from the owner(s) of each third-party copyrighted matter to be included in my work, allowing electronic distribution (if such use is not permitted by the fair use doctrine).

I hereby grant to The University of Kentucky and its agents the non-exclusive license to archive and make accessible my work in whole or in part in all forms of media, now or hereafter known. I agree that the document mentioned above may be made available immediately for worldwide access unless a preapproved embargo applies.

I retain all other ownership rights to the copyright of my work. I also retain the right to use in future works (such as articles or books) all or part of my work. I understand that I am free to register the copyright to my work.

REVIEW, APPROVAL AND ACCEPTANCE

The document mentioned above has been reviewed and accepted by the student's advisor, on behalf of the advisory committee, and by the Director of Graduate Studies (DGS), on behalf of the program; we verify that this is the final, approved version of the student's dissertation including all changes required by the advisory committee. The undersigned agree to abide by the statements above.

Ujjwal Chakraborty, Student

Dr. Peter A. Crooks, Major Professor

John Anthony, Director of Graduate Studies

OPIOID CODRUGS FOR PAIN MANAGEMENT

DISSERTATION

A dissertation submitted in partial fulfillment of the

requirements for the degree of Doctor of Philosophy in the

College of Arts and Sciences

at the University of Kentucky

By

Ujjwal Chakraborty

Lexington, Kentucky

Co-Directors: Dr. Peter A. Crooks, Professor of Pharmaceutical Sciences

and Dr. Robert B. Grossman, Professor of Department of Chemistry

Lexington, Kentucky

Copyright © Ujjwal Chakraborty 2012

ABSTRACT OF DISSERTATION

OPIOID CODRUGS FOR PAIN MANAGEMENT

Pain is an unpleasant sensory and emotional experience associated with actual or potential tissus damage or described in terms of such damage. Opioids are effective in treating moderate to severe pain, but opioid alone therapy is associated with several adverse effects, development of tolerance and addiction potential. One way to solve these problems is to administer opioids with adjuvant drugs. In this project several opioid molecules were combined with other adjuvant drugs in a single chemical entity to form a codrug.

A series of codrugs were prepared by conjugation of an opioid with *S*-(-)-nornicotine, ketamine, norketamine and gabapentin. Several of the synthesized codrugs were evaluated for analgesic activity in the rats after oral administration. Codeine-*S*-(-)-nornicotine, 3-*O*-acetylmorphine-*S*-(-)-nornicotine, and *N*-ethoxycarbonylgabapentin-codeine codrugs showed greater effectiveness as well as prolonged pain management properties as compared to the parent drugs. Stabilities of several synthesized codrugs were studied in aqueous solutions from pH 1.3-7.4, in simulated gastrointestinal fluids, in rat plasma and in brain homogenate. Only the ester-linked codrugs showed sign of hydrolysis in different solutions. Carbamate-linked codrugs didn't cleave under any hydrolytic condition. Pharmacokinetic study was performed on the following three codrugs: 3-*O*-acetylmorphine-*S*-(-)-nornicotine, *N*-acetylgabapentin-codeine, and *N*-ethoxycarbonylgabapentin-codeine. The carbamate linkage in 3-*O*-acetylmorphine-*S*-(-)-nornicotine codrug did not cleave *in vivo* to produce parent drugs. The ester linkage in *N*-acetylgabapentin-codeine codrug cleaved *in vivo* to produce codeine and *N*-acetylgabapentin, but *N*-acetylgabapentin did not undergo hydrolysis to produce gabapentin. The ester linkage in *N*-ethoxycarbonylgabapentin-codeine codrug hydrolyzed slowly in plasma to produce *N*-ethoxycarbonylgabapentin and codeine and then the carbamate linkage in *N*-ethoxycarbonylgabapentin hydrolyzed even slowly to produce gabapentin. Produced codeine also metabolized to generate some amount of morphine. Thus, the design and synthesis of an opiate and gabapentin codrug was achieved which was stable enough in the gastrointestinal tract, showed enhanced analgesic effects as

compared to the physical mixture of the parent drugs, and also produced the two parent drugs in blood plasma.

KEYWORDS: Opioid, Anticonvulsant, Codrug, Antinociception, Pharmacokinetics

Ujjwal Chakraborty

_____

_____

Date

OPIOID CODRUGS FOR PAIN MANAGEMENT

By

Ujjwal Chakraborty

Peter A Crooks
co-Director of Dissertation

Robert B. Grossman
co-Director of Dissertation

John Anthony
Director of Graduate Studies

01/14/2012

Dedication

To my parents

TABLE OF CONTENTS

List of Tables…….IX

List of Figures…….....X

List of Schemes…….…….XIX

Chapter 1: Backgroung and Literature Review and Object of the Study

1.1 Pain……1

1.2 Opioids……...3

1.2.1 Morphine…….5

1.2.2 Codeine……...6

1.2.3 Oxycodone……..6

1.3 Problems Associated with Opioid Therapy……...7

1.4 Cobbination Therapy for Pain……..10

1.4.1 Opioid-Nicotinic Receptor Agonist Combination……12

1.4.2 Opioid-NMDA Receptor Antagonist Combination……..15

1.4.3 Opioid-Gabapentin Combination……..17

1.4.4 Opioid-Cannabinoid Combination……....19

1.5 Codrugs……... 20

1.5.1 Ideal Codrug Characteristics…….21

1.5.2 Exmples of Marketed Codrugs…….23

1.5.3 Topical Codrug Therapy for the Treatment of Ophthalmic Diseases……..26

1.5.4 Codrugs for Transdermal Delivery……...34

1.5.5 Codrugs of L-DOPA for the Treatment of Parkinson's Disease…..42

1.5.6 Analgesic Codrugs containing NSAIDs……...48

1.5.7 Analgesic Codrugs of Opioids and Cannabinoids……56

1.5.8 Codrugs containing Anti-HIV Drugs……60

1.5.9 Overall Aim of the Study……..63

Chapter 2: Synthesis of Parent Drugs and Codrugs

2.1 Enantioselective Synthesis of *S*-(-)-Nornicotine ……64

2.2 *N*-Demethylation of *S*-(-)-Nicotine……..65

2.3 Synthesis of Codrugs and Analogs……..…73

2.3.1 Opioid-*S*-(-)-Nornicotine Codrug Syntheses……73

2.3.2 Opioid-Ketamine/Norketamine Codrugs Syntheses……...102

2.3.3 Opioid-Gabapentin Codrug Synthese……109

2.3.4 Synthesis of Opioid-Δ^9-Tetrahydrocannabinol Codrug……..118

2.4 Experimental Section……133

Chapter 3: The Analgesic Activities of Codrugs, Parent Drugs and Physical Mixtures of Parent Drugs

3.1 Introduction……156

3.2 Animal Models of Pain……..157

3.3 Analgesic Activity of Opioid-*S*-(-)-Nornicotine Codrugs……161

3.3.1 Animals……...161

3.3.2 Drugs……...162

3.3.3 Tail Flick Test (Measure of Analgesia/Antinociception)……...162

3.4 Chronic Constriction Nerve Injury (CCI, Neuropathic Pain)……167

3.4.1 Surgery……167

3.4.2 Mechanical Hyperalgesia……167

3.4.3 Statistical Analysis……..167

3.5 Results.....168

3.5.1 Codeine-*S*-(-)-Nornicotine Codrug Antinociception

(Tail Flick Tests).....168

3.5.2 Codeine-*S*-(-)-Nornicotine Codrug Antihyperalgesic Effect (CCI Model).....172

3.5.3 3-*O*-Acetylmorphine-*S*-(-)-Nornicotine Codrug Antinociception (Tail-Flick Test).....177

3.5.4 ED_{50} Values.....181

3.6 Analgesic Activity of *N*-Ethoxycarbonylgabapentin-Codeine Codrug

(CG-4).....183

3.6.1 Tail Flick Test (Measure of Analgesia/Antinociception).....183

Chapter 4: *In-vitro* Stability Study of the Codrugs

4.1 Introduction……190

4.2 Opioid-*S*-(-)-Nornicotine Codrugs…….192

4.2.1 Standard Curve and Quality Control Vlidation Solutions……..192

4.2.2 Kinetics of Hydrolysis of the Codrugs in Aqueous Solutions (Non-Enzymatic)……..193

4.2.3 Kinetics of Hydrolysis of the Codrugs in Simulated Gastric Fluid (SGF) and Simulated Intestinal Fluid (SIF) (Enzymatic Conditions)….193

4.2.4 Kinetics of Hydrolysis of the Codrugs in Rat Plasma (*in vitro*)….193

4.2.5 Kinetics of Hydrolysis of the Codrugs in Rat Brain Homogenate..194

4.2.6 HPLC Analysis……...194

4.3 Results……...…….198

4.3.1 Assay Validation…….198

4.3.2 Chemical and Enzymatic Stability Study……...199

4.3.3 Stability Study in Brain Homogenate…….201

4.4 Opioid-Ketamine/Norketamine Codrugs……...201

4.4.1 HPLC Assay……...202

4.4.2 Assay Validation…….204

4.4.3 Chemical and Enzymatic Stability Study……...204

4.5 Codeine-Gabapentin Codrugs……206

4.5.1 HPLC Assay……...206

4.5.2 Assay Validation…….208

4.5.3 Chemical and Enzymatic Stability Study……...208

4.5.4 HPLC Assay……...210

4.5.5 Assay Validation…….212

4.5.6 Results…….213

Chapter 5: Pharmacokinetic Analysis of the Codrugs

5.1 Introduction……215

5.2 Pharamacokinetic profile of Codeine and Gabapentin……..217

5.3 Materials and Methods……...……218

5.3.1 Chemicals and Reagents…….218

5.3.2 Animals……...218

5.4 *In vivo* Pharmacokinetic Study of 3-*O*-Acetylmorphine-*S*-(-)-Nornicotine Codrug……..219

5.4.1 Instrumentation……...219

5.4.2 HPLC and Mass Spectrometric Conditions……219

5.4.3 Plasma Pharmacokinetics……220

5.4.4 Extraction Procedure……...220

5.5 *In vivo* Pharmacokinetic Study *N*-Acetamidogabapentin-Codeine (CG-3) Codrug……..……220

5.5.1 Instrumentation……...222

5.5.2 HPLC and Mass Spectrometric Conditions……223

5.5.3 Plasma Pharmacokinetics……223

5.5.4 Standard Curves and Quality Control Validation Solutions……...224

5.5.5 Extraction Procedure……...224

5.5.6 Assay Validation…….224

5.5.7 Results…….225

5.6 *In vivo* Pharmacokinetic Study of *N*-Ethoxycarbonylgabapentin-Codeine (CG-4) Codrug……...……..226

5.6.1 Instrumentation……...226

5.6.2 HPLC and Mass Spectrometric Conditions……226

5.6.3 Plasma Pharmacokinetics……229

5.6.4 Standard Curve and Quality Control Validation Solutions…….230

5.6.5 Extraction Procedure……...230

5.6.6 Assay Validation…….231

5.6.7 Results…….231

5.6.8 Bioavailability…….235

Chapter 6: Summary

6.1 Introduction……238

6.2 Opioid-*S*-(-)-Nornicotine Codrugs…….238

6.3 Opioid-Ketamine and Opioid-Norketamine Codrugs……242

6.4 Codeine-Gabapentin Codrugs……243

References……247

Vita……..268

LIST OF TABLES

Table 1.1, Pharmacokinetic parameters of NTXOL in the Guinea pig after application of a gel formulation containing either CB-NTXOL-BUPOH or NTXOL base……..……38

Table 2.1, Comparison of three synthetic routes……...80

Table 3.1, ED_{50} values of codrug and parent drugs in tail-flick and CCI models……...182

Table 3.2, ED_{50} values of morphine, 3-*O*-acetylmorphine, *S*-(-)-nornicotine, and 3-*O*-acetylmorphine-*S*-(-)-nornicotine codrug in tail-flick model……...182

Table 3.3, AUCs for different doses of the *N*-ethoxycarbonylgabapentin-codeine codrug and an equimolar physical mixture dose of codeine and gabapentin……186

Table 3.4, ED_{50} values of codeine, gabapentin, and *N*-ethoxycarbonylgabapentin-codeine codrug in the tail-flick animal model……...187

Table 4.1, Standard curve analysis of the analytes……..199

Table 4.2, Results of the stability studies of opioid- *S*-(-)-nornicotine codrugs……..200

Table 4.3, Results of stability studies of opioid-norketamine codrugs……..……..205

Table 4.4, Rate constants for hydrolysis of codeine-gabapentin codrugs……213

Table 5.1, Linear ranges of analytes in the LC-MS/MS assay……225

Table 5.2, Optimal ion source settings for each MRM transition monitored.....228

Table 5.3, Linear ranges of the analytes in standard curves……230

Table 5.4, Pharmacokinetic parameters of the codrug and parent drugs…….234

LIST OF FIGURES

Figure 1.1, Examples of bipartate and tripartate codrugs……..21

Figure 1.2, Sultamicillin codrug and the *in vivo* hydrolysis products generated from the codrug……..24

Figure 1.3, Generation of 5-aminosalicylic acid and sulfapyridine from sulfasalazine codrug……...25

Figure 1.4, Generation of paracetamol and aspirin from hydrolysis of benorylate……...25

Figure 1.5, Structures of THS, 5-FU and the THS-BIS-5-FU codrug……...26

Figure 1.6, Cumulative release of THS and 5-FU from neat pellets containing 2 mg of the THS-BIS- 5-FU codrug in bovine vitreous humor……27

Figure 1.7, Codrugs of corticosteroids and 5-fluorouracil……30

Figure 1.8, Naproxen-5-fluorouracil codrug……..32

Figure 1.9, Ethacrynic acid-β-adrenergic receptor antagonist codrugs……33

Figure 1.10, Structures of parent drugs NTX, NTXOL, BUP, BUPOH and codrugs NTX-BUPOH and CB-NTXOL-BUPOH, which contain a cyclic carbamate prodrug moiety of BUPOH……..35

Figure 1.11, Hydrolytic behavior of the NTX-BUPOH codrug……37

Figure 1.12, Hydrolysis profile of the carbonate drug hybrid, NTX-BUPOH, in isotonic phosphate buffer at pH 7.4……37

Figure 1.13, Hydrolysis profile of the carbonate drug hybrid, CB-NTXOL-BUPOH, in Guinea Pig Plasma at 37 °C……...38

Figure 1.14, Mean (±S.D.) plasma concentration profiles in guinea pigs after topical application of a gel formulation containing either CB-NTXOL-BUPOH or 6-β-Naltrexol (control)…… ……...39

Figure 1.15, Duplex gemini prodrug of NTX……40

Figure 1.16, Structures of α-tocopherol and α-tocopherol-amino acid codrugs……41

Figure 1.17, L-DOPA-entacapone codrug……43

Figure 1.18, Codrugs of L-DOPA with benserazide……..43

Figure 1.19, (a) L-DOPA and α-lipoic acid codrugs; and (b) dopamine and α-lipoic acid codrugs……...44

Figure 1.20, (a) L-DOPA and glutathione codrugs; and (b) dopamine and glutathione codrugs.....45

Figure 1.21, Structures of (a) a 3, 4-diacetyloxy-L-DOPA methyl ester-caffeic acid codrug; and (b) a 3, 4-diacetyloxy-L-DOPA methyl ester–carnosine codrug……46

Figure 1.22, Codrugs of L-DOPA linked to cysteine, methionine and bucillamine……..47

Figure 1.23, Codrug of Flurbiprofen and PPA……..49

Figure 1.24, A series of codrugs of acetaminophen and NSAIDs……50

Figure 1.25, A series of naproxen-propyphenazone codrugs……53

Figure 1.26, Amino acid codrugs of flurbiprofen……..54

Figure 1.27, A series of codrugs of chlorozoxazone with NSAIDs……...55

Figure 1.28, Codrug of chlorozoxazone and acetaminophen……56

Figure 1.29, Structures of delta-9-THC, codeine and Cod-THC codrug……...57

Figure 1.30, (a) Dose-Response Curves for the Antinociceptive Effects of the Codeine-THC Codrug and Codeine Alone in the Tail-Flick Test. (b) Antihyperalgesic Effect of Codeine, THC and the Cod-THC Codrug in the Chronic Constriction Nerve Injury (CCI) Model……58

Figure 1.31, Hydrolysis of the Cod-THC codrug under different enzymatic conditions……...59

Figure 1.32, Plasma concentrations of codeine, Δ^9-THC and Cod-THC codrug after administration of physical mixture of codeine, 4.9 mg/kg, and Δ^9-THC, 5.1 mg/kg, (a); and Cod-THC codrug, 10 mg/kg (b)……60

Figure 1.33, Anti-HIV codrug of AZT……..62

Figure 2.1, GC-MS of synthesized *S*-(-)-nornicotine……66

Figure 2.2, Total ion chromatogram of derivatized *S*-(-)-nornicotine……...67

Figure 2.3, Mass spectrum of derivatized *S*-(-)-nornicotine……..68

Figure 2.4, Important protons for chiral analysis of the nornicotine molecule with numbering scheme……69

Figure 2.5, Proton NMR spectrum of racemic nornicotine in the presence of the chiral complexing agent *R*-(-)-1,1'-binaphthyl-2,2'-diylphosphoric acid (BNPPA) in the region 8.0-8.8 ppm……..69

Figure 2.6, Proton NMR spectrum of synthesized (-)-*S*-nornicotine in presence of the chiral complexing agent R-(-)-BNPPA in the region 8.0-8.8 ppm…..70

Figure 2.7, Proton NMR spectrum of racemic nornicotine (I), *R*-(+)-nornicotine (II) and *S*-(-)-nornicotine (III) in the presence of the chiral complexing agent R-(-)-BNPPA in the region 2.6-4.4 ppm……71

Figure 2.8, Proton NMR spectrum of synthesized nornicotine in the presence of chiral complexing agent in the region 2.5-4.4 ppm……...72

Figure 2.9, Design of codeine-*S*-(-)-nornicotine carbamate codrug……..74

Figure 2.10, Total ion chromatogram of synthetic pyrrolidine *N*-carbamoyl chloride (retention time: 3.81 min) and the pyrrolidine urea side product (retention time: 8.41 min)……..76

Figure 2.11, Mass spectrum of pyrrolidine *N*-carbamoyl chloride……77

Figure 2.12, Mass spectrum of pyrrolidine urea……77

Figure 2.13, Mass spectrum of 3-ethylphenol carbonate ester……..79

Figure 2.14, Mass spectrum of the 3-ethylphenol-pyrrolidine carbamate conjugate……79

Figure 2.15, Mass spectrum of 3-ethylphenol chloroformate……81

Figure 2.16, Mass spectrum of 3-ethylphenol-*S*-(-)-nornicotine carbamate conjugate….82

Figure 2.17, MALDI-TOFMS of codeine-*p*-nitrophenol carbonate……..85

Figure 2.18, GC-MS of the methanolic carbonate derivative of codeine……..86

Figure 2.19, Mass spectrum of the codeine-pyrrolidine carbamate conjugate……..87

Figure 2.20, Mass spectrum of the carbamate codrug of codeine and *S*-(-)-nornicotine...89

Figure 2.21, HPLC chromatogram of codeine-*S*-(-)-nornicotine carbamate (retention time: 14.485 min)……..90

Figure 2.22, GC-MS spectrum of 3-*O*-acetylmorphine……91

Figure 2.23, Mass spectrum 3-*O*-acetylmorphine-*p*-nitrophenol carbonate……..92

Figure 2.24, LC-MS chromatogram of 3-*O*-acetylmorphine-*S*-(-)-nornicotine carbamate codrug……...94

Figure 2.25, LC-MS analysis of the dicarbonate ester derivative of morphine and *p*-nitrophenol……..95

Figure 2.26, LC-MS analysis of morphine-*S*-(-)-nornicotine dicarbamate codrug……...96

Figure 2.27, GC-MS analysis of the *p*-nitrophenoxy carbamate of *S*-(-)-nornicotine….100

Figure 2.28, Mass spectrum of morphine-*S*-(-)-nornicotine carbamate (3-oxy) codrug..101

Figure 2.29, ESI-MS analysis of the mixture from the reaction of ketamine with the *p*-nitrophenoxy carbonate ester of codeine……..103

Figure 2.30, ESI-MS analysis of the *p*-nitrophenoxy carbamate of ketamine……104

Figure 2.31, ESI-MS of ketamine-codeine carbamate codrug……105

Figure 2.32, LC-MS chromatogram of codeine-norketamine codrug……107

Figure 2.33, LC-MS chromatogram of morphine-norketamine codrug……..108

Figure 2.34, Proposed structure of codeine-gabapentin ester codrug with protonated amines and chloride counterions……..109

Figure 2.35, LC-MS chromatogram of the gabapentin-codeine carbamate codrug……112

Figure 2.36, LC-MS chromatogram of *N*-acetylgabapentin……114

Figure 2.37, Single crystal X-ray structure of *N*-acetylgabapentin……114

Figure 2.38, LC-MS chromatogram of *N*-acetylgabapentin-codeine ester codrug……..115

Figure 2.39, GC-MS analysis of the *N*-ethyl carbamate of gabapentin……...117

Figure 2.40, ESI-MS analysis of carbamate N-protected ester codrug of codeine and gabapentin……118

Figure 2.41, Proposed structure of the oxycodone-Δ^9-THC codrug……119

Figure 2.42, GC-MS analysis of the product of the reaction between oxycodone and *p*-nitrophenyl chloroformate……122

Figure 2.43, ^{13}C NMR spectrum of the product from the reaction between oxycodone and *p*-nitrophenyl chloroformate……123

Figure 2.44, Proposed structure of the product from the microwave reaction between oxycodone and *p*-nitrophenyl chloroformate……...124

Figure 2.45, Single crystal X-ray structure of the oxycodone analog from the microwave reaction of oxycodone with *p*-nitrophenyl chloroformate…126

Figure 2.46, LC-MS analysis of the mixture from the reaction of oxycodone and the *p*-nitrophenoxy carbonate of tetrahydro-2-naphthol……130

Figure 2.47, ESI-MS analysis of the carbonate ester of oxycodone and DSC……135

Figure 3.1, The Tail-Flick test…….158

Figure 3.2, The Paw-Pressure test……159

Figure 3.3, The Tail-Flick latencies of orally administered codeine……...163

Figure 3.4, The Tail-Flick latencies and dose response curve of orally administered *S*-(-)-nornicotine……...164

Figure 3.5, The Tail-Flick latencies of orally administered codeine-*S*-(-)-nornicotine codrug……..166

Figure 3.6, The Tail-Flick latencies codeine-*S*-(-)-nornicotine codrug and codeine…...169

Figure 3.7, Dose-response curves for codeine, *S*-(-)-nornicotine, and codeine-*S*-(-)-nornicotine codrug in tail-flick test……..170

Figure 3.8, Comparison of %MPE at peak time for codeine-S-(-)-nornicotine codrug, physical mixture, and the individual parent drugs in tail-flick test……..171

Figure 3.9, Time-response and dose-response curves for orally administered codeine in the CCI model……..173

Figure 3.10, Time-response and dose-response curves for orally administered *S*-(-)-nornicotine in the CCI model……..174

Figure 3.11, Time-response curves for orally administered codeine-*S*-(-)-nornicotine codrug and codeine in the CCI model……..175

Figure 3.12, Dose-response curves for orally administered codeine, *S*-(-)-nornicotine, and codeine-*S*-(-)-nornicotine codrug in the CCI animal model…….176

Figure 3.13, Time-response curves for orally administered 3-*O*-acetylmorphine (MOR) in the tail-flick animal model……...178

Figure 3.14, Time-response curves for orally administered *S*-(-)-nornicotine (NNIC) in the tail-flick animal model……...178

Figure 3.15, Time-response curves for orally administered 3-*O*-acetylmorphine-*S*-(-)-nornicotine codrug (MOR-NNIC) in the tail-flick animal model……...179

Figure 3.16, Dose-response curves for 3-*O*-acetylmorphine, *S*-(-)-nornicotine, and 3-*O*-acetylmorphine-*S*-(-)-nornicotine codrug in the tail-flick animal model……180

Figure 3.17, Time-response curves for three oral doses of the *N*-ethoxycarbonylgabapentin-codeine codrug and an equimolar physical mixture dose of codeine and gabapentin in the tail-flick animal model..184

Figure 3.18, Comparison of time-response curves for *N*-ethoxycarbonylgabapentin-codeine codrug and an equivalent physical mixture dose of the parent drugs…….185

Figure 3.19, comparison of % MPE at peak time for three different doses of the *N*-ethoxycarbonylgabapentin-codeine codrug and an equimolar physical mixture dose of codeine and gabapentin in tail-flick test……188

Figure 4.1, Structures of the opioid-*S*-(-)-nornicotine codrugs used in stability studies……..192

Figure 4.2, HPLC chromatogram of morphine, *S*-(-)-nornicotine, naltrexone (IS), and 3-*O*-acetylmorphine-*S*-(-)-nornicotine codrug…….195

Figure 4.3, Individual HPLC Chromatograms of morphine, *S*-(-)-nornicotine, naltrexone (IS), and morphine-*S*-(-)-nornicotine codrug…….196

Figure 4.4, HPLC Chromatogram of *S*-(-)-nornicotine, morphine (IS), codeine, and codeine- *S*-(-)-nornicotine codrug……198

Figure 4.5, Structures of opioid-norketamine codrugs analyzed for in vitro stability….202

Figure 4.6, HPLC Chromatogram of Morphine (IS), Codeine, Norketamine, and Norketamine-Codeine codrug……..203

Figure 4.7, HPLC Chromatogram of Morphine, Naltrexol (IS), Norketamine, and Norketamine-Morphine codrug……...204

Figure 4.8, Structures of the codeine-gabapentin codrugs analyzed for their *in vitro* stabilities……..206

Figure 4.9, HPLC Chromatogram of Morphine, codeine, and CG-1 codrug……..207

Figure 4.10, HPLC Chromatogram of morphine, codeine, and CG-2 codrug…….209

Figure 4.11, HPLC Chromatogram of morphine (IS), codeine, and CG-3 codrug……..211

Figure 4.12, HPLC Chromatogram of morphine (IS), codeine, and CG-4 codrug……..212

Figure 5.1, Chromatograms of *S*-(-)-nornicotine, morphine, 3-*O*-acetylmorphine, naltrexone (IS), morphine-*S*-(-)-nornicotine, and 3-*O*-acetylmorphine-*S*-(-)-nornicotine ……221

Figure 5.2, AUC for the morphine-*S*-(-)-nornicotine codrug *versus* time plot after oral administration of *O*-acetylmorphine-*S*-(-)-nornicotine codrug……222

Figure 5.3, Mean concentrations of the analytes versus time plot after oral dosing of CG-3 codrug…….226

Figure 5.4, LC-MS/MS chromatograms of morphine, codeine, naltrexone, gabapentin, *N*-ethoxycarbonylgabapentin (gabapentin carbamate), and CG-4 codrug…….229

Figure 5.5, Mean concentrations of the analytes versus time plot after administration of 25 mg/kg oral dose of CG-4 codrug……232

Figure 5.6, Mean concentrations of the analytes versus time plot after administration of 12.5 mg/kg oral dose of CG-4 codrug…….233

Figure 5.7, Mean concentrations of the analytes versus time plot after administration of 1 mg/kg i.v. dose of CG-4 codrug……235

Figure 6.1, Structures of synthesized opioid-*S*-(-)-nornicotine codrugs……..239

Figure 6.2, Structures of synthesized opioid-ketamine and opioid-norketamine codrugs…….243

Figure 6.3, Structures of codeine-gabapentin codrugs…….244

LIST OF SCHEMES

Scheme 2.1, Enantioselective synthesis of *S*-(-)-nornicotine by Loh et al., 1999…….64

Scheme 2.2, Enantioselective synthesis of *S*-(-)-nornicotine by Swango et al., 1999…...65

Scheme 2.3, Synthesis of *S*-(-)-nornicotine……...66

Scheme 2.4, *N*-Demethylation of several *N*-methyl compounds……...73

Scheme 2.5, Different synthetic strategies to afford carbamate conjugates of a phenol and a secondary amine……...75

Scheme 2.6, Reaction of pyrrolidine with triphosgene……..76

Scheme 2.7, Synthesis of carbamate conjugate via the intermediacy of a symmetrical carbonate ester……...78

Scheme 2.8, Synthesis of a carbamate conjugate via the intermediacy of a chloroformate…….80

Scheme 2.9, Synthesis of 3-ethylphenol-*S*-(-)-nornicotine carbamate conjugate……..82

Scheme 2.10, Synthesis of the *p*-nitrophenoxy carbonate of codeine……...84

Scheme 2.11, Reaction of the *p*-nitrophenoxy carbonate of codeine with methanol in the presence of silica……..84

Scheme 2.12, Synthesis of the codeine pyrrolidine carbamate conjugate…….87

Scheme 2.13, Synthesis of the carbamate codrug of *S*-(-)-nornicotine and codeine…….88

Scheme 2.14, Synthesis of 3-*O*-acetylmorphine……90

Scheme 2.15, Synthesis of the *p*-nitrophenoxy carbonate derivative of 3-*O*-acetylmorphine ……..92

Scheme 2.16, Synthesis of 3-*O*-acetylmorphine-*S*-(-)-nornicotine carbamate codrug…..93

Scheme 2.17, Synthesis of morphine-*S*-(-)-nornicotine carbamate (6-oxy) codrug……. 93

Scheme 2.18, Synthesis of the dicarbonate ester derivative of morphine and *p*-nitrophenol……..95

Scheme 2.19, Synthesis of the morphine-*S*-(-)-nornicotine dicarbamate codrug……..96

Scheme 2.20, Reaction of morphine with 1 equivalent of *p*-nitrophenyl chloroformate in presence of DMAP at 0 °C……....97

Scheme 2.21, Reaction of morphine with 1 equivalent of *p*-nitrophenyl chloroformate in the presence of NaH……...98

Scheme 2.22, Synthesis of the *p*-nitrophenoxy carbamate derivative of *S*-(-)-nornicotine …….... 99

Scheme 2.23, Synthesis of morphine-*S*-(-)-nornicotine carbamate (3-oxy) codrug……101

Scheme 2.24, Reaction between the *p*-nitrophenoxy carbonate ester of codeine and ketamine……...102

Scheme 2.25, Synthesis of the *p*-nitrophenoxy carbamate derivative of ketamine…….104

Scheme 2.26, Synthesis of codeine-ketamine codrug (diastereomeric mixture)…….105

Scheme 2.27, Synthesis of codeine-norketamine codrug (diastereomeric mixture)……106

Scheme 2.28, Synthesis of morphine-norketamine codrug (diastereomeric mixture)….108

Scheme 2.29, Synthesis of the di-HCl salt of the codeine-gabapentin ester codrug…...110

Scheme 2.30, Proposed in vivo hydrolytic behavior of the di-HCl salt of the codeine-gabapentin ester codrug……..111

Scheme 2.31, Synthesis of the codeine-gabapentin carbamate codrug……...112

Scheme 2.32, Synthesis of the amide-protected ester codrug of codeine and gabapentin……113

Scheme 2.33, Synthesis of an *N*-carbamate protected ester codrug of codeine and gabapentin ……...116

Scheme 2.34, Reaction between oxycodone and *p*-nitrophenyl chloroformate under microwave heating conditions…….122

Scheme 2.35, Reactions of synthesized oxycodone intermediate with different phenoxides and alkoxides……125

Scheme 2.36, Reaction of allyl-protected naltrexone with *p*-nitrophenyl chloroformate under microwave irradiation conditions……..127

Scheme 2.37, Reaction of allyl protected naloxone with *p*-nitrophenyl chloroformate under microwave irradiation……128

Scheme 2.38, Model reaction for the synthesis of the 14-hydroxy carbonate ester of oxycodone and tetrahydro-2-naphthol…….129

Scheme 2.39: Reaction between *p*-nitrophenoxy carbonate of Δ^9-THC and oxycodone under microwave irradiation conditions……..131

Scheme 2.40, Reaction between oxycodone and CDI under microwave irradiation conditions ……132

Scheme 2.41, Reaction between oxycodone and DSC under microwave irradiation conditions…….132

Chapter 1

Background, Literature Review and Object of the Study

1.1 Pain

According to International Association for the Study of Pain, pain is defined as "an unpleasant sensory and emotional experience associated with actual or potential tissue damage, or described in terms of such damage" (Merksey, 1979). Pain is always subjective. We learn the application of the word 'pain' through experiences related to injury in our early lives. Without any doubt, pain is a sensation in part of the body, but also it is unpleasant, and thus also an emotional experience. Many times, pain is reported even in the absence of any tissue damage or any likely pathophysiological state; this usually happens for psychological reasons. Pain is the most common symptomatic reason for seeking medical attention (Besson, 1999). Pain affects every one of us at some point of our lives, whether it is from headache, bruises and cuts or more severely resulting from surgery. Following is the summary of some major findings from the "1999 National Pain Survey" and "Pain in America: A Research Report" carried out in 2000:

- Roughly 48 million people (24% of the Americans) in US suffer from pain lasting for six months or longer (chronic pain).
- An additional 25 million of Americans suffer from acute pain resulting from surgery or accident.
- Approximately 66% of these pain sufferers have been living with pain for more than five years.
- Around 21.6 million American adults (11% of the Americans) regularly take prescription pain medication to manage chronic pain.
- 42% of pain sufferers are unable to work due to severity of pain.
- 63% of pain sufferers experience such severe pain that they are unable to engage in routine activities of daily living.

- Approximately 4.9 million people sought medical attention for chronic pain treatment in the year of 1999.
- According to physicians' belief, about 40% of chronic pain patients could not engage in social activities due to sufferings of pain.
- 80% of - Americans believe that pain is a part of getting older.
- 60% of Americans believe that pain is just something that they have to live with.
- 28% responded that there was no solution to pain.
- 40% of - patients suffering from moderate to severe pain were unable to find adequate pain relief.
- 25% of pain patients had changed doctors at least three times due to insufficient pain relief.
- 36 million Americans missed work due to pain in the year of 1999.
- Pain affected 83 million Americans' participation in various activities.
- The most common types of pain are reported to be arthritis, lower back pain, bone/joint pain, muscle pain and fibromyalgia.

These reports show that pain is a silent epidemic in the US. It is also clear that pain remains grossly undertreated and many times mistreated. Also, the loss of productivity and daily activity due to sufferings from pain is significant. Approximately US$1 trillion is spent every year in developed countries in direct health-care expenditure, lost work time and disability payments (Melnikova, 2010). Untreated pain substantially impacts pain sufferers and their family. A sufferer's quality of life is negatively impacted by pain and it diminishes his/her ability to concentrate, work, exercise, socialize, perform daily routines, and sleep. All of these negative impacts ultimately bring depression, isolation, and loss of self-esteem. Pain as a whole is a very active research area for pharmaceutical R&D mainly because of its under-treatment and frequent mistreatment. Another reason is that the older and still widely used analgesics can cause harsh adverse side-effects (Melnikova, 2010). Global pain and inflammation market sales together accounted for US$25 billion in the year of 2001 (Melnikova, 2010). Currently, management of pain depends substantially on analgesics that have been known for a long time. Non-narcotic analgesics (acetaminophen and aspirin), narcotic analgesics (opioids) and non-steroidal

anti-inflammatory drugs (NSAIDs) are the mainstays for pain management (Melnikova, 2010). More recently, analgesic adjuvants and selective COX2 inhibitors have been added to the list of compounds for treatment of pain. Analgesic adjuvants are a class of compounds that include antidepressants, local anesthetics, and anticonvulsants. Inflammation-related pain is mostly treated by traditional NSAIDs, which have varying degrees of analgesic, anti-inflammatory and anti-pyretic activity (Scholz and Woolf, 2002). NSAIDs are effective in treating inflammation-related pain, rheumatic disorders, and are useful as multipurpose pain killers (Melzack and Wall, 1965). NSAIDs inhibit both cyclooxygenase-1 (COX1) and COX2 enzymes. Both of these enzymes are the key targets in the inflammation pathway (Flower, 2003). Use of NSAIDs is limited by their serious gastrointestinal (g.i.) toxicity. NSAIDs containing free carboxylic acid functionalities cause g.i. irritation, bleeding, ulceration, and perforation. 16,500 NSAID-related deaths are estimated in the US alone and 75,000 patients are hospitalized due to unacceptable side effects of NSAIDs every year (Flower, 2003). Other adverse effects of NSAIDs include nephrotoxicity, bronchospasm, skin rash and other allergies. Selective COX2 inhibitors were developed as analgesics due to their ability to retain analgesic/anti-inflammatory effects with less toxicity, as they do not inhibit the gastro-protective COX1 enzyme (Flower, 2003). Pfizer's celecoxib (Celebrex) and Merk & Co's rofecoxib (Vioxx) were approved by the FDA and launched as selective COX2 inhibitors (Renfrey et al., 2003). The combined total sales of these two selective COX2 inhibitor drugs in the year 2000 were US$4,774 million (Flower, 2003). Unfortunately, concern over the potential cardiovascular safety of the more selective COX2 inhibitors has risen, and this has led to a continuous decline in their market share in favor of NSAIDs and opioids (Melnikova, 2010).

1.2 Opioids

Opioids are considered to be most effective therapeutic option in our arsenal for fighting serious pain (McQuay, 1999). They hold the major share of the pain market. The global pain market was estimated to be over US$50 billion in 2009. The pain market in seven major economies (the US, Japan, France, Germany, Italy, Spain and the UK) was

valued at US$27 billion in 2009. A thirty six percent share of the pain market was held by opioid analgesics in 2009 (Melnikova, 2010).

The term opium refers to a mixture of alkaloids obtained from the plant *Papaver somniferum*. Morphine is one of the 25 alkaloids isolated from opium poppy. Opiate refers to any natural or synthetic agent derived from or structurally related to morphine. Opioids, on the other hand, are compounds having morphine-like pharmacological activity. Opioids are divided into four broad groups:

1) Endogenous opioid peptides produced by our body. Examples are the enkephalins and endorphins.
2) Naturally occurring opioid alkaloids, for example morphine and codeine.
3) Semisynthetic opioids, such as hydrocodone and oxycodone.
4) Synthetic opioids, for example fentanyl and methadone.

Radiolabeled morphine has been used to evaluate the location of the sites of action of morphine in mice, and it was found that the drug attaches to very specific areas in mouse brain. Those specific areas were classified as "morphine receptors" (Pert and Snyder, 1973). Subsequent investigations have determined that endogenous compounds exist that stimulate morphine receptors and were termed endogenous morphines or endorphins (Hughes et al., 1975). Many of the clinically relevant opioids bind to morphine receptors or mu receptors and are thus called mu agonists.

Opioid receptors are mostly found in CNS but are also ubiquitous throughout the peripheral tissues. Endogenous peptides are produced by noxious stimulation and they normally stimulate these opioid receptors. There are four major types of opioid receptors: mu, kappa, delta and sigma (Trescot et al., 2008).

Mu receptors are mostly found in the brainstem. Some well-known agonists at the mu receptor are enkephalins, morphine, meperidine, fentanyl and codeine (weak agonist). Naloxone and naltrexone, on the other hand, are antagonists at mu receptors. Mu receptors produce supraspinal analgesia, respiratory depression, euphoria, urinary retention, sedation, constipation, and physical dependence (Trescot et al., 2008).

Kappa receptors are mostly found in brainstem and spinal cord. Dynorphine A is an agonist of the kappa receptor, while morphine is a weak agonist. Naloxone and naltrexone both act as antagonists at kappa receptors. Kappa receptors are responsible for spinal analgesia, dysphoria, sedation, and respiratory depression (Trescot et al., 2008).

Delta receptors are mostly found in the brain and are responsible for supraspinal and spinal analgesia, respiratory depression, urinary retention, and physical dependence. Enkephalins and meperidine are examples of two agonists of delta receptors (Trescot et al., 2008).

Sigma receptors are no longer considered as opioid receptors. They are responsible for dysphoria and psychomimetic effects.

The following section is a brief description of the three opioids used in this current project.

1.2.1 Morphine

Morphine is a phenanthrene derivative and the prototypical mu receptor agonist. It is the gold standard opioid against with which all others are compared. It is a Schedule II substance, and is used to control moderate to severe pain. Morphine is mainly used for the treatment of non-cancer pain. Osteoarthritis is also treated with morphine rather than with NSAIDs as the latter therapeutic agents may cause gastrointestinal injury (Loeser and Melzack, 1999).

After oral administration of morphine, only 40-50% of the administered dose becomes available to central nervous system. The reason for this poor bioavailability is morphine's poor lipid solubility, avid protein binding, and rapid conjugation and metabolism. Morphine is metabolized mostly by *N*-demethylation and *O*-glucuronidation. 65% of a dose of morphine is metabolized to morphine-3-*O*-glucuronide (M3G) and morphine-6-*O*-glucuronide (M6G) primarily in the liver by the enzyme uridine-5'-diphosphate glucuronosyltransferase. M6G and M3G are produced *in vivo* in a ratio of 1:5, and approximately 5% of morphine is *N*-demethylated to form normorphine. M6G is

believed to be an opioid agonist with a potency that is 2-4 times greater than that of morphine. M3G has very low affinity for mu opioid receptors and appears to be devoid of any significant analgesic activity (Coller et al., 2009).

1.2.2 Codeine

Codeine is a weak opioid analgesic with weak affinity for mu opioid receptors. Pure codeine is a Schedule II substance; however, when given in combination with other analgesics, it is considered as a Schedule III substance. Codeine is used for the treatment of mild to moderately severe pain. Codeine is also commonly used for postpartum pain associated with episiotomy and cesarean section (Trescot et al., 2008). The analgesic potency of codeine is approximately 50% of morphine potency. Studies have shown that 80% of codeine is converted *in vivo* to codeine-6-*O*-glucuronide and 2-3% or less of codeine is metabolized to morphine. The rest of the molecules are metabolized to norcodeine (Vree et al., 2000). Some people believe that the analgesic action of codeine is due to its conversion to morphine, but recent studies have shown that the codeine metabolite codeine-6-*O*-glucuronide is also an active analgesic (Armstrong and Cozza, 2003).

1.2.3 Oxycodone

Oxycodone is also a phenanthrene class opioid and a Schedule II substance. It is a powerful opioid analgesic and has affinity for multiple opiate receptors. Oxycodone is used for the treatment of moderate to severe pain. Unlike codeine and hydrocodone, oxycodone is a very potent analgesic. Oxycodone is metabolized *in vivo* to mainly noroxycodone and oxymorphone (Poyhia et al., 1992). Oxymorphone is an active metabolite and also an analgesic drug in its own right (Poyhia et al., 1992).

1.3 Problems Associated with Opioid Therapy

Even though opioids are the most widely used analgesics for the treatment of moderate to severe pain, their use in postoperative care, and in the treatment of pain associated with life-shortening illnesses, such as cancer, is complicated by numerous side-effects associated with opioid therapy. The following is a summary of the major adverse effects produced by opioid analgesics.

Constipation and nausea are the most common opioid side effects, and usually occur with very high incidence. Constipation occurs in 40-90% of opioid-treated patients and can occur even with a single dose of morphine (Berde and Nurko, 2008). Opioids cause bowel dysfunction through several effects, including blockade of propulsive peristalsis, inhibition of secretion of intestinal fluids, and increase of intestinal fluid absorption (Kurz and Sessler, 2003). Constipation is often dismissed as a trivial side-effect, but the long term consequences of chronic constipation have an adverse effect on patient quality of life. Chronic constipation can cause hemorrhoid formation, rectal pain and burning, bowel obstruction and potential bowel rupture and death. Severe constipation can also lead to dose reduction for the opioids, resulting in decreased and inadequate analgesia. Unlike many other side effects, tolerance does not develop to the constipatory effects of opioids (Benyamin et al., 2008).

Cellular immune suppression and decreased resistance to bacterial infection has been observed in guinea pigs treated with morphine. Opioids are believed to be the cause behind the increased incidence of infection in heroin addicts. Although exogenous opioids create immunosuppression, endogenous opioids are believed to induce immunoactivation (Benyamin et al., 2008).

Opioids are known to cause hormonal changes in human body. Various studies have shown that opioids affect a variety of hormones, such as testosterone, estrogen, luteinizing hormone, dehydroepiandrosterone, andrenocorticotropin, and cortisol. Men taking prescribed or illicit opioids frequently suffer from several adverse side effects, including erectile dysfunction, decreased libido, depression, and decreased energy levels (Benyamin et al., 2008).

Opioid induced sedation is a very common side effect in opioid-naïve patients. Over time, tolerance to this side effect often develops. Dose initiation and rapid dose escalation in opioid therapy may cause sedation leading to reduced quality of life. Also, opioids exert negative effects on psychomotor/driving performance, especially in opioid-naïve patients. After initiation of opioid therapy for pain management, a patients' ability to operate heavy machinery may be diminished and the patient may not be able to drive automobiles properly. After reaching a stable opioid analgesic regimen, patients are generally allowed to drive (Pud et al., 2006).

Opioid-induced bladder dysfunction is a well-known complication in postoperative patients. Some studies have demonstrated urinary retention in 3.8-18.1% of patients taking opioids for post-operative pain management (Benyamin et al., 2008).

Some opioids are believed to have cardiovascular side effects, although the occurrence is not very common. Morphine is known to release histamine in the human body causing vasodilation and hypotension (Benyamin et al., 2008).

Development of tolerance and physical dependence are some of the very critical issues associated with opioid therapy. Tolerance refers to a phenomenon in which exposure to a drug results in the diminution of an effect, or the need for a higher dose to maintain an effect, and is one of the most common side-effects of opioid therapy. Tolerance causes decreasing effectiveness of opioids over time and ever-increasing dose requirements to provide adequate analgesia. Tolerance can be both pharmacokinetic and pharmacodynamics in origin. Pharmacokinetic tolerance is caused by changes in the metabolism of opioids after repeated administration, whereas pharmacodynamic tolerance is represented as the decreased analgesic effectiveness of opioids over time. One of the major clinical concerns when starting a patient on long term opioid therapy is the maintenance of analgesic efficacy of the opioid over time. Tolerance to some of the adverse side-effects of opioids also occurs, and this has positive benefits. Physical dependence is represented by development of an altered physiological state that is revealed by an opioid withdrawal syndrome following abrupt dose reduction, discontinuation of the drug, or administration of an antagonist drug. Physical dependence on opioids is a very common phenomenon and is expected to occur in all individuals

during continuous use of opioids for therapeutic or non-therapeutic purposes. Symptoms and signs of withdrawal syndrome include craving for opioids, restlessness, irritability, increased sensitivity to pain, nausea, abdominal cramps, insomnia and anxiety (Ballantyne, 2006).

Addiction to opioids is a complex phenomenon involving several components, such as genetic, environmental, psychological, and the inherent properties of the drug itself. Addiction in the context of pain management with opioid therapy is characterized by a persistent pattern of dysfunctional opioid use that may include: adverse consequences associated with the use of opioids, loss of control over the use of opioids, and/or preoccupation with obtaining opioids despite the presence of adequate analgesia. Studies have shown that, after a treatment period, drug craving was observed in 8.7% of the patients on morphine compared to 4.3% on placebo (Moulin et al., 1996). In another study, 16% of the active patients were found to be abusing their opioid medications (Okie, 2010).

Among all the complications associated with opioids, respiratory depression and death are the most feared ones. In the eyes of many patients, opioids are essentially legal heroin. In-between 1979 and 1990 the average drug poisoning death rates were 5.3% every year; however from 1990 to 2002 the death rates increased to 18.1% per year (Okie, 2010). During the same period of time, the number of deaths caused from opioid poisoning increased 91.2%. In 2007 there were 11,499 deaths caused by overdose of opioids, which is more than the number of deaths due to heroin and cocaine combined. Visits to the emergency department for opioid abuse more than doubled from 2004 to 2008. Admission to substance abuse treatment programs increased by 400% between 1998 and 2008, with prescription opioids being the second most prevalent type of abused drug after marijuana (Okie, 2010).

In addition to all of these complications, opioids are also associated with other side effects, which include dizziness, cognitive dysfunction, urinary retention, vomiting, loss of appetite, pruritus, and ileus.

In addition to the adverse effects, opioids are not effective for the treatment of all types of pain syndromes. Pain is broadly divided into two categories: nociceptive and neuropathic pain. Nociceptive pain occurs as a result of activation of nociceptors (free nerve endings) by noxious stimuli, such as heat, pressure, and inflammatory mediators (Loeser and Melzack, 1999). Examples of nociceptive pain include postsurgical pain, inflammatory pain and low back pain. Nociceptive pain is often described as being constant, dull and aching in nature. Nociceptive pain is responsive to opioids. On the other hand, neuropathic pain occurs as a result of damage to the peripheral or central nervous system. Examples of neuropathic pain include diabetic neuropathy, pain from stroke, and pain from spinal cord injury. Neuropathic pain is described as burning, tingling and shooting in nature. Neuropathic pain is much less responsive to opioids (Foley, 2003).

1.4 Combination Therapy for Pain

Due to the above discussed complications related to opioid therapy and the ineffectiveness of opioids-alone therapy in treating neuropathic pain, it is well established that opioids should not be used in isolation to treat pain, and that the goals of treatment will commonly require additional medications, such as anticonvulsants, antidepressants, NSAIDs and other adjuvant analgesics (Gilron and Max, 2005). The theory behind this combination therapy for pain is to lower the dose to avoid side-effects, in addition to covering a broad spectrum of pain, i.e., to treat both nociceptive and neuropathic pain. The amplification of the desired pain relief effect while decreasing, or at least not equally increasing, the adverse side-effects inherent to the individual analgesics, is the main goal of combination therapy. A logical way to achieve this target is to combine agents that have complimentary mechanisms of action (Kalso, 2005). By combining two such agents, both mechanisms are expected to contribute in additive fashion to the analgesic effect, or may even be synergistic, and the adverse effect profile is expected to be more favorable than using individual agents to achieve the same level of analgesia (Raffa et al., 2003). There may be several advantages to using combination therapy over using a single

analgesic agent, and some of the advantages are discussed below, in addition to some disadvantages of combination therapy.

- A combination strategy for pain management can produce increased efficacy in two ways. First, individual analgesic agents may not always produce complete pain relief, whereas addition of another analgesic or adjuvant may produce better efficacy. This is particularly beneficial if the combined agents are synergistic. Even if the drug combination produces just additive analgesia but there is less additivity of side-effects, the drug combination could still be clinically favorable. Secondly, a broader spectrum of pain relief can be achieved by combining analgesics of two different classes and mechanisms (Lussier et al., 2004).
- If additivity or synergism leads to maximal efficacy at lower doses, a decreased opioid dose can be achieved. This will also result in less side-effects generated from opioids use. Also, adjuvant drug may antagonize some of the opioid adverse side-effects (Raja and Haythornthwaite, 2005).
- A common aim for combination therapy is to reduce side-effects. By achieving an equivalent analgesic efficacy with reduced amounts of individual analgesic agents, combination therapy offers the potential benefit of a reduced side-effect profile for each agent (Raffa, 2001).
- Development of tolerance to opioids can be prevented by using an effective analgesic drug combination.
- Combination therapy may reduce the number of doses and may simplify the dosing schedule compared to dosing with individual analgesic agents. Greater convenience will produce greater patient compliance.
- The use of combination therapy using individual agents may increase the cost of treatment, but the decreased cost of treating adverse effects may actually decrease the overall cost of treatment.
- Concern over dose inflexibility comes into picture when agents are administered individually in a combination therapy. In case of a fixed ratio product, increasing the dose of one component without increasing the dose of the other component is not possible.

Four different combination strategies were chosen for this project based on current literature. In each of these approaches, opioids were combined with other agents having analgesic action but belonging to drug classes with different mechanisms of action. The following list represents four different combination strategies that were studied in this current project.

- Combination of opioids and nicotinic receptor agonists
- Combination of opioids and NMDA receptor antagonists
- Combination of opioids and anticonvulsants
- Combination of opioids and cannabinoids

The following section describes the rationale for choosing each of the above combination therapies.

1.4.1 Opioid-Nicotinic Receptor Agonist Combination

Given the clear indication that current analgesic drugs may not provide adequate analgesia without causing adverse side-effects, a great deal of research emphasis has been placed on identification of novel molecular targets that might form the basis for the development of new analgesic agents. Neuronal nicotinic acetylcholine receptors (nAChRs) are among these new series of molecular targets (Vincler, 2005). Nicotinic receptors are located in the central nervous system at sites known to be important in pain processing. Neuronal nicotinic receptor agonists are effective in a broad spectrum of animal pain models, including acute thermal pain models (tail-flick, hot plate) and neuropathic pain assays (spinal or sciatic nerve ligation) (Flores, 2000). Both anti-hyperalgesic and anti-allodynic effects have been observed in neuropathic pain models using nicotinic receptor agonists (Flores, 2000). Hyperalgesia refers to an exaggerated response to a noxious stimulus. Allodynia is represented by a painful response to a normally non-noxious stimulus. Neuropathic pain is characterized by several abnormal sensations. Hyperalgesia and allodynia are two of these kinds of abnormal sensations. Varieties of preclinical studies have shown that activation of neuronal nAChRs produces antinociception in various pain models and drugs acting at nicotinic receptors can be

expected to have analgesic properties (Arneric et al., 2007). Nicotine has been known to have weak analgesic activity for more than sixty years. Nicotine produces its analgesic effects by activating the neuronal nAChRs (Lippiello et al., 2007). Antinociceptive effect of nicotine in animals is typically of limited duration and is attenuated with repeated dosing. Moreover nicotine has a number of side-effects that preclude its use as a therapeutic agent. Side-effects of nicotine include adverse effects on autonomic function, its addictive nature, cardiovascular, gastrointestinal, and respiratory toxicity and tolerance (Decker and Meyer, 1999). Also, nicotine has a narrow therapeutic window and lacks selectivity for neuronal nicotinic receptors. The major issue for the successful development of analgesic agents from the class of nicotinic receptor agonists appears to be separation of efficacy from toxicity (Holladay et al., 1997).

Nornicotine is an active metabolite of nicotine. It is the *N*-desmethyl derivative of nicotine. It might be a feasible candidate to investigate as a nicotinic receptor agonist and novel analgesic agent. Nornicotine is pharmacologically and pharmacokinetically different from nicotine in several aspects; i.e., nornicotine has:

- Better oral bioavailability than nicotine (Ghosheh et al., 1999, 2001)
- A longer half-life in brain and plasma (Ghosheh et al., 1999, 2001)
- Greater brain accumulation upon repeated administration (Ghosheh et al., 1999, 2001)
- Less toxicity relative to nicotine (Papke et al., 2007)
- Less potent compared to nicotine in dependence-producing properties (Bardo et al., 1999)
- Less potent than nicotine against thermal antinociception in mice (Bardo et al., 1999)

Nornicotine exists in two enantiomeric forms as *S*-(-) and *R*-(+)-nornicotine. Holtman et al. (2010) performed a recent study to determine: (i) if either or both of the enantiomers of nornicotine have analgesic activity in well-established rodent models of acute and chronic pain; (ii) if the analgesic activities of *S*-(-) and/or *R*-(+)-nornicotine are separated from adverse side-effects; and (iii) if an enhanced analgesia and reduced side

effect profile can be achieved when either of the enantiomer of nornicotine is combined with morphine.

Several interesting facts evolved from the study. A summary of the results is provided below.

- Antihyperalgesic and antiallodynic effects of *S*-(-) and *R*-(+)-nornicotine were observed in a CCI model of neuropathic pain.
- The antihyperalgesic effect of the *S*-(-) enantiomer was approximately three-fold greater than the *R*-(+) enantiomer.
- The *S*-(-) enantiomer was more effective than the *R*-(+) enantiomer at comparable doses.
- *R*-(+)-nornicotine caused a significant decrease in locomotor activity compared to the control (saline). No statistically significant side-effects were observed in case of *S*-(-)-nornicotine. Thus, the undesirable side-effects were more pronounced with the *R*-(+) enantiomer.
- A dose of *S*-(-)-nornicotine that caused an undesirable side-effect was higher than a dose that produced a desirable analgesic effect.
- When given in combination, *S*-(-)-nornicotine at a dose that had no antinociceptive effect on its own, significantly enhanced morphine nociception in rats in the tail-flick test.
- A similar combination of dose of morphine and *R*-(+)-nornicotine produced less pronounced antinociceptive effect.
- A low dose of morphine enhanced the effectiveness of *S*-(-)-nornicotine at doses showing no antinociceptive effects on their own.
- *S*-(-)-nornicotine at doses devoid of any significant analgesic activity of their own, produced dose-related antihyperalgesia in the presence of a low dose of morphine in the CCI pain model.
- No motor effects were observed during combination therapy at the maximum antihyperalgesic doses of morphine and *S*-(-)-nornicotine.
- Thus, the analgesic property resides predominantly in *S*-(-)-nornicotine while the side- effects were more pronounced with the *R*-(+) enantiomer.

- *S*-(-)-Nornicotine had an expanded therapeutic index compared to *R*-(+)-nornicotine.
- *S*-(-)-Nornicotine might be an analgesic agent of value, either alone or in combination with a mu-opioid agonist such as morphine as a novel analgesic therapy in managing a broader range of pain.
- Enhanced analgesic activity and reduced toxicity, observed with higher doses of each drug, might be achieved by combining *S*-(-)-nornicotine with morphine.

1.4.2 Opioid-NMDA Receptor Antagonist Combination

There is evidence in the literature that pain associated with peripheral tissue or nerve injury involves activation of NMDA receptors (Petrenko et al., 2003; Parsons, 2001). Thus, NMDA receptor antagonists were expected to have analgesic behavior. Many NMDA receptor antagonists have been shown to effectively relieve pain-related behavior in preclinical animal models, as well as in clinical settings (McCartney et al., 2004). Also, attention has been focused on the concept of combining NMDA receptor antagonists with opioids in an effort to enhance analgesia, reduce side effects, and limit the development of tolerance and dependence potential. Recent research studies have shown the potential utility of combining NMDA receptor antagonists with opioids in rodents and humans (Mao, 1999). NMDA receptor antagonists are known to exhibit enhanced and prolonged opioid antinociception and reduced development of tolerance and physical dependence (Price et al., 2000). Thus, combination therapy with opioids may be useful in treating neuropathic pain, which is poorly managed by opioid alone therapy. Ketamine is a noncompetitive NMDA receptor antagonist and an intravenous anesthetic. Ketamine has been available in clinical practice for more than thirty years. Both preincisional and postincisional administration of ketamine was found to be useful as an adjuvant to opioids in several clinical trials (Hocking and Cousins, 2003). Ketamine is also considered as an additive in surgical situations with large opioid requirements (Subramaniam et al., 2004). In addition to its usefulness in surgical pain management, ketamine is also considered as a useful adjuvant for the management of pain in cancer patients (Subramaniam et al., 2004).

A recent study in rodent models of pain showed that combination of ketamine with two different opioids (morphine and methadone) resulted in a synergistic antinociceptive action in the neuropathic paw and additive antinociceptive effects in the normal paw (Pelissier et al., 2003). All the above findings support the combination of ketamine with opioids for a well-balanced pain treatment.

Ketamine is associated with side effects such as sedation, dysphoria and hallucinations. In the body, ketamine is extensively metabolized to norketamine, the *N*-desmethyl derivative of ketamine. Norketamine is also an NMDA receptor antagonist and is expected to have analgesic activity. A recent study done by Holtman et al. (Holtman et al., 2008 [1]; Holtman et al., 2008 [2]) revealed some interesting facts regarding the analgesic effects norketamine and norketamine-morphine combinations. A summary of these findings is provided below:

- Norketamine showed efficacy in two well established rodent models of persistent pain; the chronic constriction nerve injury rodent model of peripheral neuropathy (CCI) and the formalin model of tonic inflammatory pain.
- The antinociceptive effect of norketamine could be separated from significant side effects.
- Norketamine might be an effective agent for treatment of chronic pain.
- Norketamine has lower potency than ketamine in attenuation of nociception in the nerve injury assay (CCI model) or injury to peripheral tissue assay (formalin test).
- The time courses for both antihyperalgesia and motor dysfunction were of shorter duration for norketamine than for ketamine.
- Norketamine might be likely to have a better side-effect profile than ketamine.
- Norketamine, in a dose range having no antinociceptive activity, significantly increased the antinociceptive effect of low doses of morphine in the tail-flick test.
- Norketamine, at doses which are not antihyperalgesic or antiallodynic alone, enhanced the effects of morphine against mechanical hyperalgesia and tactile allodynia in rats in the CCI pain model.

- A norketamine and morphine drug combination did not produce motor dysfunction at doses that achieved maximum efficacy against thermal nociception, mechanical hyperalgesia and formalin induced flinches.
- No over toxicity was observed with a norketamine-morphine combination, as shown by a lack of sedation in rats.
- A norketamine and morphine combination had no significant effect on locomotor activity.
- A norketamine and morphine combination therapy might be useful for the treatment of a broader range of pain, including acute nociceptive, neuropathic and persistent inflammatory pain.

1.4.3 Opioid-Gabapentin Combination

Gabapentin is an anti-epileptic agent which was initially developed as a gamma-aminobutyric acid mimetic compound for the treatment of spasticity (Mao and Chen, 2000). Later, gabapentin was shown to have clinically useful anticonvulsant effects (Rose and Kam, 2002). Initially approved to treat partial seizures, gabapentin showed promise as an analgesic agent for the treatment of chronic pain syndromes, especially neuropathic pain (Mao and Chen, 2000). Both clinical and experimental studies suggest that gabapentin has analgesic effects in neuropathic pain (Gupta et al., 2004). Preclinical studies also suggested that gabapentin has antinociceptive properties in animal models of both nociceptive pain and neuropathic pain (Bennett and Simpson, 2004). Many animal experiments have also revealed that gabapentin increased the antinociceptive effects of opioids in a variety of animal pain models when given in combination with opioids (Nicholson, 2000). The following is the summary of the results obtained from several animal experiments carried out with gabapentin alone and in combination with an opioid.

- A recent study conducted by Meymandi et al. showed that a high dose of gabapentin increased the latency time significantly when compared to a control group in rat tail-flick experiments. It was also found that co-administration of gabapentin with morphine increased both tail-flick latency time and duration of

action compared to rats treated with morphine alone. Thus it can be concluded that gabapentin enhances morphine antinociception in acute models of pain (Meymandi et al., 2006).

- Another study performed by O-Arciniega et al. involving neuropathic pain induced by chronic constriction nerve injury showed synergistic antinociceptive interaction of morphine and gabapentin. Combination of a low dose of morphine with gabapentin demonstrated supra-additive effect on mechanical hyperalgesia and cold allodynia (O-Arciniega et al., 2009).
- The antinociceptive effect of a morphine and gabapentin combination was evaluated in a study by Shimoyama et al. after spinal administration of the morphine-gabapentin combination. The authors found that when sub-antinociceptive doses of morphine and gabapentin were co-administered, there was a significant antinociceptive effect in the rat tail-flick test. Furthermore, the sub-antinociceptive dose of gabapentin shifted the dose-response curve for morphine to the left, demonstrating a potentiation of the antinociceptive effects of morphine. Enhancement of antinociception resulting from the combination of spinal morphine and gabapentin suggests that the drug combination might be effective for the treatment of persistent pain syndromes in patients (Shimoyama et al., 1997).
- Gilron et al. investigated the effect of gabapentin to prevent and reverse chronic opioid tolerance. These studies demonstrated that the combination of morphine and gabapentin resulted in a maximal and supra-additive antinociceptive effect in the paw pressure and tail-flick tests. Also, visual inspection of the treated animals did not show any sign of motor impairment. It was also observed that gabapentin inhibited the development of antinociceptive tolerance to morphine. Gabapentin was also able to partially restore opioid potency in tolerant rats in the paw pressure test (Gilron et al., 2003).

In addition to the above series of animal experiments, gabapentin also showed enhancement of the analgesic effect of opioids in clinical studies. In a recent study performed by Eckhardt et al. on healthy volunteers, where analgesic effects were assessed by using the cold pressor test, the investigators showed that gabapentin significantly

enhanced the analgesic effect of morphine (Eckhardt et al., 2000). A single oral dose of 600 mg of gabapentin did not show any effect on its own in comparison to placebo. However, both pain tolerance and pain threshold were increased after the administration of morphine plus gabapentin in comparison to morphine plus placebo.

1.4.4 Opioid-Cannabinoid Combination

A body of evidence suggests the existence of independent but interacting mechanisms of modulation of antinociception by cannabinoid and opioid systems (Hohman et al., 1999). It has been shown previously that Δ^9-THC and morphine exhibit synergistic effects in the production of antinociception (Williams et al., 2006). Importantly, cannabinoids have been shown to produce analgesia through interaction with kappa opioid receptors in the spinal cord by releasing endogenous opioids (Hohman et al., 1999).

A synergism between morphine and Δ^9-THC has also been observed in the spinal cord of mice. Inactive doses of both morphine and Δ^9-THC showed a greater than additive effect when given by i.v. administration (Bidaut-Russell and Howlett, 1988; Reche et al., 1996). A mixture of these two drugs produced an analgesic effect through mu opioid receptor-mediated as well as CB1 cannabinoid receptor-mediated pathways.

The following section of Chapter 1 is taken from the published chapter "Improving the use of Drug Combinations through the Codrug Approach" (Part Three: Codrugs and Soft Drugs, Chapter 13, Page Number 347-383) coauthored by Peter A. Crooks, Harpreet K. Dhooper, and Ujjwal Chakraborty and published in the book 'Prodrugs and Targeted Delivery: Towards Better ADME Properties', edited by Jarkko Rautio. Copyright © 2010 WILEY-VCH, ISBN: 978-527-32603-7. Published in the year of 2010.

1.5 Codrug

There are advantages of delivering a single chemical entity than a physical mixture of two drugs. There are instances in prodrug design where the prodrug molecule incorporates two identical or non-identical drugs into a single chemical entity. This is often desirable when two synergistic drugs have different physicochemical and pharmacokinetic properties, and it is desirous to have the parent drugs released concomitantly at the site of action to obtain a synergistic pharmacodynamic effect that is not attainable by delivering a physical mixture of the two drugs. Also, one of the drugs in the codrug structure may be incorporated to counterbalance the known side-effects associated with the other parent drug, or may amplify the pharmacodynamic effect of the other parent drug through an action at another biological target. Thus, codrugs can be designed to overcome various barriers to drug formulation and delivery, such as poor aqueous solubility, chemical instability, insufficient oral absorption, rapid pre-systemic metabolism, inadequate brain penetration, toxicity and local irritation. Structurally, a codrug (also known as a mutual prodrug, or hybrid drug) comprises two or more different drugs within a single chemical entity where the drugs must each contain an appropriate chemical functionality to enable them to be connected together, either directly or by means of a cleavable, biolabile covalent linker (Hamad et al., 2006). Such codrugs can be either bipartate or tripartate in nature (Silverman, 2004) (Fig.1. 1) and the design of the linker moiety can be adopted from current linker design strategies and chemistry already established in the broad area of prodrug design.

Thus, a codrug strategy can be useful when:

- Synergistic drugs need to be given concomitantly to act at the same time, either at the same or different biological targets.
- The physicochemical properties of two synergistic drugs are not favorable for delivery of the two drugs as a physical mixture, but can be improved by chemical combination of the two drugs.
- Improved pharmacokinetics results from a chemical combination of two synergistic drugs compared to those of a physical mixture of the two drugs.

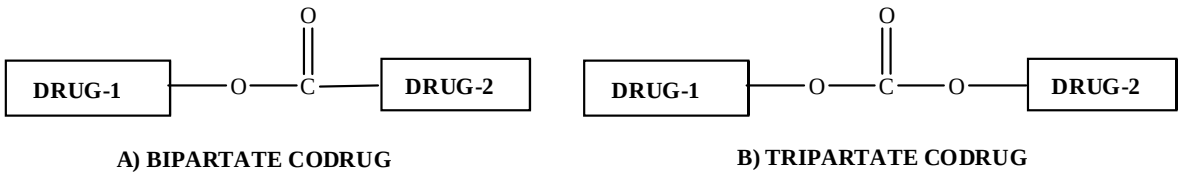

A) BIPARTATE CODRUG **B) TRIPARTATE CODRUG**

Fig. 1.1: Examples of bipartate and tripartate codrugs: A) conjugation of a carboxylic drug with an alcoholic drug to form a bipartate codrug where the two drugs are connected by an ester linkage which cleaves in vivo to release only the two parent drugs; B) conjugation of two alcoholic drug molecules via a carbonate ester linker to form a tripartate codrug which cleaves in vivo to form the two parent drugs and an equivalent of carbonic acid.

As with prodrugs, the codrug structure can incorporate two drugs joined together by linker moieties such as ester, carbonate, amide, carbamate, etc., which are then cleaved enzymatically in vivo to release the active drugs at a required site in the body. By appropriate structural design of these linkers, it may be possible to control the release kinetics of one or both drugs. When the two drugs are chemically combined together, the resulting codrug will usually have different physicochemical properties to those of the individual parent drugs, which may provide superior properties for delivery of the two drugs when compared to delivery of a physical mixture of the drugs (Howard, 2007).

1.5.1 Ideal Codrug Characteristics

An ideal codrug will generate the parent drugs with high recovery rates, and will incorporate linkers that give rise to non-toxic linker residues upon *in vivo* cleavage. There may be other advantages in delivering of two drugs as a single chemical entity *versus* a physical mixture. These include, for example, improved chemical stability of the formulation (i.e. no chemical interaction of the two parent drugs within the formulation), improved metabolic stability (especially with regard to possible protection of either drug from high first pass metabolism), as well as improved targeting of drugs to the site of

action (e.g., the central nervous system), and more desirable pharmacokinetic properties, in particular for drugs with different physicochemical properties (e.g., differences in lipid solubility or polarity).

There are also certain disadvantages that are associated with a codrug strategy. One disadvantage is that codrugs are usually large molecules with molecular weights that are often greater than 500. Thus, codrugs with large molecular weights may well violate Lipinsky's rule of five (Lipinski et al., 2001) as unfavorable molecules for oral or topical dosage form development, or for CNS delivery. In addition, by the very nature of their structural design, these cleavable molecules may possess poor stability profiles for formulation development. Thus, it must be initially established that the codrug is resilient enough to withstand the rigors of formulation development, but must not be too stable that it will not efficiently cleave to the parent drugs *in vivo*.

Another important aspect of codrug design is the toxicological significance of delivering a codrug to an individual. Since codrugs are novel chemical entities (although the parent drugs they generate may or may not be novel), they will have to be treated as new xenobiotics by the FDA, as are all new drugs entities that have never been previously administered to humans. Thus, there are important toxicological and safety issues associated with the development of codrugs, as they move toward clinical status.

Several important criteria are required for codrugs to be effective. The codrug must be well absorbed and distribution, metabolism and elimination of the codrug should be superior to the physical mixture of the parent drugs. Both parent drugs should be released concomitantly and quantitatively after absorption, and the maximal effect of the drug combination should occur when a simple molar ratio, i.e. 1:1, 2:1, or 3:1, is utilized.

Before designing the codrug, one needs to know the route of administration. Routes of administration can be broadly divided into topical, enteral and parenteral routes. The topical route involves a local drug effect. The drug is directly applied where the action is desired, e.g. asthma medications, eye or eardrops, and decongestant nasal sprays. In the enteral route, drug administration involves any part of the gastrointestinal tract. The effect is non-local. Sublingual, oral and rectal are all enteral routes. In

sublingual administration, the drug is placed under the tongue, is rapidly absorbed and avoids first-pass metabolism. The first-pass effect term refers to the hepatic metabolism of a drug when it is absorbed from the gastrointestinal tract and delivered to the liver via the hepatic portal circulation. The greater the first-pass effect, the lower the concentration of drug that reaches the systemic circulation. In the oral route, the drug is swallowed. It passes through the whole gastrointestinal tract. Drugs taken orally are usually less expensive to manufacture than ones administered by any other route, and can easily be self-administered (minimal invasiveness) by the patient. The disadvantage of oral delivery is that the drug has to be absorbed from the gastrointestinal tract and experience the first pass effect. Sometimes this route of administration is inefficient because only part of the drug may be absorbed; also a significant first-pass effect may occur. In addition, some orally administered drugs can cause irritation of the gastric mucosa, and cause nausea and vomiting.

Note: drugs given orally take more time than any other route to show a pharmacological response, but the oral route is considered to be the safest, pain-free and cheapest method of drug administration. Other routes are used if there is an emergency situation where the effect of the drug is needed immediately (Silverman, 2004).

1.5.2 Examples of Marketed Codrugs

A good example of an effective and marketed codrug is the antibiotic sultamicillin (Unasyn Oral), a tripartate codrug of ampicillin and penicillanic acid sulfone (Fig. 1.2) (Baltzer et al., 1980; Hartley and Wise, 1982). Ampicillin is a well-known β-lactam antibiotic, but suffers from ineffectiveness against resistant bacteria that excrete high concentrations of the bacterial enzyme, β-lactamase. β-Lactamase degrades penicillins such as ampicillin by hydrolysis of the β-lactam ring with consequent loss of antibacterial activity. Subsequent co-administration of a β-lactam antibiotic with a β-lactamase inhibitor was utilized as a strategy for treating resistant strains of bacteria. For example, the antibiotic Augmentin is a mixture of the β-lactam penicillin, amoxicillin and the β-lactamase inhibitor, potassium clavulanate (Fig. 1.2). One of the problems of

administering the two synergistic drugs together (as a physical mixture) is that they may not have similar pharmacokinetic profiles, and thus may not arrive at the target site at the same time or at the same concentration. The codrug sultamicillin incorporates a labile linker, which on hydrolysis by a plasma esterase affords the two synergistic parent drugs in equimolar amounts together with a molar equivalent of formaldehyde.

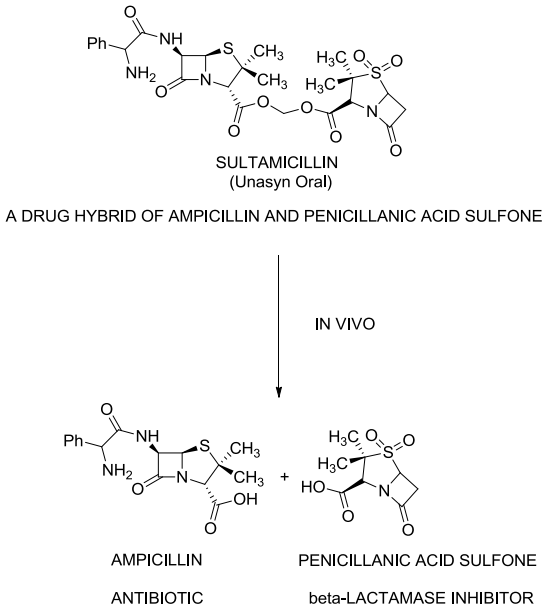

Fig.1.2: Sultamicillin codrug and the *in vivo* hydrolysis products generated from the codrug.

Another example of a marketed codrug is sulfasalazine (Svartz, 1942), which is prescribed for the treatment of ulcerative colitis. Ulcerative colitis is a chronic inflammatory disease characterized by a diffuse inflammation the mucosa which is mainly restricted to the colon. Aminosalicylates are the mainstay of treatment in case of active ulcerative colitis. Sulfasalazine is the prototype of this drug class and releases 5-aminosalicylic acid and antibacterial sulfonamide, sulfapyridine in the colon. After oral administration, 80-90% of the drug is delivered to the colon intact. 10-20% of the drug is absorbed from small intestine and undergoes enterohapatic circulation without biotransformation and is excreted in the bile (Das et al., 1973). In the colon, the azo bond

in sulfasalazine is cleaved by colonic bacterial azoreductases liberating sulfapyridine and 5-aminosalicylic acid (Peppercorn and Goldman, 1972; Khan et al., 1983) (Fig. 1.3).

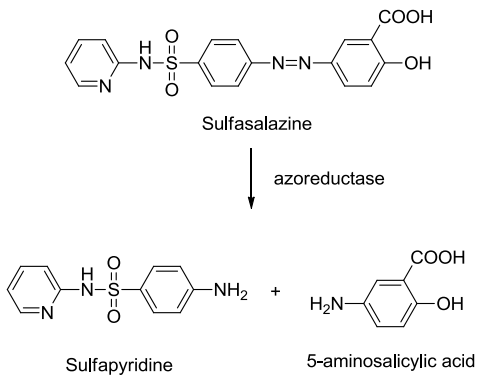

Fig.1.3: Generation of 5-aminosalicylic acid and sulfapyridine from sulfasalazine codrug.

Benorylate is another good example of a marketed codrug used in the treatment of rheumatoid arthritis. Benorylate is an ester of acetylsalicylic acid and paracetamol and is an effective analgesic and anti-inflammatory drug with less potential for gastric irritation. The antipyretic activity of benorylate is similar to that of acetylsalicylic acid (aspirin) and paracetamol (Beales et al., 1972). The pharmacological actions of benorylate are due to the effects of both aspirin and paracetamol released by hydrolytic cleavage. Benorylate is actively hydrolyzed by liver cytosol and plasma to generate the two parent drugs (Fig. 1.4). Only paracetamol and salicylate can be detected in plasma after oral administration of benorylate (Robertson et al., 1972).

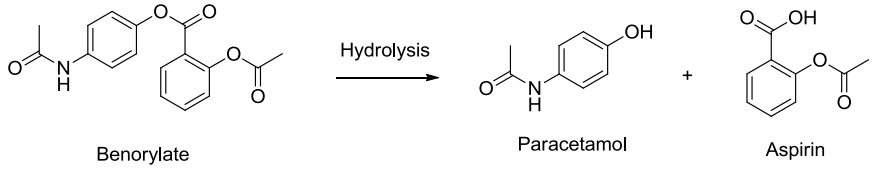

Fig.1.4: Generation of paracetamol and aspirin from hydrolysis of benorylate.

1.5.3 Topical Codrug Therapy for the Treatment of Ophthalmic Diseases

Codrugs for the treatment of diabetic retinopathy

The codrug strategy has previously been utilized when the physicochemical and/or pharmacokinetic properties of two synergistic drugs are not favorable for delivery of the two drugs as a physical mixture, but can be improved by chemical combination of the two drugs. For example, 5-fluorouracil (5-FU) is a polar, water-soluble antiviral and cytotoxic drug that is rapidly cleared from the vitreous when delivered topically to the eye. In a topical drug combination treatment consisting of 5-FU and the lipophilic, water-insoluble, anti-inflammatory drug, trihydroxy steroid (THS), a codrug strategy was utilized which provided a superior sustained release delivery of these two synergistic parent drugs for the treatment of diabetic retinopathy (Howard-Sparks et al., 2005; Howard et al., 2007). The individual physicochemical properties of 5-FU and THS are not favorable for sustained release of a physical mixture of the two drugs. However, utilizing a codrug approach, the chemical combination of 5-FU and THS in a 2:1 molar ratio, respectively (for optimal synergistic activity) afforded a molecule with greatly improved physicochemical characteristics for sustained delivery compared to formulations of the two drugs as a physical mixture (Howard-Sparks et al., 2005). Fig. 1.5 shows the structure of THS, 5-FU and the THS-BIS-5-FU codrug.

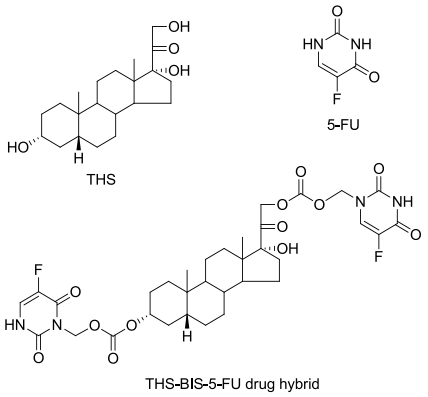

Fig. 1.5: Structures of THS, 5-FU and the THS-BIS-5-FU codrug.

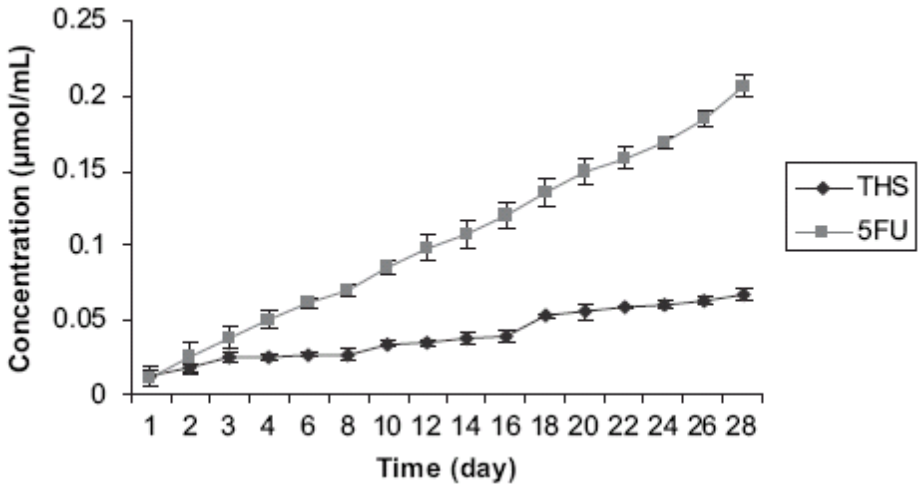

Fig. 1.6: Cumulative release of THS and 5-FU from neat pellets containing 2 mg of the THS-BIS- 5-FU codrug in bovine vitreous humor (Reprinted from Journal of Enzyme Inhibition and Medicinal Chemistry, Howard et al., 2005, copyrighted by Informa Healthcare, used by permission).

The 5-FU-THS codrug was designed as a "chemical delivery" system (Howard-Sparks et al., 2005) which joined together the two drugs via a labile linker moiety. The physicochemical properties of the codrug were favorable for formulation as a sutured ophthalmic pellet, and for slow dissolution of the codrug pellet in the vitreous humor. The labile linker was specifically designed to undergo rapid hydrolysis once the codrug pellet had dissolved, providing sustained release of the parent drugs, which was dependent on the rate of dissolution of the codrug pellet. This concept of a chemical delivery system, where the target tissue is never exposed to dissolved codrug, has been patented (Ashton et al., 2000), and represents a unique form of a codrug formulation, which may be considered as just another formulation for delivery of the parent drugs; the important concept is that the body is never exposed to the new codrug entity, and thus, issues of codrug toxicity would not be relevant. One molar equivalent of the codrug produces one molar equivalent of THS, two molar equivalents of 5-FU, and two molar equivalents of both formaldehyde and carbon dioxide after hydrolysis. Another important consideration in the design of the 5-FU-THS codrug was the structure of the labile linker.

The two drugs were linked together via a linker that afforded hydrolysis products that were considered to be non-toxic. The pellets containing the THS-BIS-5-FU codrug simultaneously released THS and 5-FU in 0.1 M phosphate buffer, (pH=7.4), in human serum, and in bovine vitreous humor. Fig. 1.6 shows the release of THS and 5-FU from the codrug in bovine vitreous humor. The results demonstrate that a neat pelleted THS-5-FU codrug can be utilized as a sustained release ocular delivery form of the parent compounds, and that the unique physicochemical properties of the codrug allow both slow dissolution and rapid release of the two parent drugs (Fig. 1.6).

Codrugs containing corticosteroids for proliferative vitreoretinopathy

Proliferative vitreoretinopathy (PVR) refers to migration and proliferation of cells into the subretinal space, vitreous cavity and onto the retinal surface and undersurface. Subsequent collagen production and cell-mediated contraction of the resulting collagenous scar leads to retinal detachment and loss of vision (Machemer, 1988). Different pharmacological adjuncts have been examined in animal models and human trials to reduce the formation of fibrocellular membranes in PVR, but due to the short half lives of these drugs when delivered by intravitreal injection, repeated post-operative intraocular injections are necessary. When administered systemically, toxic effects are observed as a consequence of the high doses needed to achieve therapeutic intraocular drug levels. This also limits the clinical usefulness of these therapeutic agents. An intraocular device providing therapeutic intraocular drug levels for several months via sustained delivery of the drugs is needed for the treatment of PVR, since re-proliferation and recurrent retinal detachment can occur in the first few months after initial retinal reattachment surgery. An implantable, non-erodible intraocular device has been developed, and has shown potential in the treatment of experimental uveitis (Cheng et al., 1995). Both 5-FU (a cytotoxic agent) and corticosteroids such as dexamethasone (DX) and triamcinolone (TA) are known to be effective in the treatment of experimental PVR. The following are some pros and cons associated with 5-FU and corticosteroids as therapeutic agents for the treatment of PVR.

- Both DX and TA are known to reduce incidents of retinal detachment in a rabbit model of PVR (Tano et al., 1980 [1]; Tano et al., 1980 [2])
- Although corticosteroids are advantageous in suppressing the inflammatory arm of the wound healing response, their weak anti-proliferative properties reduce their clinical potential
- 5-FU is known to be a potent inhibitor of rabbit dermal fibroblast proliferation in cell culture (Blumenkranz et al., 1981)
- 5-FU is also well tolerated in the rabbit when administered intra-vitreally at high doses
- Due to a very short half-life and rapid clearance of 5-FU from the eye, repeated injections of 5-FU are required to achieve a clinically significant effect of the drug when given alone
- Repeated injections of ophthalmic drugs can cause endophthalmitis and retinal detachment, and is also inconvenient and uncomfortable for the patient
- 5-FU is toxic to the cornea and retina when given in high doses (Stern et al., 1983)

In a recent study, codrugs of 5-FU covalently linked to either DX or TA have been prepared and evaluated in a rabbit model of PVR (Berger et al., 1996). The corticosteroid-5-FU codrugs retain the anti-inflammatory properties of the corticosteroids and incorporate the anti-proliferative properties of 5-FU.

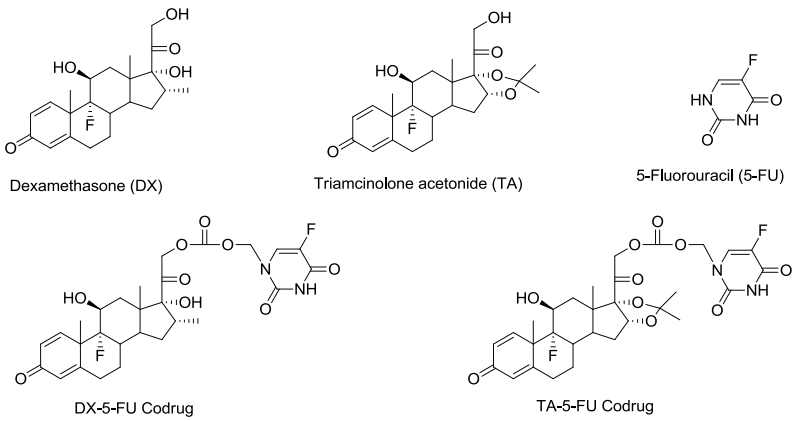

Fig. 1.7: Codrugs of corticosteroids and 5-fluorouracil.

The codrugs of 5-FU and corticosteroids were designed to take advantage of the best characteristics of the individual drugs, and to reduce their individual disadvantages (Fig. 1.7). The parent drugs possessed unfavorable physicochemical properties for sustained delivery; however, when converted the codrug form the molecules were found to possess good characteristics for sustained delivery of the parent drugs. An implantable sustained-release formulation containing the DX-5-FU codrug was developed and surgically implanted into the right eyes of New Zealand white rabbits. In separate experiments, as an alternate to DX-5-FU pellets, a suspension of the more insoluble TA-5-FU codrug was injected into the vitreous of the right eye of the rabbits. TA is less soluble than DX and as a result TA-5-FU codrug is less soluble and therefore longer lasting than DX-5-FU codrug. It was observed that the DX-5-FU device fully released the parent drugs after approximately one week, whereas the TA-5-FU suspension took an extended period of time (1 month) to release the parent drugs. In vitro pharmacokinetic data showed that the DX-5-FU pellet was effective but allowed the disease to progress at the later time points, due to insufficient amount of the drug left in the pellet as a consequence of high solubility of DX-5-FU pellet. However, the TA-5-FU codrug was much more effective in causing regression of PVR severity especially at the later time points. Thus, intravitreal sustained release of the DX-5-FU device and the TA-5-FU suspension were both effective against progression of PVR in the rabbit model.

Codrugs containing non-steroidal anti-inflammatory agents for treatment of proliferative vitreoretinopathy

Although corticosteroids have been used to prevent and treat intraocular inflammation, these therapeutic agents might interfere more severely with wound healing, exacerbate infection, or cause an increase in intraocular pressure. The development of non-steroidal anti-inflammatory drugs (NSAIDs) provides the ocular surgeon with an alternative way to control inflammation and to avoid the problems associated with corticosteroid therapy. Also, a sustained release of the drug with prolonged effects is expected to be more effective in the treatment of experimental post-traumatic PVR than the transient nature of the free drug form, and it is also known that single intra-vitreal injections of either 5-FU or the NSAID naproxen have too short a half life to provide an adequate therapeutic effect (Algyere and Bill, 1981). Based on these observations and on the encouraging data from the 5-FU-corticosteroid codrugs, a naproxen-5-FU codrug (Fig. 1.8) was synthesized for the treatment of experimental post-traumatic PVR. It was also hypothesized that treatment with a NSAID and 5-FU together might be more effective than either of the drugs alone, and that such a drug combination could simultaneously down-regulate the inflammatory and proliferative components of the wound healing response. Bio-erodible implantable sustained release pellets containing a naproxen-5-FU codrug were developed and tested in a rabbit trauma model of PVR. The naproxen-5-FU pellets were found to release 5-FU and naproxen linearly over a 30-day time course in *in vitro* release experiments. Rabbits, after administering codrug as sutured corneal pellet implants, showed a significant decrease in retinal detachment rate compared with the control group (untreated eye) at almost all time points. The codrug pellet did not exhibit any toxic effects on the retina when examined electro-physiologically or histologically. The overall results of the study showed that the napreoxen-5-FU codrug device effectively inhibited the frequency and severity of PVR in a rabbit trauma model without any observable toxic effects of the codrug on the retina.

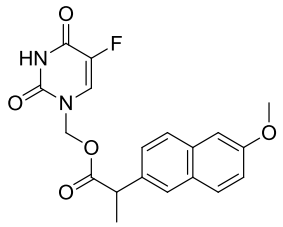

Fig. 1.8: Naproxen-5-fluorouracil codrug.

Codrugs containing ethacrynic acid for treatment of elevated intraocular pressure

Elevated intraocular pressure (IOP) is one of the major risk factors leading to glaucomatous damage of the optic nerve and a consequent cause of blindness. It is known that ethacrynic acid (ECA), a diuretic drug, can reduce IOP in rabbit and monkey eyes (Tingey et al., 1992, Epstein et al., 1997). Intracameral injection of ECA into the eye can also reduce IOP in humans (Melamed et al., 1992). These observations suggest ECA as a potential glaucoma drug. However, topical administration of ECA shows many adverse effects, and limitations. For example:

- Eyelid edema, conjunctival hyperaemia, and moderate diffuse superficial corneal erosion are some of the side effects of long term topical administration of ECA.
- Due to the low pKa (2.8) of ECA, the molecule exists exclusively in the anionic form at physiological pH (pH=7.4), and the very low lipophilicity of the anionic form of ECA limits its ability to effectively penetrate cornea to provide a therapeutic dose at the site of action.
- Oral administration of ECA does not produce any significant effect on IOP (Peczon and Grant, 1968).

On the other hand, β-adrenergic receptor antagonists such as atenolol (ATL) and timolol (TML) are effective against a variety of hypertensive disorders, ischemic heart disease, some arrhythmias and ocular hypertensive effects (Shargel et al., 1997).

Diuretics produce additive antihypertensive effects when co-administered with β-adrenergic receptor antagonists (Safran et al., 1993). Thus, ECA delivered together with a β-adrenergic receptor antagonists, can act synergistically to lower elevated IOP, since these two classes of drug work via different physiological mechanisms. To overcome the unsuitable physicochemical properties of ECA for ocular delivery and to utilize the synergistic interaction between ECA and β-adrenergic receptor antagonists, codrugs of ECA with ATL and TML have been synthesized and evaluated (Fig. 1.9).

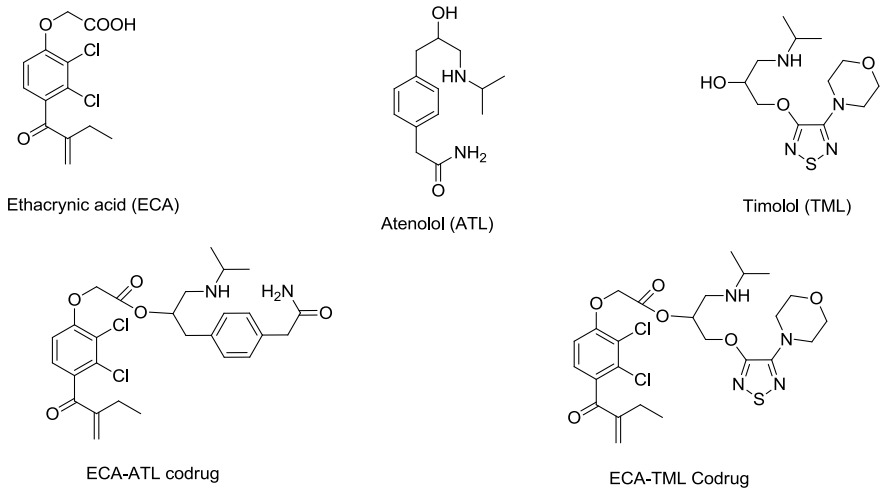

Fig. 1.9: Ethacrynic acid-β-adrenergic receptor antagonist codrugs.

ECA was coupled with ATL and TML through an ester linkage using 1,1-carbonyldiimidazole (CDI) as the coupling reagent. The stability of the ECA-ATL codrug was studied in non-enzymatic aqueous buffer at pH 7.4 and enzymatic hydrolysis was studied using human serum. The codrug was hydrolyzed in both buffer (half life =14 h) and human serum (half life = 30 min) to produce the parent drugs. The stability study confirmed that biotransformation of the codrug would occur after penetration into the vitreous. The main target behind the codrug approach was to overcome the solubility and clearance problems associated with the parent drugs, and thus improve the delivery of the parent drugs through topical membranes.

1.5.4 Codrugs for Transdermal Delivery

Many currently available drugs do not have suitable physicochemical properties for transdermal delivery. For a drug to permeate across the skin, it must be able to partition into and diffuse across the lipophilic region of stratum corneum, and also the more hydrophilic underlying epidermis. Many different strategies have been utilized to enhance topical drug delivery. One of these startegies is to chemically modify the structure of the penetrant. Prodrug and codrug approaches to drug delivery come under this category.

Codrugs for the treatment of alcohol abuse and tobacco dependence

Naltrexone (NTX) is an opioid antagonist and useful drug for the treatment of alcohol dependence (Volpicelli et al., 1992) and cigarette smoking is known to be a social cue for alcoholics. Many alcoholics are also chronic smokers. Naltrexol (NTXOL) is the active metabolite of NTX (Rukstalis et al, 2000; Wang et al., 2001). Currently NTX is used in the form of an oral tablet for the treatment of the above-mentioned morbidities. It has been shown that alcohol dependence can be reduced by 50% in adult alcoholics after administering NTX orally (Volpicelli et al., 1997). However, there are adverse g.i. side effects associated with NTX oral therapy, such as abdominal pain, constipation, nausea and vomiting. NTX is also a hepatotoxin, having the ability to cause dose-related hepatocellular injury. Due to this hepatotoxicity, dosage cannot be increased above 50 mg/day, and patients who need a dosage regimen of more than 50 mg/day cannot benefit from oral NTX therapy. In addition to these adverse effects, in humans, NTX undergoes extensive first pass metabolism, which reduces the oral bioavailability of NTX to about 5-40% (PDR Generics, 1996). Thus, these adverse effects, along with the low bioavailability limit the clinical utility of oral NTX therapy and poor patient compliance is observed. Neither NTX nor NTXOL is deliverable in therapeutic concentrations via the transdermal route (Kiptoo et al., 2006). A codrug approach was applied to attempt to solve these problems. Hydroxybupropion (BUPOH) is the active metabolite of the orally active smoking cessation agent, bupropion (Zyban) (Cooper et al, 1994; Ascher er at.,

1995; Sanchez and Hyttel, 1999; Slemmer et al., 2000). A transdermal NTX-BUPOH codrug should have improved transdermal delivery characteristics, lower toxicity, offer patients the freedom from intravenous injections and surgical implantations, and afford better patient compliance. This single codrug entity would have the potential to treat both alcohol and nicotine abusers when delivered transdermally. Fig. 1.10 shows the structure of NTX, NTXOL, BUP, BUPOH and two codrugs of BUPOH covalently linked to either NTX or NTXOL.

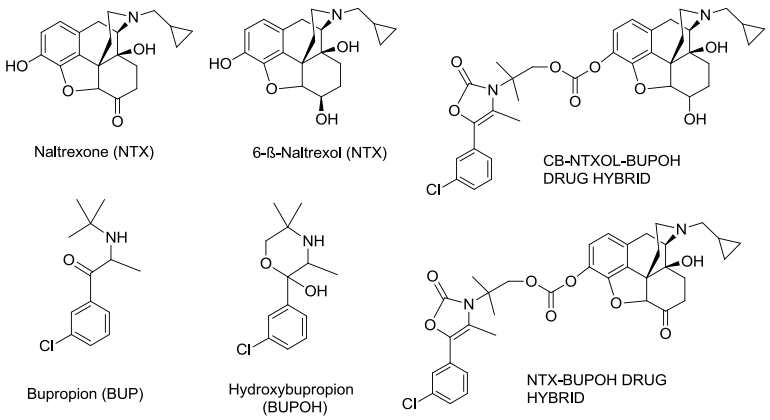

Fig. 1.10: Structures of parent drugs NTX, NTXOL, BUP, BUPOH and codrugs NTX-BUPOH and CB-NTXOL-BUPOH, which contain a cyclic carbamate prodrug moiety of BUPOH.

In order to determine the stability of the codrugs, hydrolytic studies were carried out in isotonic phosphate buffer at pH 7.4 (physiological pH). The results showed that the codrugs were susceptible to hydrolysis and produced the parent drugs at physiological pH. NTX, NTXOL and BUPOH were stable in the buffer solution and NTX-BUPOH and CB-NTXOL-BUPOH codrugs underwent slow hydrolysis in the buffer solution with half-lives of 36.68 and 28.88 h respectively. The proposed hydrolytic conversion of the NTX-BUPOH codrug to the parent drugs is shown in detail in Fig. 1.11. The NTX-BUPOH codrug undergoes cleavage of the carbonate bond to generate NTX, and a relatively stable cyclic carbamate intermediate of BUPOH, which subsequently

undergoes hydrolysis to generate BUPOH. The chemical stability of the NTX-BUPOH codrug was studied in isotonic phosphate buffer at pH 7.4 over 4 days. The disappearance of the codrug and the appearance of the two parent drugs over time are shown in Fig. 1.12. The rate of appearance of NTX was identical to the rate of disappearance of the codrug. However, the rate of formation of BUPOH was found to be slower than the rate of disappearance of the codrug, involving the formation of a relatively stable intermediate, which was identified as the 5-membered cyclic carbamate analogue of BUPOH (Hamad et al., 2006).

The stability of the carbonate codrug of 6-β-naltrexol and hydroxybupropion (CB-NTXOL-BUPOH) was also evaluated in Guinea pig plasma. Fig. 1.13 illustrates the hydrolytic profile of the carbonate codrug and the time course of formation of the two active parent drugs in the plasma. The release of 6-β-naltrexol from the codrug was a one-step process, as confirmed by the rate of appearance of 6-β-naltrexol correlating with the rate of disappearance of the carbonate codrug. The release of BUPOH involved the initial formation of the cyclic carbamate analogue of BUPOH, which was then converted subsequently to the parent drug, BUPOH. The rate of hydrolysis of the CB-NTXOL-BUPOH codrug in plasma was 3 times faster compared to the rate of hydrolysis in isotonic phosphate buffer at pH 7.4 (Kiptoo et al., 2008).

The CB-NTXOL-BUPOH codrug and 6-β-naltrexol were administered transdermally to hairless Guinea pigs. The plasma concentration profiles of the analytes following topical application of either CB-NTXOL-BUPOH or 6-β-naltrexol are shown in Fig. 1.14. The results showed a fivefold enhancement in the transdermal delivery of 6-β-naltrexol when given in the form of the codrug. Also, the codrug delivered a significant amount of BUPOH to the plasma when administered transdermally. The cyclic carbamate intermediate of BUPOH was not detected in the plasma of codrug-treated Guinea pigs. The calculated pharmacokinetic parameters for the CB-NTXOL-BUPOH codrug and 6-β-naltrexol are listed in Table 1.1 (Kiptoo et al., 2008).

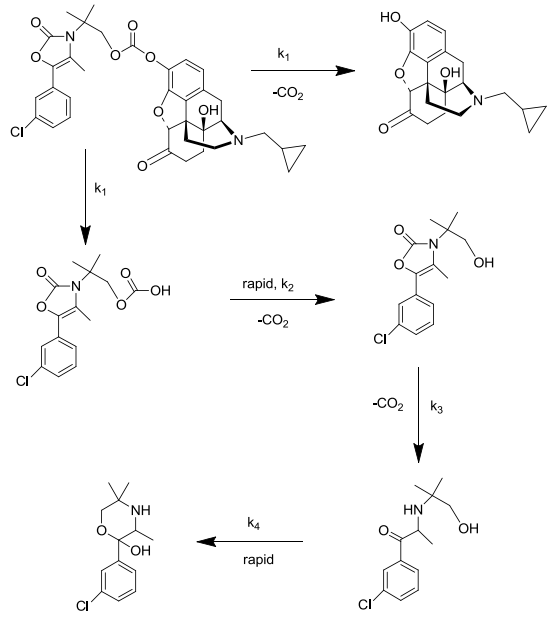

Fig. 1.11: Hydrolytic behavior of the NTX-BUPOH codrug.

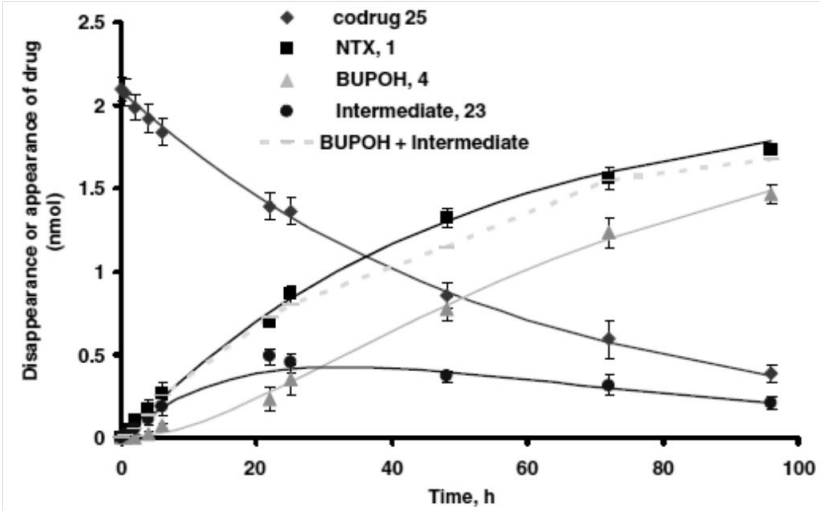

Fig 1.12: Hydrolysis profile of the carbonate drug hybrid, NTX-BUPOH, in isotonic phosphate buffer at pH 7.4 (Reprinted from Journal of Bioorganic and Medicinal Chemistry Hamad et al., 2006, copyrighted by Elsevier, used by permission).

Table 1.1: Pharmacokinetic parameters of NTXOL in the Guinea pig after application of a gel formulation containing either CB-NTXOL-BUPOH or NTXOL base (Reprinted from European Journal of Pharmaceutical Sciences, Kiptoo et al., 2008, copyrighted by Elsevier, used by permission).

Parameter	NTXOL	NTXOL from CB-NTXOL-BUPOH
AUC_{0-48} (ng/ml h)	66.4 ± 7.9	282.0 ± 14.5
C_{max} (ng/ml)	1.5 ± 0.2	6.6 ± 0.4
T_{max} (h)	28.1 ± 1.5	10.1 ± 0.9
T_{lag} (h)	5.1 ± 0.7	5.0 ± 1.1
Observed C_{SS} (ng/ml)	1.3 ± 0.5	6.4 ± 0.9
Predicted C_{SS} (ng/ml)[a]	0.2 ± 0.1	0.7 ± 0.3
Enhancement factor	1	5.3

Data is represented as mean ± S.D. $n = 5$ for NTXOL and $n = 6$ for CB-NTXOL-BUPOH.

[a] Predicted from *in vitro* human skin diffusion data.

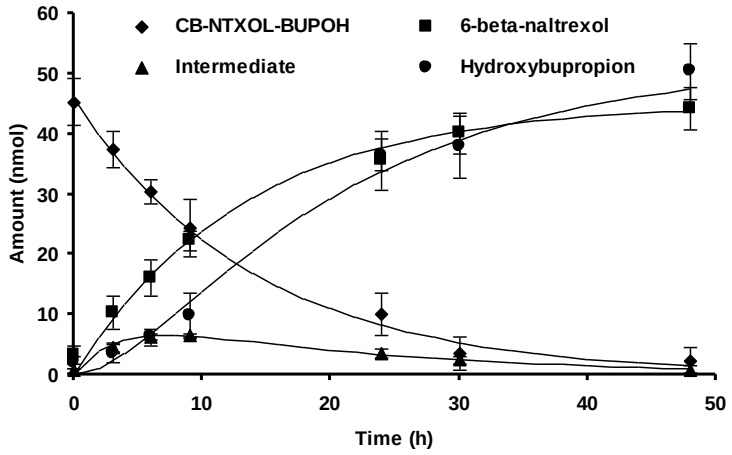

Fig 1.13: Hydrolysis profile of the carbonate drug hybrid, CB-NTXOL-BUPOH, in Guinea Pig Plasma at 37 °C (Reprinted from European Journal of Pharmaceutical Sciences, Kiptoo et al., 2008, copyrighted by Elsevier, used by permission).

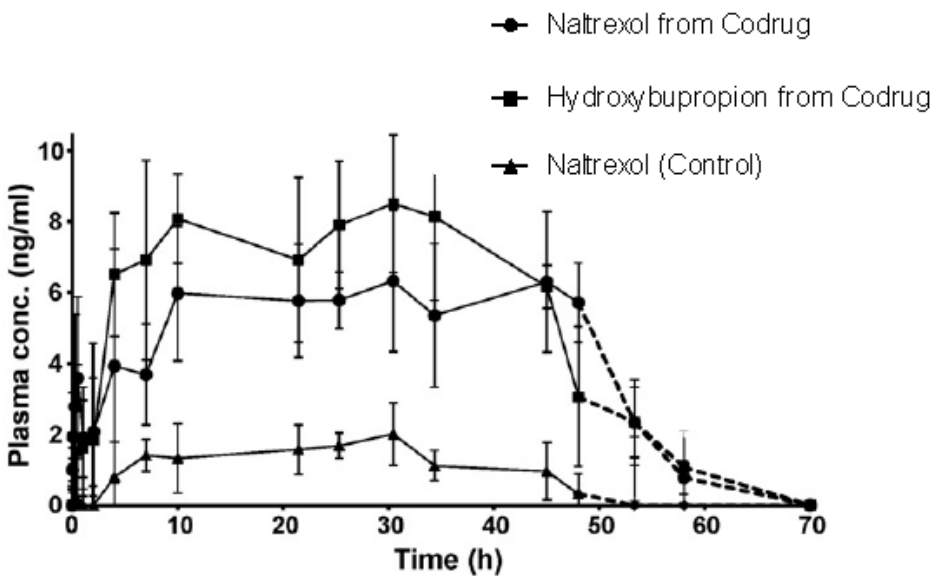

Fig 1.14: Mean (±S.D.) plasma concentration profiles in guinea pigs after topical application of a gel formulation containing either CB-NTXOL-BUPOH or 6-β-Naltrexol (control). The dotted line (----) indicates the plasma concentration after the removal of the formulation (Reprinted from European Journal of Pharmaceutical Sciences, Kiptoo et al., 2008, copyrighted by Elsevier, used by permission).

Duplex codrugs of naltrexone for transdermal delivery

The problem of dealing with a released linker moiety was partially solved in the study of an NTX "Gemini", or duplex codrug. Although the transdermal patch provides a sustained release of drug, NTX does not have the ideal physicochemical properties that allow delivery of therapeutic doses of the drug across the skin. Stinchcomb et al. addressed this problem in a recent study of transdermal delivery of NTX (Hammell et al., 2004). A synthetic dimer of NTX termed a "duplex gemini prodrug" (NTX-NTX) (Fig. 1.15) was synthesized, and then evaluated in *in vitro* diffusion studies utilizing human cadaver skin samples.

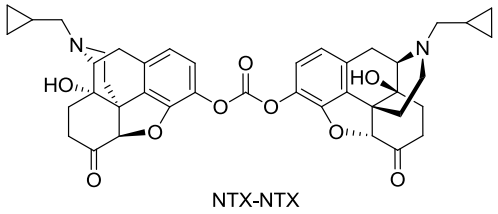

Fig. 1.15: Duplex gemini prodrug of NTX.

It was observed that NTX-NTX was hydrolyzed in the skin to afford two equivalents of NTX and one equivalent of harmless carbon dioxide (half-life = 31 min), and appeared primarily as NTX in the receiver solution of an in vitro Franz cell. It was also observed that the maximum flux from the duplex drug, in terms of NTX equivalents, was twice as high as that from NTX alone (6.2 and 3.0 nmol/cm^2/hr from the duplex codrug and NTX, respectively). According to the authors, the main reason for the increased flux from the NTX-NTX duplex was due to rapid bioconversion causing a difference in the concentration gradient profile for the NTX-NTX codrug.

Codrugs containing α-tocopherol for skin hydration

Proper hydration conditions of human skin are maintained by natural moisturizing factors, which contain different amino acids, pyroglutamic acid and some other water-soluble molecules (Morganti, 1999). Water retention inside the stratum corneum is maintained by fatty acids and cholesterol present on the skin surface. α-Tocopherol (VE) is one of the lipophilic antioxidants and carries out several important functions in the skin. Some of the important properties of VE are listed below.

- VE along, with ascorbic acid, form an antioxidant network in the skin to protect the skin from oxidative damage (Thiele et al., 2000)
- VE also protects polyunsaturated fatty acids (PUFA) and biological membranes against attack by free radicals that initiate lipid peroxidation

- Biological membranes containing high levels of PUFA are protected against oxidizing radicals by VE as it penetrates into the lipid bi-layers and acts as a radical scavenger

- VE functions as a moisturizer by reducing *trans*-epidermal water loss

Although possessing many useful properties, the VE molecule has some disadvantages. It is very readily degraded by oxidants, moisture, and UV irradiation. The stability of VE towards oxidation is generally increased by converting it to either an acetate or succinate ester (Henegouwen et al., 1995; Lampen et al, 2003; Gensler et al., 1996). However, during this process the bioavailability of VE becomes dependent on the enzyme-catalyzed hydrolysis of the ester linkage. Bearing in mind that amino acids are components of natural moisturizing factors, Santi et al. synthesized ester codrugs of VE with amino acids such as alanine and glycine (Fig. 1.16) (Ostacolo et al., 2004).

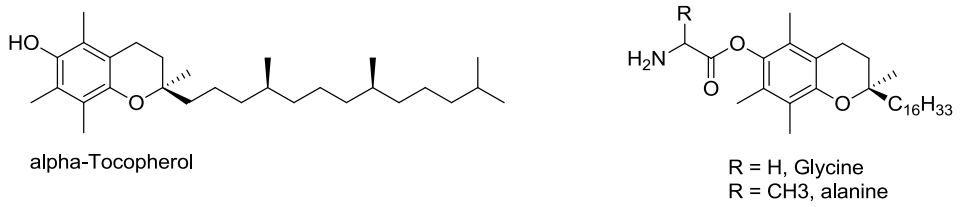

Fig. 1.16: Structures of α-tocopherol and α-tocopherol-amino acid codrugs.

As VE is the main active moiety in the codrug, the ester linkage should be cleavable by hydrolytic enzymes to produce the parent compounds. Porcine liver esterase was used to examine the stability of the ester bond between VE and various amino acids; these molecules can also be regarded as prodrugs. Under the experimental conditions utilized, the codrug concentration decayed exponentially, and the concentration of the parent compound (VE) increased exponentially. The experimentally determined half-lives of the glycine and alanine codrugs of VE were 49.5 and 142 hours, respectively. Skin accumulation and metabolism experiments were performed on freshly excised rabbit ear skin that is considered to be similar to human skin in terms of drug permeability. The

extent of metabolism for the glycine codrug was higher than that of the alanine codrug, a trend that was followed in the in vitro stability of the two codrugs. Experiments also showed that the alanine and glycine codrugs accumulated in skin in significant concentrations. The amount of VE found in the dermis after 6 hours was almost double compared to the amount in dermis when VE was administered alone.

1.5.5 Codrugs of L-DOPA for the Treatment of Parkinson's Disease

L-DOPA Codrugs that incorporate inhibitors of L-DOPA metabolism

Dopamine is deficient in the brains of patients suffering from Parkinson's disease. Unfortunately, dopamine cannot be given as a drug for this disease because it cannot cross the blood-brain barrier. L-3,4-Dihydroxyphenylalanine (L-DOPA) is a precursor of dopamine, and is used in the treatment of Parkinson's disease. L-DOPA crosses the blood-brain barrier via facilitated transport, and is then converted to dopamine in the brain by the enzyme DOPA decarboxylase. For the treatment of Parkinson's disease, L-DOPA is given in combination with a peripheral DOPA decarboxylase inhibitor such as carbidopa, to prevent degradation of L-DOPA in the systemic circulation. Entacapone is a catechol-O-methyltransferase (COMT) inhibitor, which is also currently used with L-DOPA to treat Parkinson patients; entacapone inhibits the metabolism of L-DOPA by COMT to afford the inactive O-methylated metabolite. Since oral L-DOPA bioavailability is low, a codrug approach was utilized, by combining L-DOPA and entacapone via an ester linkage to improve L-DOPA brain delivery (Fig. 1.17). The codrug showed stability in aqueous media at different pHs and was hydrolysed to the parent drugs in liver homogenate, fulfilling the codrug criteria (Leppanen et al., 2002).

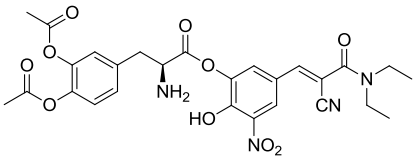

Fig.1.17: L-DOPA-entacapone codrug.

Similar to carbidopa, benserazide is a DOPA-decarboxylase inhibitor. An L-DOPA codrug that incorporates benserazide was demonstrated to have good lipophilicity as compared to either L-DOPA or benserazide (Fig. 1.18). The codrug was also stable in aqueous buffer solutions. In plasma, the catechol esters and amide bonds in the codrug structure were efficiently cleaved, releasing the parent drugs in one step (Stefano et al., 2006 [1]).

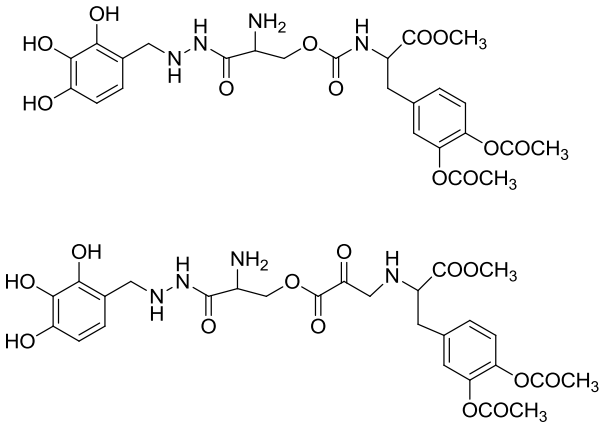

Fig. 1.18: Codrugs of L-DOPA with benserazide.

L-DOPA-antioxidant codrugs

A series of codrugs have also been designed by linking L-DOPA and dopamine with antioxidant compounds such as α-lipoic acid, glutathione, caffeic acid, carnosine,

benserazide and *N*-acetylcysteine (Stefano et al., 2006 [2]; Stefano et al., 2007; Piera et al., 2008; Stefano et al.; 2006 [3], Pinnen et al., 2009).

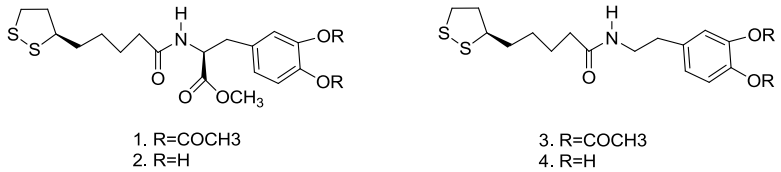

(a) (b)

Fig. 1.19: (a) L-DOPA and α-lipoic acid codrugs; and (b) dopamine and α-lipoic acid codrugs.

As shown in Fig.1.19, L-DOPA and dopamine can be conjugated directly to α-lipoic acid via an amide linkage (Stefano et al., 2006 [2]). α-Lipoic acid is an effective antioxidant. It exists as dihydrolipoate *in vivo*, which can regenerate (reduce) antioxidants such as glutathione, vitamin C and vitamin E (Biewenga et al., 1997; Packer at al., 1995). The strained 5-membered ring conformation of lipoic acid contributes to its good scavenging activity (Haenen and Bast, 1991). All the four codrugs in Fig. 1.19 showed good stability in the gastrointestinal tract and are cleaved enzymatically in rat and human plasma to release the parent drugs. The prolonged release of L-DOPA showed the effectiveness of the L-DOPA codrugs. Codrugs 1 and 2 were used to test antioxidant efficacy using superoxide dismutase (SOD) and glutathione peroxidase (GPx) markers. These enzymes have a central role in the control of reactive oxygen species (ROS). SOD dismutates highly reactive superoxide into oxygen and hydrogen peroxide, and GPx reduces hydrogen peroxide to water by oxidizing GSH. The oxidized form of GSH (GSSG) is reduced back to GSH by glutathione reductase, as shown in the equations below:

$$H_2O_2 + 2GSH \longrightarrow GSSG + 2H_2O$$

$$GSSG + NADPH + H^+ \longrightarrow 2GSH + NADP^+$$

Codrugs 1 and 2 afforded an increase in GPx activity as compared to L-DOPA alone, which indicating a decreased production of free radicals. Also, these codrugs induced a decrease in the activity of SOD as compared to L-DOPA alone, indicating a reduced production of superoxide anions.

Similar results were obtained when codrugs of L-DOPA and glutathione were constructed with amide linkages joining the two drug entities (Fig. 1.20) (Stefano et al., 2007). Glutathione is involved in the decomposition of toxic peroxide molecules, and protects enzymes by maintaining their SH groups in a reduced state; it is also involved in the repair of oxidized iron-sulfur centers of the mitochondrial complex. No hydrolysis of the glutathione-L-DOPA codrugs was observed in gastrointestinal fluids and L-DOPA was shown to be released in plasma via enzymatic hydrolysis. The codrugs also exhibited an antioxidant effect as indicated using SOD and GPx markers.

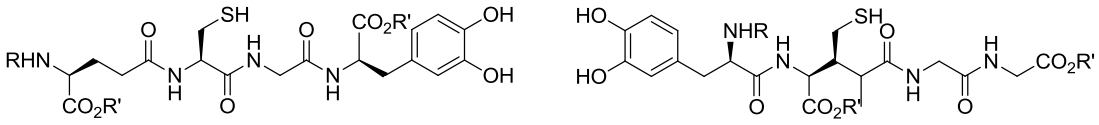

(a) (b)

Fig. 1.20: (a) L-DOPA and glutathione codrugs; and (b) dopamine and glutathione codrugs.

Like glutathione and α-lipoic acid, two other antioxidants, caffeic acid and carnosine, have also been conjugated with L-DOPA (Fig. 1.21), and the resulting codrugs assessed by evaluating plasma activities utilizing SOD and GPx markers in rats (Piera et al., 2008). These codrugs were devoid of significant antioxidant activity, although the literature lists many reports that caffeic acid and carnosine act as natural antioxidants with hydroxyl radical-scavenging and lipid-peroxidase activities.

To overcome the pro-oxidant effects of L-DOPA, other antioxidants utilized in L-DOPA codrug design were sulfur containing compounds, such as *N*-acetyl cysteine (NAC), methionine and bucillamine (Fig. 1.22). *N*-Acetylation of cysteine speeds up cysteine absorption and distribution when given orally. NAC helps in increasing the intracellular concentration of glutathione by elevating intracellular cysteine levels. NAC is rapidly absorbed, enters cells, and is rapidly hydrolyzed to cysteine. Methionine is also an intermediate in the synthesis of cysteine, and helps PC 12 cells against DA–induced nigral cell loss in Parkinson's disease by binding to oxidative metabolites of dopamine (Grinberg et al., 2005; Offen et al., 1996; Martinez et al., 1999). Bucillamine is a synthetic cysteine derivative used for the treatment of rheumatoid arthritis (Horwitz, 2003). It contains two thiol groups, which makes it a more powerful antioxidant as compared to NAC and methionine. It can be easily transported into cells to restore glutathione under conditions of oxidative stress and glutathione depletion (Hammond et al., 2001).

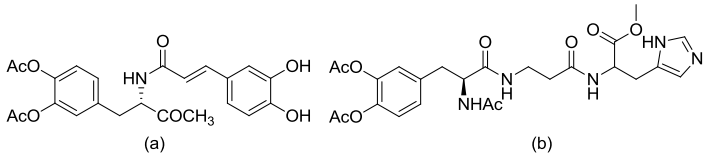

Fig. 1.21: Structures of (a) a 3, 4-diacetyloxy-L-DOPA methyl ester-caffeic acid codrug; and (b) a 3, 4-diacetyloxy-L-DOPA methyl ester–carnosine codrug.

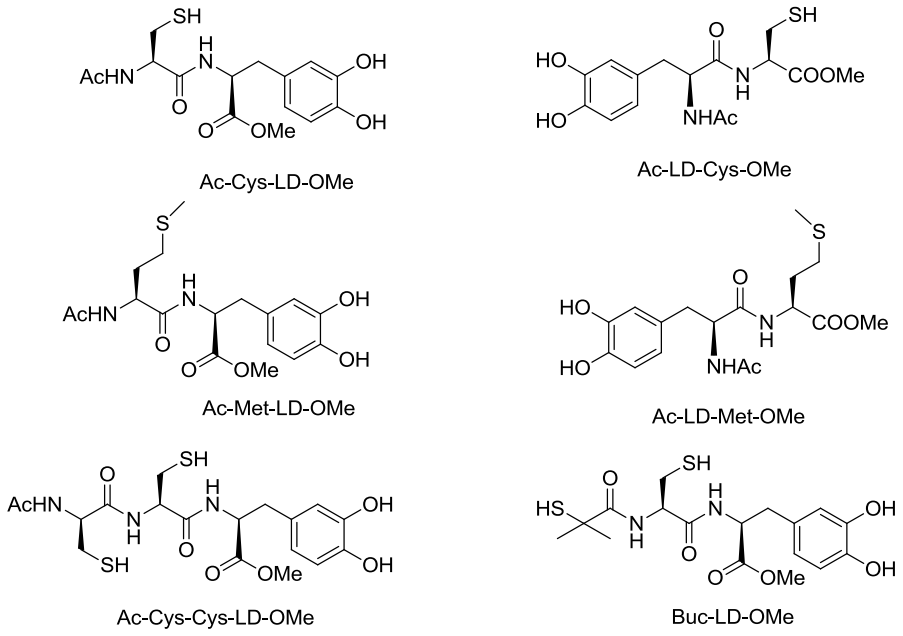

Fig. 1.22: Codrugs of L-DOPA linked to cysteine, methionine and bucillamine.

Six codrugs have constructed using L-DOPA as one of the parent drugs and NAC/methionine/bucillamine as the other parent drug (Pinnen et al., 2009). All the codrugs showed good lipophilicity and water solubility for optimal intestinal absorption. Stability studies at pH 1.3 and in SGF indicated that the codrugs would be stable enough to pass un-hydrolyzed through the stomach mucosa after oral administration. At pH 7.4, the codrugs were shown to be stable enough to be absorbed intact from the intestine. In rat and human plasma, the codrugs hydrolyzed to release the parent drugs, although the release of L-DOPA was very slow. The antioxidant efficacy of the codrugs was evaluated using a chemiluminescent assay, and compared with NAC; all the codrugs showed a superior antioxidant effect as compared to NAC. The physicochemical and pharmacokinetic data showed high levels of L-DOPA in the plasma and brain, even 12 h after administration. Ac-Met-LD-OMe and Ac-LD-Met-OMe Codrugs were able to induce a sustained release of L-DOPA and dopamine in rat striatum with respect to an equimolar dose of L-DOPA. When Ac-LD-Met-OMe codrug was injected intracerebroventricularly, it afforded levels of dopamine in the striatum that were higher

than those in L-DOPA-treated rats, and indicated that the codrug had a longer half-life in brain than L-DOPA (Pinnen et al., 2009).

1.5.6 Analgesic Codrugs Containing Non-steroidal Anti-inflammatory Agents

The clinical usefulness of non-steroidal anti-inflammatory drugs (NSAIDs) has been documented for decades, and these drugs constitute a mainstay in the treatment of rheumatic disorders and other degenerative and inflammatory joint diseases, in sports medicine, and as a multipurpose pain killer. However, NSAIDs containing carboxylic acids are known to have g.i. toxicity, causing upper g.i. irritation, bleeding, ulceration, and perforation, due to the presence of a free carboxylic acid group, and due to local inhibition of the cytoprotective actions of prostaglandins on gastric mucosa. In addition, NSAIDs may have an indirect effect attributed to their ion-trapping properties. One common way to solve the g.i toxicity problem is to design ester prodrugs of NSAIDs by masking the carboxylic acid group in the molecule. A recent and more effective approach is the design of codrugs of NSAIDs with another drug molecule by forming an ester linkage with the carboxylic acid group of the NSAID.

Flurbiprofen-histamine-H_2 antagonist codrugs

The first codrug of this category was synthesized and examined by Otagiri et al. (Otagiri and Fukuhara, 1999). Flurbiprofen (FP) was chosen as a model NSAID and linked to an anti-ulcer histamine H_2-antagonist agent to reduce the gastric mucosal damage caused by the NSAID. *N*-[3-{3-(1-Piperidinylmethyl)phenoxy}propyl]-2-(2-hydroxyethylthio)acetamide (PPA) was chosen as the histamine-H_2 antagonist (Fig. 1.23). The FP-PPA codrug showed high hydrophilicity and lipophilicity, suggesting that the codrug would not have an adverse effect on FP absorption. The codrug was also stable in the aqueous buffers over the pH range 1-7.4, and was also stable in the presence of the enzymes pepsin and trypsin. The codrug rapidly hydrolyzed in 10% plasma (half-life = 35 s). The pharmacokinetic results showed that the codrug was nearly completely absorbed into systemic circulation after oral delivery, and was sufficiently hydrolyzed to produce both the parent drugs. The acute anti-inflammatory effects of both the FP-PPA

codrug and parent drug (FP) were analyzed by measurement of the inhibition of carrageenan-induced edema. No difference was observed when the inhibitory effects of FP and the FP-PPA codrugs were compared, demonstrating that the codrug had the same anti-inflammatory effect as FP. Pharmacokinetic data in rats also supported this result. However, experimental data showed the occurrence of gastric damage after FP administration; and when PPA was co-administered with FP as a physical mixture the gastric damage by FP was not reduced. On the other hand, while the FP-PPA codrug inhibited ulcer formation induced by FP, the codrug was effective in reducing the gastric damage caused by FP alone, and this was attributed to the masking of the carboxylic acid group of FP by linking it to the histamine-H_2 antagonist, PPA.

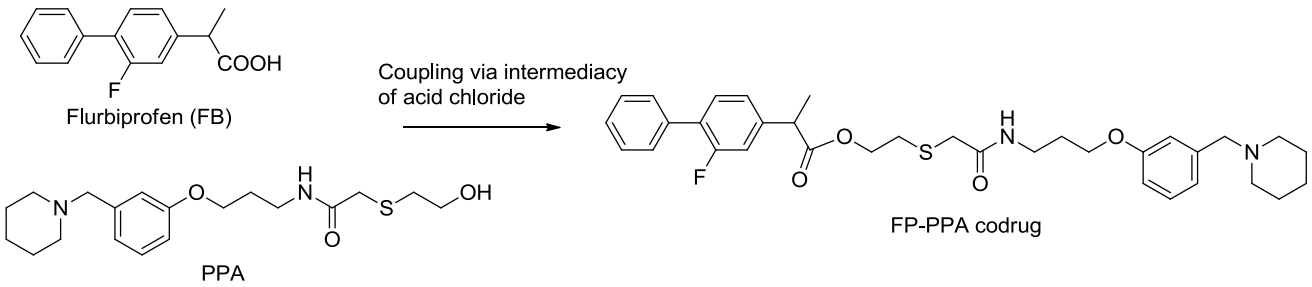

Fig. 1.23: Codrug of Flurbiprofen and PPA.

NSAID-acetaminophen codrugs

In another approach, Omar et al. utilized a well-known analgesic, acetaminophen, to mask the carboxylic acid group of NSAIDs (Fig. 1.24) (Fadl and Omar, 1998). Although, acetaminophen is relatively safe at therapeutic doses, large overdoses can produce the toxic metabolite, *N*-acetyl-*p*-benzoquinoneimine (NAPQI). Codrugs of acetaminophen with NSAIDs would reduce the g.i. adverse effects of NSAIDs and could also reduce formation of the toxic metabolite NAPQI from acetaminophen. A series of ester-linked codrugs of acetaminophen with NSAIDs were synthesized and evaluated, and the stability of these codrugs was examined at pH 1.3 and 7.4 in non-enzymatic aqueous buffers, and 80% human plasma. Result showed appreciable stability of the codrugs in both non-enzymatic simulated gastric fluid (pH 1.3) (half-life = 6.7-43 h) and

in non-enzymatic simulated intestinal fluid (pH 7.4) (half-life = 1.5-25 h). The codrugs exhibited much shorter half-lives in human plasma (half-life = 13.9-38.4 min) and in rat liver homogenate (half-life = 12.6-42.9 min). From the hydrolytic study it was found that the susceptibility of the codrugs to enzymatic hydrolysis was dependent upon the type of NSAID covalently linked to the acetaminophen molecule. The aspirin-acetaminophen codrug having the smallest acyl moiety, was found to be the most susceptible to enzymatic degradation. Codrugs with bulkier acyl moieties were found to be least susceptible to enzymatic hydrolysis. Based on in vitro data, the codrug of ibuprofen and acetaminophen was selected for bioavailability studies. No appreciable concentration of the codrug was detected in plasma after oral administration of the codrug, confirming very fast hydrolysis of the ester linkage in vivo compared to in vitro hydrolysis. Over a 24 time course, the ibuprofen-acetaminophen codrug produced higher concentration of ibuprofen in the plasma compared to a physical mixture of the two parent drugs, indicating a higher bioavailability of the codrug due to improved lipophilicity.

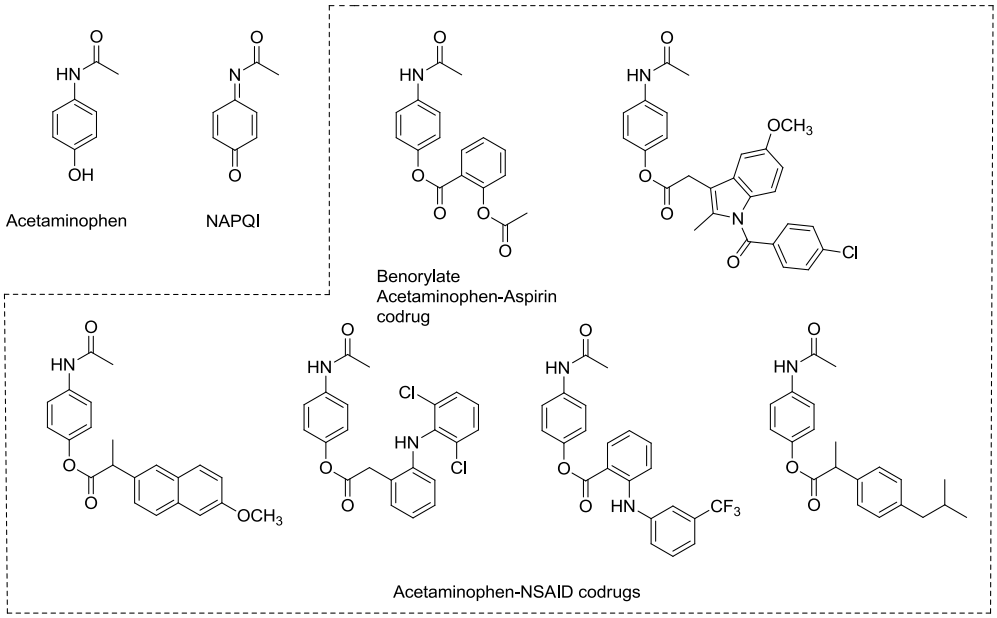

Fig. 1.24: A series of codrugs of acetaminophen and NSAIDs.

A codrug of diclofenac and acetaminophen was chosen for an ulcerogenicity study, and was compared with an equivalent physical mixture of the two parent drugs. Mice treated with a physical mixture of the two drugs showed significant damage of the mucous layer and ulceration of submucosal cells. However, mice treated chronically with the corresponding codrug did not show any significant gastric mucosal injury. The analgesic activities of the codrugs and the corresponding physical mixtures were analyzed using the mouse hot-plate assay. The results showed a significant increase in the analgesic activity of the codrug over time, compared to the physical mixture of the parent drugs. All the synthesized codrugs showed significantly higher analgesic activity than the control groups (equivalent physical mixture of parent drugs).

Naproxen-propyphenazone codrugs

In another study aimed at suppressing the g.i. toxicity of NSAIDs without affecting their anti-inflammatory activity, codrugs of naproxen (NAP) and propyphenazone were synthesized and evaluated (Fig. 1.25) (Shehaa et al., 2002). NAP is a potent carboxylic acid-containing NSAID, and has moderate analgesic activity associated with g.i. irritation (Shanbhag et al., 1992). Previously reported alkyl ester and thioester prodrugs of NAP showed reduced g.i. erosive properties and similar anti-inflammatory activity but significantly reduced analgesic potency (Venuti et al., 1989). On the other hand, propyphenazone is a non-acidic pyrazole drug with good analgesic and antipyretic activity and no anti-inflammatory activity (Burne, 1986). The metabolism of propyphenazone is known to proceed via the formation of its active metabolite, 3-hydroxymethylpropyphenazone (HMP), which has similar activity as the parent drug (Goromaru et al., 1984; Neugebauer et al., 1997). A NAP-propyphenazone codrug strategy was considered a rational approach to achieving an anti-inflammatory and synergistic analgesic effect with a reduction in g.i. irritation associated with the NSAID. Propyphenazone was first converted to HMP or 3-aminomethylpropyphenazone (AMP). In one of the codrug molecules HMP was directly linked to NAP to afford the NAP-HMP codrug. In the second codrug design, HMP was linked to the endogenous amino acid glycine through an ester linkage, and the free amino group of glycine was then covalently

linked to NAP via an amide bond. In the third codrug molecule, a different linker, glycolic acid, was utilized to link AMP and NAP. Since the carboxylic acid group of NAP is essential for its analgesic activity, the release of NAP from the various codrugs was studied initially in non-enzymatic aqueous buffer solutions at pH 1.2 and 7.4, and in liver homogenates having activated esterase enzymes. Stability studies of the codrugs in aqueous buffers showed significant stability (half-life = 60-91 h at pH 1.2, and 10-19 h at pH 7.4). The codrugs showed a high susceptibility towards hydrolysis in rat liver homogenate (half-life 54-85 min). The analgesic activity of the codrugs compared to equimolar doses of the two parent drugs were tested in the mouse hot-plate assay. As a general trend, the codrugs showed improved analgesic activity over time compared to the parent drugs, reaching a maximum effective dose after about 4-6 hours due to improved codrug bioavailability and efficient hydrolysis to the parent drugs. Comparative anti-inflammatory activity of the codrugs and NAP was determined by measuring the swelling of the paw after intraplantar injection of carrageenan in the rat. The codrug of NAP and HMP linked through glycolic acid also reduced inflammation in a pattern similar to an equimolar dose of NAP. This codrug was analyzed for its ulcerogenic activity and compared to those of the parent drugs, NAP and HMP. The NAP-treated mice, and to some extent the HMP-treated mice, showed complete damage of the mucous layer in addition to ulceration of the sub-mucosal cells of the g.i. tract, while the codrug-treated group and the control group (treated with vehicle only) did not show any ulcerogenic activity.

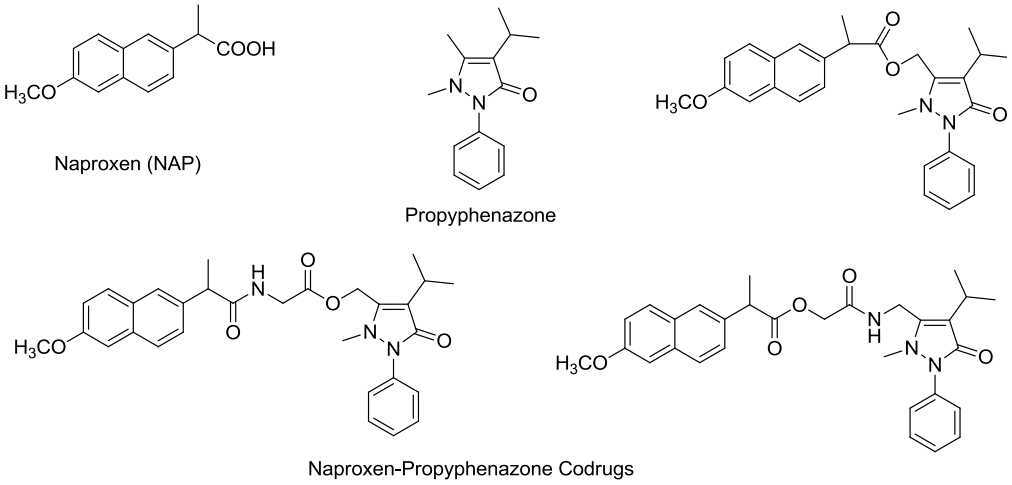

Fig. 1.25: A series of naproxen-propyphenazone codrugs.

Flurbiprofen-amino acid codrugs

In another approach, the adverse G.I. effects of the NSAID, flurbiprofen, were reduced by masking the carboxylic acid group through the formation of an amide bond with a series of amino acids. The anti-inflammatory activity of amino acids against gelatin induced hind paw edema in rats and their healing effects on gastric lesions produced by NSAIDs have been reported in literature (Meyers et al., 1979). Thus, conjugates of flurbiprofen with anti-inflammatory amino acids can clearly be considered as codrugs, since they would produce amino acids as hydrolytic products having synergistic anti-inflammatory effects with NSAIDs, and would also afford g.i. protective effect against NSAIDs. By covalently linking appropriate amino acids to NSAIDs, codrugs with optimal polarity, solubility profile and acid-base properties can be designed. Thus, a series of amide codrugs of flurbiprofen with methyl esters of L-tryptophan, L-histidine, L-phenylalanine, and DL-alanine (Fig. 1.26) were synthesized and evaluated (Gairola et al., 2005). The stability of the codrugs was studied in hydrochloric acid buffer (pH=1.2), phosphate buffer (pH=7.4) and 80% human plasma. The codrugs were found to be stable in hydrochloric acid buffer but underwent hydrolysis in phosphate buffer with half-life values ranging from 30.19 min to 70.09 min. This result suggested that the codrugs were likely to be stable enough to be absorbed intact from the intestine. The

comparatively shorter half-lives of the codrugs in plasma (ranging from 16.2 min to 29.3 min) indicated that rapid production of the parent drugs in the systemic circulation was likely. Results from the evaluation of the anti-inflammatory properties of the codrugs revealed that flurbiprofen-phenylalanine and flurbiprofen-alanine codrugs were superior to flurbiprofen alone; the flurbiprofen-tryptophan and flurbiprofen-histidine codrugs were comparable to flurbiprofen in terms of anti-inflammatory activity.

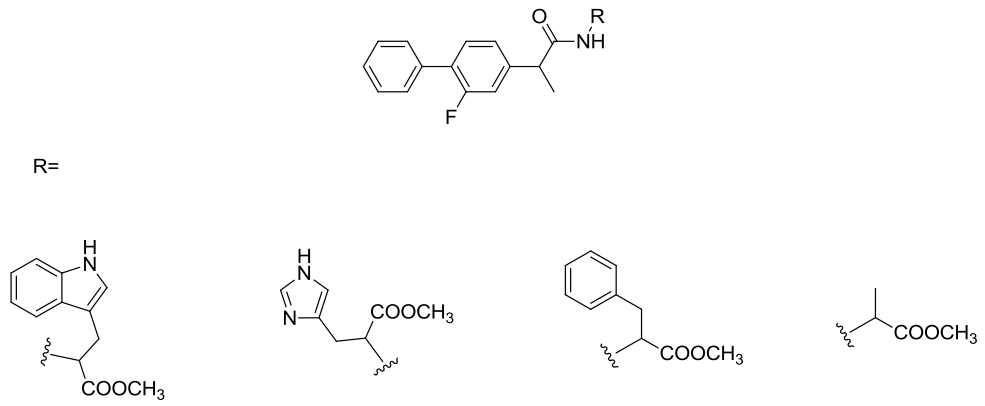

Fig. 1.26: Amino acid codrugs of flurbiprofen.

NSAID-chlorzoxazone codrugs

In a recent study, an active muscle relaxant drug was used to mask the carboxylic acid group of NSAIDs via the formation of a codrug (Abdel-Azeem et al., 2009). Chlorzoxazone is an active muscle relaxant, and is marketed as a single component drug or in combination with NSAIDs. On the basis of these observations, codrugs of chlorzoxazone with three different NSAIDs were synthesized in an attempt to minimize the adverse gastrointestinal effects of NSAIDs, and to improve the pharmacokinetic properties of the parent drugs while retaining anti-inflammatory and skeletal muscle relaxant activities (Fig. 1.27). Chlorzoxazone was first converted to the key intermediate, hydroxymethylchlorzoxazone and then coupled with the carboxylic acid group of the appropriate NSAID to form ester-linked codrugs. Hydrolysis of these codrugs was studied in non-enzymatic aqueous buffers at pH 1.2 and 7.4 and in 80% human plasma.

The hydrolysis data showed that the codrugs were sufficiently stable at pH 1.2 and 7.4 to be absorbed almost unchanged from the g.i. tract. The codrugs showed susceptibility towards hydrolysis in 80% human plasma (half-life = 34-37 min). In the carrageenan-induced paw edema bioassay ibuprofen and the ibuprofen-chlorzoxazone codrug showed the greatest inhibition of inflammation followed by the naproxen-chlorzoxazone and mefenamic acid-chlorzoxazone codrugs. The overall data showed that the codrugs exhibited comparable anti-inflammatory activity to their parent NSAIDs. The muscle relaxant activity of the codrugs in comparison with that of the muscle relaxant chlorzoxazone was examined using rat sciatic nerve tibialis muscle preparation. Muscle relaxant activity was exhibited by all the codrugs, while that of the ibuprofen-chlorzoxazone codrug was comparable with chlorzoxazone. Importantly, the ibuprofen-chlorzoxazone codrug treated animals showed far less damage to the mucous layer of the gastrointestinal tract compared to that produced by ibuprofen alone.

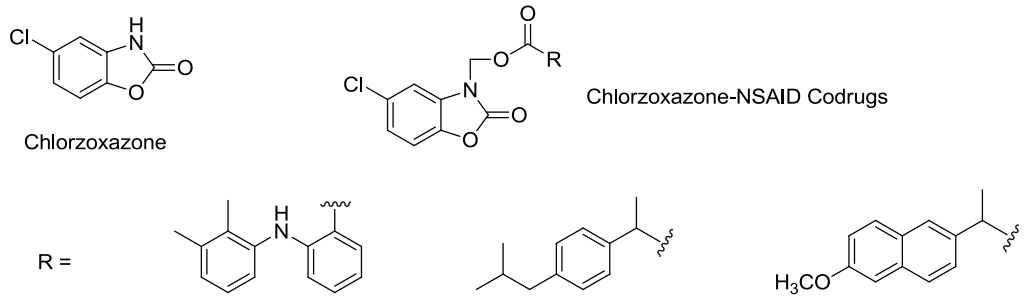

Fig. 1.27: A series of codrugs of chlorozoxazone with NSAIDs.

Acetaminaphen-chlorzoxazone codrug

In a related study, a codrug molecule incorporating chlorzoxazone and acetaminophen has been reported (Fig. 1.28) (Vigroux and Bergon, 1995). The main reason for the synthesis of this codrug was the observed synergistic effects of these two drugs when administered together. The rate of liberation of the parent drugs from this codrug was studied at pH 7.4 in phosphate buffer, and in human and rat plasma. The codrug regenerated chlorzoxazone and acetaminophen simultaneously and quantitatively

under the experimental conditions. The codrug showed a higher susceptibility to formation of parent drugs in phosphate buffer than in either human or rat plasma, indicating that the release of chlorzoxazone from the codrug did not need to be enzyme-mediated.

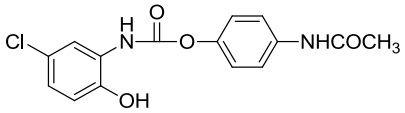

Fig. 1.28: Codrug of chlorozoxazone and acetaminophen.

1.5.7 Analgesic Codrugs of Opioids and Cannabinoids

There is a continuing need for analgesic medications that are able to provide high efficacy pain relief while providing more favorable pharmacokinetics and reducing the possibility of undesirable side effects. Enhancement of the analgesic effect of opioids with cannabinoids has been previously described (Cichewicz et al., 1999). These two classes of drug work via opioid and cannabinoid receptors, which are found throughout the central and peripheral nervous system. Synergy between Δ^9-THC and opioids is well documented in the literature (Bloom and Dewey, 1978; Cichewicz and McCarthy, 2002). In addition, these two classes of drug produce similar effects on calcium levels and cyclic AMP accumulation through G protein-mediated pathways. However, appropriate dosing of these active agents to their site of action, e.g., the brain or spinal column, can be difficult because of their differential pharmacokinetics. A codrug approach can be useful in overcoming the differential physicochemical and pharmacokinetic properties of opioid and cannabinoid drugs. In addition, opioids exert their analgesic effect on nociceptive pain while cannabinoids are effective in modulating neuropathic pain. Thus, an opioid-cannabinoid codrug might be able to cover a broader range of pain. Keeping these points in mind, a series of opioid-cannabinoid codrugs were designed and synthesized and a codrug of codeine and Δ^9-THC (Cod-THC) was fully evaluated in pain models, stability

indicating assays and *in vivo* pharmacokinetic studies (Holtman et al., 2006; Dhooper et al., 2008).

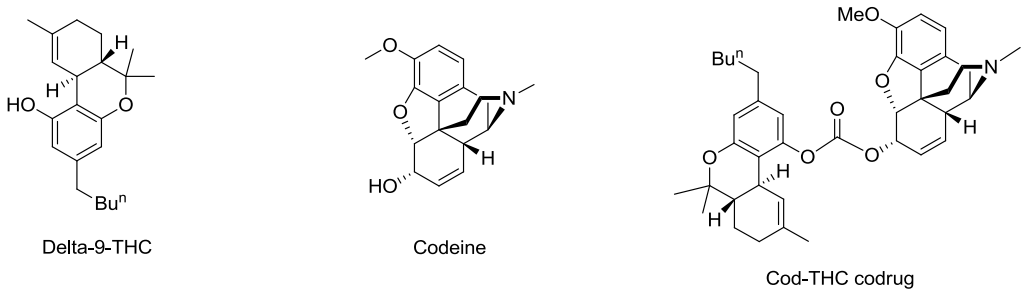

Fig. 1.29: Structures of delta-9-THC, codeine and Cod-THC codrug.

The effect of the Cod-THC codrug after oral administration in nociceptive and neuropathic pain models utilizing tail-flick and chronic constriction injury pain models in the rat was evaluated. The oral efficacies of each of the parent drugs, codeine and Δ^9-THC, were also compared with the Cod-THC codrug as pain modulators in the above pain models to determine their relative effectiveness. In both pain models, the codrug showed improved effectiveness, as well as more prolonged pain management properties, when compared to the parent drugs (Fig. 1.30).

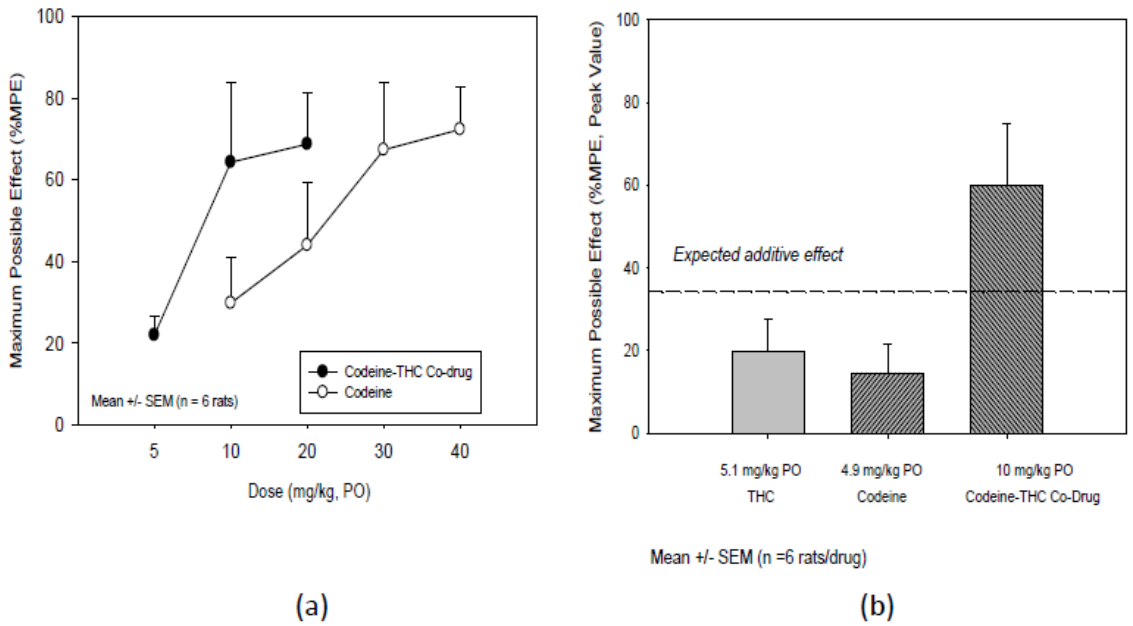

Fig. 1.30: (a) Dose-Response Curves for the Antinociceptive Effects of the Codeine-THC Codrug and Codeine Alone in the Tail-Flick Test. (b) Antihyperalgesic Effect of Codeine, THC and the Cod-THC Codrug in the Chronic Constriction Nerve Injury (CCI) Model.

The Cod-THC codrug was initially evaluated for its stability in buffers ranging from pH 1 to pH 9, as well as in simulated gastric and intestinal fluids (SGF and SIF, respectively), and in rat plasma and brain homogenate. The codrug was found to have a favorable drug stability profile for oral administration, being stable in aqueous solutions over a wide range of physiologically relevant pHs from 1 to 7.4, and was also stable in simulated gastric fluid, simulated intestinal fluid and rat brain homogenate. In rat plasma, the codrug was hydrolyzed to the two parent drugs, codeine and Δ^9-THC with a rate constant of 0.282 hr^{-1} (Fig. 1.31).

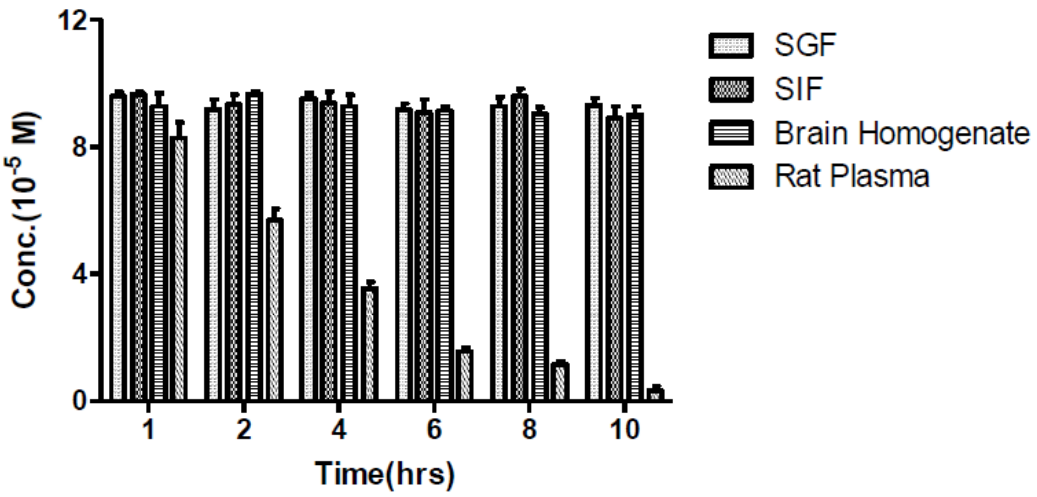

Fig. 1.31: Hydrolysis of the Cod-THC codrug under different enzymatic conditions.

The pharmacokinetic profile of the Cod-THC codrug was evaluated in the rat after oral administration and compared with the pharmacokinetic profile of an equimolar physical mixture of the parent drugs. Several groups have reported low bioavailability of THC (2 to 6%) and codeine (4 to 8%) after oral administration in rats, due to poor absorption from the gastrointestinal tract (Chiang and Barnett, 1984; Shah and Mason, 1990). Rat plasma concentrations of the Cod-THC codrug were determined after oral and i.v. administration. These resulting data were compared with those obtained after oral administration of an equimolar physical mixture of the two parent drugs, codeine and Δ^9-THC. The plasma concentrations of codeine and Δ^9-THC were found to be much higher after oral administration of the codrug in the rat, compared to plasma concentrations of these drugs after oral administration of the equimolar physical mixture of the two parent drugs. The parent drugs were clearly released from the codrug molecule in 1:1 ratio in plasma, while administration of the physical mixture did not afford equimolar concentrations of codeine and Δ^9-THC in the plasma (Fig. 1.32). This is likely due to the different pharmacokinetic profiles of the two parent drugs, and to the different pharmacokinetic profile of the Cod-THC codrug. Also, the parent drugs were present in plasma for a longer period of time after oral administration of codrug, likely due to the sustained release of the parent drugs from the codrug in the plasma.

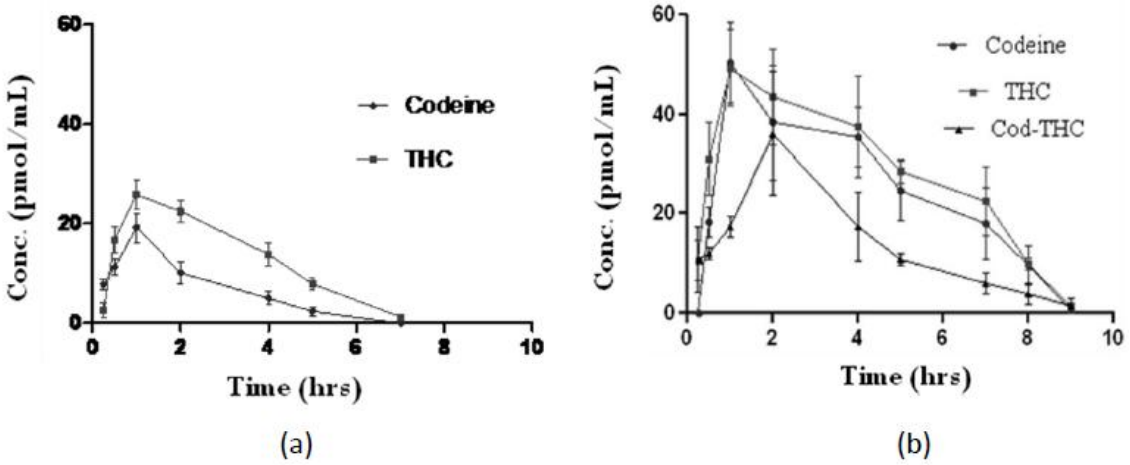

Fig. 1.32: Plasma concentrations of codeine, Δ^9-THC and Cod-THC codrug after administration of physical mixture of codeine, 4.9 mg/kg, and Δ^9-THC, 5.1 mg/kg, (a); and Cod-THC codrug, 10 mg/kg (b).

1.5.8 Codrugs containing Anti-HIV Drugs

The rapid spread of the human immunodeficiency virus (HIV), the etiological agent of acquired immunodeficiency syndrome (AIDS), has stimulated intensive efforts worldwide to develop chemotherapeutic agents effective against HIV. 2',3'-Dideoxynucleosides (ddNs) are one of the most potent series of compounds active against HIV (Mitsuya and Broder, 1986; De Clercq, 1997). The expression of activity of these drugs requires bioconversion into their corresponding 5'-O-triphosphate analogs (Furman et al., 1986, Hao et al., 1988; Balzarini and De Clercq, 1999). The resulting triphosphate analogs may inhibit the replication of the virus by competitive inhibition of viral reverse transcriptase (RT) and/or by incorporation into, and subsequent chain termination of the growing viral DNA strand (Cheng et al., 1987). Six drugs from the ddN family have been marketed: zidovudine (AZT, Retrovir), stavudine (d4T, Zerit), zalcitabine (ddC, Hivid), didanosine (ddI, Videx), lamivudine (3TC, Epivir) and abacavir (1592U89, Ziagen). AZT was the first drug to be approved by FDA (Mitsuya et al., 1985). Some other families of compounds have also been approved by FDA and are now commercially available as anti-HIV therapeutic agents, for example: nucleoside analogs (adefovir, dipivoxil), non-

nucleoside reverse transcriptase inhibitors, also known as NNRTIs (nevirapine), and protease inhibitors (indinavir). AZT is still one of the most effective anti-HIV agents used, although it is the oldest compound approved by FDA. Although AZT therapy has reduced the mortality rate and frequency of opportunistic infections in AIDS patients, it is associated with some adverse effects and unsuitable pharmacokinetic properties. These adverse effects are provided below:

- AZT administration is associated with significant dose-related toxicity leading to anemia and leucopenia (Fischl et al., 1987; Richman et al., 1987)
- Pharmacokinetic studies in phase I trials revealed that the plasma half-life of AZT was only 1 hour (Klecker et al., 1987), requiring frequent administration of AZT to maintain therapeutic plasma concentration of the drug
- Bone marrow toxicity was caused by the high doses of AZT needed to achieve adequate concentrations in cerebrospinal fluid (CSF)
- AZT does not penetrate into brain tissue from the CSF (Terasaki and Pardridge, 1988), and thus causes no suppression of viral replication in the brain

Designing lipophilic prodrugs of AZT is one approach to increase its permeability through plasma membranes and to improve blood-brain barrier permeability. Combination therapy of AZT with other nucleoside derivatives, or certain NNRTIs, or different protease inhibitors, has been found to be more effective than AZT therapy alone (De Clercq, 1995). Based on these observations and the need for improvements in chemotherapeutic agents to treat AIDS, a series of codrugs of AZT has been synthesized and evaluated.

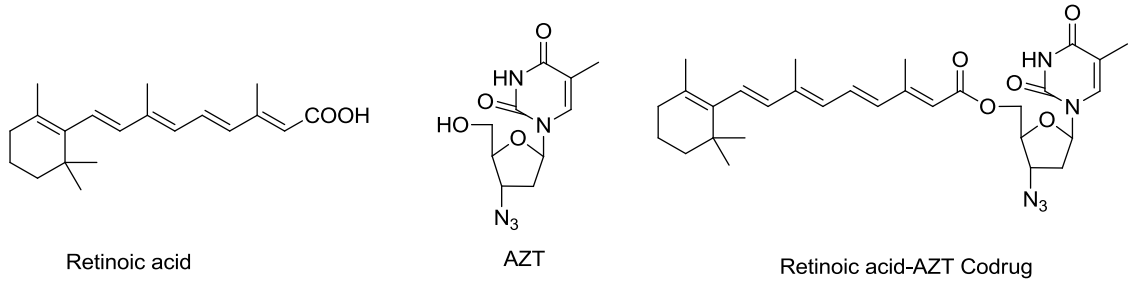

Fig. 1.33: Anti-HIV codrug of AZT.

AZT-retinoic acid codrug

Agrawal et al. synthesized a series of mutual prodrugs of AZT with improved permeability properties to achieve higher concentrations of AZT in the both the central nervous system (CNS) and in targeted HIV-infected cells. Among these was a codrug of retinoic acid and AZT linked through an ester moiety (Fig. 1.33) (Aggarwal et al., 1990). Retinoic acid has previously been shown to inhibit HIV replication. The synthesized AZT-retinoic acid codrug and the parent drug AZT were partitioned between n-octanol and phosphate buffer (0.2 M, pH 7.4) to determine their partition coefficients (PC), and the codrug (PC = 17.9) was found to be more lipophilic than AZT (PC = 1.2). The hydrolysis of the codrug to the parent compounds was examined in phosphate buffer (pH=7.4) and in human plasma. The codrug was found to be stable in phosphate buffer, and the half-life of the codrug was found to be 120 minutes in human plasma. The stability of the codrug was also studied upon incubation with hepatic microsomes isolated from rat. The half-life of the codrug was found to be 60 minutes, indicating relatively rapid and complete microsomal enzymatic hydrolysis to the two parent drugs. The extent of cell membrane permeability of AZT and the retinoic acid-AZT codrug was measured by comparing the uptake of the radiolabeled drugs into H9 cells. The data showed that the uptake of the retinoic acid-AZT codrug in H9 cells was highest among all the synthesized AZT derivatives, and that the uptake the retinoic acid-AZT codrug was 4 times greater than the parent compound, AZT. The anti-viral activity of the retinoic acid-AZT codrug and AZT against HIV-1 was determined in vitro in peripheral blood lymphocytes (PBL) obtained from HIV-seronegative donors. The codrug was found to have similar anti-viral

activity to AZT, although cellular uptake of the codrug was much higher than that of AZT, and this may indicate incomplete cellular hydrolysis of the codrug under in vitro conditions. Although retinoic acid is known to inhibit HIV replication, the codrug did not exhibit synergistic effects, most likely due to only partial release of retinoic acid.

1.5.9 Overall Aim of the Study

The object of the study is to first design and synthesize a series of codrugs combining an opioid drug with either a nicotinic receptor agonist or an NMDA receptor antagonist or an anticonvulsant or a cannabinoid drug, then to study the stabilities of the codrugs in different enzymatic and nonenzymatic conditions and finally to determine the pharmacological and pharmacokinetic profiles of some of the synthesized codrugs.

Copyright © Ujjwal Chakraborty 2012

Chapter 2

Synthesis of Parent Drugs and Codrugs

2.1 Enantioselective Syntheses of *S*-(-)-Nornicotine

For the syntheses of the first series of codrugs containing *S*-(-)-nornicotine and opioids, *S*-(-)-nornicotine was required to be prepared. There are few enantioselective syntheses of *S*-(-)-nornicotine reported in literature. Schemes 2.1 and 2.2 summarize previously reported enantioselective synthetic strategies. As both the synthetic strategies involve several steps and afford only moderate yields, it would be beneficial if the naturally occurring, chirally pure, and inexpensive tobacco alkaloid *S*-(-)-nicotine could be *N*-demethylated without compromising the chirality of the pyrrolidine 2'-carbon, to afford *S*-(-)-nornicotine.

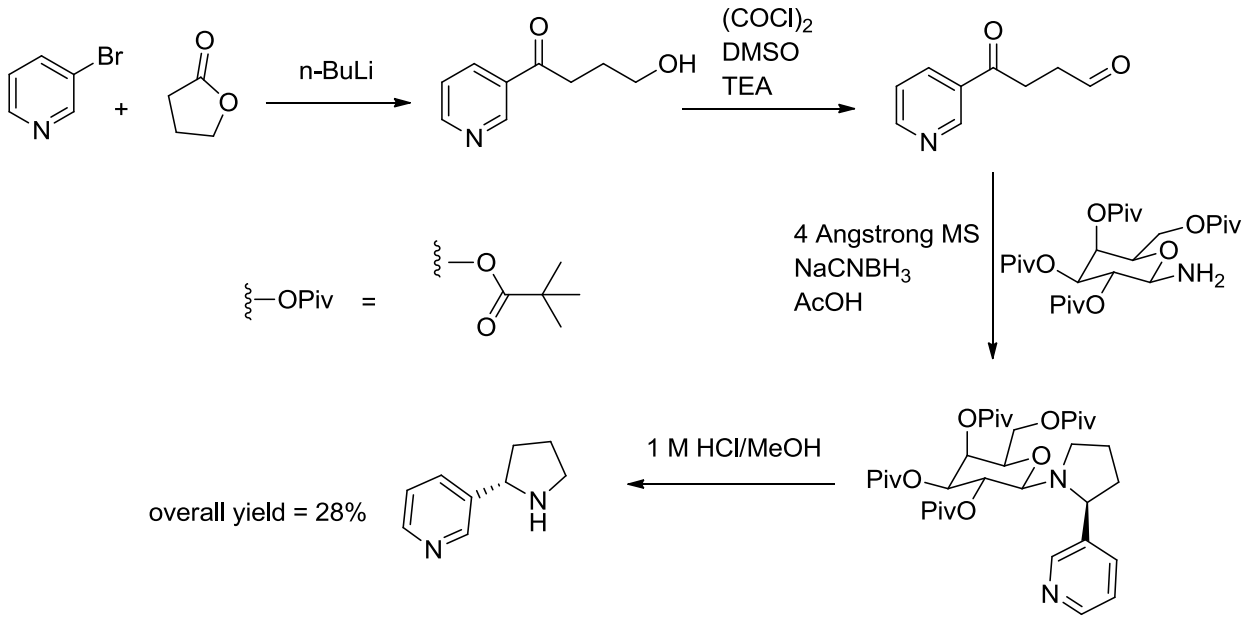

Scheme 2.1: Enantioselective synthesis of *S*-(-)-nornicotine by Loh et al., 1999. The key step in the synthesis involved reductive aminocyclization of a 1,4-ketoaldehyde with

2,3,4,6-tetra-*O*-pivaloyl-β-D-galactosylamine in presence of sodium cyanoborohydride. This step diastereoselectively afforded the desired stereoisomer.

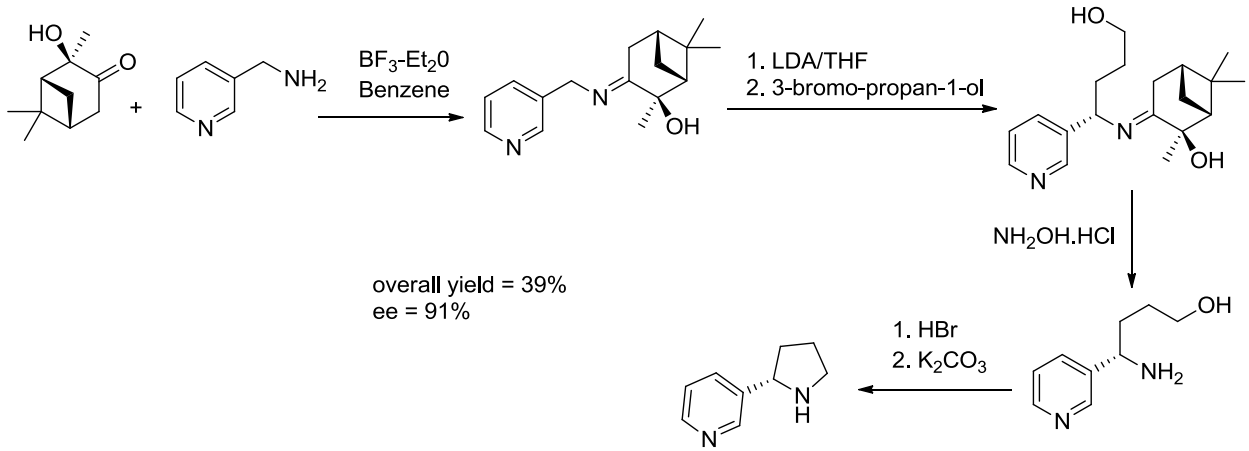

Scheme 2.2: Enantioselective synthesis of *S*-(-)-nornicotine by Swango et al., 1999. The key step in the synthesis involved alkylation of a chiral ketimine with 3-bromopropan-1-ol. In later steps, the ketimine was cleaved followed by base catalyzed intramolecular ring closure.

2.2 *N*-Demethylation of *S*-(-)-Nicotine

A new method was developed for the *N*-demethylation of *S*-(-)-nicotine to afford *S*-(-)-nornicotine. Several oxidative conditions with or without high oxidation state metal oxides are reported in literature for dealkylation purpose (Nehru et al., 2007; McCamley et al., 2003; Rosenau et al., 2004). Based on the literature evidence that metal oxides can be used for *N*-dealkylation reactions, MnO_2 was selected for *N*-demethylation of *S*-(-)-nicotine. *S*-(-)-Nicotine was refluxed in 0.3 N H_2SO_4 in the presence of MnO_2. After work up, *S*-(-)-nornicotine was obtained as an oil in 35% yield (Scheme 2.3).

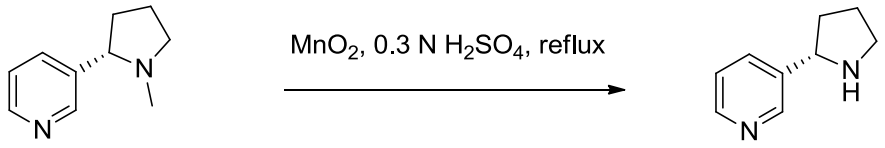

Scheme 2.3: Synthesis of *S*-(-)-nornicotine.

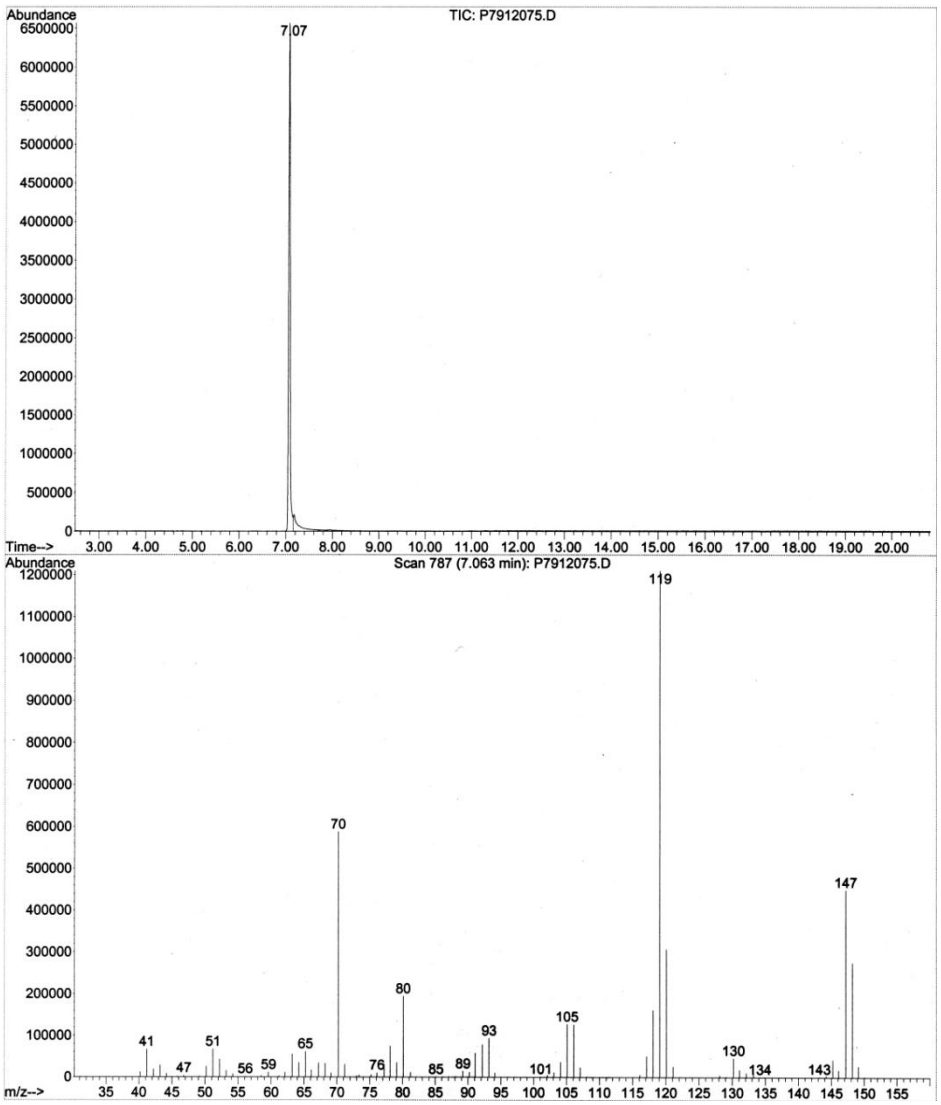

Fig. 2.1: GC-MS of synthesized *S*-(-)-nornicotine.

Chiral analysis of the *S*-(-)-nornicotine product was performed *via* derivatization with (-)-menthyl chloroformate, followed by chiral GC/MS analysis. The GC/MS retention time for the derivatized *S*-(-)-nornicotine (Fig. 2.2) was 9.12 minutes (NOTE: the (-)-menthyl *R*-(+)-nornicotine derivative has a retention time of 9.37 minutes). The compound showed a parent molecular ion (m/z = 329) using electron impact mass spectrometry (Fig. 2.3). The *S*-(-)-nornicotine product was found to have an enantiomeric excess (*ee*) of greater than 99 percent.

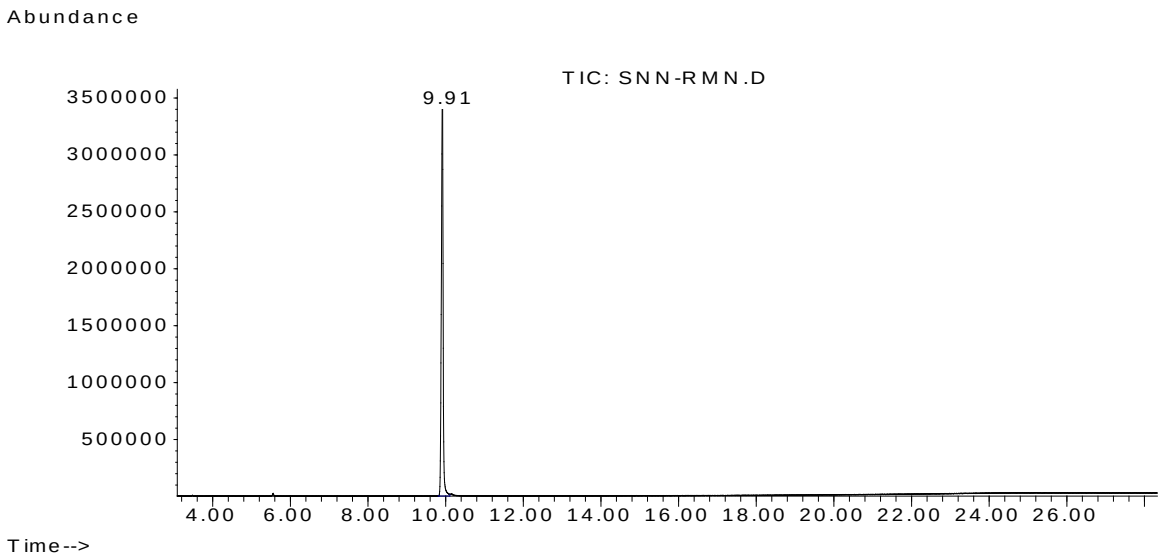

Fig. 2.2: Total ion chromatogram of derivatized *S*-(-)-nornicotine.

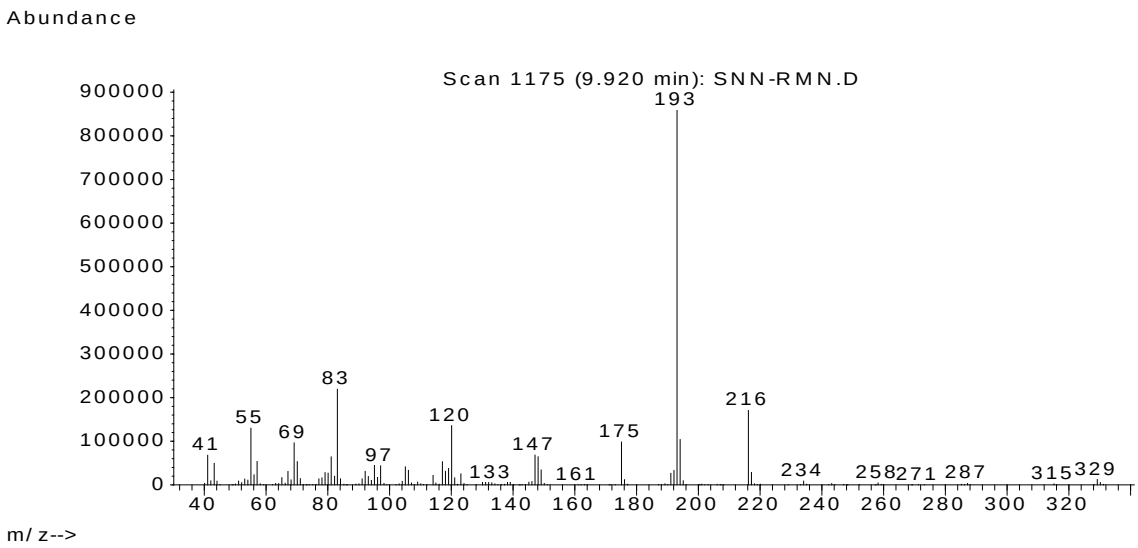

Fig. 2.3: Mass spectrum of derivatized *S*-(-)-nornicotine.

Chiral purity of the synthesized *S*-(-)-nornicotine was also determined by utilizing a chiral complexing agent, 1,1'-binaphthyl-2,2'-diylphosphoric acid (BNPPA) (Ravard and Crooks, 1996). Enantiopure (-)-*R*-BNPPA was used as the chiral complexing agent. When racemic nornicotine was treated with (-)-*R*-BNPPA a mixture of diastereomeric salts was formed; the 2-H and 6-H pyridinyl signals of racemic nornicotine could be seen as separate signals and were integratable. These two proton signals could be used for chiral purity analysis without any interference from the aromatic signals from the chiral complexing agent. If the sample of nornicotine contains two enantiomers then both of the enantiomers will form complex with (-)-*R*-BNPPA and produce a mixture of two diastereomeric salts. 2-H and 6-H pyridinyl hydrogens from the two diastereomeric salts have different chemical shifts and show up as separate peaks in the spectrum and thus can be used to determine chiral purity of a nornicotine sample. Along with the pyridinyl protons, the 5'-H protons of the pyrrolidine ring were also found to be useful for chiral analysis. In presence of the chiral complexing agent, the 5'-H protons of (+)-*R*-nornicotine were observed as a single broad multiplet. In the case of (-)-*S*-nornicotine, the 5'-H protons were split into two broad multiplets. Synthesized *S*-(-)-nornicotine was treated with 1.6 equivalents of (-)-*R*-BNPPA and the resulting salt was analyzed by ^{1}H NMR spectroscopy. The spectrum showed only two signals above 8 ppm, corresponding

to the 2-H and 6-H pyridinyl protons of the (-)-*S*-nornicotine enantiomer complex. No signals were observed for the 2-H and 6-H pyridinyl protons that corresponded to the (+)-*R*-nornicotine enantiomer complex. Similarly, analysis of the 2.6-4.2 ppm region of the spectrum revealed two broad multiplets centered around 3.1 and 2.8 ppm. These two multiplets correspond to the 5' protons of the (-)-*S*-nornicotine enantiomer complex. A broad multiplet centered at 2.95 ppm corresponding to the 5'-H protons of the (+)-*R*-nornicotine enantiomer complex was barely negligible (noise level), and below levels of integration. Thus, the analysis of the proton NMR spectrum of synthesized nornicotine in presence of the chiral complexing agent demonstrated that (-)-*S*-nornicotine was exclusively obtained by the oxidative *N*-demethylation of (-)-*S*-nicotine.

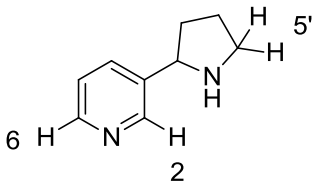

Fig. 2.4: Important protons for chiral analysis of the nornicotine molecule with compound numbering scheme.

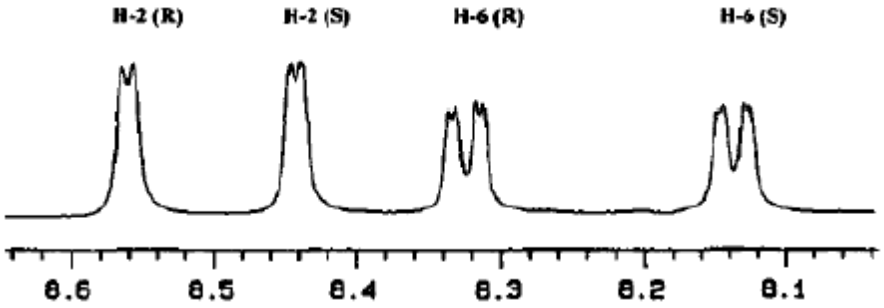

Fig. 2.5: Proton NMR spectrum of racemic nornicotine in the presence of the chiral complexing agent *R*-(-)-1,1'-binaphthyl-2,2'-diylphosphoric acid (BNPPA) in the region 8.0-8.8 ppm. (Reprinted from Chirality, Ravard and Crooks, 1996, with permission)

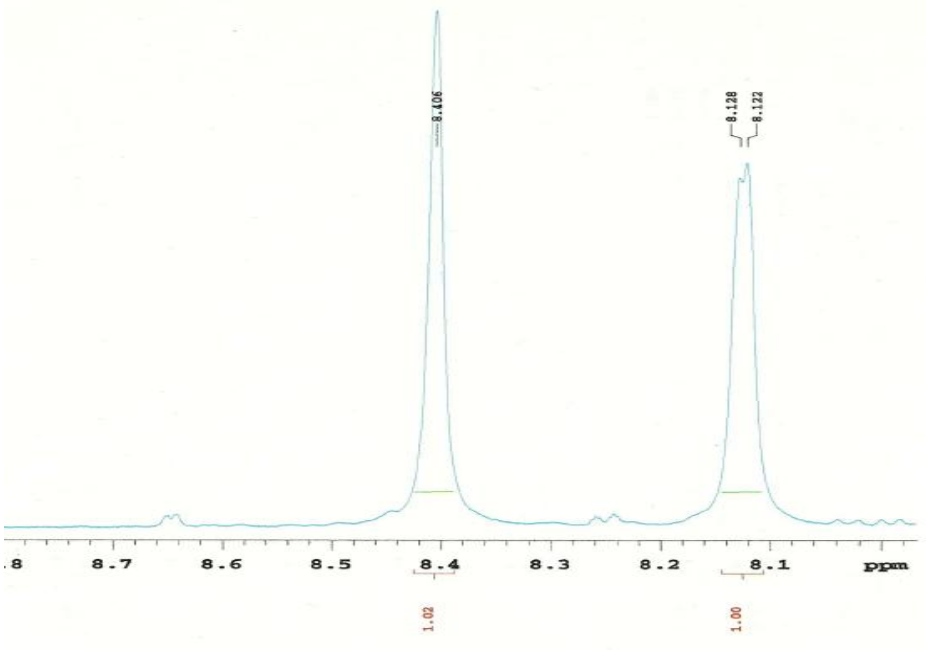

Fig. 2.6: Proton NMR spectrum of synthesized (-)-*S*-nornicotine in presence of the chiral complexing agent R-(-)-BNPPA in the region 8.0-8.8 ppm.

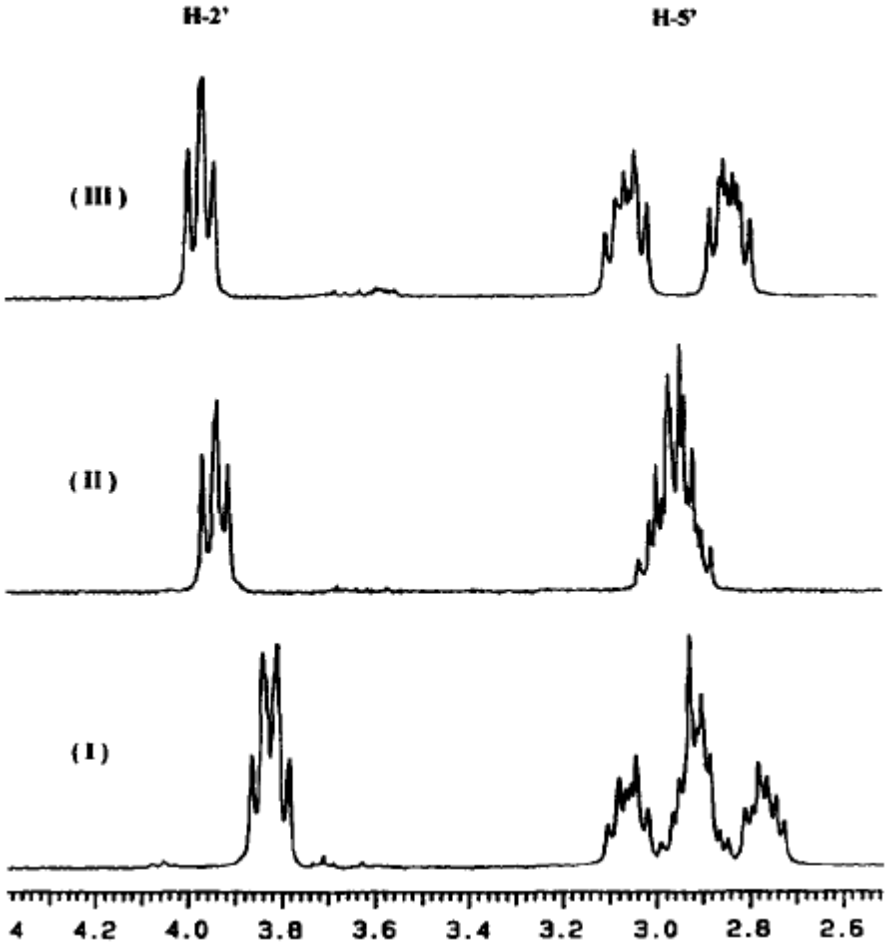

Fig. 2.7: Proton NMR spectrum of racemic nornicotine (I), *R*-(+)-nornicotine (II) and *S*-(-)-nornicotine (III) in the presence of the chiral complexing agent R-(-)-BNPPA in the region 2.6-4.4 ppm. (Reprinted from Chirality, Ravard and Crooks, 1996, with permission)

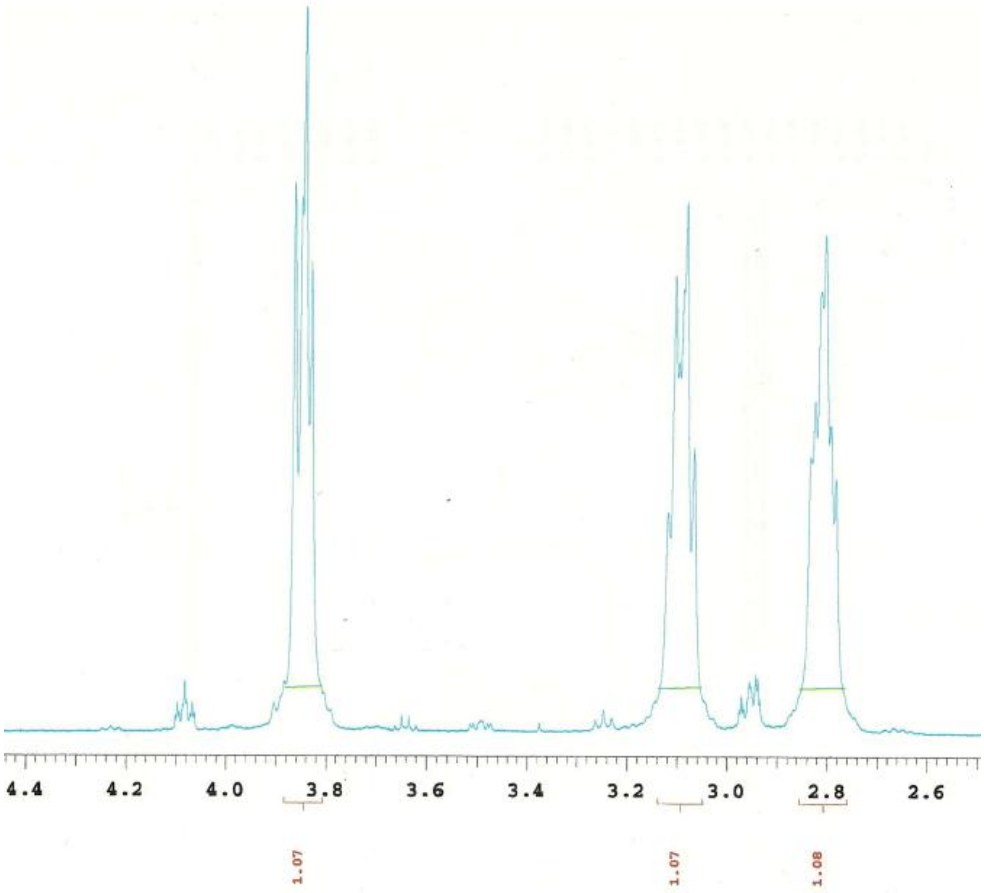

Fig. 2.8: Proton NMR spectrum of synthesized nornicotine in the presence of chiral complexing agent in the region 2.5-4.4 ppm.

To determine if this *N*-demethylation procedure could be utilized as a general procedure for the *N*-demethylation of tertiary amino compounds bearing an *N*-methyl group. Several other *N*-methyl compounds were treated with MnO_2 and 0.3 N H_2SO_4 under reflux conditions and the products were analyzed by GC-MS. The following scheme (Scheme 2.4) summarizes the outcomes of these oxidative *N*-demethylation reactions. It can be concluded from the obtained results, that MnO_2 can be used for oxidative *N*-demethylation reactions without compromising the chirality of any adjacent stereocenters present in such molecules. It is observed that the presence of a double bond is not compatible with the above methodology, affording extensive oxidation at the C=C moiety.

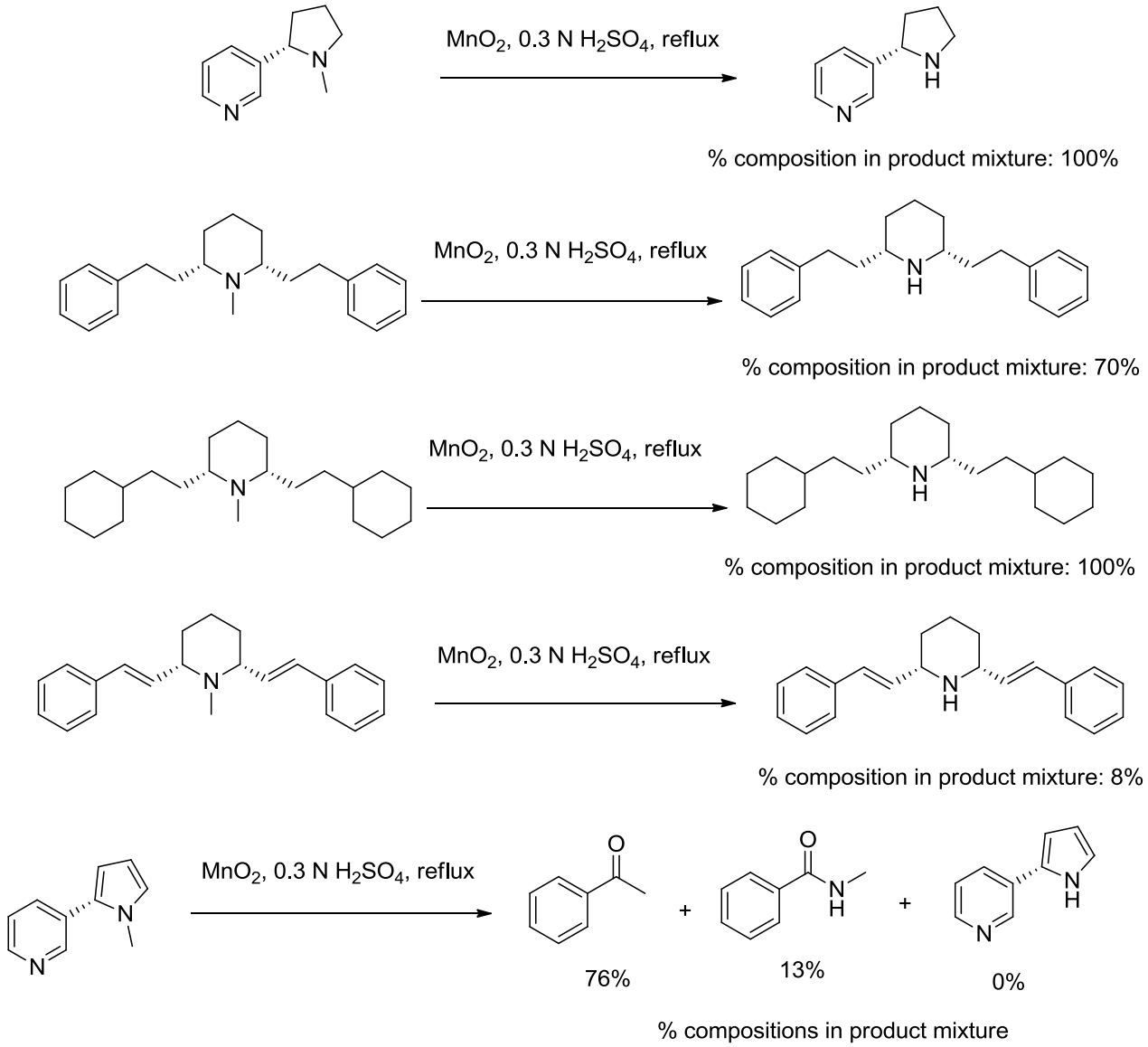

Scheme 2.4: *N*-Demethylation of several *N*-methyl compounds.

2.3 Synthesis of Codrugs and Analogs

2.3.1 Opioid-*S*-(-)-Nornicotine Codrugs Syntheses

A series of codrugs were designed combining an opioid or a prodrug of an opioid with *S*-(-)-nornicotine. Codeine, morphine and 3-*O*-acetylmorphine (a prodrug of morphine) were chosen as the opioid molecules. Codeine, morphine and 3-*O*-

acetylmorphine contain either an alcoholic OH group or a phenolic OH group. On the other hand, *S*-(-)-nornicotine contains a secondary amino group. The most logical way to join these molecules is through a carbamate bond between OH groups of opioids and the amino group of *S*-(-)-nornicotine. The first codrug in this series that was aimed for synthesis was a carbamate codrug combining codeine and *S*-(-)-nornicotine through a carbamate bond.

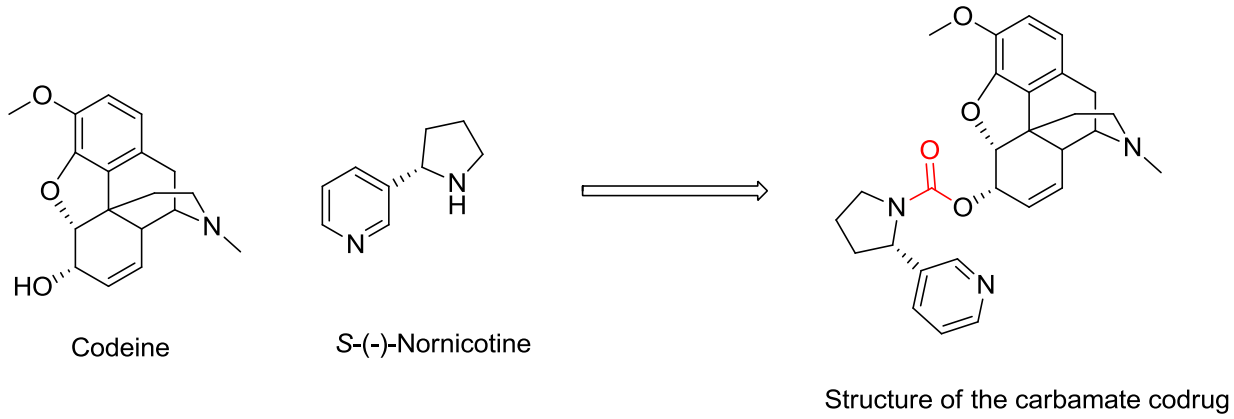

Fig. 2.9: Design of codeine-*S*-(-)-nornicotine carbamate codrug.

Since the essential conjugation chemistry in the synthesis of the codeine-*S*-(-)-nornicotine codrug is the formation of a carbamate linkage, reactions were initiated to generate carbamate linkages between an amine and a phenol. Before commencing the synthetic work with expensive controlled substances such as codeine and *S*-(-)-nornicotine, coupling reactions were initially carried out with model compounds or chemical-mimics of the drug molecules to optimize the desired chemistry. 3-Ethylphenol was chosen as the model compound for codeine and morphine, and pyrrolidine was selected as a chemical mimic for the *S*-(-)-nornicotine molecule. Initially, three retrosynthetic schemes were devised for the synthesis of a carbamate conjugate of the two desired molecules (Scheme 2.5). The first approach (route A) involves the intermediacy of the *N*-carbamoyl chloride analogue of pyrrolidine, followed by its

reaction with a phenol to generate the desired carbamate conjugate. The second approach (route B) involves conversion of the phenol to a symmetrical carbonate ester, followed by nucleophilic substitution of one of the carbonate moieties with the desired amine. The last approach (route C) involves the formation of a chloroformate derivative of the phenol followed by reaction with pyrrolidine, to generate the desired carbamate conjugate.

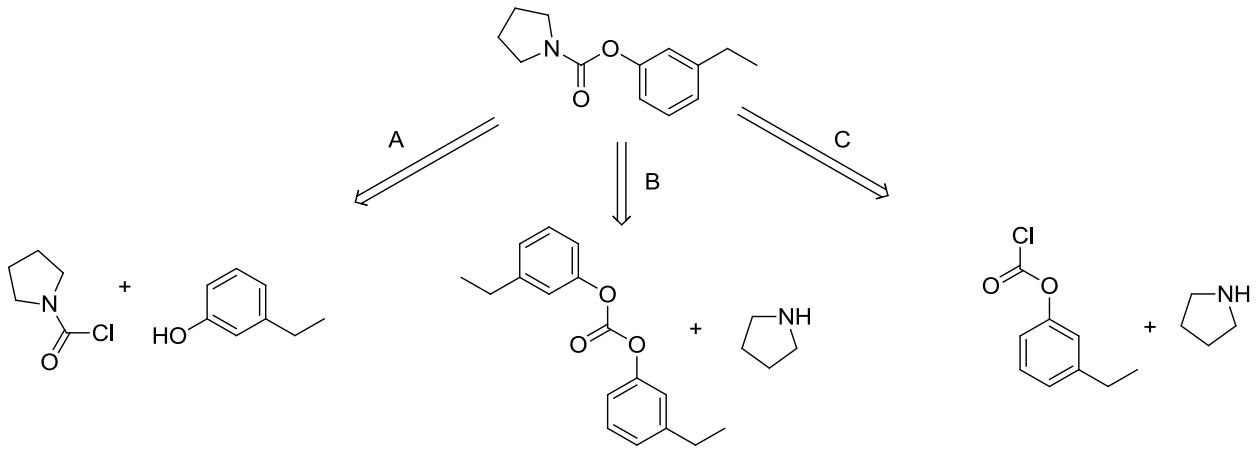

Scheme 2.5: Different synthetic strategies to afford carbamate conjugates of a phenol and a secondary amine.

In the first synthetic approach (route A), to generate the carbamate linkage, pyrrolidine was allowed to react with triphosgene to form the desired *N*-carbamoyl chloride derivative of pyrrolidine (Gulin et al., 2006). The reaction was followed by GC-MS monitoring. The reaction yielded the desired intermediate, along with a urea side product (Scheme 2.6 and Fig. 2.10). This side reaction not only decreased the yield of the desired product, but also caused complications in the purification of the carbamoyl chloride intermediate. Urea formation would significantly increase the cost of the final process, as it would consume the expensive parent drugs during the actual synthesis of the codeine-*S*-(-)-nornicotine codrug. The mass spectra of the *N*-carbamoyl chloride and the urea side product are shown in Fig. 2.11 and 2.12.

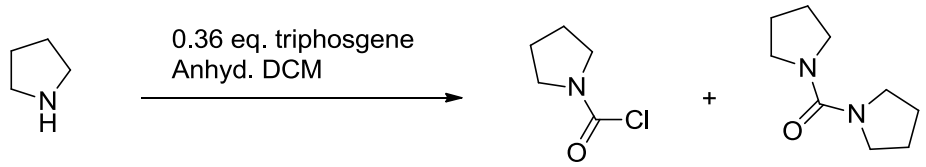

Scheme 2.6: Reaction of pyrrolidine with triphosgene.

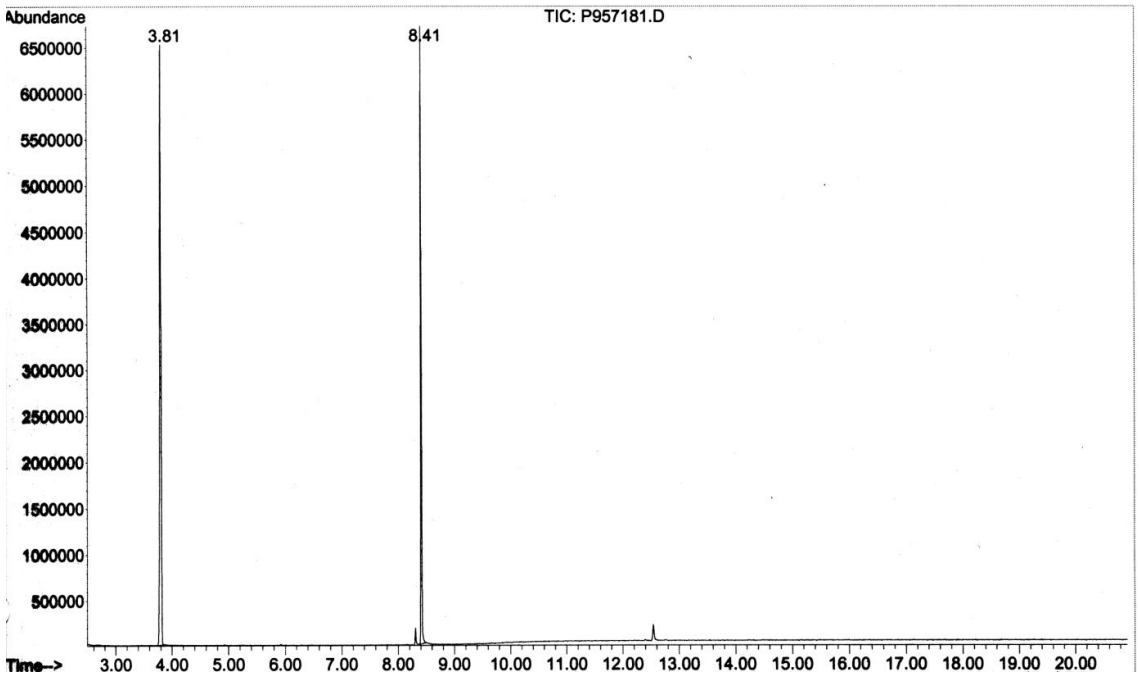

Fig. 2.10: Total ion chromatogram of synthetic pyrrolidine *N*-carbamoyl chloride (retention time: 3.81 min) and the pyrrolidine urea side product (retention time: 8.41 min).

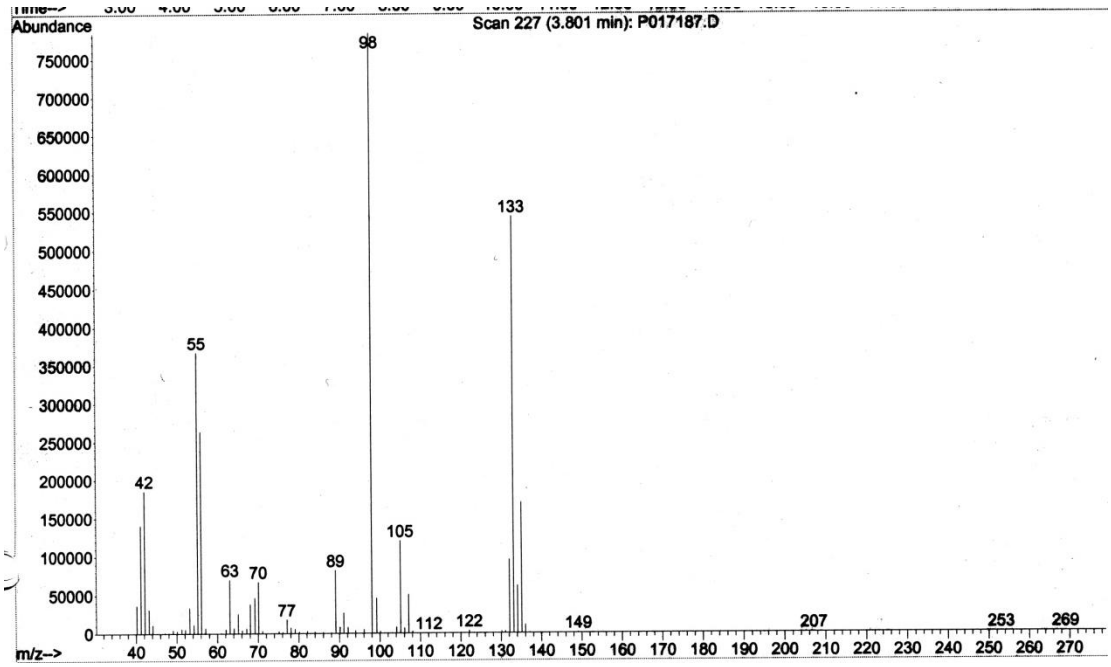

Fig. 2.11: Mass spectrum of pyrrolidine *N*-carbamoyl chloride.

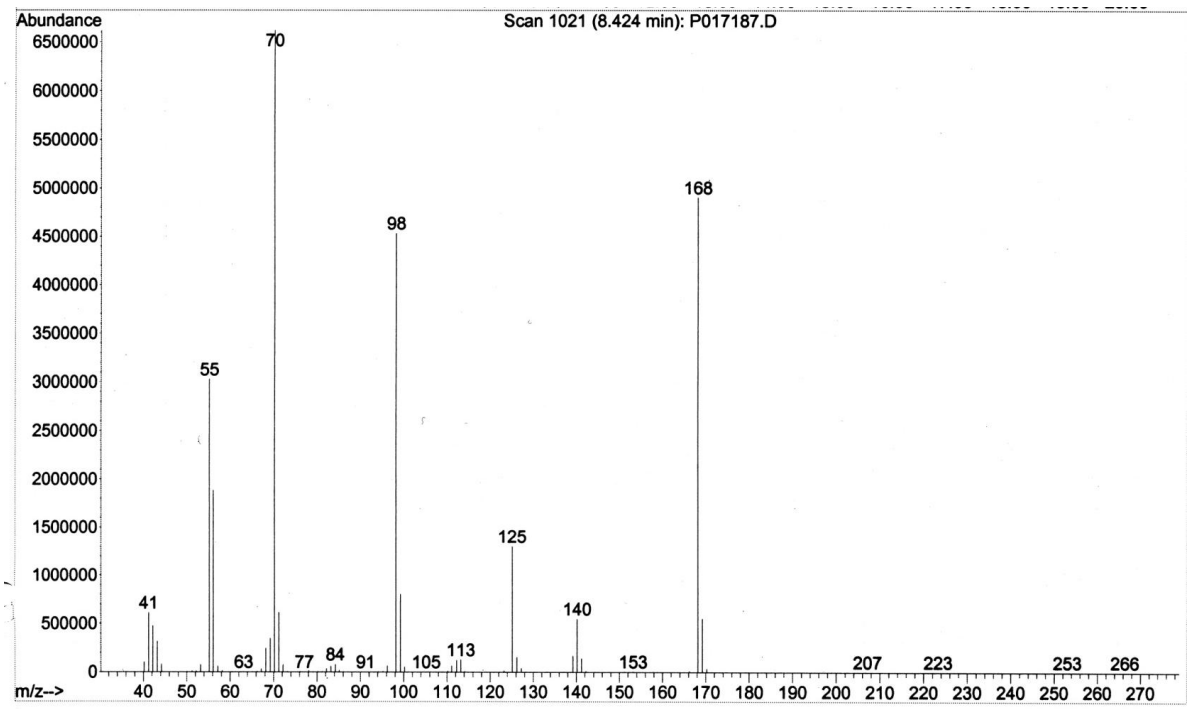

Fig. 2.12: Mass spectrum of pyrrolidine urea.

In the second synthetic approach (route B), the symmetrical carbonate of the phenolic compound was formed by reacting the phenol with triphosgene (Burk and Roof, 1993). The carbonate intermediate was then allowed to react with pyrrolidine to form the desired carbamate conjugate (Scheme 2.7). Both reactions were monitored by GC-MS. The reactions were comparatively cleaner than the reaction in the previous synthetic approach, but suffered from the loss of half equivalent of the phenolic compound as a byproduct. This would cause an increase in cost when the final opioid (codeine and morphine)-nornicotine codrug molecule was synthesized. The mass spectra of the symmetrical carbonate of 3-ethylphenol and the 3-ethylphenol-pyrrolidine carbamate conjugate are shown in Fig. 2.13 and 2.14.

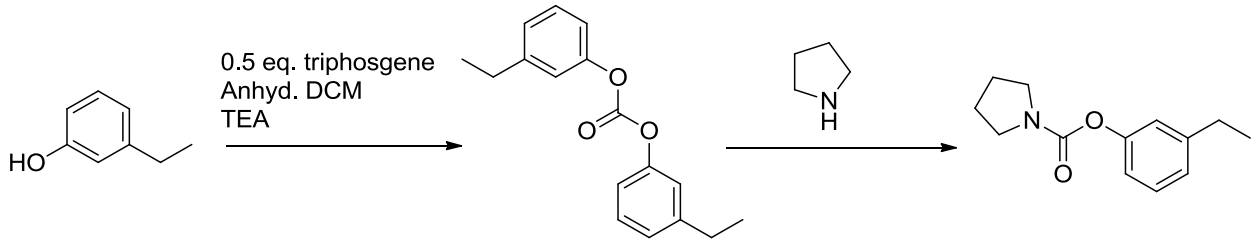

Scheme 2.7: Synthesis of carbamate conjugate via the intermediacy of a symmetrical carbonate ester.

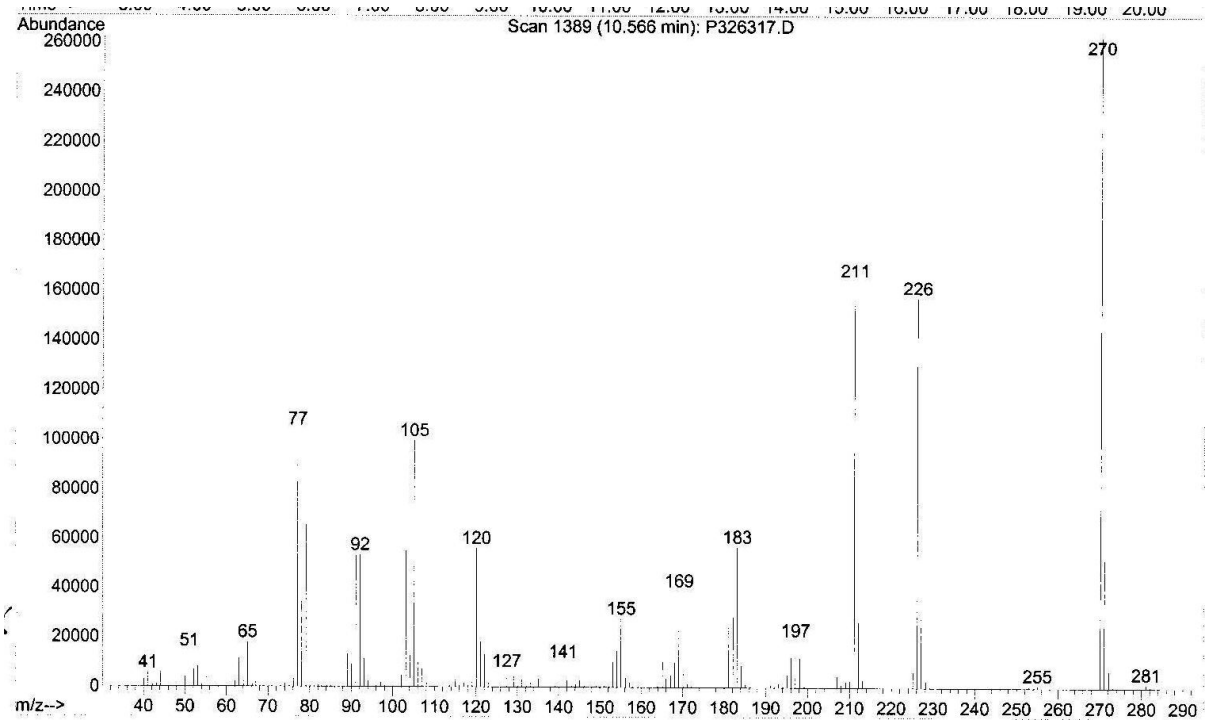

Fig. 2.13: Mass spectrum of 3-ethylphenol carbonate ester.

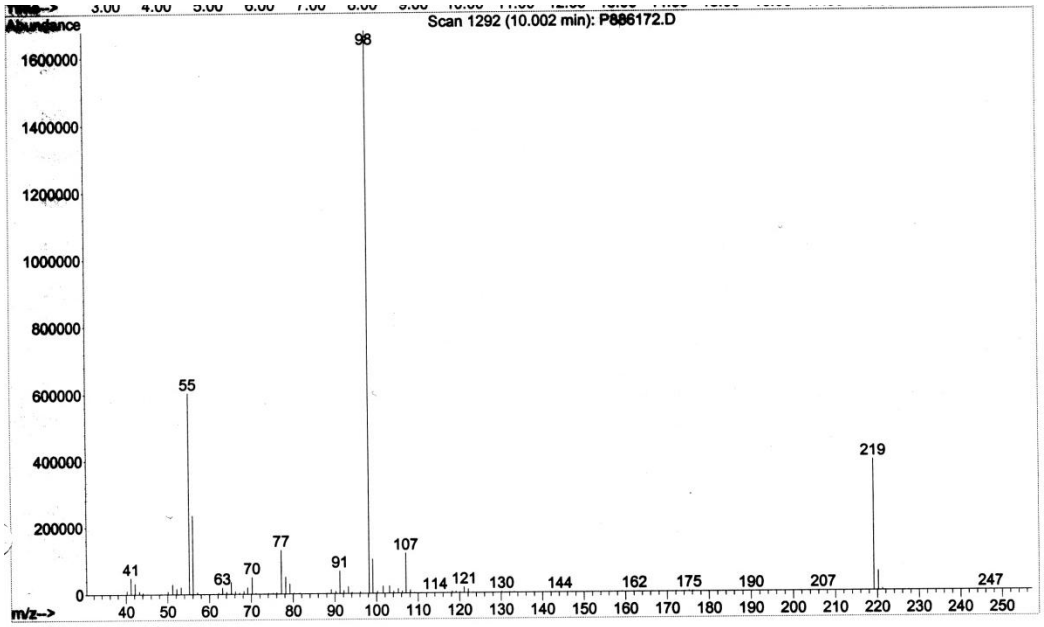

Fig. 2.14: Mass spectrum of the 3-ethylphenol-pyrrolidine carbamate conjugate.

A third synthetic approach (route C) was explored in an attempt to solve the problems faced in the first two approaches. Following this retrosynthetic route, a chloroformate derivative of the phenolic starting material was synthesized by reacting the phenol with triphosgene reagent in the presence of a base (pyridine) (Martin et al., 2006). The chloroformate derivative was then allowed to react with pyrrolidine to yield the carbamate conjugate (Scheme 2.8). This route was found to be the best choice among the three approaches investigated. Nevertheless, some minor problems were observed. Formation of a symmetrical carbonate side product during the synthesis of chloroformate derivative was one of the minor problems in this approach. The mass spectrum of the chloroformate intermediate of 3-ethylphenol is shown in Fig. 2.15.

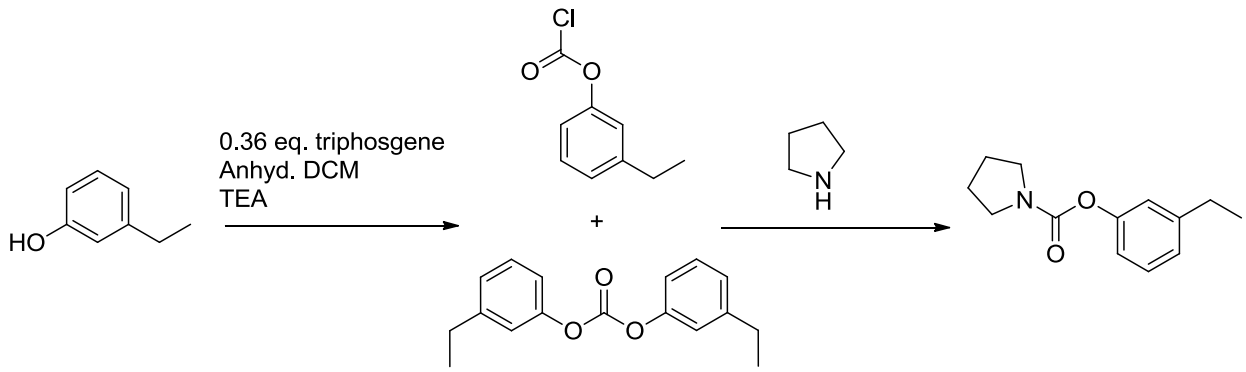

Scheme 2.8: Synthesis of a carbamate conjugate via the intermediacy of a chloroformate.

Table 2.1: Comparison of three synthetic routes.

Route	GC yield of the intermediate	GC yield of the product	Problem
A	50%	88%	50% of the starting material amine wasted as urea intermediate
B	82%	79%	50% of the starting material phenol wasted at the last step
C	62%	87%	Minor problem of symmetrical carbonate formation

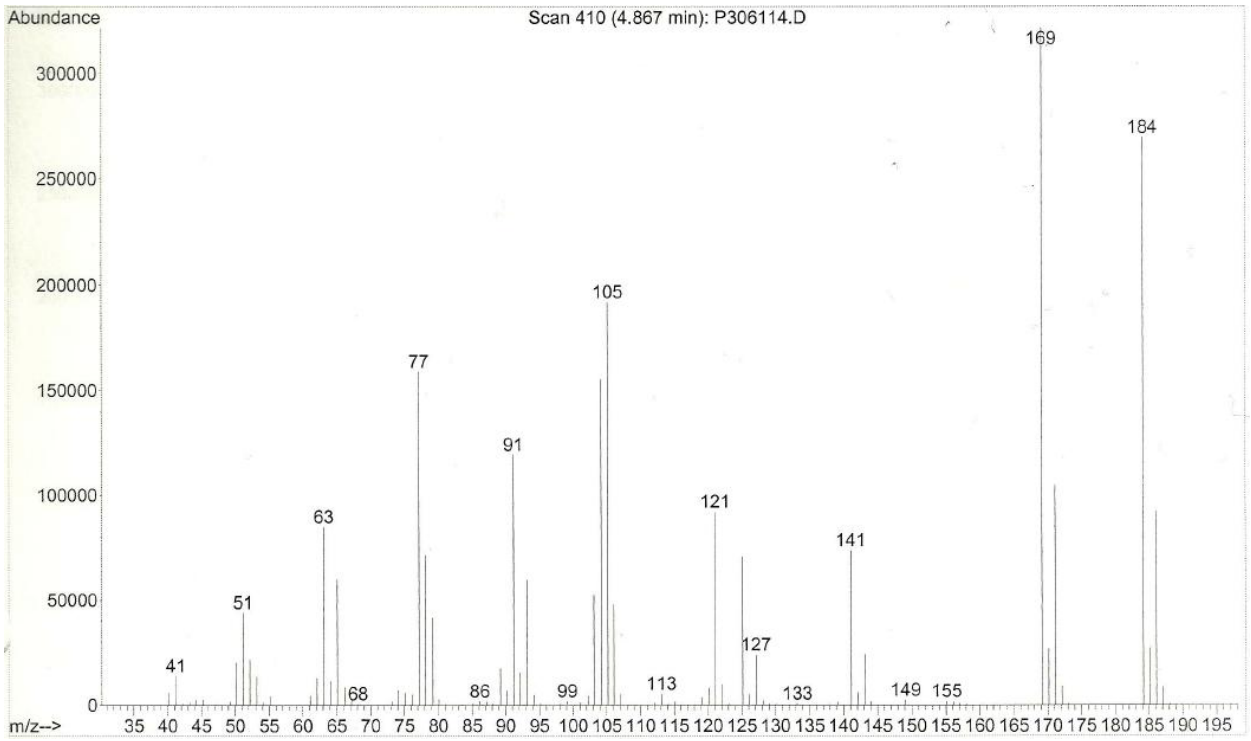

Fig. 2.15: Mass spectrum of 3-ethylphenol chloroformate.

In the next series of reactions, one of the chemical mimics was replaced by the actual drug molecule. Pyrrolidine was replaced with the *S*-(-)-nornicotine molecule. The chloroformate derivative of the model phenolic compound was synthesized utilizing the same methodology as previously described, and then it was allowed to react with *S*-(-)-nornicotine in presence of triethylamine (TEA). The reaction was monitored by GC-MS, which confirmed the formation of the carbamate conjugate of 3-ethylphenol and *S*-(-)-nornicotine.

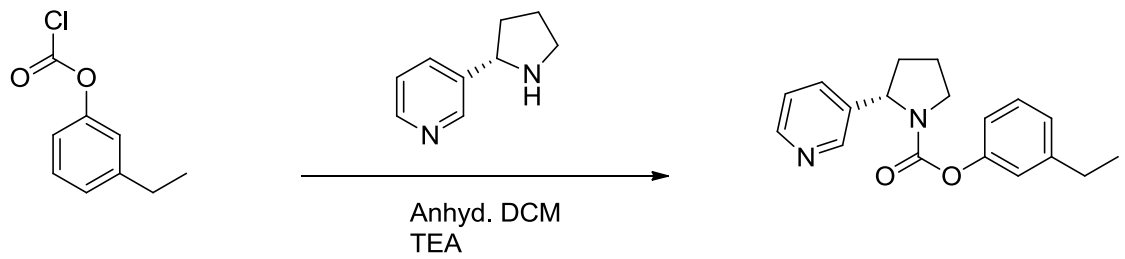

Scheme 2.9: Synthesis of 3-ethylphenol-*S*-(-)-nornicotine carbamate conjugate.

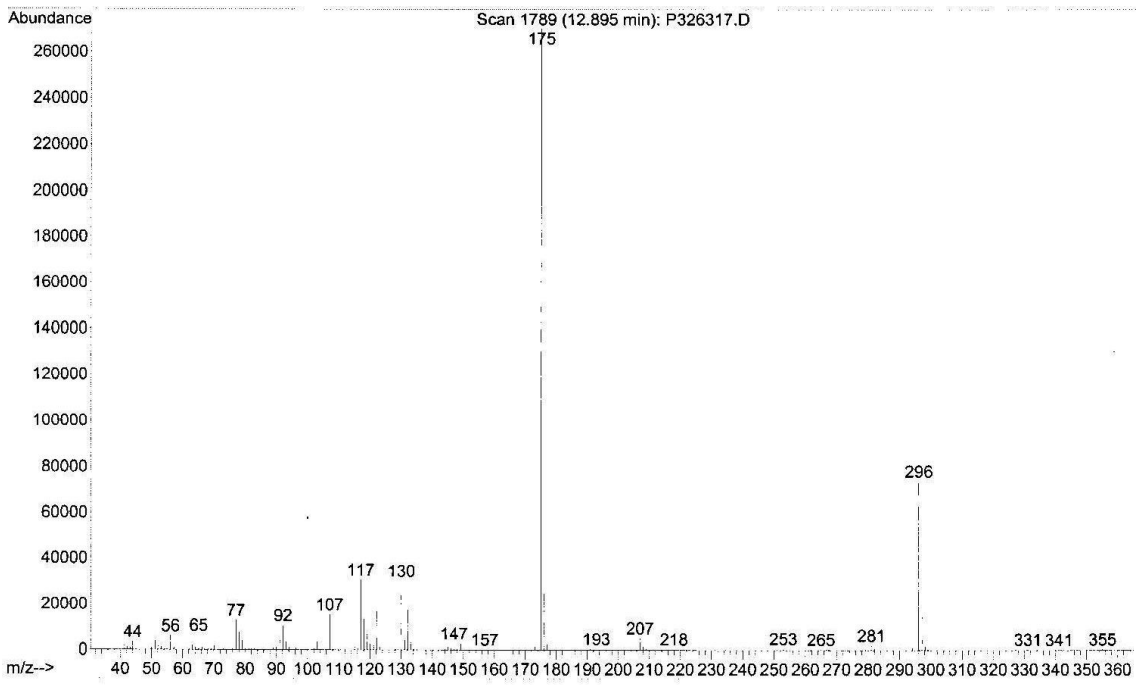

Fig. 2.16: Mass spectrum of 3-ethylphenol-*S*-(-)-nornicotine carbamate conjugate.

After the successful formation of the carbamate conjugate of *S*-(-)-nornicotine and 3-ethylphenol, the carbamate conjugates of morphine and *S*-(-)-nornicotine and codeine and *S*-(-)-nornicotine were undertaken. Morphine or codeine was added to dry THF along with pyridine or triethylamine and the reaction temperature was maintained at 0 °C. Triphosgene solution was then added drop-wise to the reaction mixture. An immediate white precipitation was observed after the addition of triphosgene to the morphine or codeine solution. GC-MS analysis of the each of the precipitates from these two reactions

showed a product with the molecular mass of morphine and codeine, respectively. ^{13}C NMR spectra of the two precipitates did not show any carbonyl peak in the region where a chloroformate carbon would show up. The precipitates were identified to be protonated morphine and codeine. A series of different solvents and bases were utilized in these reactions, but in all the different situations, precipitation of the starting materials always occurred. Due to this problem a new synthetic method was sought for the formation of the carbamate codrugs.

In attempting to solve the above problem it was found that *p*-nitrophenylchloroformate analogues have been utilized in the literature for the formation of unsymmetrical carbonates and carbamates (Anderson and McGregor, 1957). Initially, an alcohol is reacted with *p*-nitrophenylchloroformate (*p*NPCF) to form the carbonate conjugate of the alcohol and *p*-nitrophenol. This intermediate is then reacted with an amine to form the carbamate conjugate of an alcohol and an amine. In the second step, the good leaving group property of the *p*-nitrophenol moiety is advantageous in the selective formation of the desired carbamate conjugate.

Utilizing this approach, codeine was first allowed to react with *p*NPCF in the presence of *N*,*N*-dimethylamino pyridine (DMAP) in anhydrous dichloromethane (DCM) to yield the *p*-nitrophenyl carbonate analog of codeine (i.e. cod-pnp). The structure of this compound was confirmed by ^{1}H- and ^{13}C-NMR spectroscopy and mass spectrometry. *p*-Nitrophenol was generated as a side-product of the reaction, and was difficult to remove from the desired product. Washing the DCM solution of the cod-pnp carbonate with saturated aqueous $NaHCO_3$ solution reduced the *p*-nitrophenol contamination, but could not remove it completely. An attempt to purify the carbonate intermediate of codeine and *p*-nitrophenol using column chromatography with DCM-MeOH as eluent yielded the methanolic carbonate analog of codeine; the structure of this product was determined by mass spectrometry and ^{1}H- and ^{13}C-NMR spectroscopy. This carbonate conjugate between methanol and codeine may be utilizable as a novel prodrug of codeine.

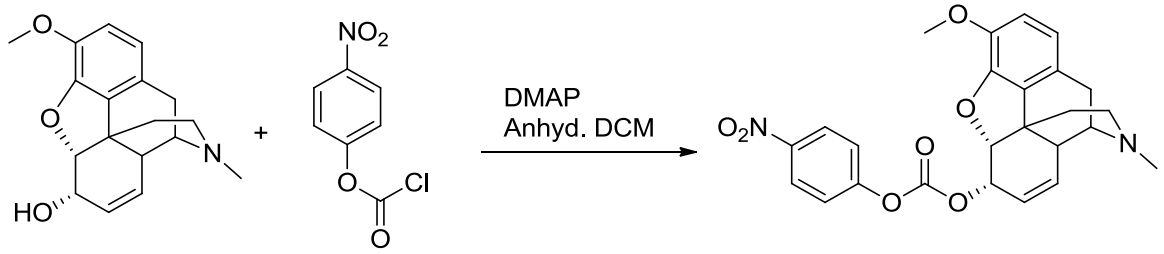

Scheme 2.10: Synthesis of the *p*-nitrophenoxy carbonate of codeine.

Scheme 2.11: Reaction of the *p*-nitrophenoxy carbonate of codeine with methanol in the presence of silica.

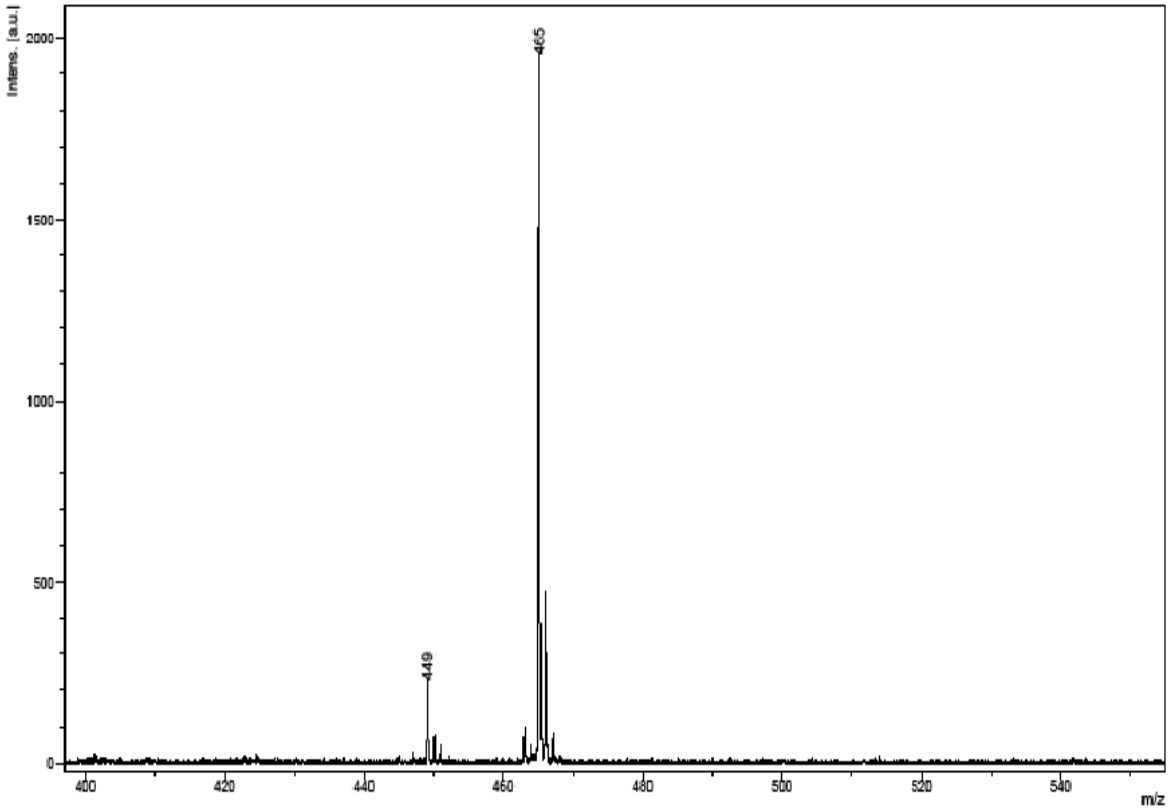

Fig. 2.17: MALDI-TOFMS of codeine-*p*-nitrophenol carbonate.

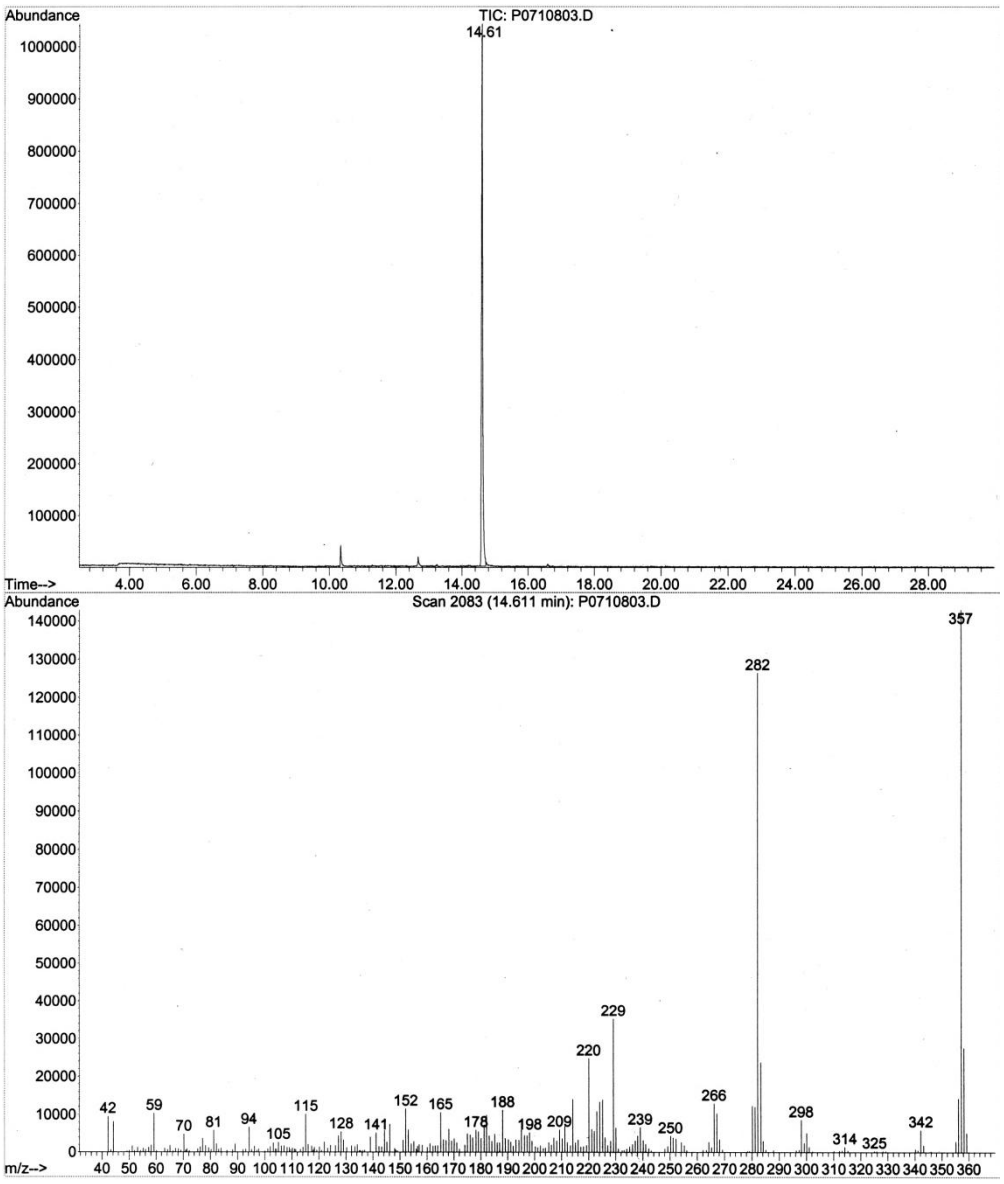

Fig. 2.18: GC-MS of the methanolic carbonate derivative of codeine.

Codeine-*p*-nitrophenyl carbonate was then allowed to react with the model compound pyrrolidine under reflux conditions in the presence of TEA. The progress of the reaction was followed by TLC, and after the completion of the reaction, the desired carbamate conjugate of codeine and pyrrolidine was obtained as a solid product. The structure of the conjugate was confirmed by ^{1}H- and ^{13}C-NMR spectroscopy and mass spectrometry.

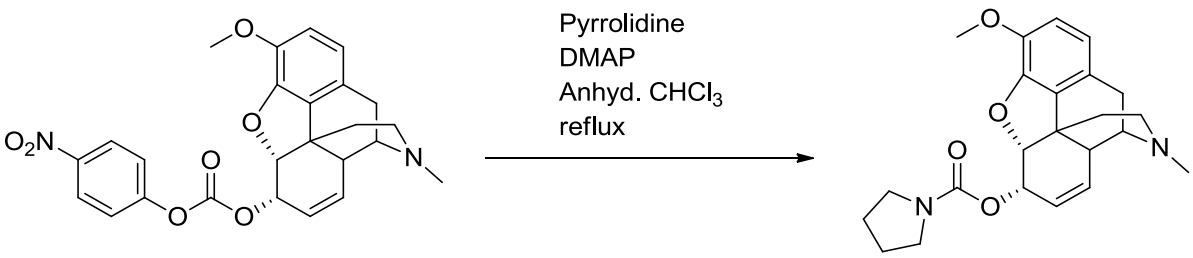

Scheme 2.12: Synthesis of the codeine pyrrolidine carbamate conjugate.

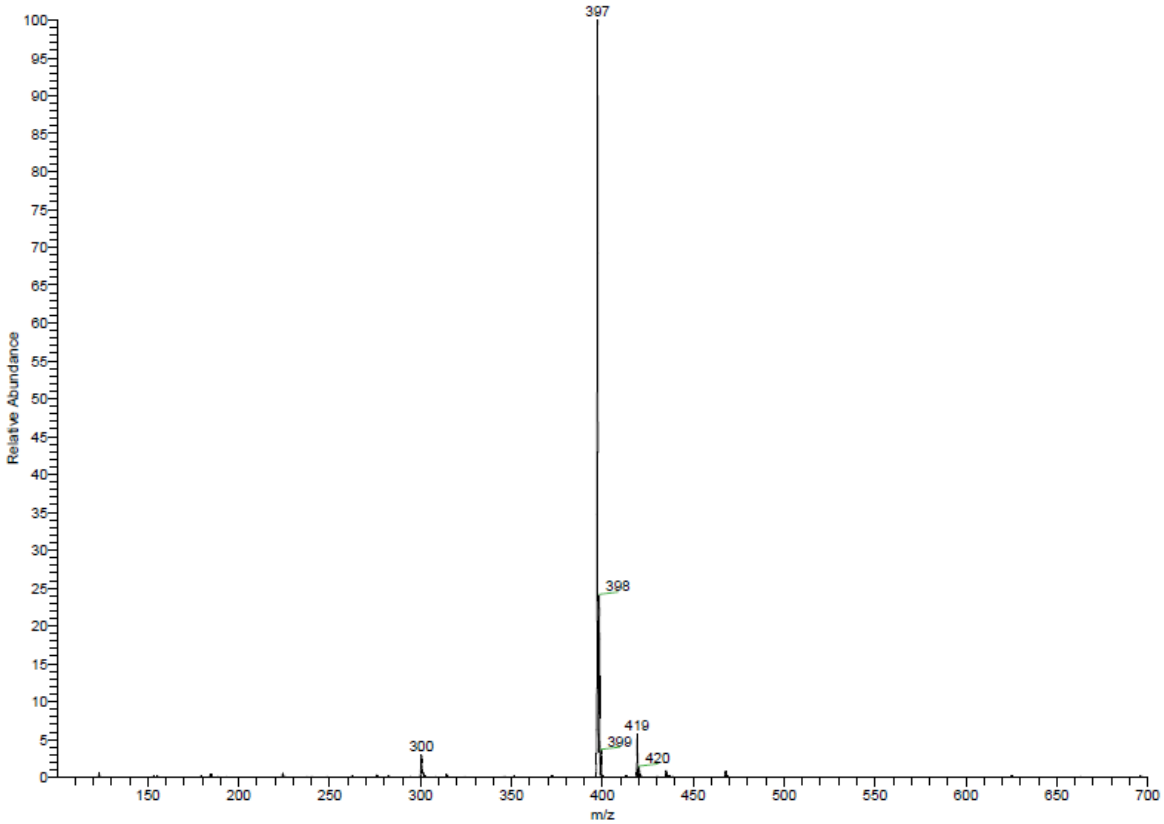

Fig. 2.19: Mass spectrum of the codeine-pyrrolidine carbamate conjugate.

After the success of generating the carbamate conjugate between codeine and pyrrolidine, synthesis of the codrug containing codeine and *S*-(-)-nornicotine was attempted using the same synthetic methodology. Cod-pnp carbonate was allowed to

react with *S*-(-)-nornicotine under reflux conditions yielding the desired codrug. The structure of the codeine-*S*-(-)-nornicotine carbamate codrug was confirmed by ^{1}H- and ^{13}C-NMR spectroscopy and mass spectrometry and the purity of the codrug was determined using HPLC-diode array assay.

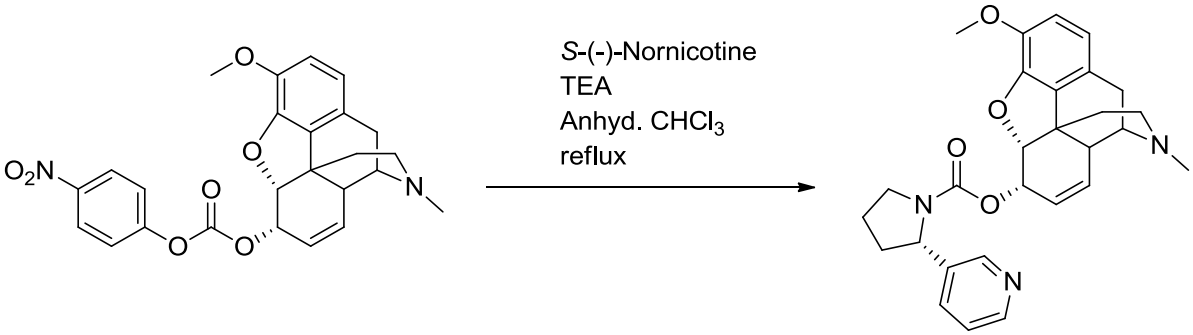

Scheme 2.13: Synthesis of the carbamate codrug of *S*-(-)-nornicotine and codeine.

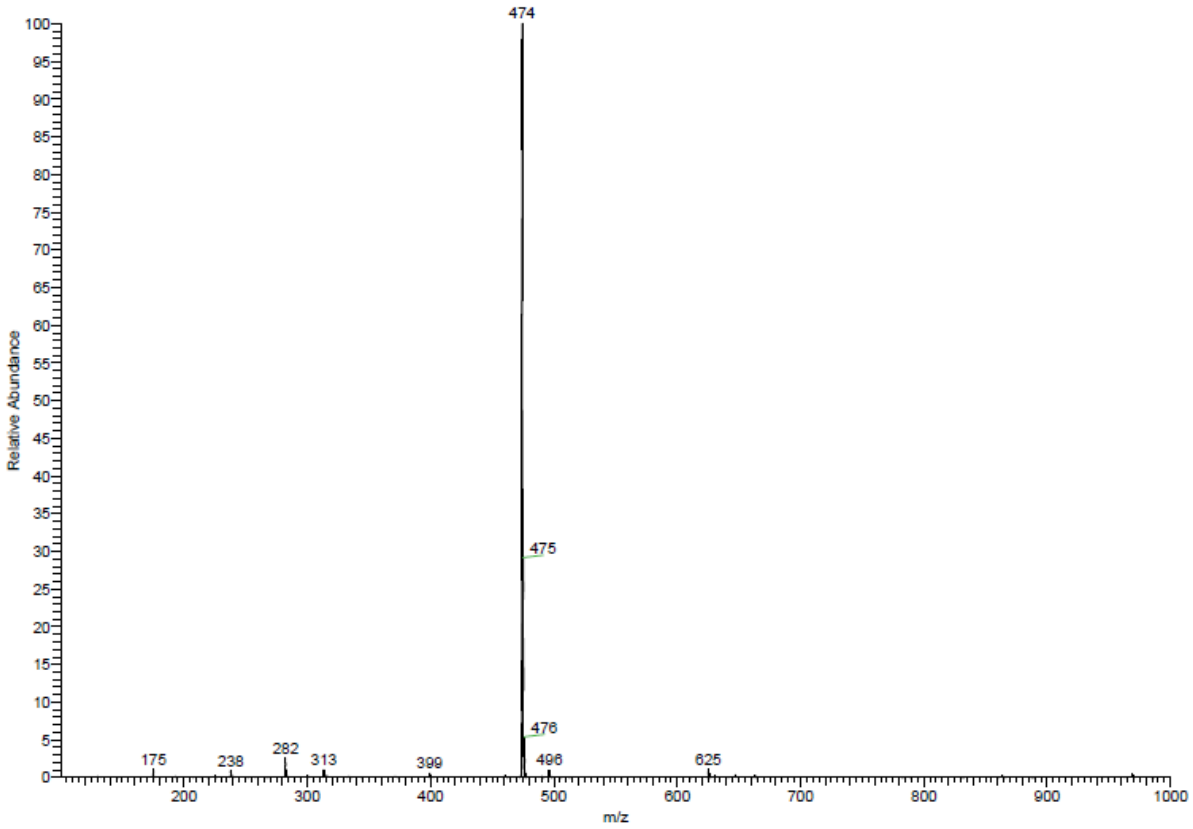

Fig. 2.20: Mass spectrum of the carbamate codrug of codeine and *S*-(-)-nornicotine.

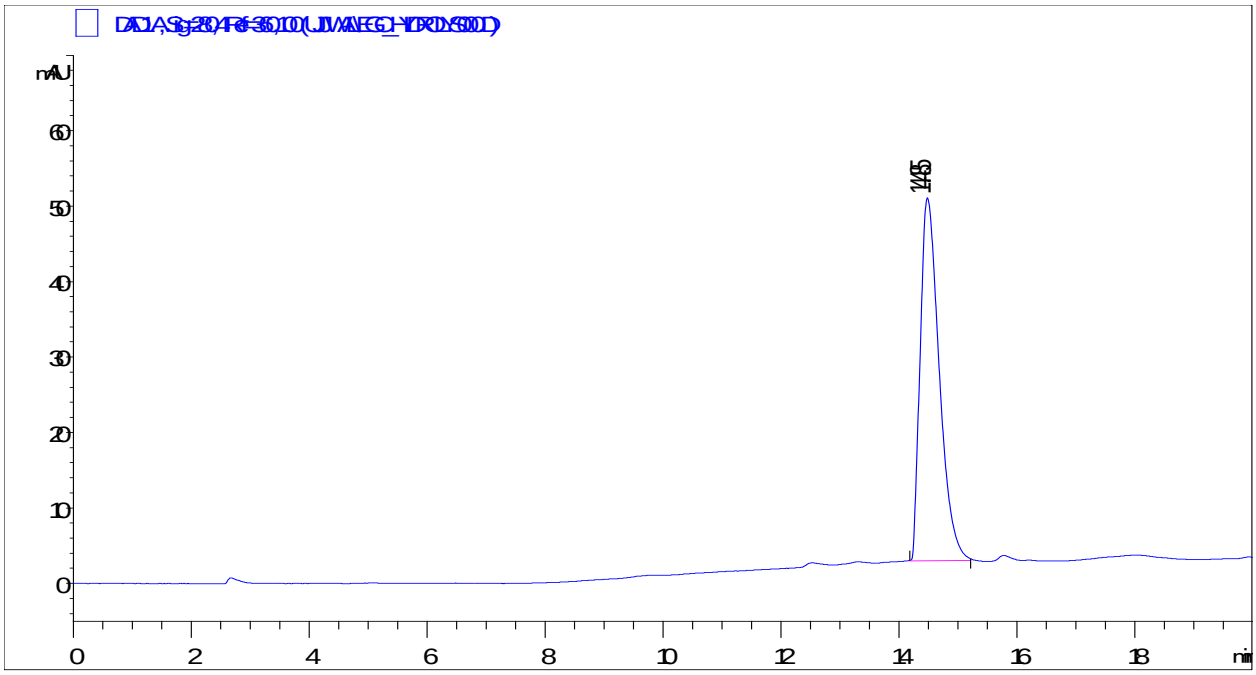

Fig. 2.21: HPLC chromatogram of codeine-*S*-(-)-nornicotine carbamate (retention time: 14.485 min).

The synthesis of a second series of codrugs were then pursued that incorporated the opioid alkaloid morphine and *S*-(-)-nornicotine. The first codrug prepared in this series was the carbamate codrug of *S*-(-)-nornicotine and morphine; carbamate conjugation was through the 6-hydroxy group of the morphine molecule. Morphine was first converted into 3-*O*-acetylmorphine by acetylation with acetic anhydride/$NaHCO_3$.

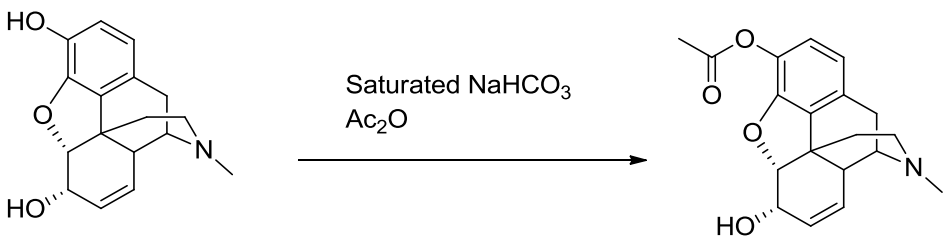

Scheme 2.14: Synthesis of 3-*O*-acetylmorphine.

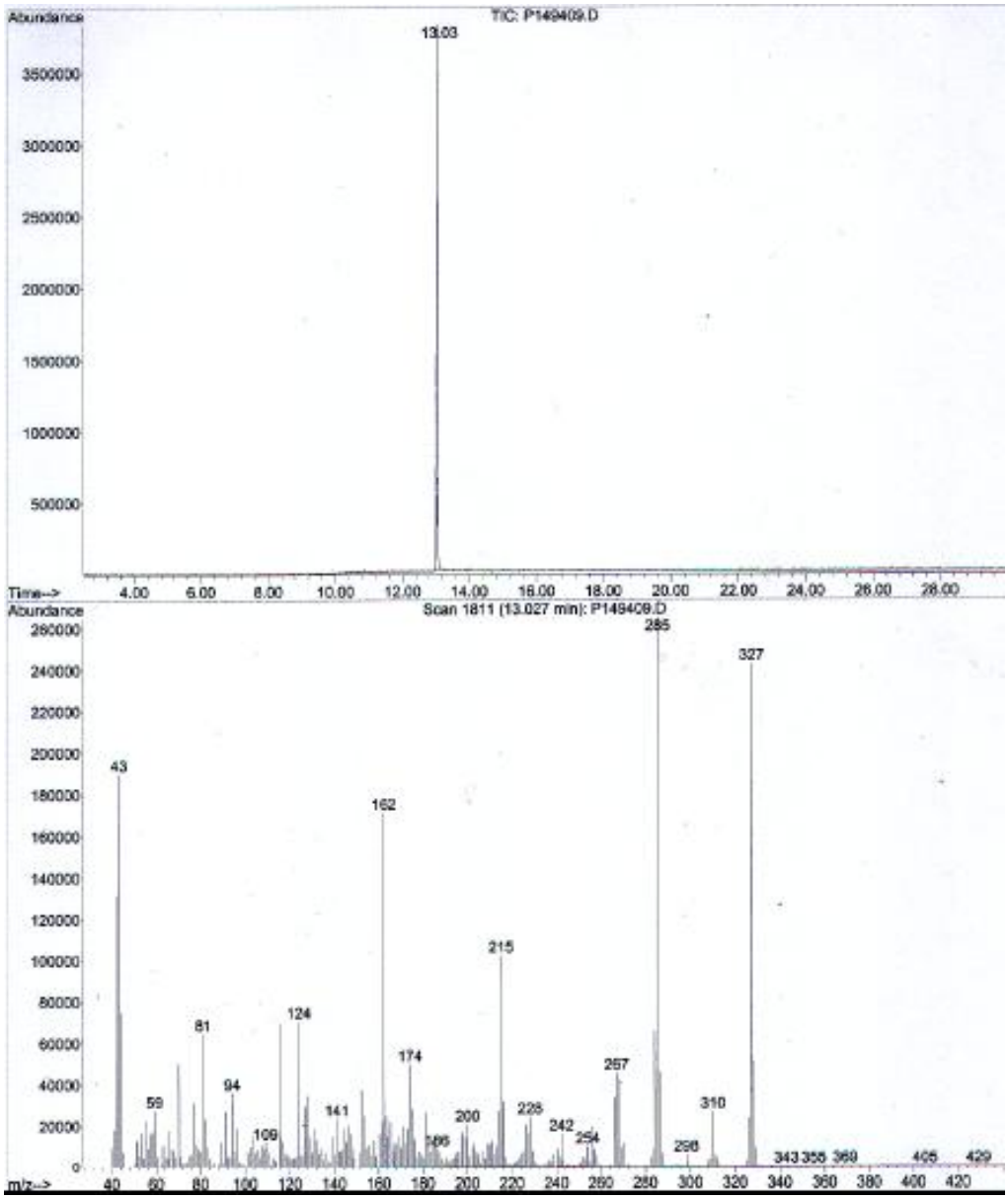

Fig. 2.22: GC-MS spectrum of 3-*O*-acetylmorphine.

3-*O*-Acetylmorphine was converted into its *para*-nitrophenoxycarbonate ester. The structure of the intermediate was confirmed by ^{1}H- and ^{13}C-NMR spectroscopy and mass spectrometry.

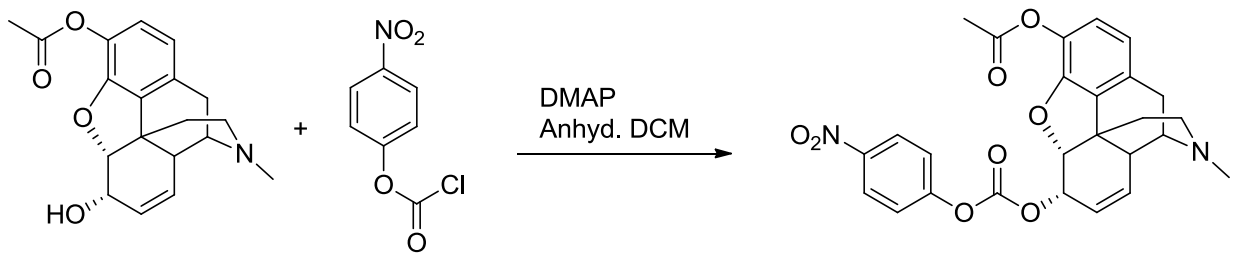

Scheme 2.15: Synthesis of the *p*-nitrophenoxy carbonate derivative of 3-*O*-acetylmorphine.

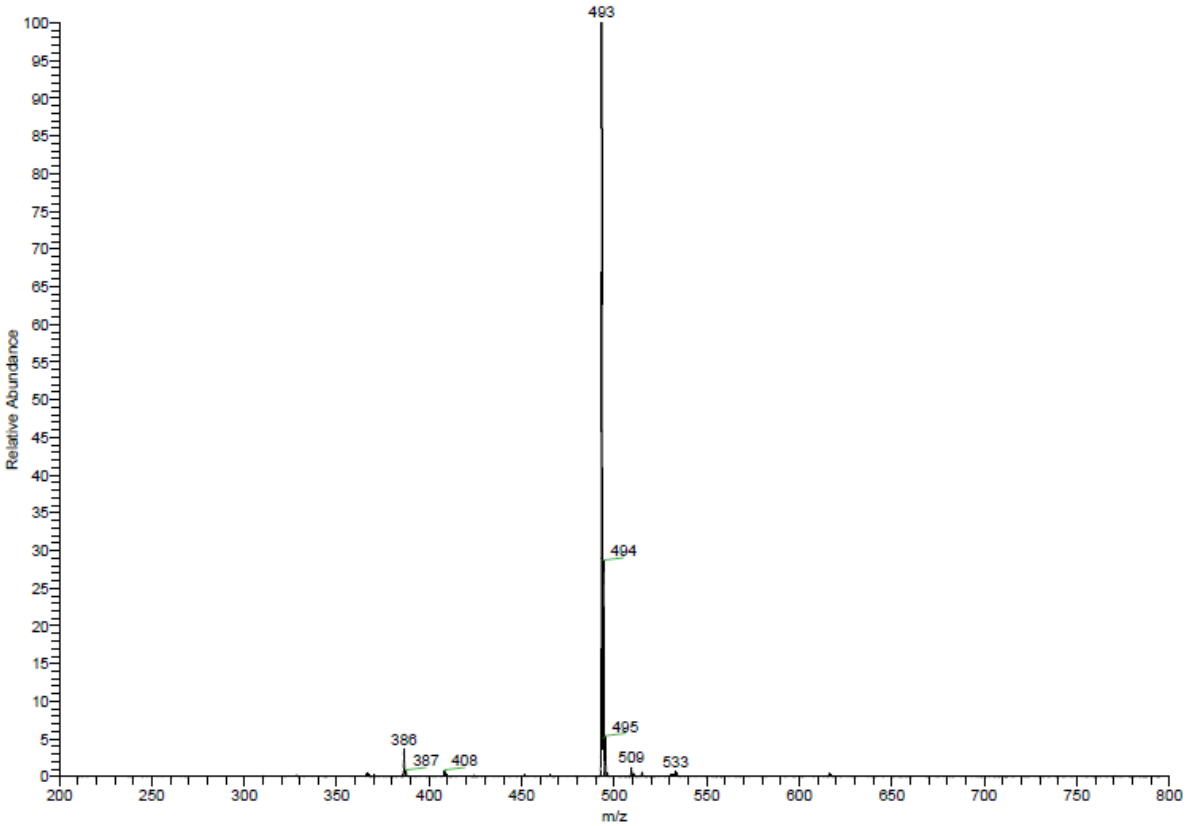

Fig. 2.23: Mass spectrum 3-*O*-acetylmorphine-*p*-nitrophenol carbonate.

The reactive carbonate intermediate was then allowed to react with *S*-(-)-nornicotine to afford the 3-*O*-acetylmorphine-*S*-(-)-nornicotine codrug. The acetyl protected codrug was subsequently *O*-deacetylated in the presence of LiOH to provide the desired carbamate codrug of morphine and *S*-(-)-nornicotine. The 3-*O*-acetyl

protected codrug was considered to be a useful structural modifaction of the target morphine-*S*-(-)-nornicotine codrug, since it represents a derivative that may have improved bioavailability over the codrug, due to increased lipophilicity and reduced number of sites for metabolism.

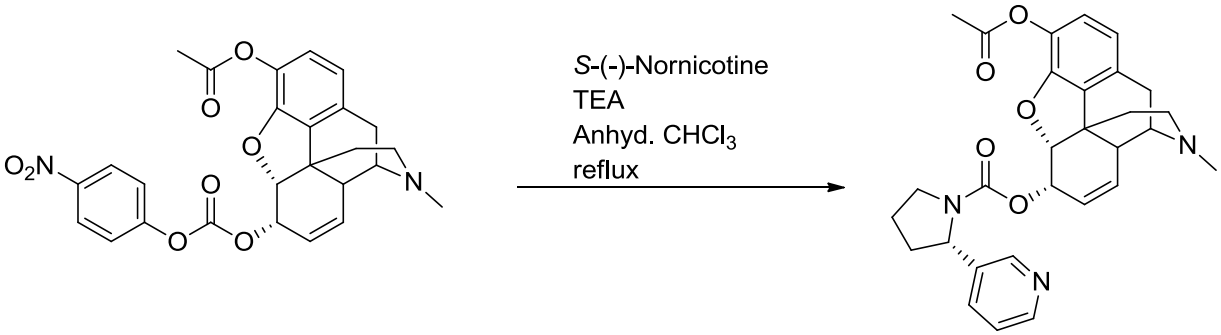

Scheme 2.16: Synthesis of 3-*O*-acetylmorphine-*S*-(-)-nornicotine carbamate codrug.

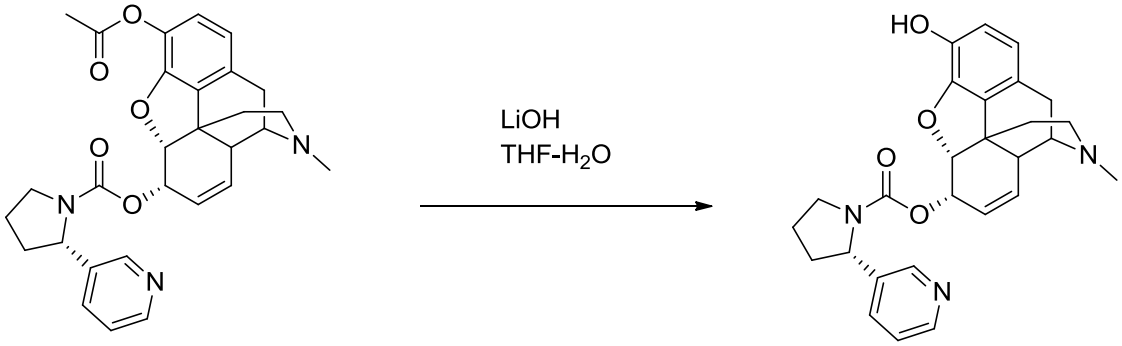

Scheme 2.17: Synthesis of morphine-*S*-(-)-nornicotine carbamate (6-oxy) codrug.

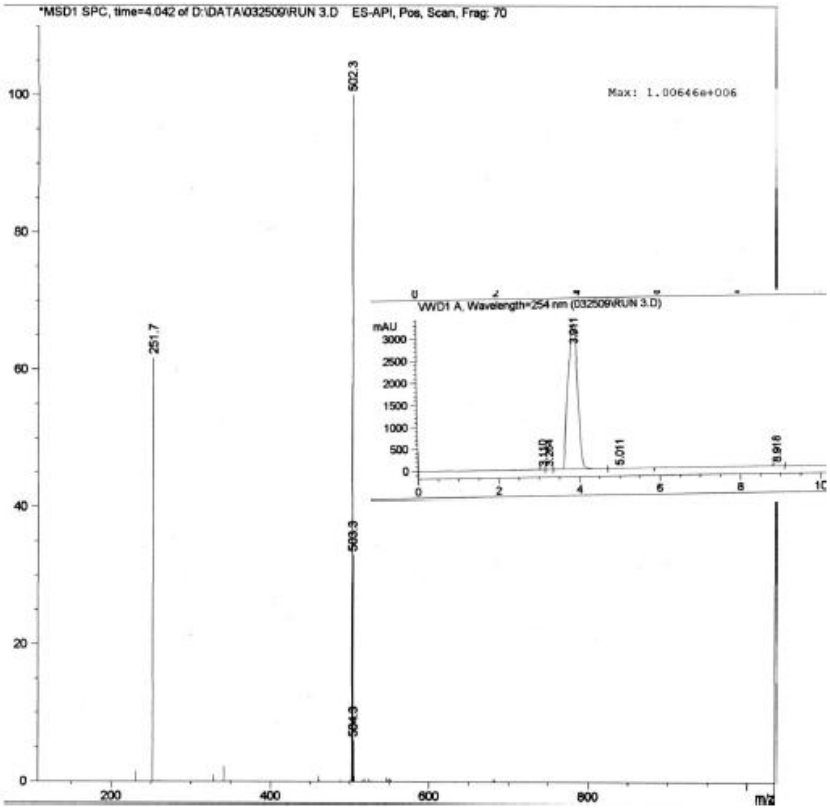

Fig. 2.24: LC-MS chromatogram of 3-*O*-acetylmorphine-*S*-(-)-nornicotine carbamate codrug.

A second codrug was synthesized in this series which incorporated two molecules of *S*-(-)-nornicotine with one molecule of morphine. In the preparation of this novel codrug, morphine was allowed to react with excess of *p*-nitrophenyl chloroformate to afford a dicarbonate ester derivative of morphine with two equivalents of *p*-nitrophenol (Scheme 2.18). The structure of the intermediate in this synthesis was confirmed by mass spectrometry and ^{1}H- and ^{13}C-NMR spectroscopy.

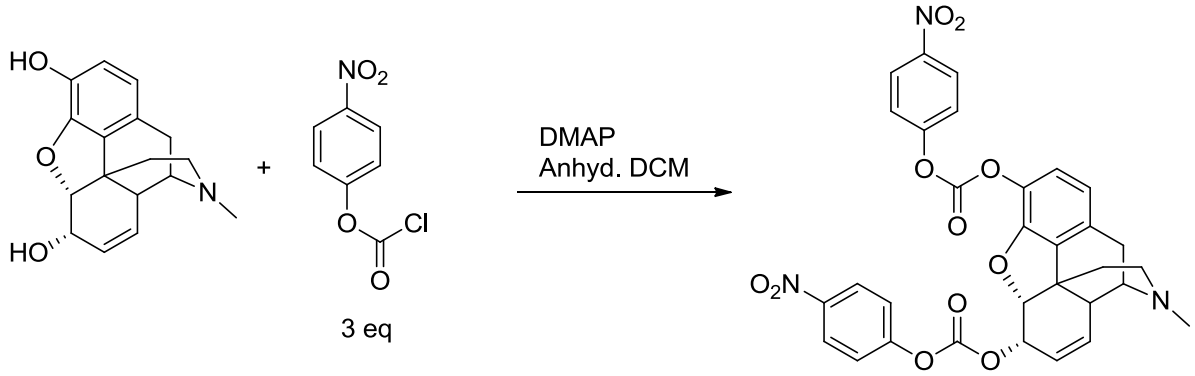

Scheme 2.18: Synthesis of the dicarbonate ester derivative of morphine and *p*-nitrophenol.

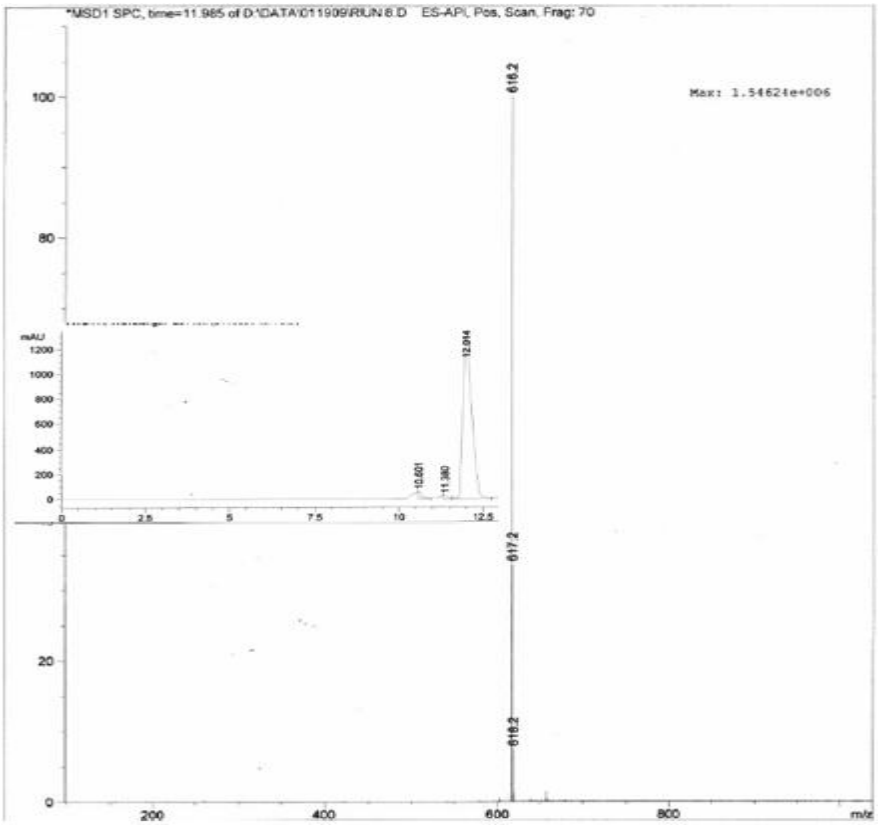

Fig. 2.25: LC-MS analysis of the dicarbonate ester derivative of morphine and *p*-nitrophenol.

The *p*-nitrophenol dicarbonate ester of morphine was then allowed to react with *S*-(-)-nornicotine to yield morphine-*bis*-*S*-(-)-nornicotine codrug. The structure of the codrug was confirmed by LC-MS.

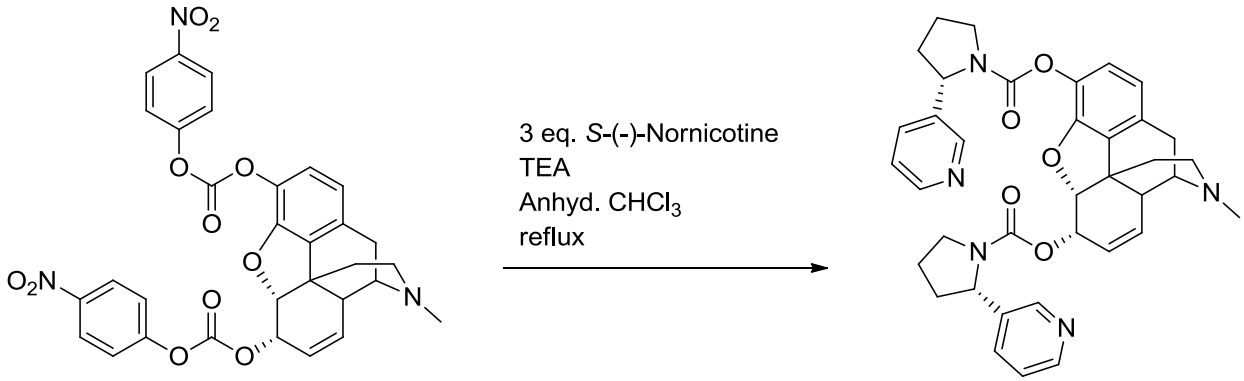

Scheme 2.19: Synthesis of the morphine-*S*-(-)-nornicotine dicarbamate codrug.

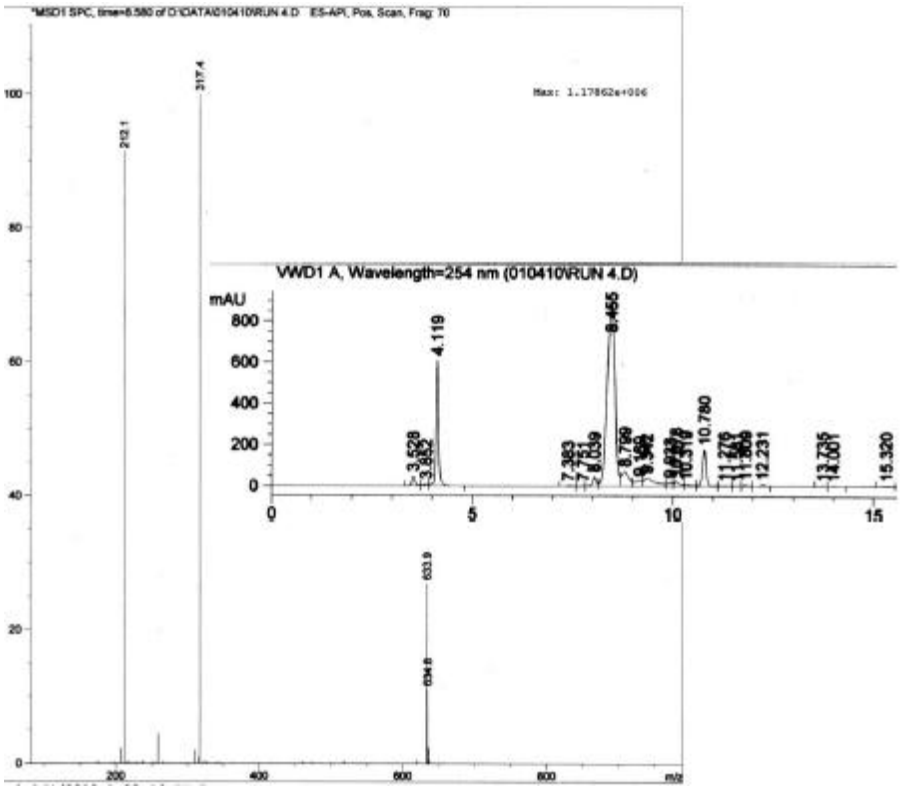

Fig. 2.26: LC-MS analysis of morphine-*S*-(-)-nornicotine dicarbamate codrug.

The last codrug to be synthesized in this series was the *S*-(-)-nornicotine-morphine carbamate codrug in which the *S*-(-)-nornicotine moiety was connected to the 3-hydroxy group of morphine (instead of the 6-hydroxy group). Initially, conjugation reactions were carried out utilizing different bases and conditions to selectively form the 3-oxy carbonate (avoiding formation of 6-oxy carbonate product). In the first attempt, morphine was allowed to react with 1 equivalent of *p*-nitrophenyl chloroformate in presence of 1 equivalent of DMAP at 0 °C. This reaction turned out to be non-selective, producing a mixture of three different carbonate conjugates of morphine, as shown in Scheme 2.20.

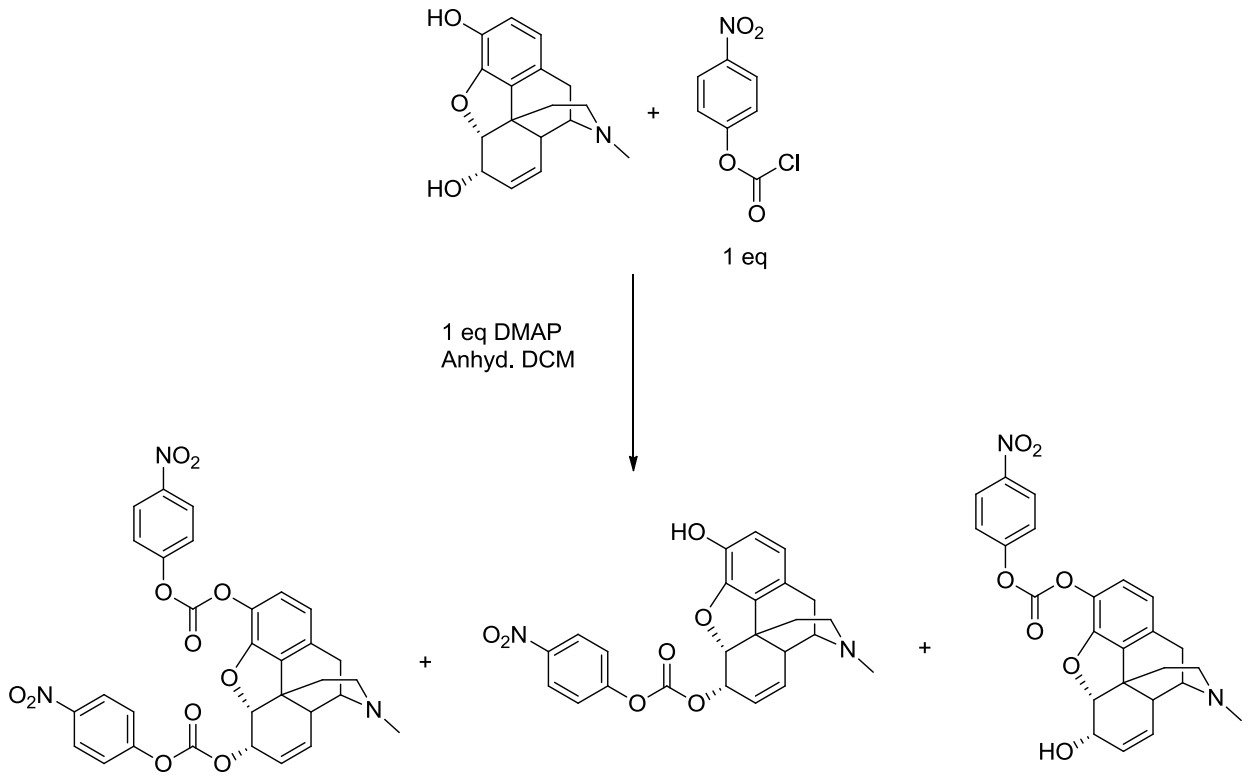

Scheme 2.20: Reaction of morphine with 1 equivalent of *p*-nitrophenyl chloroformate in presence of DMAP at 0 °C.

In another attempt, 1 equivalent of a strong alkali base (NaH) was utilized along with 1 equivalent of *p*-nitrophenyl chloroformate to form the desired 3-oxy carbonate of morphine and *p*-nitrophenol. This reaction showed better regioselectivity although formation of 6-oxy carbonate could not be completely avoided. The purification of the 3-oxy carbonate from the mixture of 3-oxy and 6-oxy carbonates was nearly impossible, due to their very similar R_f values, and also due to the reactivity of the *p*-nitrophenoxy carbonate conjugates with methanol in presence of silica; thus, a different synthetic scheme was sought.

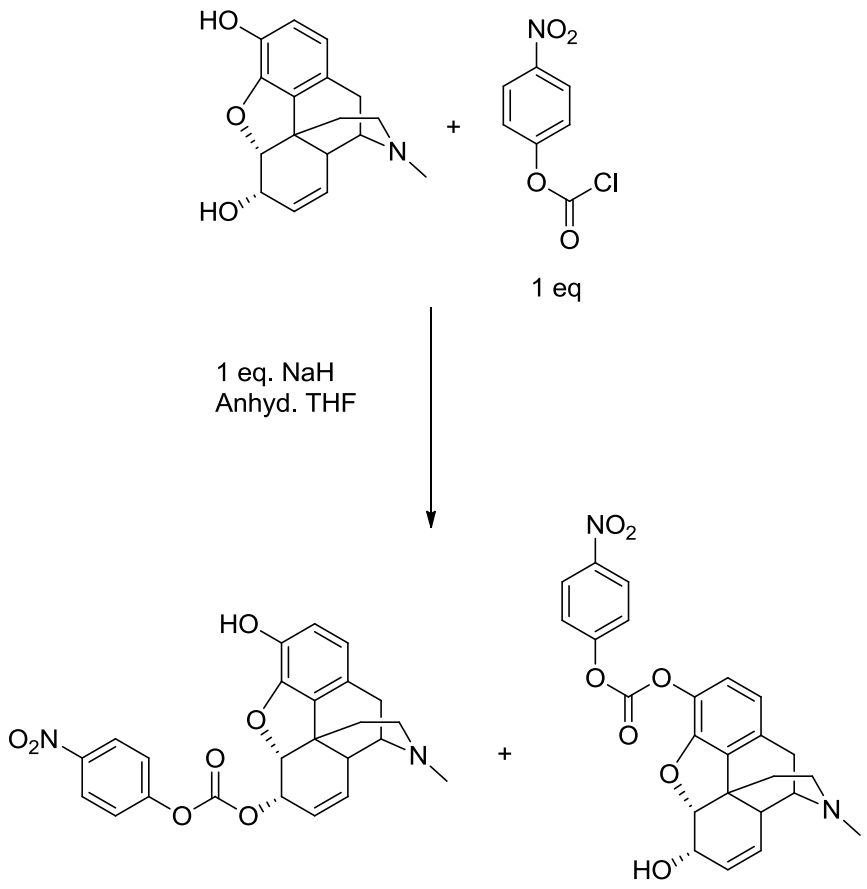

Scheme 2.21: Reaction of morphine with 1 equivalent of *p*-nitrophenyl chloroformate in the presence of NaH.

In a different synthetic strategy *S*-(-)-nornicotine was converted into its *p*-nitrophenoxy carbamate derivative using *p*-nitrophenyl chloroformate (Scheme 2.22). The structure of the carbamate conjugate was confirmed by GC-MS analysis and ^{1}H- and ^{13}C-NMR spectroscopy.

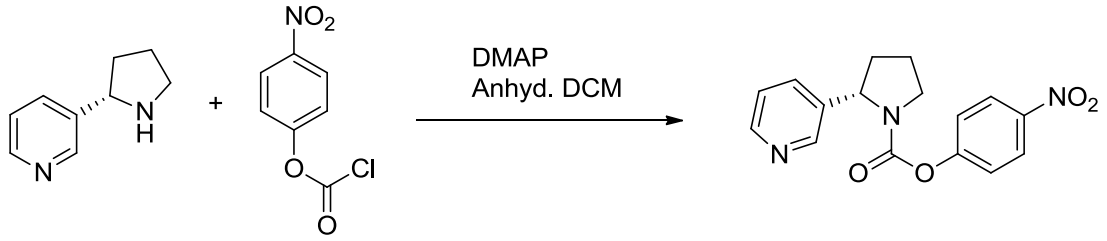

Scheme 2.22: Synthesis of the *p*-nitrophenoxy carbamate derivative of *S*-(-)-nornicotine.

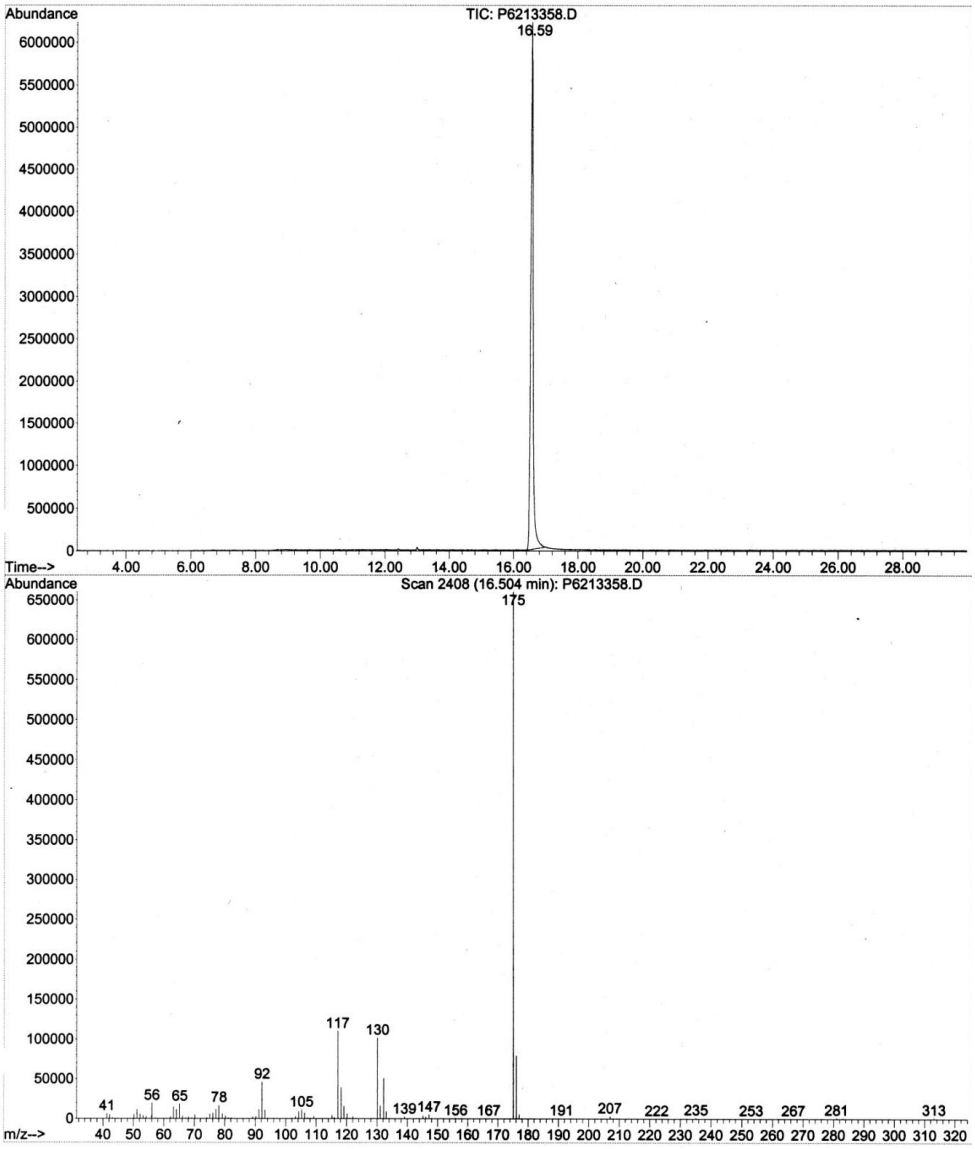

Fig. 2.27: GC-MS analysis of the *p*-nitrophenoxy carbamate of *S*-(-)-nornicotine.

The *p*-nitrophenoxy carbamate of *S*-(-)-nornicotine was then allowed to react with morphine in the presence of 1 equivalent of NaH. This reaction yielded the 3-oxycarbamate conjugate of morphine linked with *S*-(-)-nornicotine.

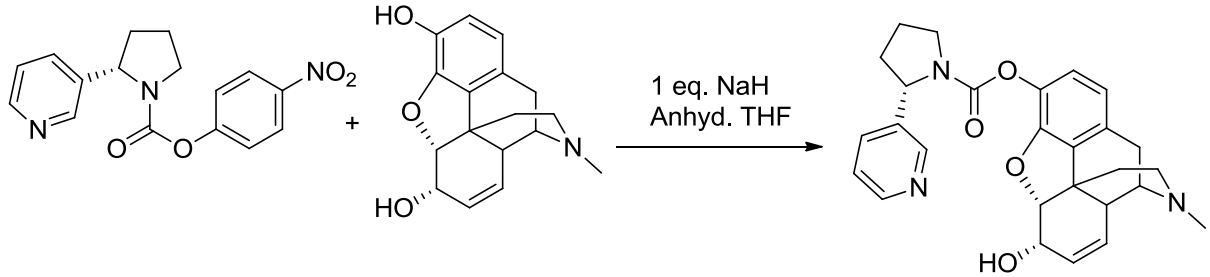

Scheme 2.23: Synthesis of morphine-*S*-(-)-nornicotine carbamate (3-oxy) codrug.

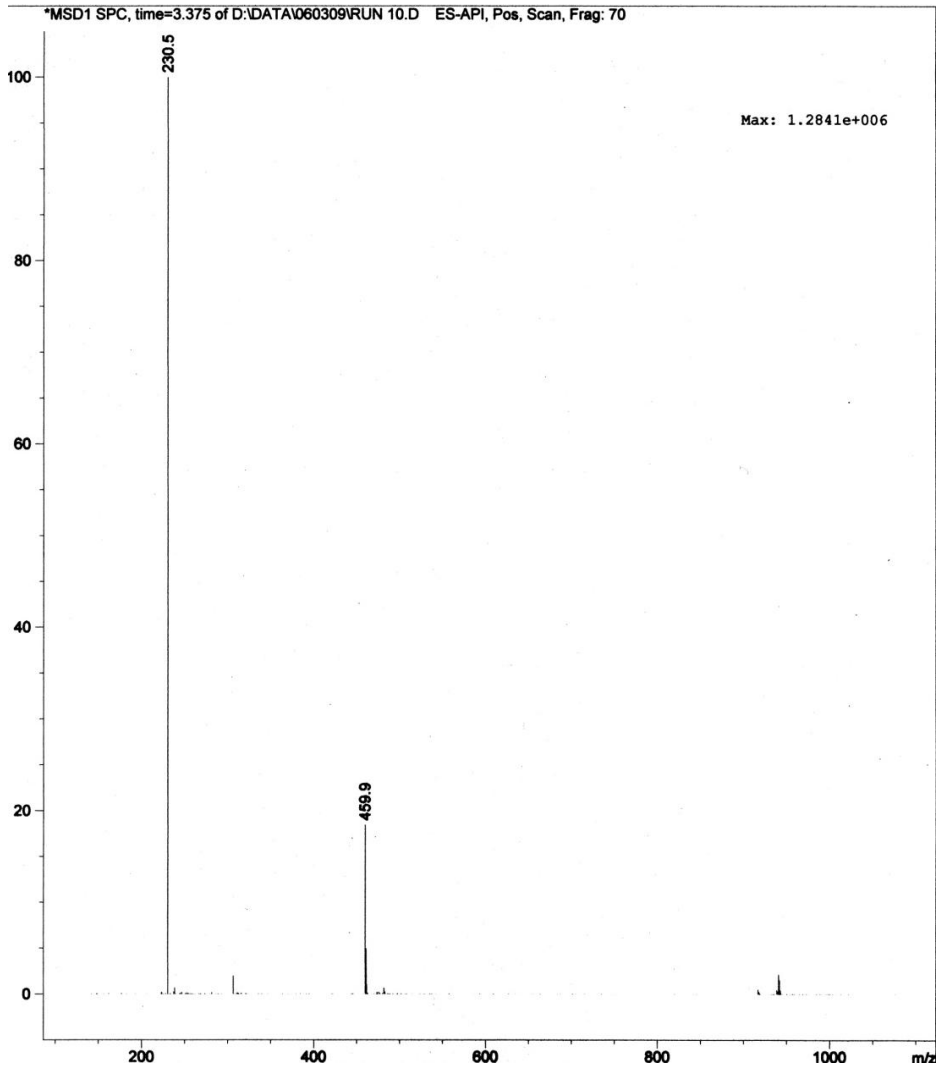

Fig. 2.28: Mass spectrum of morphine-*S*-(-)-nornicotine carbamate (3-oxy) codrug.

2.3.2 Opioid-Ketamine/Norketamine Codrugs Syntheses

After completing the syntheses of the opioid-*S*-(-)-nornicotine codrug series, the next series of codrugs to be synthesized were opioid - NMDA receptor antagonist conjugates. Racemic ketamine and racemic norketamine were chosen as NMDA receptor antagonist molecules. As racemic ketamine and racemic norketamine were used for the synthesis of opioid-ketamine and opioid-norketamine codrugs, a mixture of diastereomeric codrugs were obtained in each case. The first synthetic target was a codrug containing ketamine and codeine. Since codeine contains an allylic alcohol and ketamine is a secondary amine, a carbamate linkage was utilized to conjugate these two molecules. The previously developed synthetic strategies to form carbamate linkages in the previous examples were utilized for synthesis of the desired opioid-ketamine codrugs. The *p*-nitrophenoxy carbonate ester of codeine was allowed to react with ketamine in the presence of DMAP. The progress of the reaction was monitored by TLC. Reflux conditions utilizing several different solvents were attempted but none afforded product. ESI-MS analysis of the reaction mixture did not afford any proof of product formation. Failure of the carbamoylation reaction could be due to steric hindrance around the secondary amino group of the ketamine molecule.

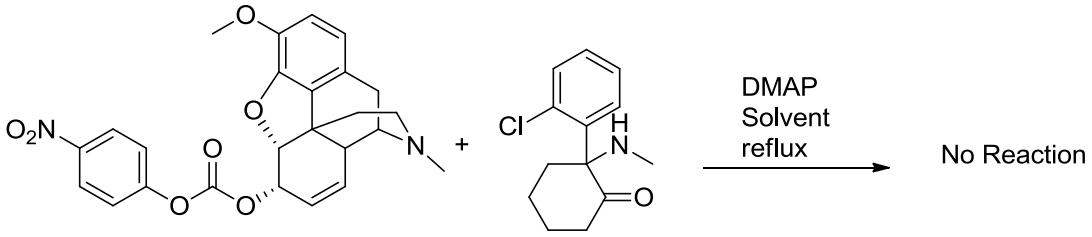

Scheme 2.24: Reaction between the *p*-nitrophenoxy carbonate ester of codeine and ketamine.

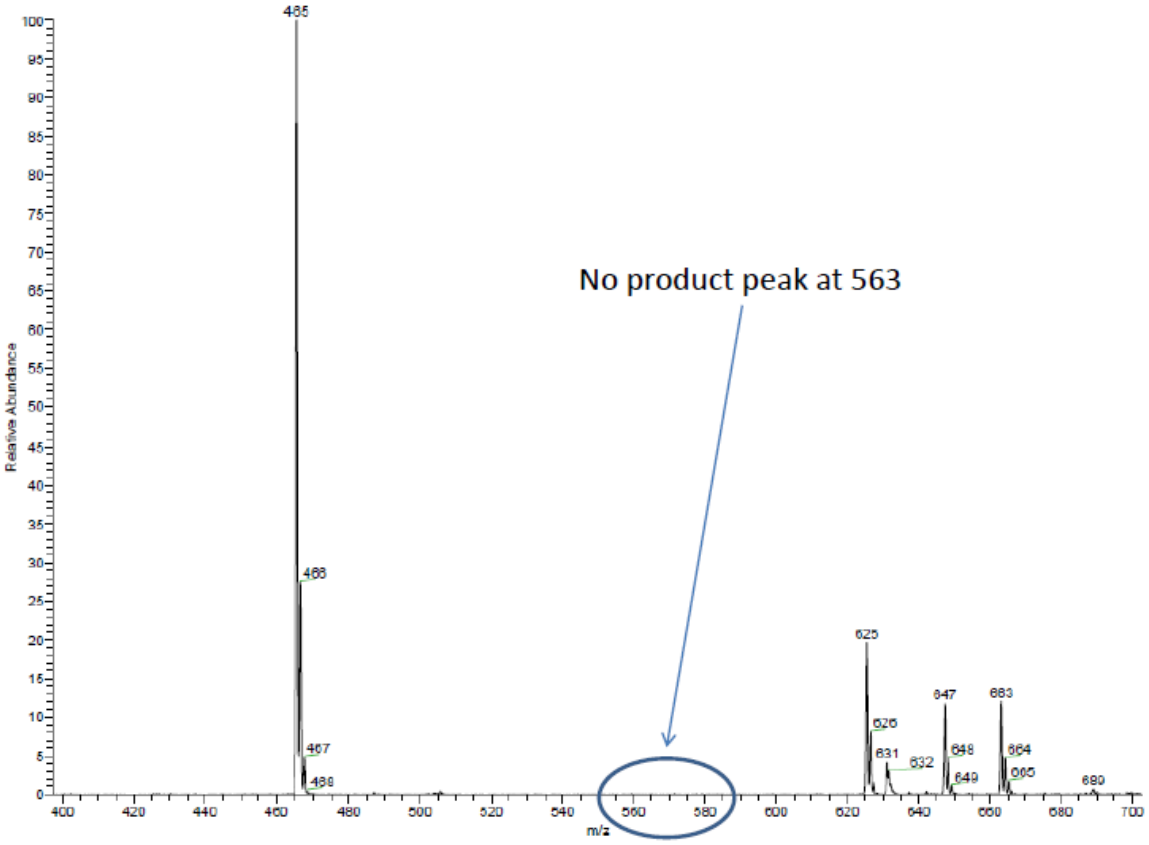

Fig. 2.29: ESI-MS analysis of the mixture from the reaction of ketamine with the *p*-nitrophenoxy carbonate ester of codeine.

In a second attempt to form the ketamine-codeine carbamate conjugate, an initial reaction was carried out to synthesize the *p*-nitrophenoxy carbamate of ketamine followed by subsequent reaction with codeine. Thus, a mixture of ketamine and *p*-nitrophenyl chloroformate was refluxed in presence of Na_2CO_3. This reaction yielded the desired carbamate product (Crooks and Rivera, 2004).

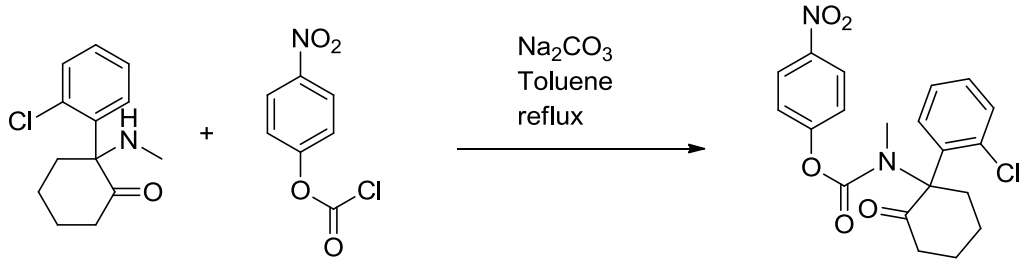

Scheme 2.25: Synthesis of the *p*-nitrophenoxy carbamate derivative of ketamine.

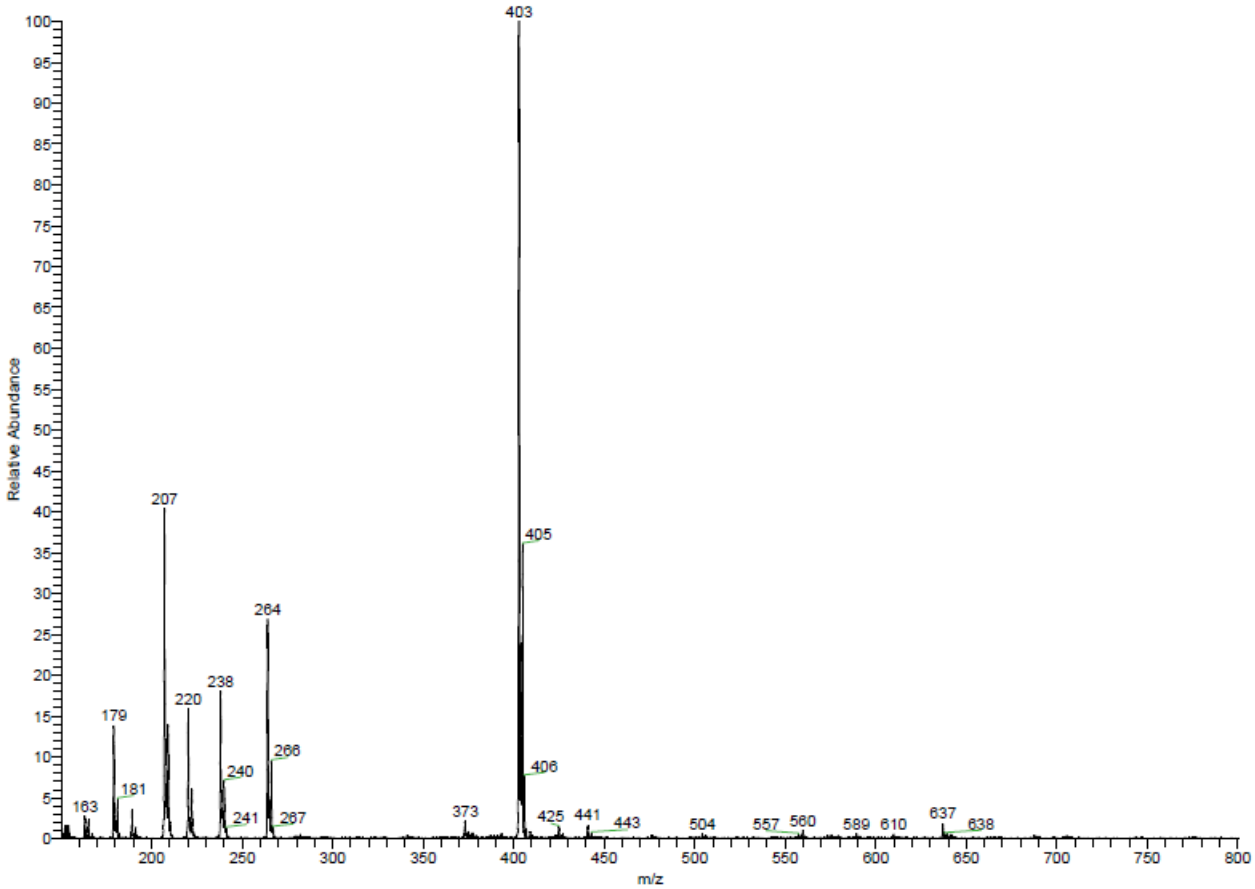

Fig. 2.30: ESI-MS analysis of the *p*-nitrophenoxy carbamate of ketamine.

The *p*-nitrophenoxy carbamate conjugate of ketamine was then allowed to react with codeine in presence of NaH. Since the ketamine utilized was racemic ketamine, the

reaction yielded a diastereomeric mixture of two codeine-ketamine codrugs. The two diastereomers of the desired codrug could not be separated by column chromatography.

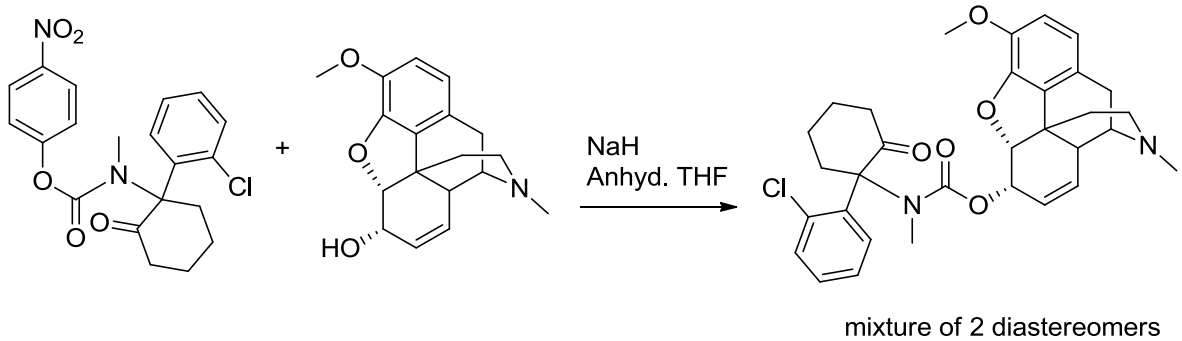

Scheme 2.26: Synthesis of codeine-ketamine codrug (diastereomeric mixture).

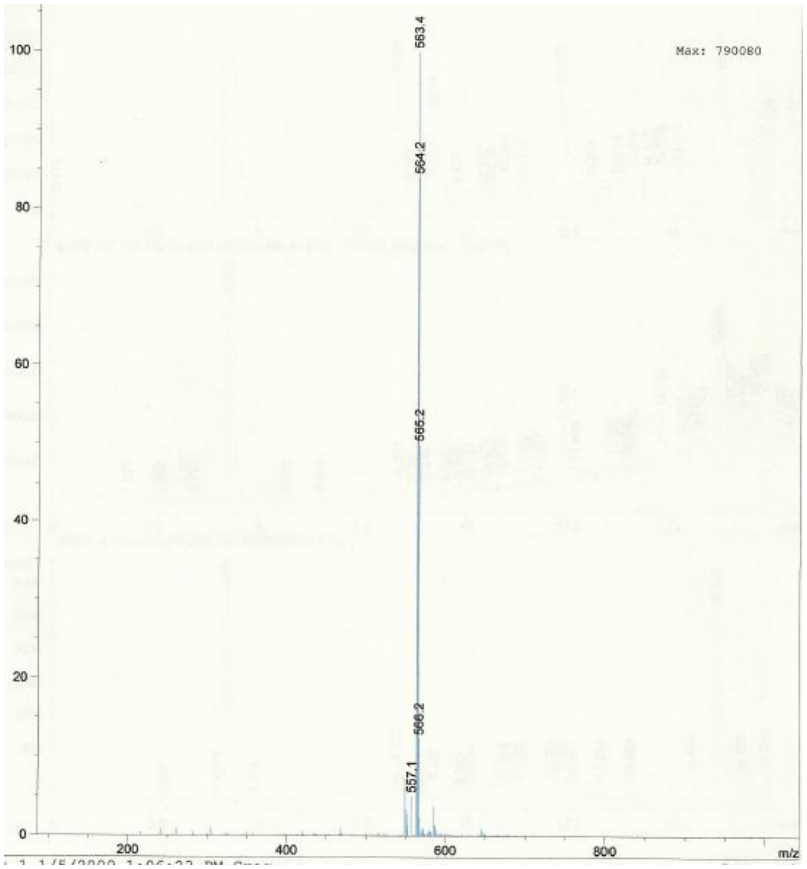

Fig. 2.31: ESI-MS of ketamine-codeine carbamate codrug.

A codeine-norketamine codrug was synthesized by first converting racemic norketamine into the *p*-nitrophenoxy carbamate conjugate followed by reaction with codeine in the presence of NaH. The reaction produced a diastereomeric mixture of two codeine-norketamine codrugs. The two diastereomers could not be separated by column chromatography, but under HPLC analysis the diastereomeric mixture exhibited two separate peaks.

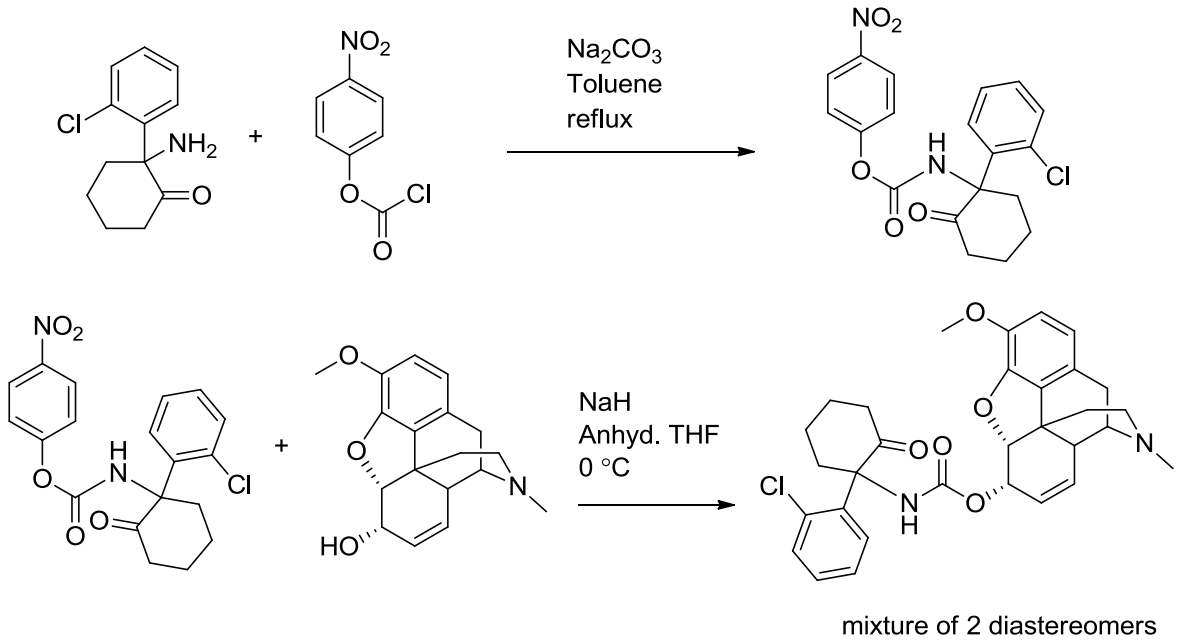

Scheme 2.27: Synthesis of codeine-norketamine codrug (diastereomeric mixture).

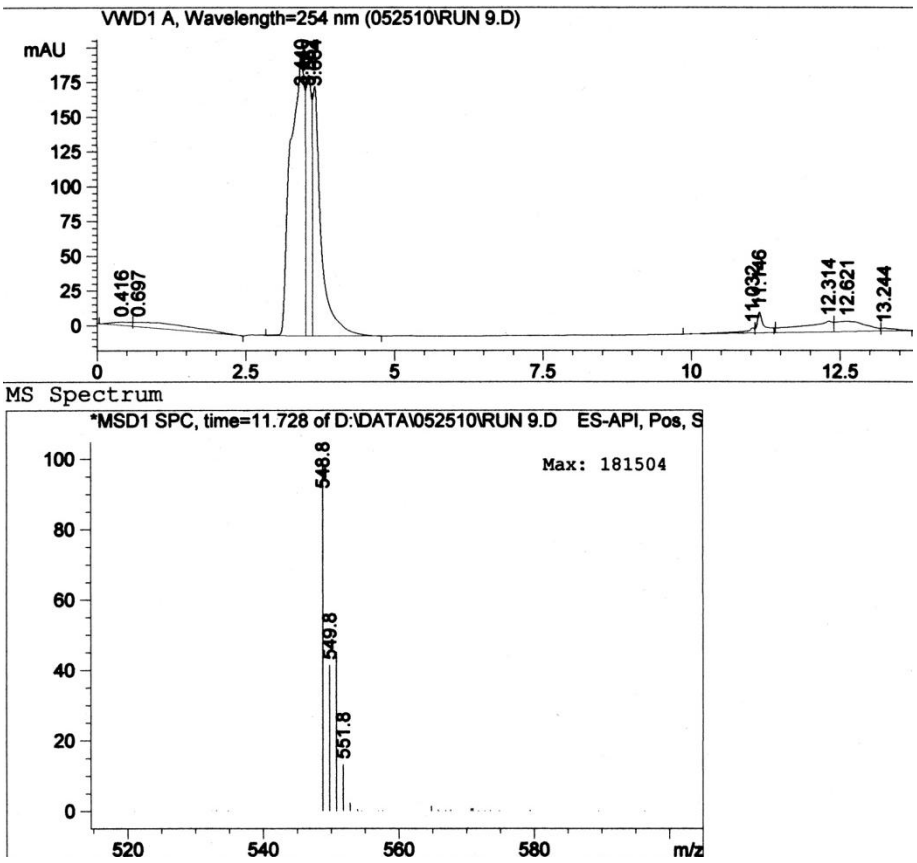

Fig. 2.32: LC-MS chromatogram of codeine-norketamine codrug.

Using a similar synthetic strategy, a codrug containing morphine and racemic norketamine was synthesized. The *p*-nitrophenoxy carbamate conjugate of norketamine was allowed to react with morphine in the presence of 1 equivalent of NaH. This yielded a diastereomeric mixture of the carbamate codrug of morphine and racemic norketamine. One equivalent of NaH allowed the selective deprotonation of the 3-hydroxy group of morphine followed by its nucleophlic attack on the carbamate linkage of the norketamine-*p*-nitrophenol conjugate. Formation of the desired carbamate codrug was confirmed by ^{1}H- and ^{13}C-NMR spectroscopy and mass spectrometry. Column chromatographic separation of the two diastereomers could not be achieved due to the very similar R_f values of both diastereomers. Peaks corresponding to the two diastereomeric codrugs could be observed in the HPLC-diode array assay.

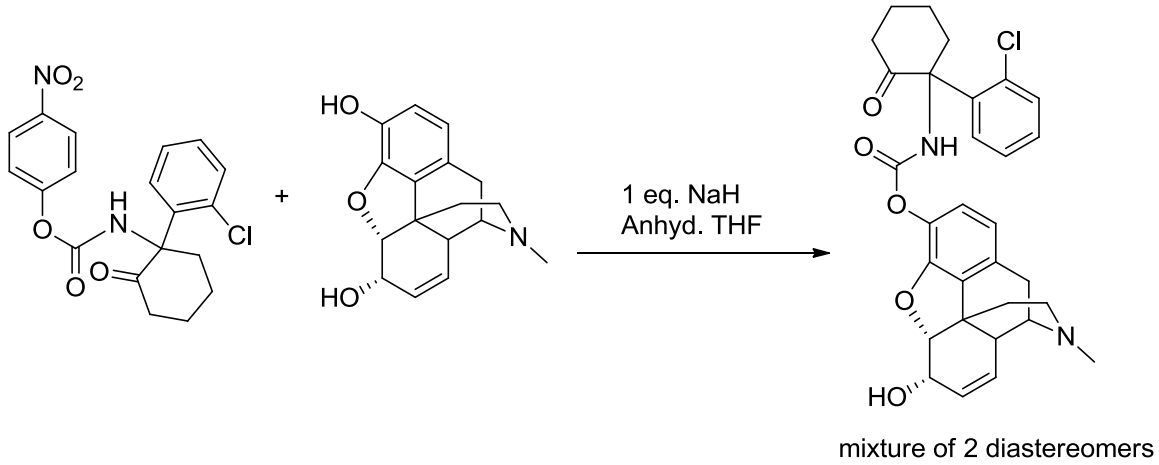

Scheme 2.28: Synthesis of morphine-norketamine codrug (diastereomeric mixture).

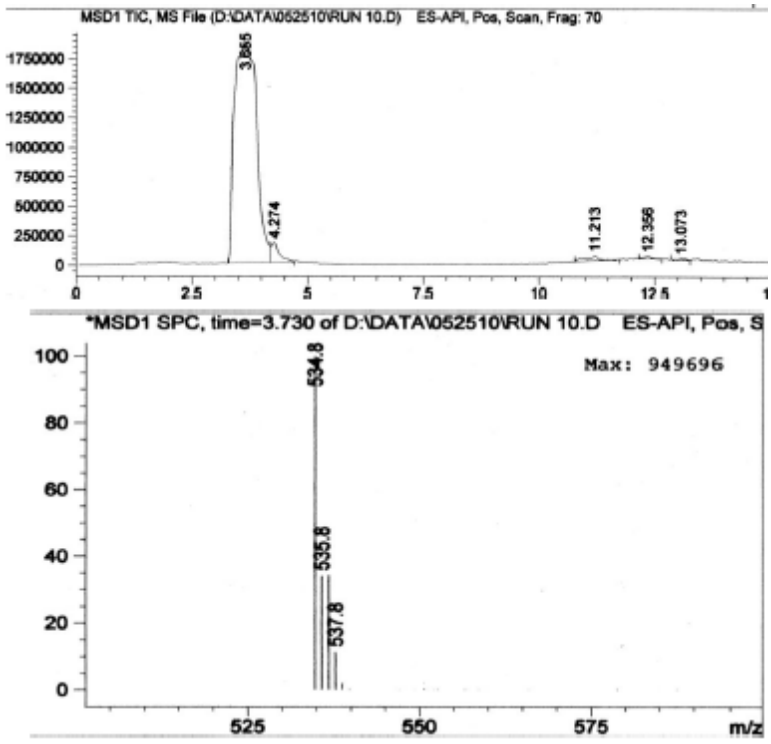

Fig. 2.33: LC-MS chromatogram of morphine-norketamine codrug.

2.3.3 Opioid-Gabapentin Codrugs Syntheses

The next series of codrugs that were synthesized were codrugs combining an opioid molecule with gabapentin (an anticonvulsant). The presence of a primary amino group and a carboxylic acid group in the gabapentin molecule makes this molecule more versatile in terms of its conjugation chemistry. Opioids can be joined to gabapentin through its amino group yielding a carbamate codrug, or can be connected to gabapentin via its carboxylic acid group yielding an ester codrug. Since an ester linkage is more susceptible to hydrolysis than a carbamate linkage, the first drug to be considered in this series was an ester codrug containing codeine as the opioid molecule. To prevent the likely internal cyclization of this codrug molecule, gabapentin has to be kept in the diprotonated amine form. The structure of the proposed ester codrug is shown in Fig. 2.34.

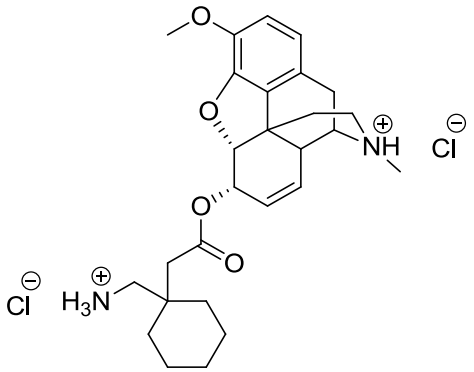

Fig. 2.34: Proposed structure of codeine-gabapentin ester codrug with protonated amines and chloride counterions.

Since all the codrugs thus far were targeted for oral delivery, the proposed codrug of codeine and gabapentin (Fig. 2.34) will likely be relatively stable in the acid pH of the stomach, but will be deprotonated in the alkaline pH of the intestine, which will generate a free primary amino group that will attack the adjacent ester moiety, leading to rapid ester cleavage of the codrug in the g.i. tract. Cleavage of the ester linkage will afford a 5-

membered lactam derivative of gabapentin as well as free codeine. This reaction would produce a very stable cyclic lactam of gabapentin, which might not be easily cleaved in vivo to produce gabapentin. Also, due to this intramolecular nucleophilic substitution, the codrug would likely cleave completely in the intestine before entering the systemic circulation. . To examine this hypothesis, the designed ester codrug was synthesized and its stability was determined in pH 7.4 buffer (the pH of the small intestine). Results of the stability studies will be discussed in the *in vitro* stability studies section of chapter 4.

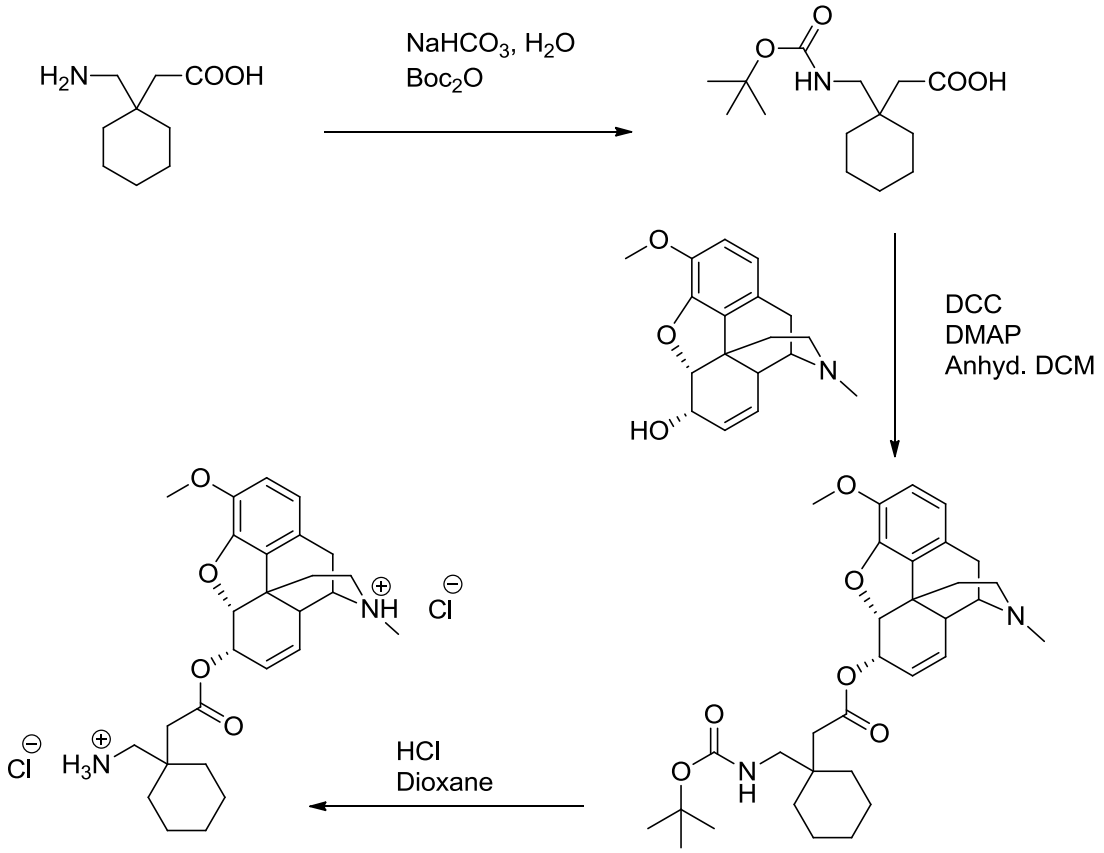

Scheme 2.29: Synthesis of the di-HCl salt of the codeine-gabapentin ester codrug.

In the preparation of the ester codrug, the primary amino group of gabapentin was protected initially with a BOC protecting group (Green and Wuts, 1999). The free carboxylic acid group of BOC-protected gabapentin was coupled with the alcoholic

group of codeine in the presence of DCC to generate an ester conjugate. The BOC-protected amino group of the ester conjugate was then deprotected to form the dihydrochloride salt of the ester codrug of codeine and gabapentin (Green and Wuts, 1999).

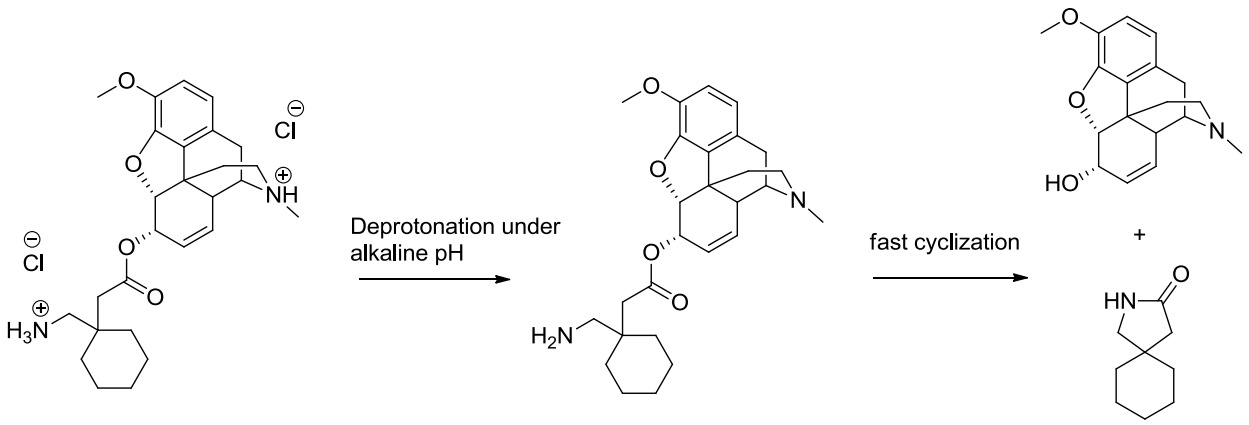

Scheme 2.30: Proposed in vivo hydrolytic behavior of the di-HCl salt of the codeine-gabapentin ester codrug.

Since the above ester codrug of codeine and gabapentin may suffer from instability in intestine, a carbamate codrug of gabapentin and codeine was designed by directly conjugating the amino group of gabapentin with the hydroxyl group of codeine. The *p*-nitrophenoxy carbonate ester of codeine was allowed to react with gabapentin to afford the desired carbamate codrug (Scheme 2.31) (Bolla et al., 2005). The structure of the desired codrug was confirmed by mass spectrometry and ^{1}H- and ^{13}C-NMR spectroscopy. The purity of the codrug was also determined by HPLC-diode array assay.

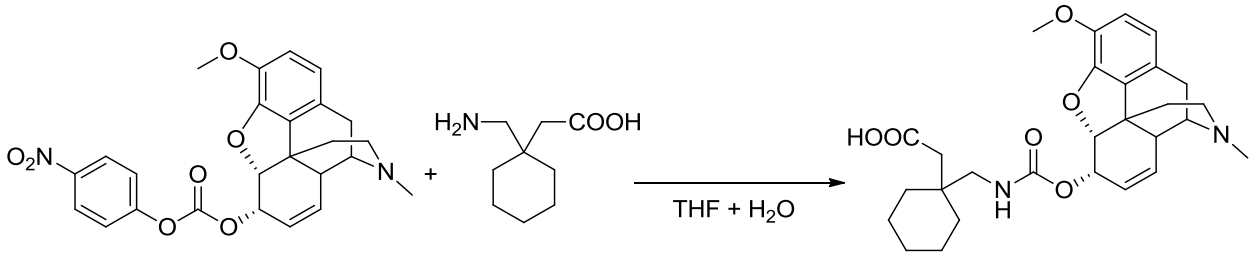

Scheme 2.31: Synthesis of the codeine-gabapentin carbamate codrug.

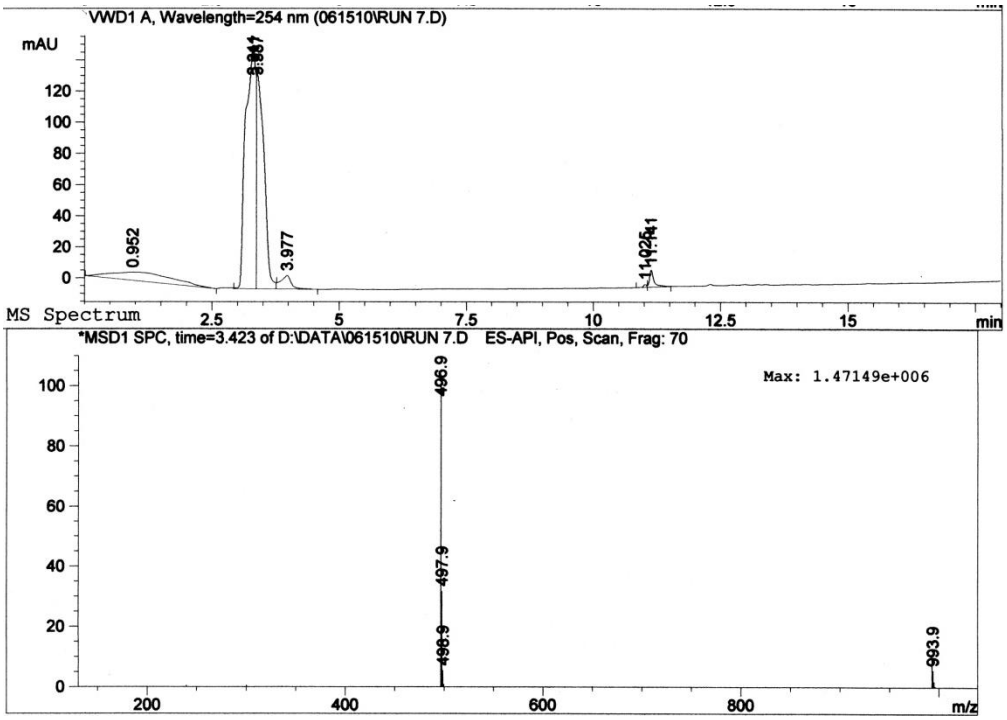

Fig. 2.35: LC-MS chromatogram of the gabapentin-codeine carbamate codrug.

Several other codrugs were designed by protecting the free amino group of gabapentin as a labile amide or carbamate and conjugating the carboxylic acid group of gabapentin with the 6-hydroxyl group of codeine through an ester linkage. In the first attempt, the amino group of gabapentin was protected as a simple amide which was then conjugated with codeine in the presence of DCC to form an ester linkage. The structure of the resulting codrug and the intermediate were confirmed by mass spectrometry and ^{1}H- and ^{13}C-NMR spectroscopy.

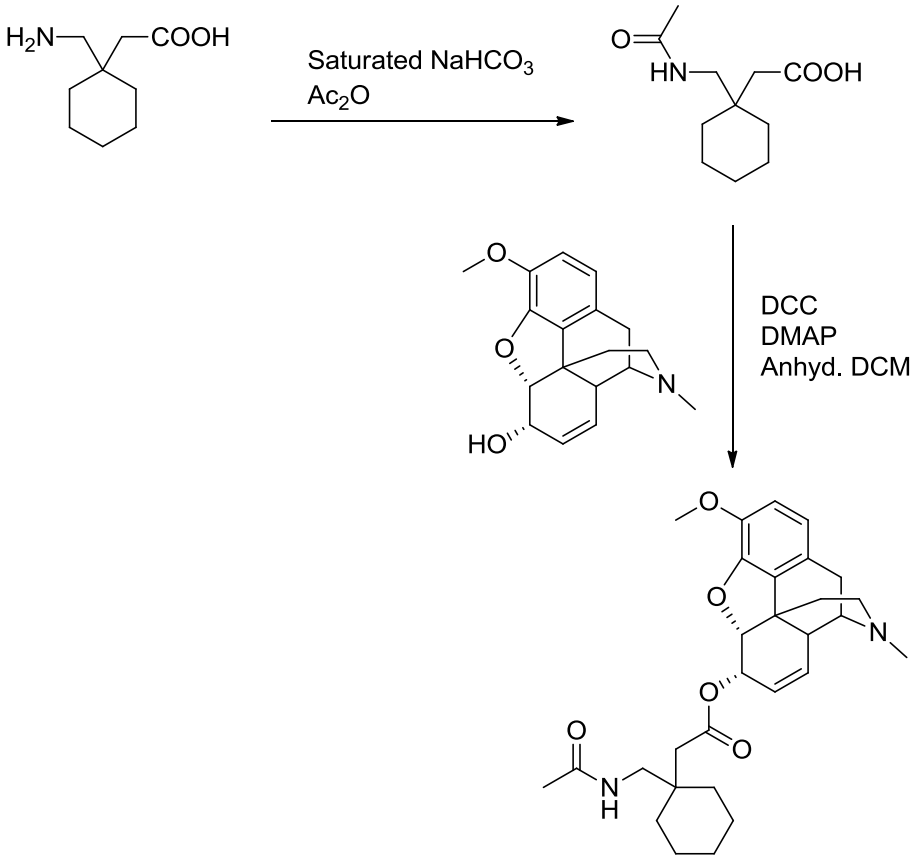

Scheme 2.32: Synthesis of the amide-protected ester codrug of codeine and gabapentin.

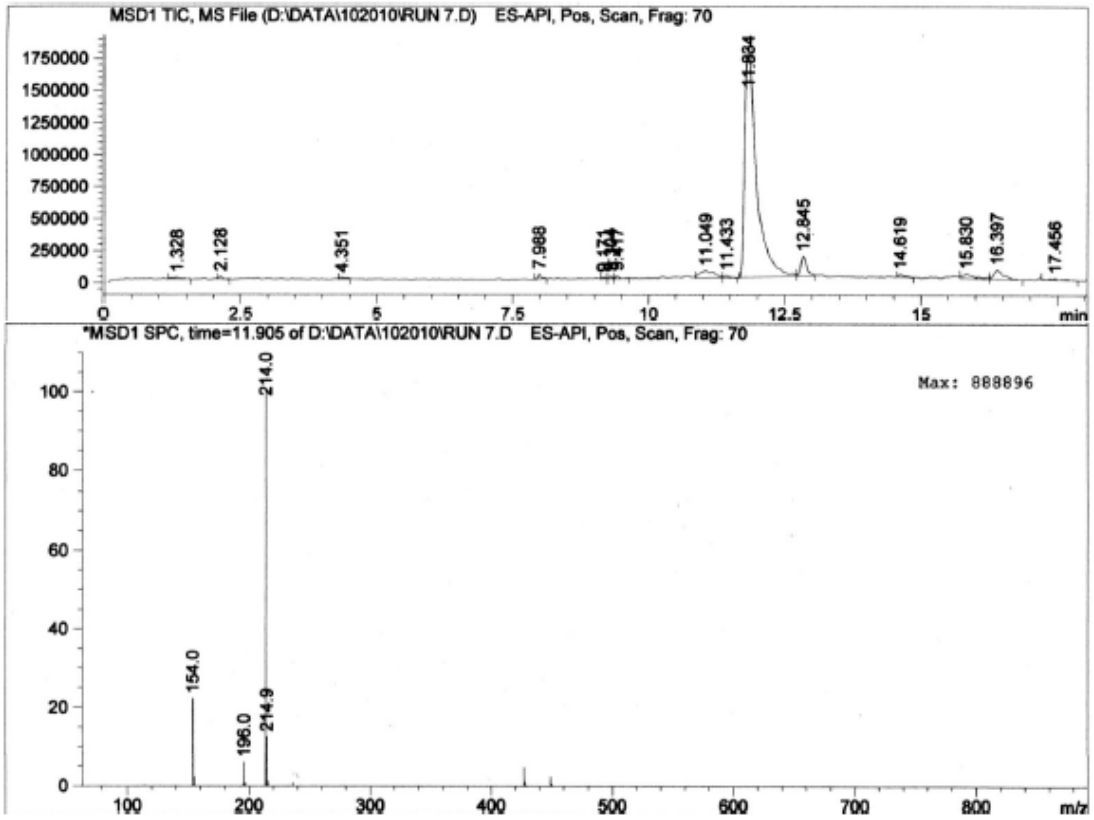

Fig. 2.36: LC-MS chromatogram of *N*-acetylgabapentin.

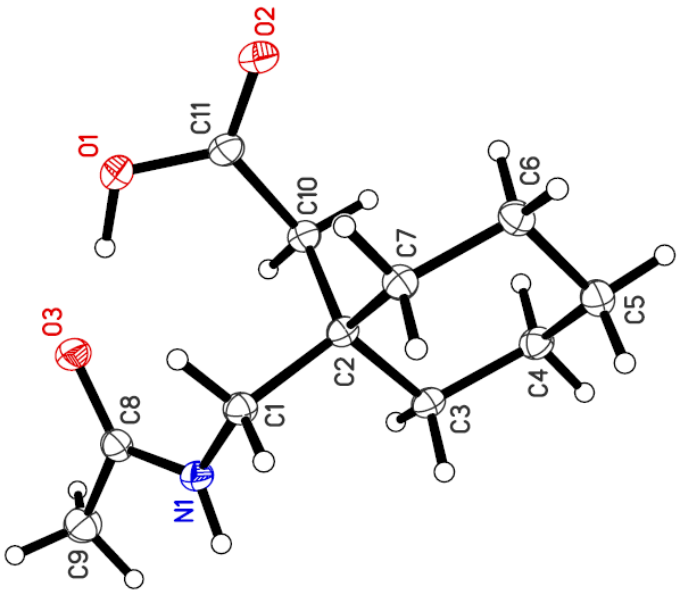

Fig. 2.37: Single crystal X-ray structure of *N*-acetylgabapentin.

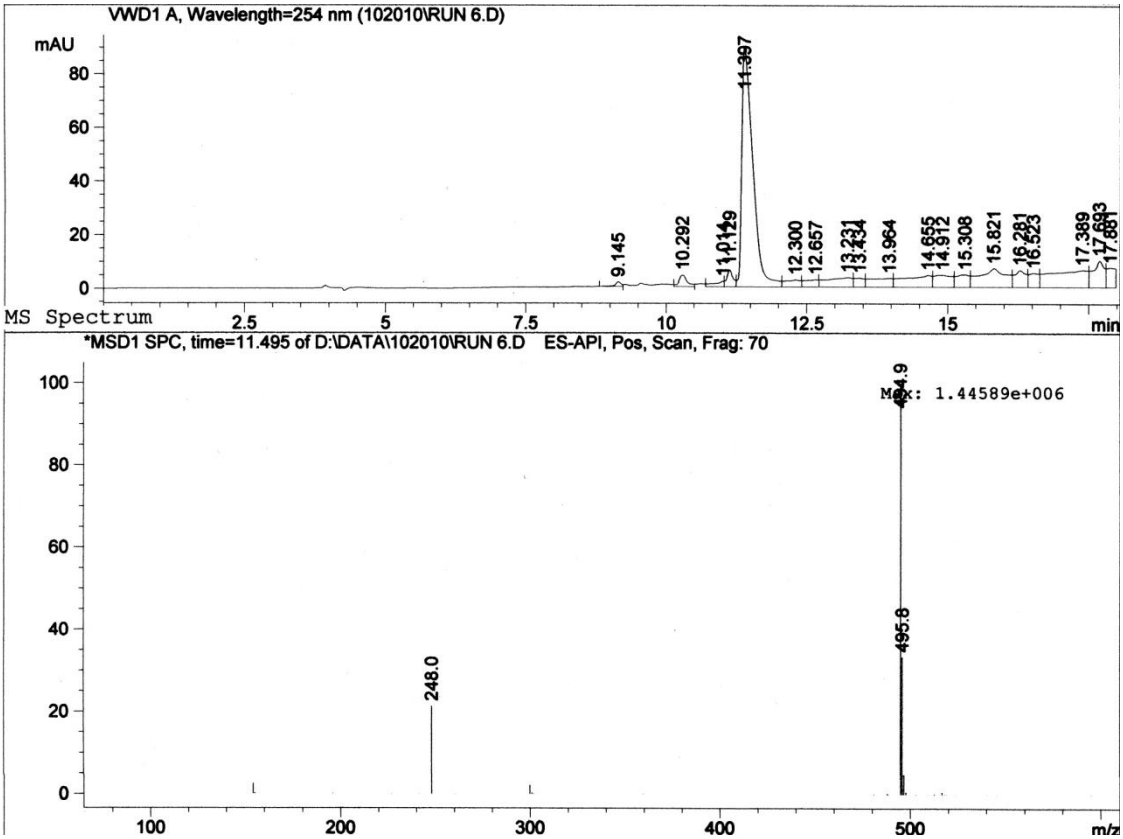

Fig. 2.38: LC-MS chromatogram of *N*-acetylgabapentin-codeine ester codrug.

In another attempt, the free amino group of gabapentin was protected as an ethanolic carbamate (Cundy et al., 2004) and then coupled with codeine following the same chemistry as previously described, to obtain a different ester linked codrug of gabapentin and codeine (Scheme 2.33).

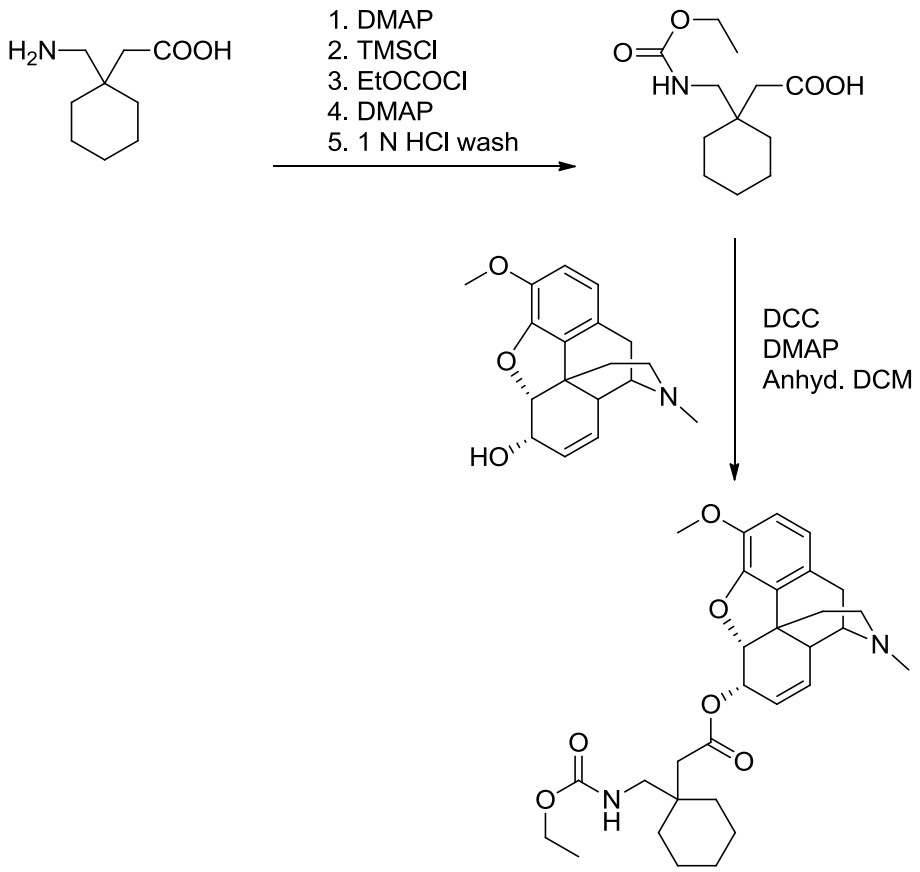

Scheme 2.33: Synthesis of an *N*-carbamate protected ester codrug of codeine and gabapentin.

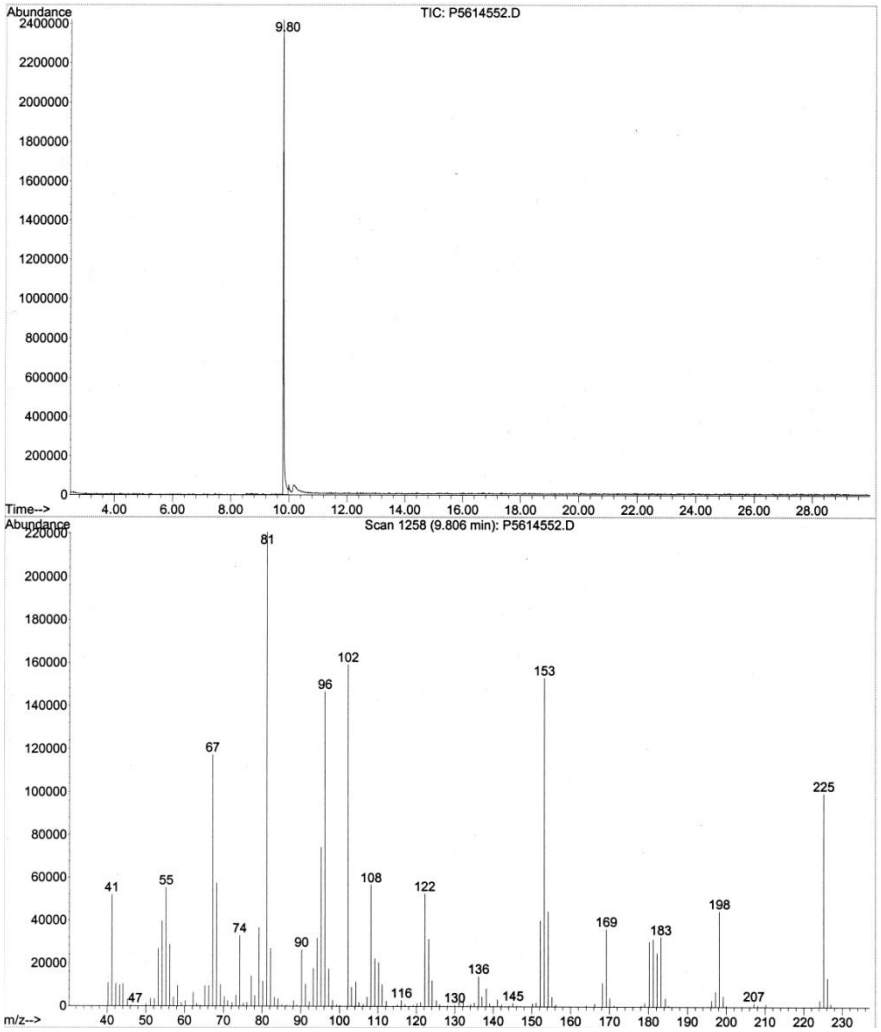

Fig. 2.39: GC-MS analysis of the *N*-ethyl carbamate of gabapentin (molecular mass corresponds to dehydration product).

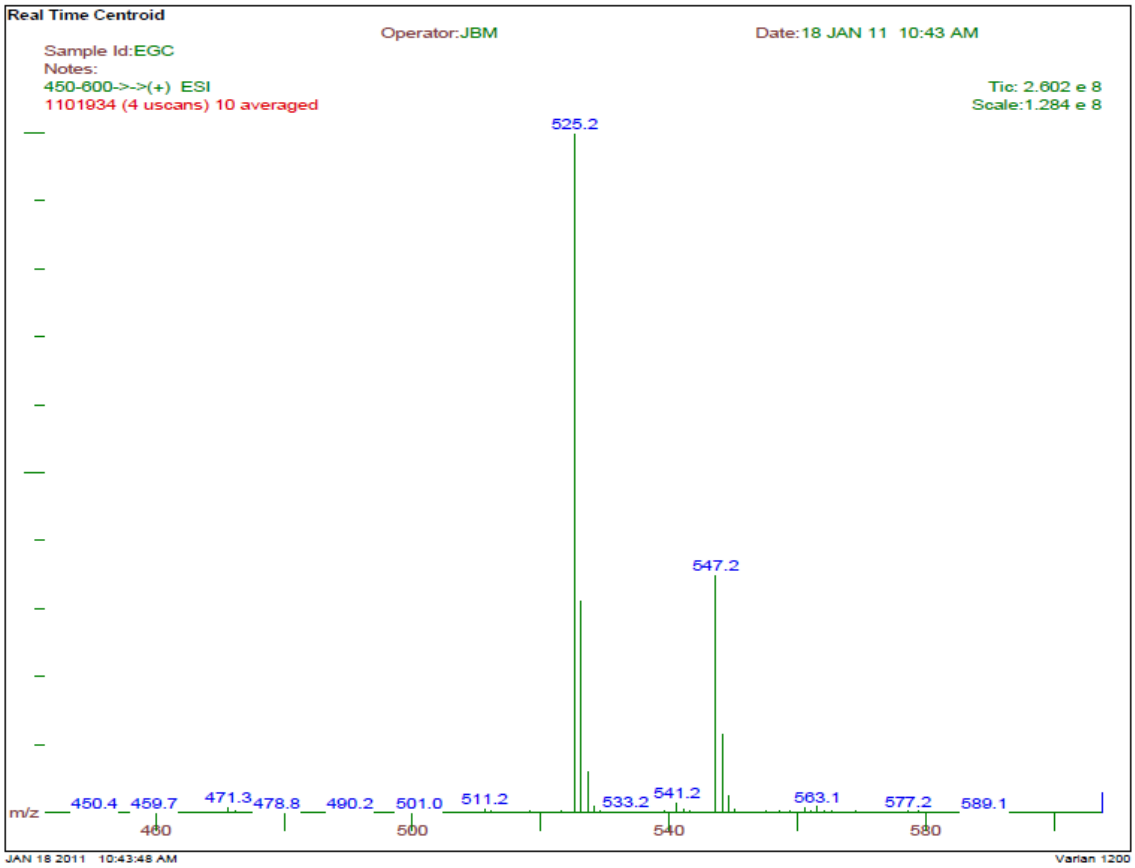

Fig. 2.40: ESI-MS analysis of carbamate N-protected ester codrug of codeine and gabapentin.

2.3.4 Attempt to Synthesis of Opioid-Δ^9-Tetrahydrocannbinol Codrug

The next series of codrugs to be synthesized were opioid-Δ^9-tetrahydrocannbinol (Δ^9-THC) codrugs. Morphine-Δ^9-THC and codeine-Δ^9-THC codrugs were synthesized and studied by Dhooper et al. (2006). Thus a different opioid (oxycodone) was chosen for this project. The proposed structure oxycodone-Δ^9-THC codrug contains a carbonate linkage between hydroxyl group of oxycodone and phenolic group of Δ^9-THC.

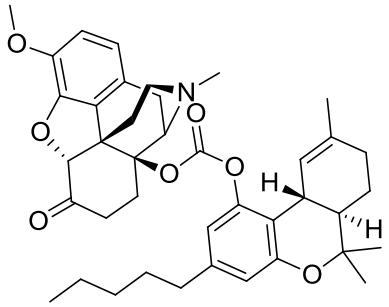

Fig. 2.41: Proposed structure of the oxycodone-Δ^9-THC codrug.

Several synthetic strategies can be planned to synthesize the desired codrug. The first synthetic route was based on conversion of oxycodone to its *p*-nitrophenoxy carbonate ester and then reaction between Δ^9-THC and *p*-nitrophenoxy carbonate ester of oxycodone to afford the carbonate codrug. In contrast to codeine and morphine, oxycodone does not contain a phenolic or allylic hydroxyl group; instead it has a very sterically hindered tertiary alcoholic group (the 14-hydroxy group). There are very few literature references that report any chemical modification of the 14-hydroxy group of oxycodone. Only two esters of oxycodone have previously been synthesized (Cami-Kobeci et al., 2009; Moynihan et al., 2009). It was initially planned to convert oxycodone to its *p*-nitrophenoxy carbonate analog to afford one component for the subsequent conjugation reaction with a second drug. A solution containing oxycodone, *p*-nitrophenyl chloroformate and DMAP was refluxed in anhydrous THF. After two days of continuous reflux, one new faint spot was observed by TLC analysis. GC-MS analysis of the reaction mixture showed a new peak of molecular mass 377 bearing the signature of the presence of one chlorine atom in the molecule. To enhance the rate of the reaction microwave irradiation was investigated.

Microwave heating has become a widely accepted, non-conventional heating source for improving the yields of organic reactions. The major advantage of using microwave irradiation as a source of heating is the spectacular acceleration of the reaction kinetics as compared to conventional heating. In addition to shorter reaction times, higher yields are generally achieved in microwave assisted organic synthesis

(Gabriel et al., 1998). Some reactions which cannot be performed by conventional heating can be done using microwave irradiation (Gabriel et al., 1998). Greatly accelerated reaction rates under microwave heating are generally explained in terms of a combination of thermal and non-thermal effects. Thermal effects may include overheating, hotspots and selective heating, and non-thermal effects incorporate changes in mobility and diffusion increasing the probabilities of effective contacts and the effects of a highly polarizing field (Roberts and Straus, 2005).

Thermal Effects

The microwave heating technique utilizes the ability of some compounds to transform electromagnetic irradiation into heat. Conventional heating, in contrast, relies on convection and conduction of heat. Microwave heating is rapid and volumetric, meaning the whole material is heated up simultaneously and very rapidly. On the other hand, conventional heating is superficial and relatively slow. The magnitude of heating in the case of microwave irradiation depends on the dielectric properties of the solvent or the reactants, thus making it a selective heating procedure (Lew et al., 2002).

Overheating of polar liquids through microwave irradiation is also instrumental in rate enhancement in microwave assisted organic synthesis. Generally overheating in the range of 13-26 °C above the normal boiling point is observed in polar liquids when heated under microwave conditions (Hoz et al., 2004). The major reason behind the overheating is inverted heat transfer, i.e. heating occurs from the irradiated mass towards the exterior. Overheating under microwave condition is helpful in improving the yields and efficiency of many chemical reactions. “Hot spots” in microwave irradiated samples are also considered as one of the thermal effects. Hot spots are defined as certain zones within the sample being irradiated with microwaves whose temperature is much greater than the macroscopic temperature of the sample. This effect is caused by the inhomogeneity of the applied field. In addition to these thermal effects, another advantage of microwave heating is its selective nature. Microwaves cause rapid heating of polar substances while nonpolar substances are not able to absorb microwave radiation, and as a consequence are not heated (Jacob et al., 1995).

Non-thermal effects

The presence of non-thermal effects in addition to thermal effects is still being debated. In an experiment carried out by Berlan et al.,(1999) cycloaddition reactions were carried out under reflux conditions in nonpolar solvents under conventional heating and under microwave conditions at the same temperature. Reaction rates were observed to be faster under microwave irradiation, even though the temperature was maintained the same and poorly microwave absorbing nonpolar solvents were used. The authors proposed a decreased free energy of activation through a change in the entropy of the system as an explanation of the observed phenomenon. It is also believed that microwave causes rapid rotation of the polarized dipoles in the molecules generating heat due to friction, and also increases the probability of contact between molecules and atoms. Increased probability of contact will increase the rate of the reaction and also will decrease the activation energy (Hoz et al., 2004).

Since the microwave approach is proven to be more efficient than conventional heating, microwave irradiation was utilized in an attempt to increase the rate of reaction between oxycodone and *p*-nitrophenyl chloroformate. Oxycodone, *p*-nitrophenyl chloroformate and DMAP were dissolved in anhydrous THF and the reaction mixture was irradiated in a microwave unit to achieve a reaction temperature of 170 °C. The reaction temperature was maintained at 170 °C for 4 minutes. GC-MS analysis of the reaction mixture showed an intense peak of molecular mass 377. This mass does not correspond to the molecular mass of the desired *p*-nitrophenoxy carbonate ester of oxycodone and the pattern of isotopic peaks in the mass spectrum of the compound indicated the presence of chlorine in the synthesized compound.

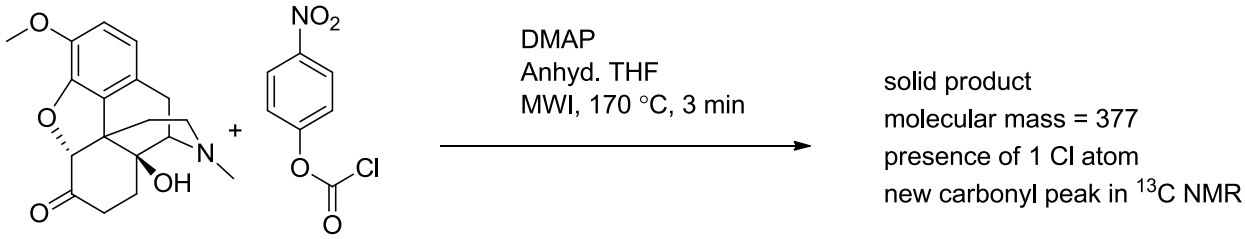

Scheme 2.34: Reaction between oxycodone and *p*-nitrophenyl chloroformate under microwave heating conditions.

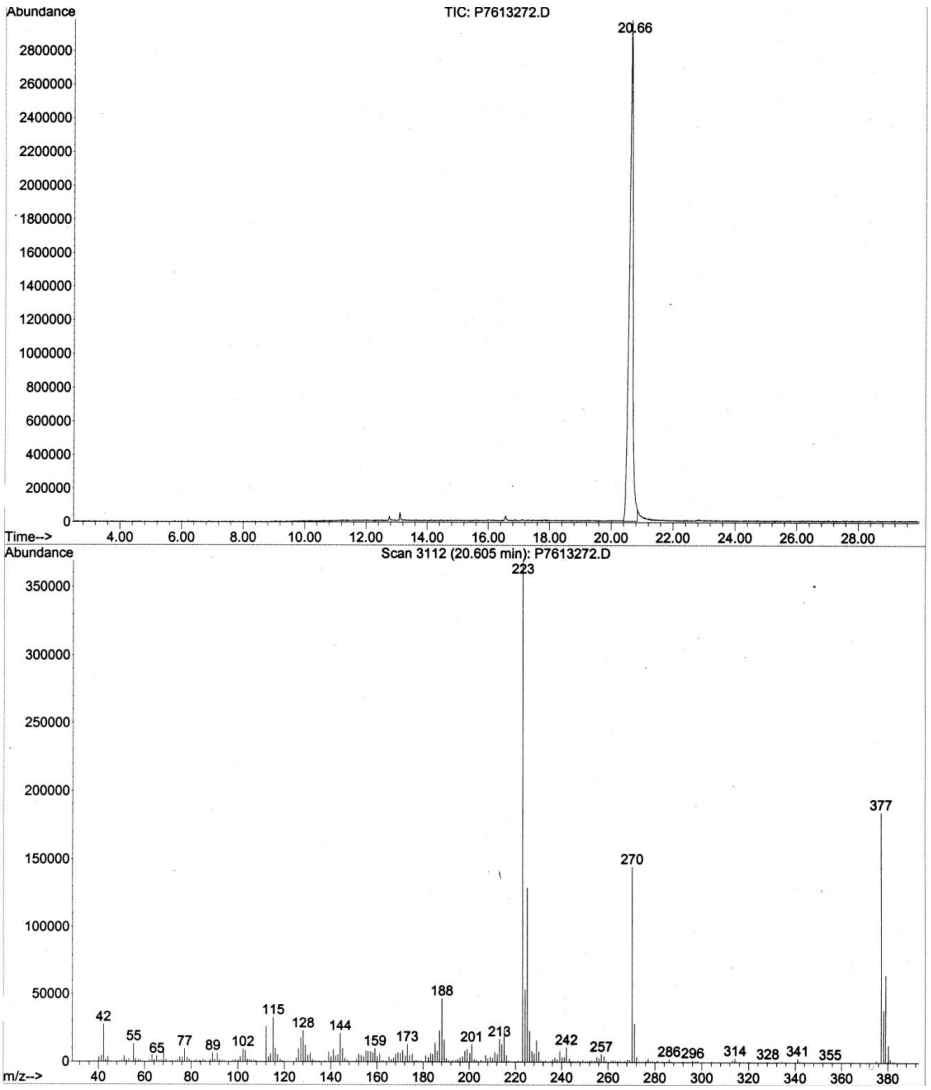

Fig. 2.42: GC-MS analysis of the product of the reaction between oxycodone and *p*-nitrophenyl chloroformate.

To determine the structure of the newly generated oxycodone analog, the compound was purified followed by ^{1}H and ^{13}C NMR spectral analysis. The ^{13}C NMR spectrum of the compound showed one new peak at 156.33 ppm which was absent in the ^{13}C NMR spectrum of oxycodone. A literature search showed that the carbonyl carbon of a chloroformate group shows up at around 156 ppm in ^{13}C NMR spectra (Mizuno et al., 2002; Olofson et al., 1978).

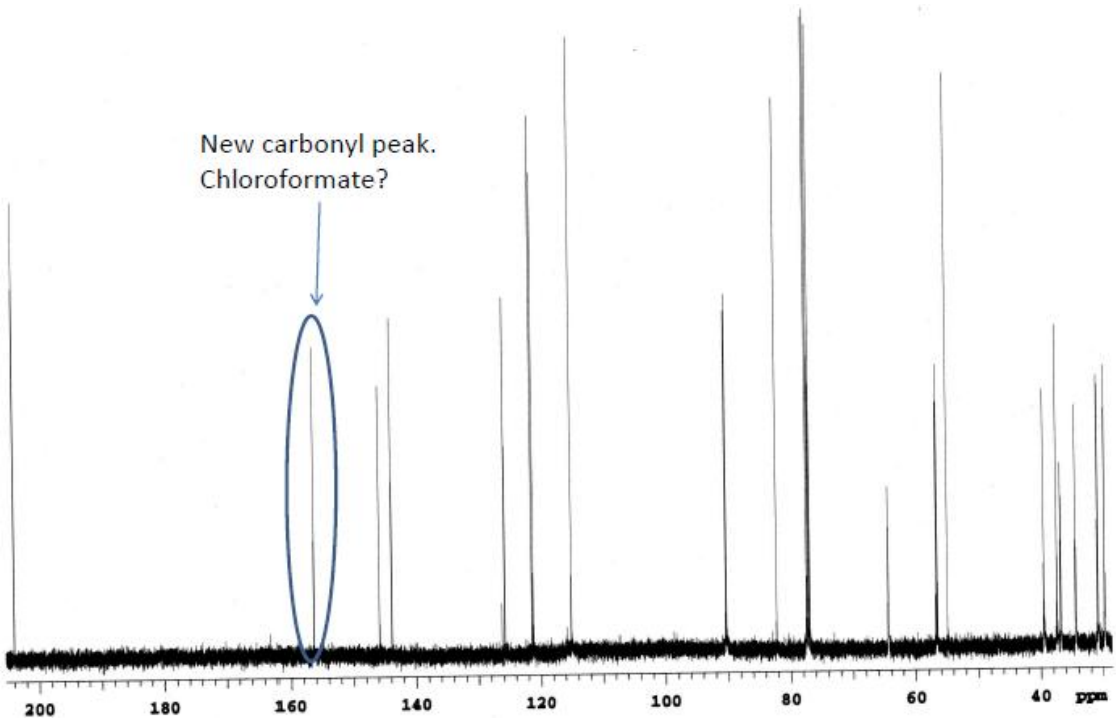

Fig. 2.43: ^{13}C NMR spectrum of the product from the reaction between oxycodone and *p*-nitrophenyl chloroformate.

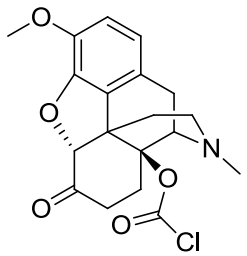

Oxycodone Chloroformate
Chemical Formula: $C_{19}H_{20}ClNO_5$
Exact Mass: 377.10

Fig. 2.44: Proposed structure of the product from the microwave reaction between oxycodone and *p*-nitrophenyl chloroformate.

The 377 m/z molecular mass of the product was also a match with the molecular mass of the expected chloroformate derivative of oxycodone. To analyze the chemical behavior of the compound several reactions were attempted with different phenolic and alcoholic nucleophiles in presence of different bases. The outcomes of those chemical reactions are summarized in the Scheme 2.35. The behavior of the molecule in the above mentioned reactions indicated that the molecule is likely not a chloroformate, unless it is a highly sterically hindered one (which could not be ruled out). X-ray crystallography was used to determine the crystal structure of the molecule.

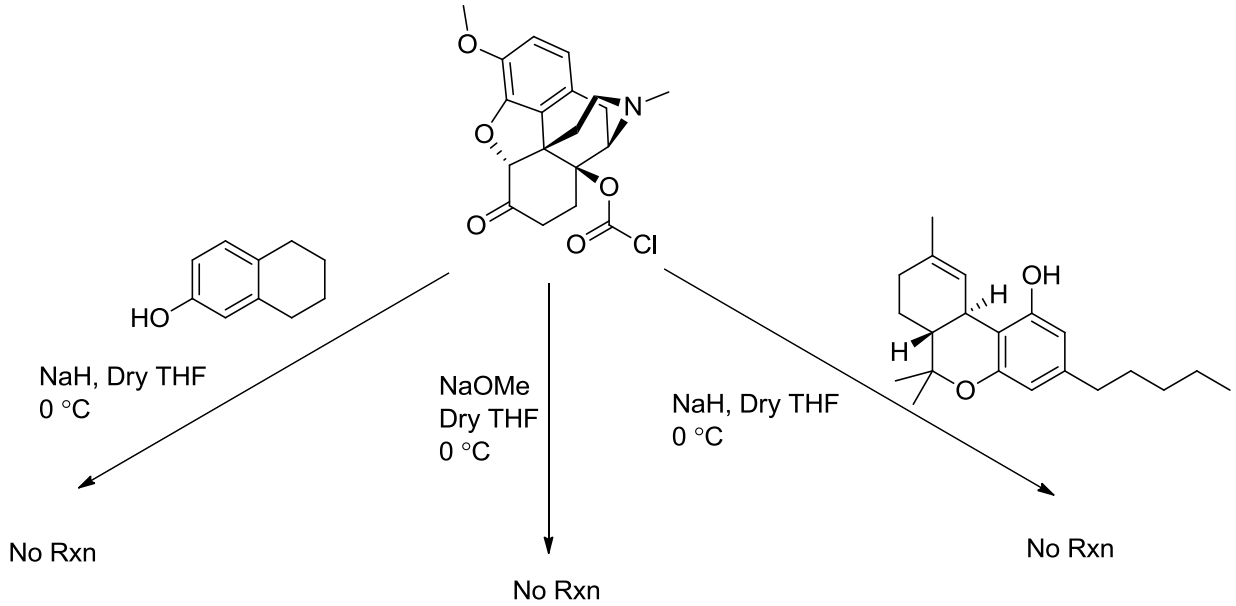

Scheme 2.35: Reactions of synthesized oxycodone intermediate with different phenoxides and alkoxides.

Crystals of the product from the above microwave reaction were formed from ethyl acetate solution, and analyzed by X-ray crystallography. X-ray crystallographic analysis of the compound indicated that the molecule was not the desired chloroformate derivative of oxycodone, but was a cyclic carbamate with incorporation of a chlorine atom (Fig. 2.45). The 14-hydroxy group and the amine group of oxycodone formed a carbamate ring. Also, one of the six membered rings (containing N) opened up with incorporation of a chlorine atom. Formation of the 5-membered cyclic carbamate can be explained as a result of initial formation of *p*-nitrophenoxy intermediate followed by simultaneous ring closure and ring opening.

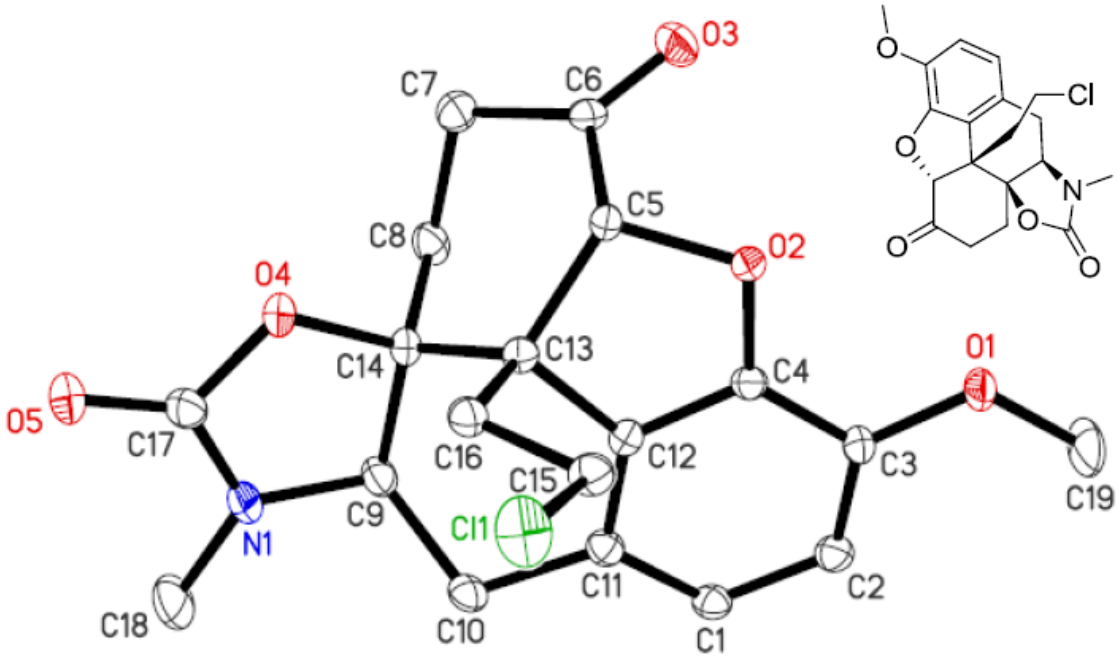

Fig. 2.45: Single crystal X-ray structure of the oxycodone analog from the microwave reaction of oxycodone with *p*-nitrophenyl chloroformate.

Since the oxycodone skeletal rearrangement chemistry was interesting, similar reactions were carried out with other opioids containing a 14-hydroxy functionality. Two other opioids containing a 14-hydroxy group are naltrexone and naloxone. Along with 14-hydroxy group, both the opioids have phenolic hydroxyl groups. The phenolic hydroxyl group of naltrexone was protected as an allyl ether (Scheme 2.36) (Green and Wuts, 1999) and then the compound was allowed to react with *p*-nitrophenyl chloroformate under the same microwave irradiation conditions as previously described. The reaction was monitored by TLC and LC-MS. No new spots in TLC analysis or new peaks in LC-MS were observed, even after 10 minutes of microwave heating at 170 °C.

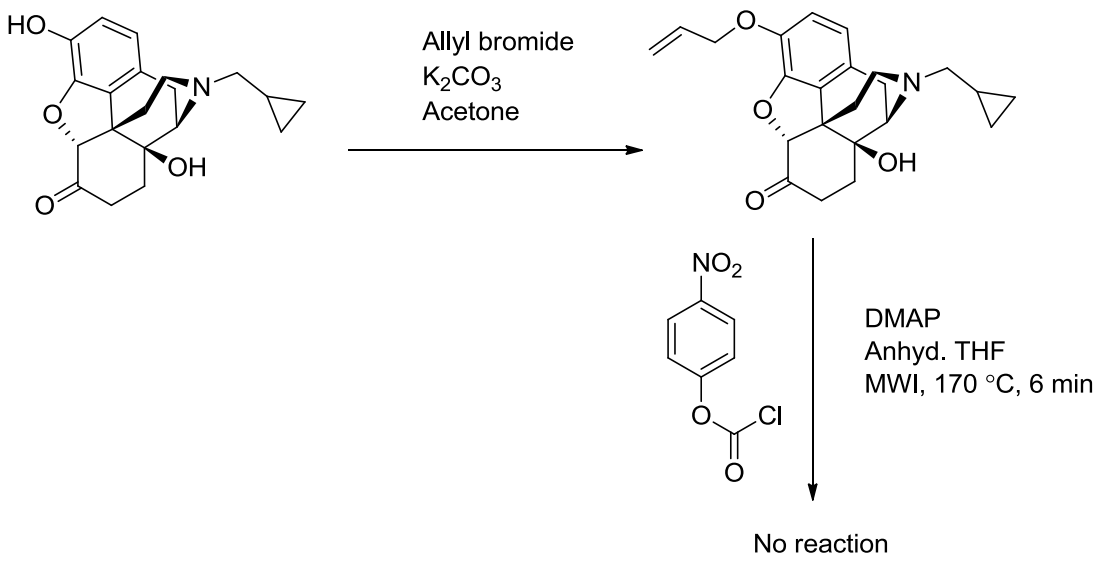

Scheme 2.36: Reaction of allyl-protected naltrexone with *p*-nitrophenyl chloroformate under microwave irradiation conditions.

Similar non-reactivity was observed in case of naloxone. Naloxone was first converted into 3-oxyallyl ether derivative (Green and Wuts, 1999) and then allowed to react with *p*-nitrophenyl chloroformate in the presence of DMAP under microwave heating at 170 °C. No new product formation was observed. The presence of an *N*-cyclopropylmethyl group in the case of naltrexone, and an *N*-allyl group in the case of naloxone, on the tertiary *N*-atom rather than presence of a *N*-methyl group (in the case of oxycodone) may be the reason behind naltrexone and naloxone not exhibiting similar skeletal rearrangement chemistry that was observed with oxycodone.

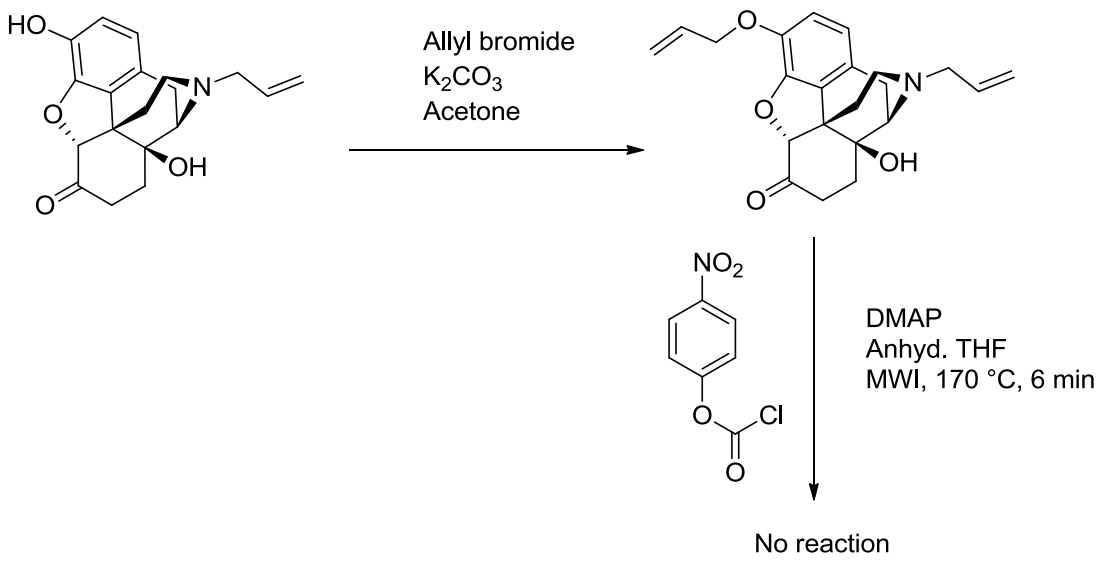

Scheme 2.37: Reaction of allyl protected naloxone with *p*-nitrophenyl chloroformate under microwave irradiation.

Since the *p*-nitrophenoxy carbonate ester of oxycodone could not be formed, a new synthetic approach was investigated, involving the coupling of Δ^9-tetrahydrocannbinol (Δ^9-THC) with oxycodone via a carbonate linkage. Thus, Δ^9-THC would be converted into its *p*-nitrophenoxy carbonate ester and then reacted with oxycodone. To determine the feasibility of the chemistry, reactions were initially carried out with model compounds. Tetrahydro-2-naphthol was used as a model compound for Δ^9-THC. The phenolic compound was converted into its *p*-nitrophenoxy carbonate ester by reaction with *p*-nitrophenyl chloroformate and then the resulting carbonate derivative was allowed to react with oxycodone in the presence of DMAP under microwave conditions. The progress of the reaction was followed by monitoring of the reaction mixture by LC-MS. LC-MS analysis of the reaction mixture showed a peak corresponding to the mass of desired carbonate conjugate of tetrahydro-2-naphthol and oxycodone, but the yield of the product was low (14%, from analysis of the LC-MS chromatogram).

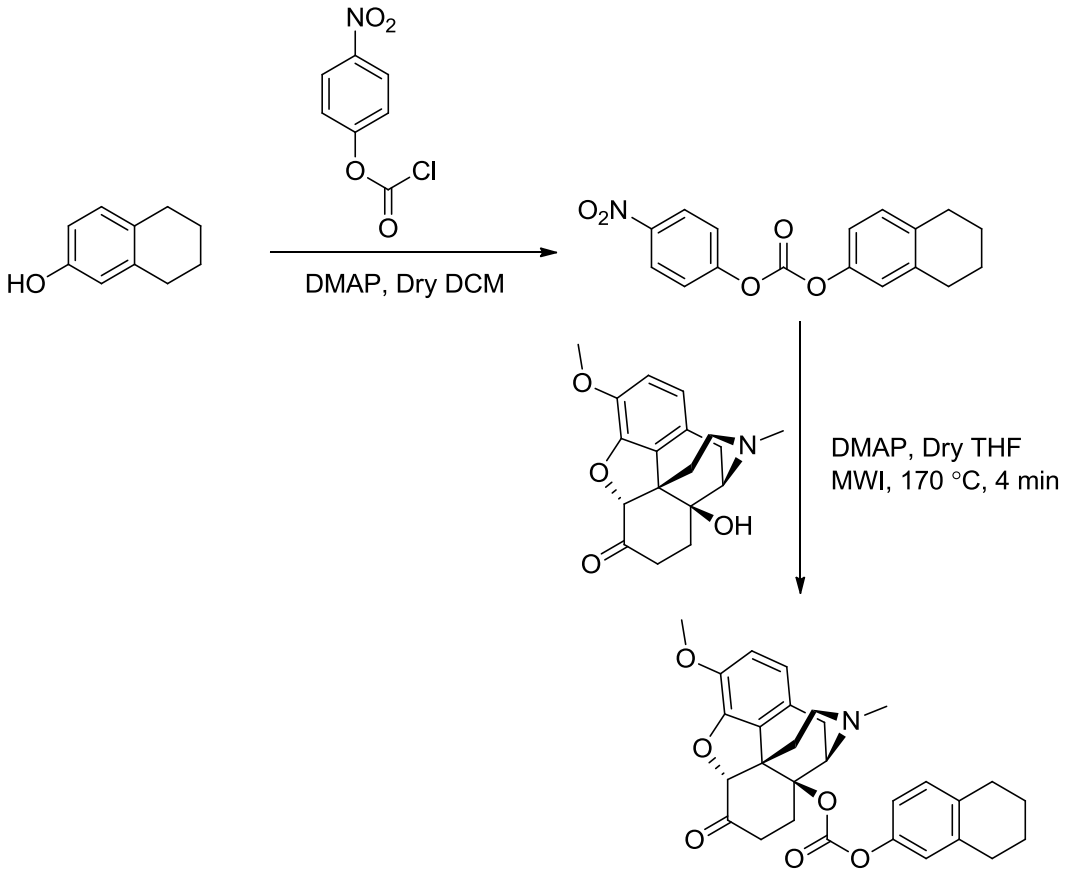

Scheme 2.38: Model reaction for the synthesis of the 14-hydroxy carbonate ester of oxycodone and tetrahydro-2-naphthol.

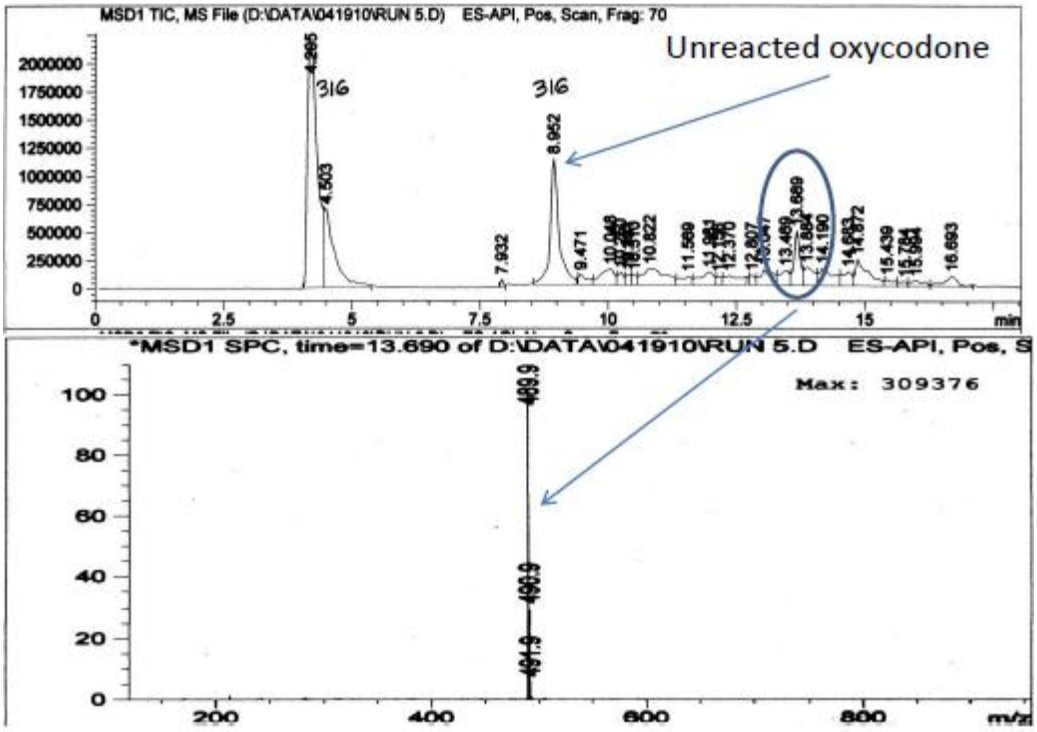

Fig. 2.46: LC-MS analysis of the mixture from the reaction of oxycodone and the *p*-nitrophenoxy carbonate of tetrahydro-2-naphthol.

As a consequence of the results from the above model reaction, Δ^9-THC was converted into its *p*-nitrophenoxy carbonate ester by reaction with *p*-nitrophenyl chloroformate and the resulting intermediate was allowed to react with oxycodone in presence of DMAP under microwave heating at 170 °C. The progress of the reaction was followed by TLC and LC-MS monitoring of the reaction mixture. Several new spots were observed in the TLC but LC-MS analysis did not show any peak corresponding to the molecular mass of the Δ^9-THC-oxycodone carbonate codrug. The two most intense spots observed by TLC were isolated by silica column chromatography, and the compounds were analyzed by GC-MS and NMR spectroscopy. The two isolated compounds were identified as Δ^9-THC and Δ^8-THC. The observed result can be explained as a thermal breakdown of the *p*-nitrophenoxy carbonate ester of Δ^9-THC into Δ^9-THC followed by subsequent conversion of Δ^9-THC into the more stable Δ^8-THC isomer. Conversion of

Δ^9-THC into Δ^8-THC is already reported in the literature (Neumeyer and Shagoury, 2006).

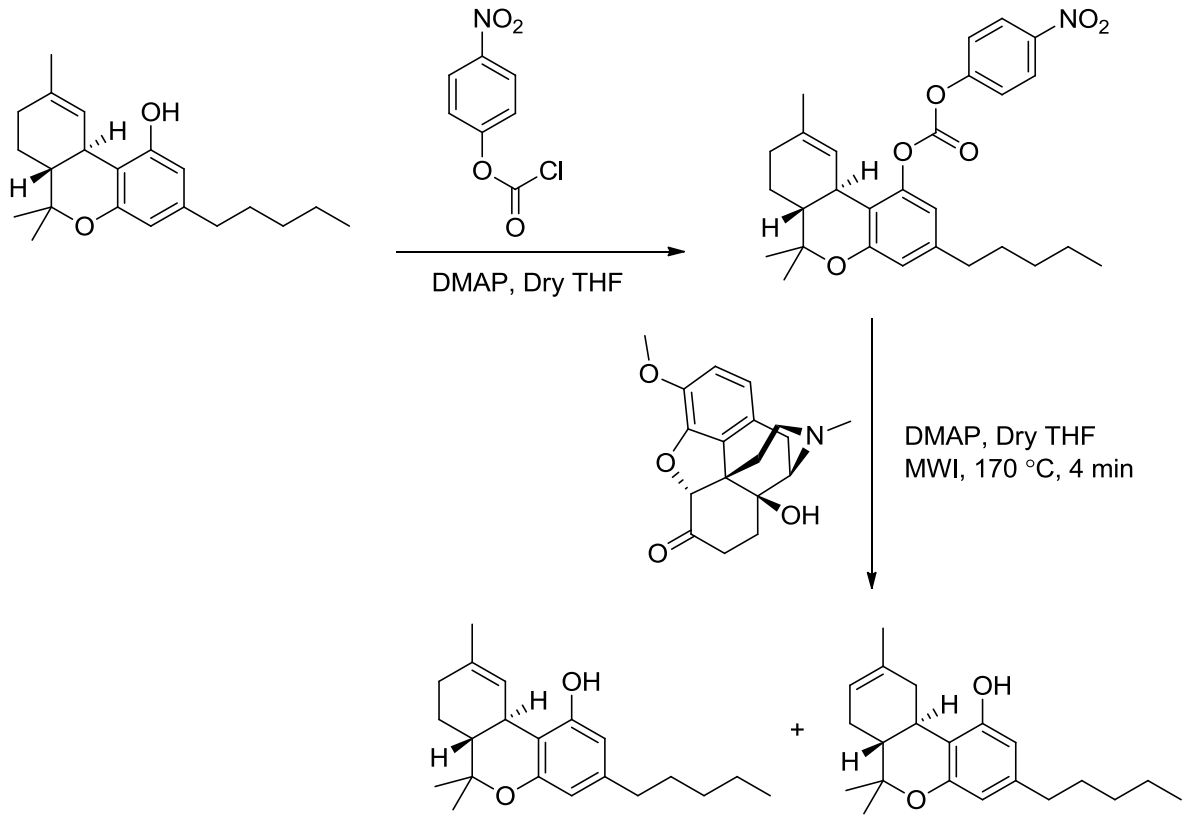

Scheme 2.39: Reaction between *p*-nitrophenoxy carbonate of Δ^9-THC and oxycodone under microwave irradiation conditions.

Since the coupling chemistry between Δ^9-THC and oxycodone was not successful utilizing *p*-nitrophenyl chloroformate, new coupling chemistry was tried. Two commonly used coupling reagents are 1,1'-carbonyldiimidazole (CDI) and *N*,*N*'-disuccinimidyl carbonate (DSC).

In intial attempts, oxycodone was allowed to react with CDI under microwave conditions and the reaction was monitored by TLC and LC-MS analysis. Heating the reaction mixture at 180 °C did not produce any of the desired products, as confirmed by TLC and LC-MS chromatograms.

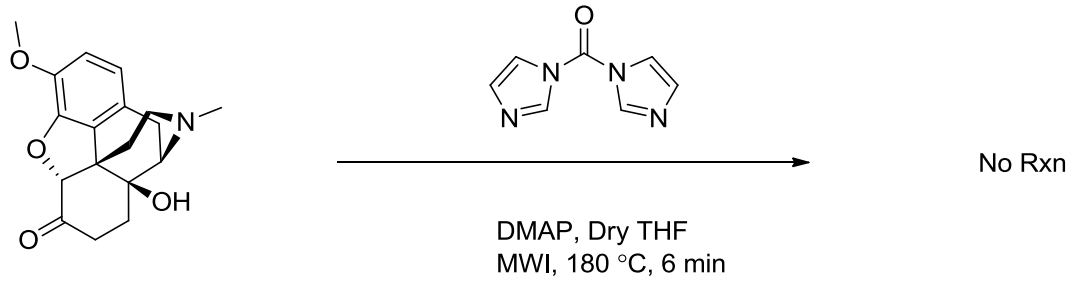

Scheme 2.40: Reaction between oxycodone and CDI under microwave irradiation conditions.

In the next attempt, oxycodone was mixed with DSC in the presence of DMAP in anhydrous THF and the mixture was heated at 180 °C under microwave irradiation conditions. TLC of the reaction mixture did not show any new spots. LC-MS analysis of the reaction mixture showed a very small peak corresponding to the molecular mass of the DSC-oxycodone carbonate. Prolonged heating under microwave condition did not result in isolable yields of the DSC-oxycodone carbonate.

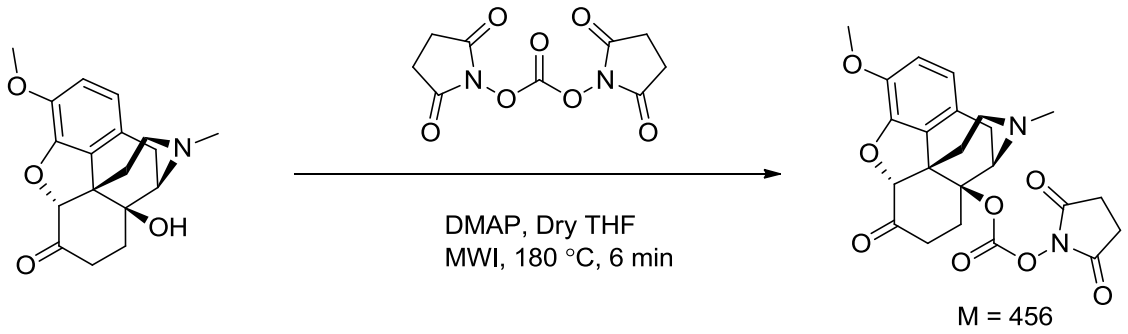

Scheme 2.41: Reaction between oxycodone and DSC under microwave irradiation conditions.

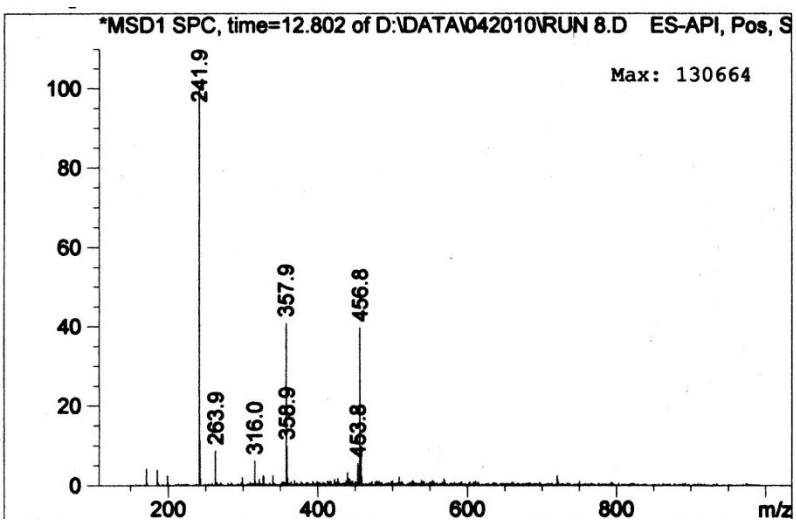

Fig. 2.47: ESI-MS analysis of the carbonate ester of oxycodone and DSC.

Several coupling reagents and strategies were used (as discussed above) in the synthesis of Δ^9-THC-oxycodone carbonate; however, none were successful in yielding the desired product. The reason for this failure was attributed to the sterically hindered nature of the 14-hydroxy group of oxycodone and to the thermal instability of the Δ^9-THC molecule. More synthetic endeavor is required for the synthesis of this desirable codrug.

2.4 Experimental Section

General Procedures. All experimental procedures were carried out under nitrogen and in oven-dried glassware unless otherwise mentioned. Solvents and reagents were obtained from commercial vendors. All solvents were removed by evaporation using a rotary evaporator unless indicated otherwise.

^{1}H and ^{13}C NMR spectra were recorded on Varian 300 MHz, 400 MHz and 500 MHz spectrometers. HPLC analyses were carried on an Agilent 1100 series Quatpump, equipped with a photodiode array detector and a computer integrating apparatus. GC-MS analyses were carried out on an Agilent 6890 GC instrument attached to a 593 mass-selective detector. Microwave reactions were carried out on a Biotage 355422-AD

microwave synthesizer. ESI and MALDI mass spectrometry was performed by the University of Kentucky Mass Spectrometry facility. X-ray crystallography was performed by the University of Kentucky Crystallographic facility.

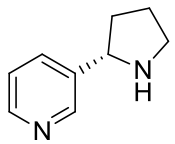

_S_-(-)-Nornicotine

S-(-)-Nicotine free base (6 g, 37 mmol), with a specific rotation of $[\alpha]_D^{25}$ = -169.9° (neat), was added with stirring to a mixture of 0.3 N aqueous sulfuric acid (120 ml) and manganese dioxide (36 g). The mixture was stirred and heated to reflux under a condenser for 10-12 hours. After cooling to room temperature, the resulting mixture was filtered through a Kimax Büchner Funnels with Fritted Disc and solid was washed with 0.3 N sulfuric acid (10 ml x 2 times) and water (100 ml). The filtrate was washed with chloroform or methylene chloride (50 ml x 5 times, total volume 250 ml), and the resulting aqueous solution was basified with 2.5N NaOH to pH 10-11. The resulting basic mixture was first filtered and then extracted with chloroform (100 ml x 4 times, total volume 400 ml), and the chloroform layer was decolorized with charcoal, filtered through celite and then concentrated under reduced pressure to afford *S*-(-)-nornicotine (1.92 g, 35% yield), recovered as an oil. The product showed over 99% purity by GC/MS analysis and HPLC analysis. ^{1}H NMR (300 MHz, $CDCl_3$): δ 8.533 (1H, d), 8. 415 (1H, dd), 7.657 (1H, dt), 7.183 (1H, dd), 4.101 (1H, t), 3.060 (2H, m), 2.310 (1H, broad), 1.940-1.563 (4H, m) ppm; ^{13}C NMR (300 MHz, $CDCl_3$): δ 148.8, 148.4, 140.6, 134.2, 123.5, 60.2, 47.1, 34.5, 25.6 ppm; GC-MS M^+ 148 *m/z*.

Same synthetic procedure was used for all other *N*-demethylation reactions.

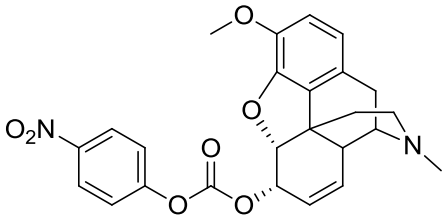

Codeine-*p*-nitrophenol carbonate

All glasswares were oven-dried and cooled under a nitrogen atmosphere. Codeine (0.6 g, 2.01 mmol) was placed in a round bottom flask under a nitrogen atmosphere and was dissolved in 6 mL of dry chloroform. The solution was cooled to 0 °C. DMAP (0.295 g, 2.41 mmol) was then added to the solution and the mixture stirred for 5 min. *para*-Nitrophenylchloroformate (0.486 g, 2.41 mmol) was dissolved in 5 mL of dry chloroform and the solution was added to the reaction mixture drop-wise, the mixture was allowed to warm to the ambient temperature. The progress of the reaction was monitored by TLC. After completion of the reaction, the mixture was diluted with chloroform (50 mL). The chloroform layer was washed 5 times with 30 mL 50% $NaHCO_3$ solution and with brine (30 mL), dried over anhydrous sodium sulfate and concentrated to afford a solid yellow colored product (0.532 g, 57% yield). ^{1}H NMR (300 MHz, $CDCl_3$): δ 8.27 (2H, dd), 7.45 (2H, dd), 6.66 (1H, d), 6.56 (1H, d), 5.70 (1H, dd), 5.52 (1H, dd), 5.16 (2H, m), 3.82 (3H, s), 3.36 (1H, m), 3.04 (1H, d), 2.75 (1H, m), 2.58 (1H, dd), 2.43 (3H, s), 2.36 (1H, dt), 2.29 (1H, dd), 2.03 (1H, dt), 1.88 (1H, d) ppm; ^{13}C NMR (300 MHz, $CDCl_3$): δ 156.1, 152.2, 146.7, 145.3, 142.7, 130.4, 127.4, 126.7, 126.6, 125.6, 122.2, 121.9, 119.9, 115.0, 114.5, 87.4, 72.4, 59.5, 56.9, 46.9, 43.1, 42.6, 40.5, 35.3, 20.6 ppm; MS (ESI): (M+1) 465 *m/z*.

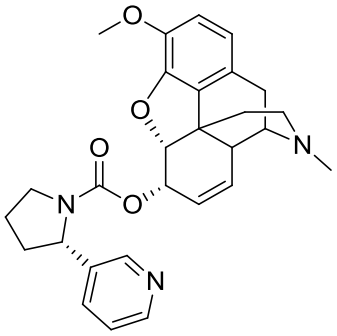

Codiene-*S*-(-)-nornicotine carbamate

Codeine-*p*-nitrophenol carbonate (0.5 g, 1.08 mmol) was dissolved in dry chloroform (8 mL) and then DMAP (0.158 g, 1.3 mmol) and *S*-(-)-nornicotine (0.192 g, 1.3 mmol) was added to the solution. The reaction mixture was refluxed and progress of the reaction was monitored by running TLC samples. After completion, the reaction mixture was diluted with 25 mL of chloroform and washed three times (15 mL each time) with 50% aqueous solution of $NaHCO_3$. Organic layer was dried with anhydrous sodium sulfate and concentrated to afford a solid product. The crude product was purified using silica gel column chromatography and a methylene chloride-methanol mixture as eluent, to afford the pure product (0.28 g, 54% yield). ^{1}H NMR (500 MHz, $CDCl_3$): δ 8.519 (1H, s), 8.465 (1H, d), 7.539 (1H, d), 7.225 (1H, dd), 6.671 (1H, d), 6.552 (1H, d), 5.696 (1H, d), 5.413(1H, d), 5.082 (1H, s), 5.25 (1H, dd), 3.852 (3H, s), 3.772 (1H, t), 3.733-3.572 (2H, m), 3.37 (1H, m), 3.032 (1H, d), 2.758 (1H, s), 2.599 (1H, dd), 2.445 (3H, s), 2.421-2.378 (2H, m), 2.349 (1H, dt), 2.304 (1H, d), 2.066-1.944 (2H, m), 1.906 (1H, m), 1.88 (1H, d) ppm; ^{13}C NMR (500 MHz, $CDCl_3$): δ 154.5, 148.4, 147.9, 146.9, 142.2, 139.0, 133.6, 130.9, 129.2, 129.0, 127.0, 123.4, 119.2, 113.8, 88.5, 68.7, 59.6, 59.3, 56.7, 47.4, 46.8, 43.1, 42.6, 40.5, 35.3, 34.8, 24.1, 20.6; MS (ESI): (M+1) 474 *m/z*.

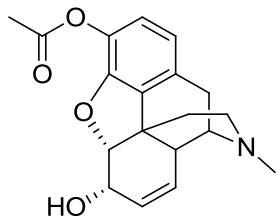

3-*O*-Acetylmorphine

Morphine free base (1.102 g, 3.87 mmol) was suspended in saturated sodium bicarbonate solution (55 mL). To the stirred suspension, 1.1 mL (11.68 mmol) of acetic anhydride was added drop-wise. Reaction mixture was stirred at ambient temperature and the progress of the reaction was monitored by running TLC. After completion of the reaction, aqueous phase was extracted with chloroform (5 x 20 mL), dried over sodium sulfate and concentrated under reduced pressure to afford a white solid product (1.21 g, 96%). ^{1}H NMR (300 MHz, $CDCl_3$): δ 6.73 (1H, d), 6.60 (1H, d), 5.74 (1H, dd), 5.27 (1H, dd), 4.92 (1H, m), 4.16 (1H, m), 3.38 (1H, m), 3.06 (1H, d), 2.60 (1H, m), 2.54 (1H, dd), 2.43 (3H, s), 2.37 (1H, dt), 2.32 (3H, s), 2.29 (1H, dd), 2.05 (1H, dt), 1.88 (1H, d) ppm; ^{13}C NMR (300 MHz, $CDCl_3$): δ 168.6, 148.7, 134.2, 132.7, 132.3, 131.7, 127.8, 121.1, 119.8, 92.5, 66.0, 59.1, 46.0, 43.3, 42.3, 41.6, 35.4, 21.4, 20.9 ppm; MS (ESI): (M+1) 328 *m/z*.

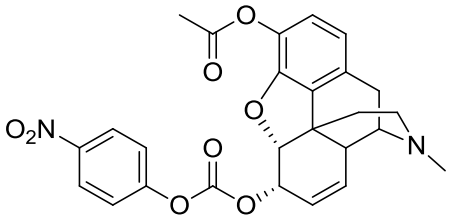

3-*O*-Acetylmorphine-*p*-nitrophenol carbonate

3-*O*-Acetylmorphine (2.0 g, 6.12 mmol) was placed in a round bottom flask under a nitrogen atmosphere and was dissolved in dry chloroform (10 mL). The solution was cooled to 0 °C. DMAP (0.9 g, 7.34 mmol) was added to the solution and allowed to stir for 5 min. *p*-Nitrophenylchloroformate (1.48 g, 7.34 mmol) dissolved in dry chloroform (8 mL) was added to the reaction mixture drop-wise and the mixture was allowed to come to room temperature. Progress of the reaction was monitored by running TLC. After completion of the reaction, the mixture was diluted with chloroform (20 mL). The chloroform layer was washed 5 times with 25 mL 50% $NaHCO_3$ solution and with brine

(20 mL), dried over anhydrous sodium sulfate and concentrated under reduced pressure to afford a solid product (1.69 g, 56%). ^{1}H NMR (300 MHz, $CDCl_3$): δ 8.30 (2H, dd), 7.51 (2H, dd), 6.82 (1H, d), 6.64 (1H, d), 5.71 (1H, dd), 5.58 (1H, dd), 5.24 (1H, m), 5.19 (1H, m), 3.42 (1H, m), 3.09 (1H, d), 2.80 (1H, m), 2.62 (1H, dd), 2.45 (3H, s), 2.41 (1H, dt), 2.19 (3H, s), 2.09 (1H, dt), 1.92 (1H, d) ppm; ^{13}C NMR (300 MHz, $CDCl_3$): δ 168.5, 155.9, 151.8, 149.2, 145.6, 132.2, 131.9, 130.4, 127.8, 126.4, 125.5, 122.3, 122.2, 121.8, 119.9, 113.8, 88.2, 72.6, 59.1, 46.7, 43.8, 42.9, 40.7, 35.3, 21.0, 20.8 ppm; MS (ESI): (M+1) 493 *m/z*.

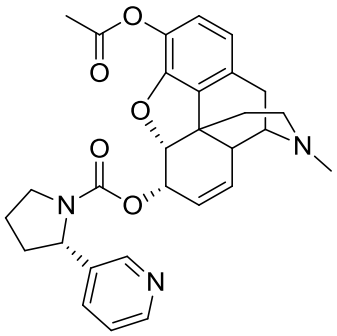

3-*O*-Acetylmorphine-*S*-(-)-nornicotine carbamate

3-*O*-acetylmorphine-*p*-nitrophenol carbonate (1.2 g, 2.44 mmol) was dissolved in dry chloroform (18 mL) and then DMAP (0.358 g, 2.93 mmol) and *S*-(-)-nornicotine (0.433 g, 2.93 mmol) was added to the solution. The reaction mixture was refluxed and progress of the reaction was monitored by running TLC samples. After completion, the reaction mixture was diluted with 30 mL of chloroform and washed three times with 50% aqueous solution of $NaHCO_3$. Organic layer was dried over anhydrous sodium sulfate and concentrated to afford a solid product. The crude product was purified using silica gel column chromatography and a methylene chloride-methanol mixture as eluent, to afford the pure product (0.623 g, 51% yield). ^{1}H NMR (300 MHz, $CDCl_3$): δ 8.492 (1H, s), 8.440 (1H, d), 7.515 (1H, d), 7.204 (1H, dd), 6.739 (1H, d), 6.560 (1H, d), 5.646 (1H, d), 5.370 (1H, d), 5.074 (2H, m), 4.990 (1H, dd), 3.726 (2H, m), 3.639 (2H, m), 3.330 (1H, m), 3.026 (1H, d), 2.686 (1H, broad), 2.569 (1H, dd), 2.433 (3H, s), 2.406- 2.295 (2H, m), 2.275 (3H, s), 2.100-1.852 (4H, m); ^{13}C NMR (300 MHz, $CDCl_3$): δ 168.2, 154.2, 149.5, 148.2, 147.6, 138.7, 133.4, 132.4, 131.7, 131.6, 129.1, 128.9, 123.3, 121.8,

119.2, 89.5, 68.9, 59.4, 58.9, 47.3, 46.5, 43.1, 43.0, 42.9, 40.7, 35.3, 34.9, 24.2, 20.9; MS (ESI): (M+1) 502 *m/z*.

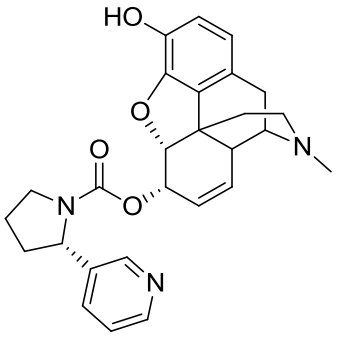

Morphine-*S*-(-)-nornicotine carbamate (6-oxy)

3-*O*-acetylmorphine-*S*-(-)-nornicotine carbamate (0.9 g, 1.8 mmol) was dissolved in 10 mL 1:1 mixture of water and THF and then LiOH (0.095 g, 3.96 mmol) was added to the solution. Reaction mixture was stirred at room temperature and progress of the reaction was followed by running TLC. After completion, reaction mixture was diluted with chloroform and washed two times with water. Organic layer was then dried over anhydrous sodium sulfate and then concentrated to afford a solid product (0.727 g, 88%). ^{1}H NMR (300 MHz, $CDCl_3$): δ 8.825 (1H, d), 8.473 (1H, dd), 7.642 (1H, dt), 7.318 (1H, dd), 6.710 (1H, d), 6.470 (1H, d), 5.532 (1H, d), 5.370 (1H, dt), 5.239 (1H, m), 4.890 (1H, dd), 4.753 (1H, dd), 3.718 (2H, m), 3.339 (1H, dd), 3.026 (1H, d), 2.662 (1H, m), 2.570-2.437 (4H, m), 2.426 (3H, s), 2.416-1.940 (5H, m), 1.554 (1H, dd); ^{13}C NMR (300 MHz, $CDCl_3$): δ 154.2, 150.6, 147.3, 146.6, 138.7, 137.7, 134.0, 130.3, 130.0, 128.5, 125.4, 123.6, 119.1, 118.6, 89.8, 70.8, 58.9, 58.5, 47.8, 46.6, 44.2, 43.3, 41.7, 36.1, 34.3, 24.3, 20.9; MS (ESI): (M+1) 460 *m/z*.

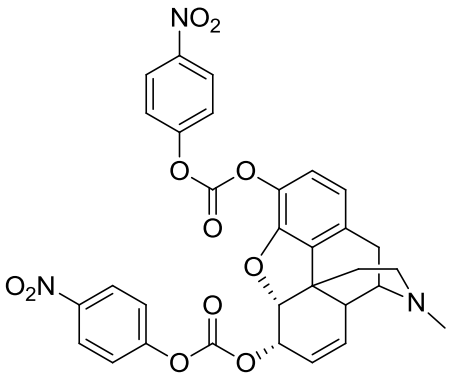

Morphine-bis-*p*-nitrophenol carbonate

All glasswares were oven-dried and cooled under a nitrogen atmosphere. Morphine (0.6 g, 2.11 mmol) was placed in a round bottom flask under a nitrogen atmosphere and was dissolved in 16 mL of dry THF. The solution was cooled to 0 °C. DMAP (0.566 g, 4.64 mmol) was then added to the solution and the mixture stirred for 5 min. *para*-Nitrophenylchloroformate (1.28 g, 6.33 mmol) was dissolved in 4 mL of dry THF and the solution was added to the reaction mixture drop-wise, the mixture was allowed to warm to the ambient temperature. The progress of the reaction was monitored by TLC. After completion of the reaction, the mixture was diluted with chloroform (50 mL). The chloroform layer was washed 5 times with 25 mL 50% aqueous $NaHCO_3$ solution and with brine (25 mL), dried over anhydrous sodium sulfate and concentrated to afford a solid product (0.623 g, 48%). ^{1}H NMR (500 MHz, $CDCl_3$): δ 8.252 (2H, d), 8.231 (2H, d), 7.432 (2H, d), 7.414 (2H, d), 6.987 (1H, d), 6.695 (1H, d), 5.745 (1H, d), 5.554 (1H, dt), 5.306 (1H, m), 5.198 (1H, m), 3.456 (1H, dd), 3.132 (1H, d), 2.839 (1H, t), 2.671 (1H, dd), 2.480 (3H, s), 2.410 (1H, m), 2.130 (1H, td), 1.959 (1H, dd) ppm; ^{13}C NMR (300 MHz, $CDCl_3$): δ 155.5, 155.3, 151.9, 150.3, 148.8, 145.6, 132.4, 131.5, 129.7, 127.5, 125.7, 125.4, 121.9, 121.6, 120.3, 88.5, 72.2, 59.4, 46.8, 42.9, 40.0, 34.7, 21.3; MS (ESI): (M+1) 616 *m/z*.

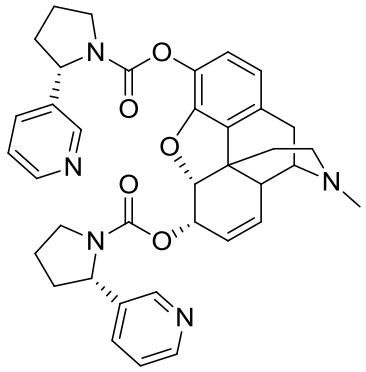

Morphine-bis-*S*-(-)-nornicotine carbamate

Morphine-bis-*p*-nitrophenol (0.6 g, 0.98 mmol) carbonate was dissolved in dry chloroform (15 mL) and then DMAP (0.263 g, 2.16 mmol) and *S*-(-)-nornicotine (0.435 g, 2.94 mmol) were added to the solution. The reaction mixture was refluxed and progress of the reaction was monitored by running TLC samples. After completion, the reaction mixture was diluted with 50 mL of chloroform and washed three times with 50% aqueous solution of $NaHCO_3$ (25 mL each time) and with brine (25 mL), dried over anhydrous sodium sulfate and concentrated to afford a solid product (0.111 g, 18%). MS (ESI): (M+1) 634 *m/z*.

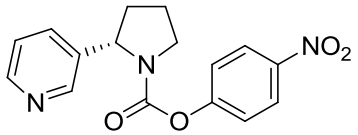

***S*-(-)-Nornicotine-*p*-nitrophenol carbamate**

All glasswares were oven-dried and cooled under a nitrogen atmosphere. *S*-(-)-nornicotine (0.3 g, 2.03 mmol) was placed in a round bottom flask under a nitrogen atmosphere and was dissolved in 5 mL of dry chloroform. The solution was cooled to 0 °C. DMAP (0.3 g, 2.44 mmol) was then added to the solution and the mixture stirred for 5 min. *para*-Nitrophenylchloroformate (0.492 g, 2.44 mmol) was dissolved in 5 mL of dry chloroform and the solution was added to the reaction mixture drop-wise, the mixture was allowed to warm to the ambient temperature. The progress of the reaction was monitored by TLC. After completion of the reaction, the mixture was diluted with chloroform (25 mL). The chloroform layer was washed 5 times with 50% aqueous $NaHCO_3$ solution (15 mL each time) and with brine (15 mL), dried over anhydrous

sodium sulfate and concentrated to afford the product (0.426 g, 67%). The product was used in the next synthetic step without any further purification. GC-MS M^+ 313 *m/z*.

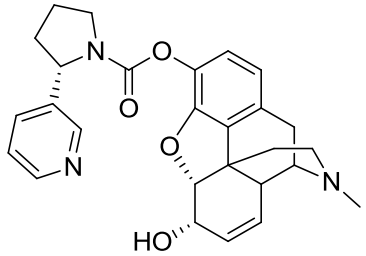

Morphine-*S*-(-)-nornicotine carbamate (3-oxy)

All glasswares were oven dried and cooled under a nitrogen atmosphere. Morphine (0.437 g, 1.53 mmol) was placed in a round bottom flask under a nitrogen atmosphere and was dissolved in 6 mL of dry THF. The solution was cooled down to 0 °C. NaH (0.037 g, 1.53 mmol) was added to the solution and allowed to stir for 5 min. *p*-Nitrophenol-*S*-(-)-nornicotine carbamate (0.4 g, 1.28 mmol), dissolved in 5 mL of dry THF was added to the reaction mixture drop-wise and the mixture was allowed to warm to the ambient temperature. The progress of the reaction was monitored by TLC. After the completion of the reaction, the mixture was filtered through a pad of celite and then the organic filtrate was concentrated under reduced pressure to afford yellow oil. The organic residue was dissolved in chloroform (50 mL), the organic layer was washed with 50% aqueous sodium bicarbonate solution (5 x 20 mL) and brine (20 mL), dried over sodium sulfate and concentrated under reduced pressure to afford a solid. The crude product was purified using silica gel column chromatography and a methylene chloride-methanol mixture as eluent, to afford the pure product (0.212 g, 36%). ^{1}H NMR (500 MHz, $CDCl_3$): δ 8.828 (1H, s), 8.475 (1H, dd), 7.640 (1H, d), 7.316 (1H, dd), 6.708 (1H, d), 6.469 (1H, d), 5.540 (1H, d), 5.371(1H, dt), 5.258 (1H, dd), 4.892 (1H, dd), 4.751 (1H, d), 3.740 (1H, m), 3.635 (1H, m), 3.339 (1H, dd), 3.029 (1H, d), 2.662 (1H, t), 2.542 (1H, dd), 2.427 (3H, s), 2.386 (1H, dd), 2.271 (1H, dd), 2.161(1H, m), 2.076 (1H, m), 2.043-1.953 (3H, m), 1.752 (1H, d), 1.88 (1H, d) ppm; ^{13}C NMR (300 MHz, $CDCl_3$): δ154.2, 150.6, 147.4, 146.6, 138.8, 137.7, 134.0, 130.4, 130.1, 128.5, 125.5, 123.6, 119.2, 118.6, 89.8, 70.8, 59.0, 58.6, 47.9, 46.6, 44.3, 43.4, 41.8, 36.2, 34.3, 24.3, 20.9; MS (ESI): (M+1) 460 *m/z*.

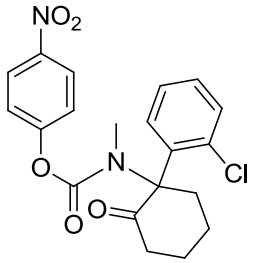

Ketamine-*p*-nitrophenol carbamate

All glasswares were oven dried and cooled under a nitrogen atmosphere. Ketamine (0.062 g, 0.26 mmol) was placed in a round bottom flask under a nitrogen atmosphere and was dissolved in 2 mL of dry toluene. Na_2CO_3 (0.1 g, 0.94 mmol) was added to the solution and allowed to stir for 5 min. *para*-Nitrophenylchloroformate (0.158 g, 0.78 mmol), dissolved in 3 mL of dry toluene was added to the reaction mixture drop-wise and the mixture was refluxed under nitrogen. The progress of the reaction was monitored by TLC. After the completion of the reaction, the mixture was filtered and then the organic filtrate was concentrated under reduced pressure to afford yellow oil. The organic residue was dissolved in chloroform (20 mL), the organic layer was washed with 50% sodium bicarbonate solution (3 x 10 mL), 1N HCl solution (2 X 10 mL) and brine (10 mL), dried over sodium sulfate and concentrated under reduced pressure to afford a brownish solid. The crude product was purified using silica gel column chromatography and a methylene chloride-methanol mixture as eluent, to afford the pure product (0.065 g, 62%). ^{1}H NMR (300 MHz, $CDCl_3$): δ 8.083 (2H, d), 7.347 (1H, dd), 7.215-7.055 (5H), 3.385 (1H, m), 3.153 (3H, s), 2.734 (2H, m), 2.006-1.584 (5H, m); ^{13}C NMR (300 MHz, $CDCl_3$): δ 202.4, 155.6, 154.8, 154.1, 134.1, 132.8, 129.8, 129.2, 126.7, 125.4, 124.9, 122.1, 121.7, 76.0, 41.2, 34.9, 36.6, 27.2, 22.4; MS (ESI): (M+1) 403 *m/z*.

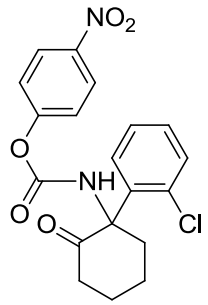

Norketamine-*p*-nitrophenol carbamate

Norketamine-*p*-nitrophenol carbamate was synthesized following the same methodology. Obtained yield: 69%. ^{1}H NMR (500 MHz, $CDCl_3$): δ 8.154 (2H, d), 7.868 (1H, dd), 7.401-7.293 (3H, m), 7.216 (2H, d), 3.838 (1H, dd), 2.504 (1H, m), 2.404 (1H, m), 2.121 (1H, m), 1.878- 1.736 (5H, m); ^{13}C NMR (300 MHz, $CDCl_3$): δ 208.4, 155.7, 150.5, 144.6, 133.8, 133.7, 131.7, 131.2, 130.0, 125.6, 126.1, 125.0, 122.0, 115.6, 67.5, 39.3, 38.5, 30.9, 22.5; MS (ESI): (M+1) 389 *m/z*.

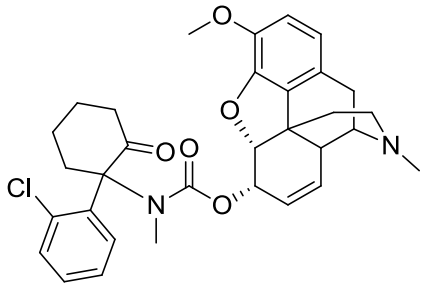

mixture of 2 diastereomers

Ketamine-codeine carbamate

All glasswares were oven dried and cooled under a nitrogen atmosphere. Codeine (0.045 g, 0.15 mmol) was placed in a round bottom flask under a nitrogen atmosphere and was dissolved in 2 mL of dry THF. The solution was cooled down to 0 °C. NaH (0.05 g, 0.195 mmol) was added to the solution and allowed to stir for 5 min. Ketamine-*p*-nitrophenol carbamate (0.050 g, 0.124 mmol), dissolved in 3 mL of dry THF was added to the reaction mixture drop-wise and the mixture was allowed to warm to the ambient temperature. The progress of the reaction was monitored by TLC. After the completion of the reaction, the mixture was filtered through a pad of celite and then the organic filtrate was concentrated under reduced pressure to afford yellow oil. The organic residue was dissolved in chloroform (20 mL), the organic layer was washed with 50% sodium

bicarbonate solution (3 x 10 mL) and brine (10 mL), dried over sodium sulfate and concentrated under reduced pressure to afford a brown solid. The crude product was purified using silica gel column chromatography and a methylene chloride-methanol mixture as eluent, to afford a diastereomeric mixture of the product (0.034 g, 48%). MS (ESI): (M+1) 563 *m/z*.

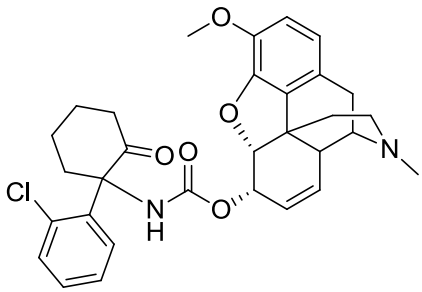

mixture of 2 diastereomers

Norketamine-codeine carbamate

Norketamine codeine carbamate was synthesized following the procedure same as the synthetic method used for synthesizing ketamine-codeine carbamate. Obtained yield: 42%. MS (ESI): (M+1) 549 *m/z*.

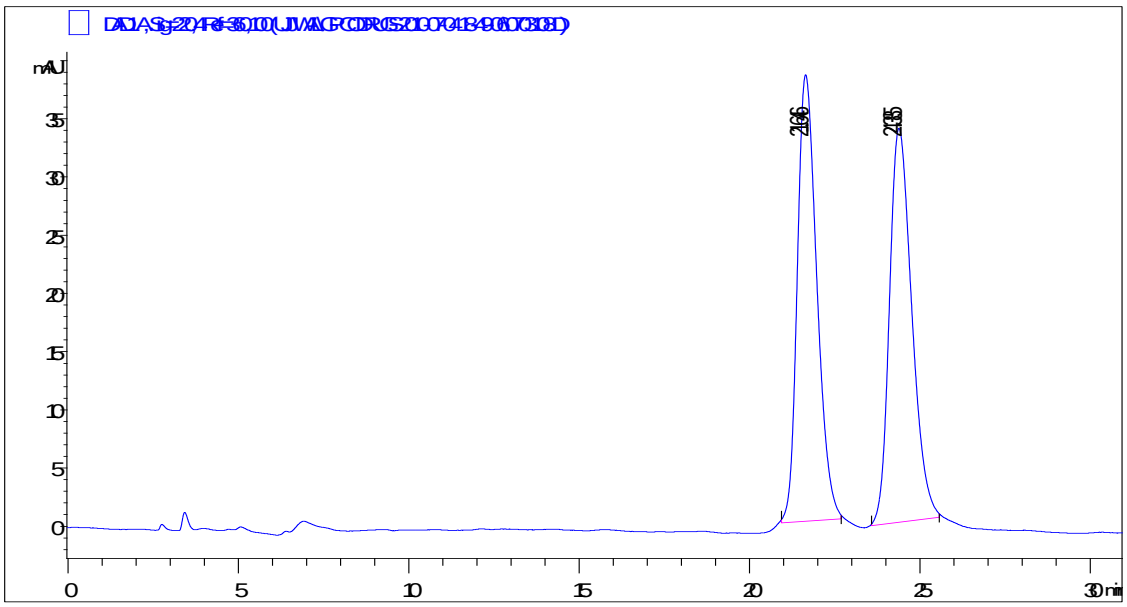

Fig. 2.48: HPLC chromatogram of two diastereomers of norketamine-codeine carbamate codrug.

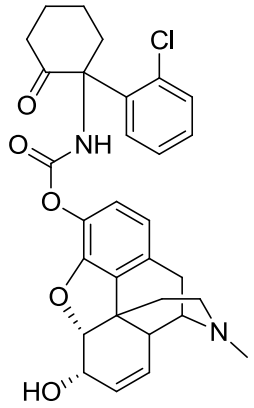

mixture of 2 diastereomers

Norketamine-morphine carbamate

All glasswares were oven dried and cooled under a nitrogen atmosphere. Morphine (0.08 g, 0.28 mmol) was placed in a round bottom flask under a nitrogen atmosphere and was dissolved in 2 mL of dry THF. The solution was cooled down to 0 °C. NaH (0.007 g, 0.3 mmol) was added to the solution and allowed to stir for 5 min. Norketamine-*p*-nitrophenol carbamate (0.084 g, 0.22 mmol), dissolved in 3 mL of dry THF was added to the reaction mixture drop-wise and the mixture was allowed to warm to the ambient temperature. The progress of the reaction was monitored by TLC. After the completion of the reaction, the mixture was filtered through a pad of celite and then the organic filtrate was concentrated under reduced pressure to afford yellow oil. The organic residue was dissolved in chloroform (20 mL), the organic layer was washed with 50% sodium bicarbonate solution (3 x 10 mL) and brine (10 mL), dried over anhydrous sodium sulfate and concentrated under reduced pressure to afford a brown solid. The crude product was purified using silica gel column chromatography and a methylene chloride-methanol mixture as eluent, to afford a diastereomeric mixture of the product (0.047 g, 40%). MS (ESI): (M+1) 535 *m/z*.

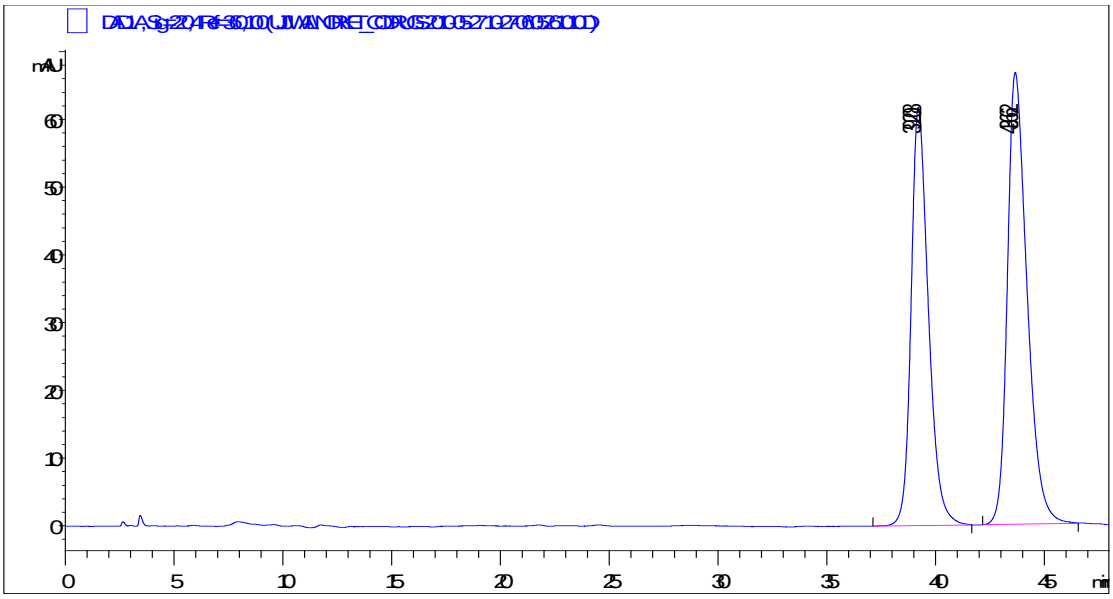

Fig. 2.49: HPLC chromatogram of two diastereomers of norketamine-morphine carbamate codrug.

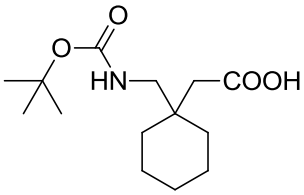

Boc-protected gabapentin

Gabapentin (0.3 g, 1.75 mmol) was placed in a round bottom flask and dissolved in 5 mL water. Sodium bicarbonate (0.368 g, 4.38 mmol) was added to the solution and stirred for 5 min. Boc anhydride (0.458 g, 2.1 mmol) was dissolved in THF (5 mL) and added to the reaction mixture. The reaction mixture was allowed to stir overnight at room temperature. The reaction mixture was then acidified with 1N HCl and the product was extracted into chloroform. Chloroform layer was dried over anhydrous sodium sulfate and concentrated under reduced pressure to produce a white colored solid product (0.413 g, 87%). ^{1}H NMR (500 MHz, $CDCl_3$): δ 5.076 (1H, t), 3.156 (2H, d), 2.306 (2H, s), 1.518-1.243 (19H, m); ^{13}C NMR (300 MHz, $CDCl_3$): δ 176.1, 157.4, 80.2, 47.5, 41.2, 37.9, 34.2, 28.6, 26.1, 21.6.

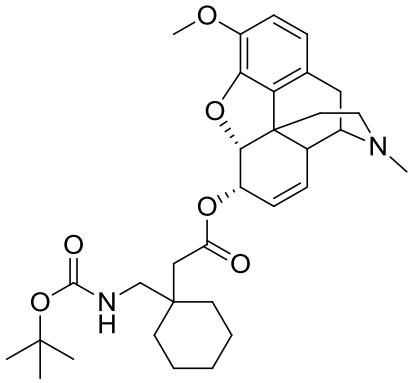

Boc-protected gabapentin-codeine ester

Boc-protected gabapentin (0.233 g, 0.86 mmol), codeine (0.257 g, 0.86 mmol), and DMAP (0.042 g, 0.34 mmol) were placed in a round bottom flask and dissolved in 12 mL DCM. The mixture was cooled to 0 °C and then DCC (0.213 g, 1.03 mmol) was added to the stirred solution. The reaction mixture was allowed to come to room temperature and stirred at room temperature. Progress of the reaction was followed by running TLC. After the reaction was over, reaction mixture was diluted with 40 mL DCM and washed with 50% sodium bicarbonate solution (3 x 20 mL) and brine (20 mL), dried over sodium sulfate and concentrated under reduced pressure to afford a solid. The crude product was purified using silica gel column chromatography and a methylene chloride-methanol mixture as eluent, to afford the pure product (0.328 g, 69%). ^{1}H NMR (500 MHz, $CDCl_3$): δ 6.656 (1H, d), 6.538 (1H, d), 5.612 (1H, d), 5.160 (1H, dt), 5.200-5.120 (2H, m), 5.096 (1H, dd), 3.819 (3H, s), 3.357 (1H, dd), 3.249 (2H, d), 3.038 (1H, d), 2.733 (1H, m), 2.579 (1H, dd), 2.436 (3H, s), 2.412- 2.253 (4H, m), 2.045 (1H, td), 1.852 (1H, d), 1.551-1.367 (19H, m); ^{13}C NMR (300 MHz, $CDCl_3$): δ 172.2, 156.7, 147.3, 142.5, 130.9, 130.0, 128.6, 127.3, 119.4, 114.0, 88.4, 78.9, 68.9, 59.2, 56.8, 47.2, 46.7, 43.2, 43.1, 41.2, 40.9, 38.2, 35.7, 34.2, 28.6, 26.1, 21.7, 20.5; MS (ESI): (M+1) 553 *m/z*.

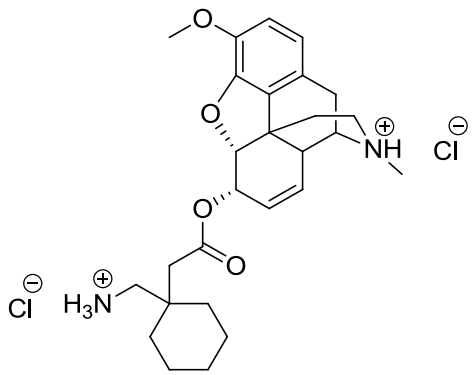

Boc deprotection of Boc-protected gabapentin-codeine ester

Boc protected gabapentin-codeine ester codrug (0.1 g, 0.18 mmol) was placed in an oven dried round bottom flask and kept under nitrogen. 4N HCl solution in anhydrous dioxane (5 mL) was added drop wise and the reaction mixture was stirred at room temperature under nitrogen atmosphere. Progress of the reaction was followed by running TLC. After completion, reaction mixture was diluted with 8 mL ether and stirred vigorously for 15 mins. The dihydrochloride salt separates out as brownish solid and was filtered out from the reaction mixture. The product (0.052 g, 52%) was dried under reduced pressure and stored under nitrogen atmosphere. ^{1}H NMR (300 MHz, DMSO-D_6): δ 11.01 (1H, broad), 7.864 (2H, broad), 6.790 (1H, d), 6.649 (1H, d), 5.685 (1H, d), 5.503 (1H, d), 5.176 (2H, m), 3.748 (2H, s), 3.565 (3H, s), 3.416-3.205 (4H, m), 3.005 (2H, m), 2.849 (2H, d), 2.512 (3H, s), 2.506 (1H, m), 2.349 (1H, m), 1.902 (1H, d), 1.508-1.290 (10H, m); ^{13}C NMR (300 MHz, $CDCl_3$): δ 170.2, 146.0, 142.0, 129.5, 128.6, 126.8, 123.7, 119.8, 114.1, 86.6, 67.7, 66.3, 59.3, 58.8, 58.0, 56.1, 46.3, 44.7, 41.8, 36.9, 34.9, 32.5, 32.3, 31.9, 25.1, 20.7, 20.6.

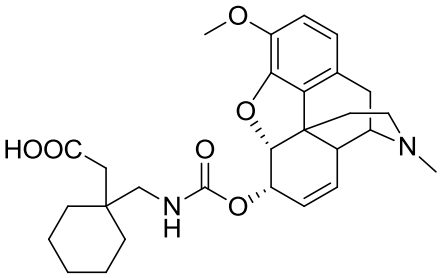

Gabapentin-codeine carbamate

Codeine-*p*-nitrophenol Carbonate (0.262 g, 0.56 mmol) and gabapentin (0.106, 0.62 mmol) were placed in a round bottom flask and dissolved in 8 mL 1:1 mixture of

water and THF. The reaction mixture was stirred at room temperature and progress of the reaction was followed by running TLC. After completion, reaction mixture was concentrated under reduced pressure and then diluted with 40 mL DCM. The organic layer was washed with 50% sodium bicarbonate solution (5 x 20 mL) and brine (20 mL), dried over sodium sulfate and concentrated under reduced pressure to afford a white solid. The crude product was purified using silica gel column chromatography and a methylene chloride-methanol mixture as eluent, to afford the pure product (0.164 g, 59%). ^{1}H NMR (500 MHz, $CDCl_3$): δ 10.820 (1H, broad), 7.003 (1H, broad), 6.670 (1H, d), 6.542 (1H, d), 5.649 (1H, d), 5.508 (1H, broad), 5.322 (1H, d), 5.248 (1H, d), 3.852 (3H, s), 3.704 (1H, broad), 3.318 (2H, m), 3.126 (1H, broad), 3.041 (2H, d), 2.636 (3H, s), 2.586 (2H, m), 2.385 (1H, m), 2.308 (2H, s), 1.913 (1H, d), 1.524-1.330 (10H, m); ^{13}C NMR (300 MHz, $CDCl_3$): δ 177.2, 156.2, 147.0, 142.5, 130.6, 129.8, 127.0, 124.5, 119.3, 114.7, 88.8, 68.1, 58.9, 56.7, 48.6, 46.3, 43.2, 41.9, 41.4, 41.2, 38.2, 37.2, 33.9, 33.3, 26.1, 21.6.

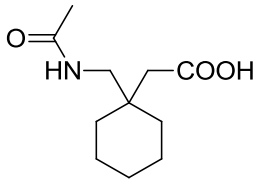

***N*-Acetylgabapentin**

Gabapentin (0.2 g, 1.17 mmol) was placed in a round bottom flask and dissolved in 8 mL saturated aqueous sodium bicarbonate solution. Acetic anhydride (0.262 g, 2.57 mmol) was added drop wise to the solution and the reaction mixture was stirred overnight at room temperature. The reaction mixture was then acidified with 1N HCl and the product was extracted into chloroform. Chloroform layer was dried over anhydrous sodium sulfate and concentrated under reduced pressure to produce a white colored solid product (0.234 g, 94%). ^{1}H NMR (500 MHz, $CDCl_3$): δ 6.939 (1H, broad), 3.262 (2H, d), 2.304 (2H, s), 2.061 (3H, s), 1.513-1.308 (10H, m); ^{13}C NMR (300 MHz, $CDCl_3$): δ 174.4, 172.7, 47.4, 41.7, 37.6, 34.5, 26.1, 23.4, 21.6; MS (ESI): (M+1) 214 *m/z*.

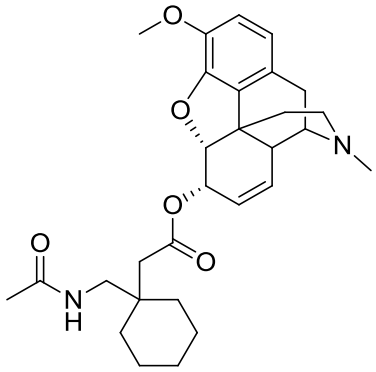

***N*-Acetylgabapentin-codeine ester codrug (CG-3)**

N-acetylgabapentin (0.149 g, 0.7 mmol), codeine (0.209 g, 0.7 mmol), and DMAP (0.34 g, 0.28 mmol) were placed in a round bottom flask and dissolved in 5 mL DCM. The mixture was cooled to 0 °C and then DCC (0.187 g, 0.91 mmol) was added to the stirred solution. The reaction mixture was allowed to come to room temperature and stirred at room temperature. Progress of the reaction was followed by running TLC. After the reaction was over, reaction mixture was diluted with 40 mL DCM and washed with 50% sodium bicarbonate solution (3 x 20 mL) and brine (20 mL), dried over sodium sulfate and concentrated under reduced pressure to afford a white solid. The crude product was purified using silica gel column chromatography and a methylene chloride-methanol mixture as eluent, to afford the pure product (0.229 g, 66%). ^{1}H NMR (500 MHz, $CDCl_3$): δ 6.665 (1H, d), 6.566 (1H, d), 6.406 (1H, t), 5.615 (1H, d), 5.452 (1H, dt), 5.184 (1H, m), 5.076 (1H, dd), 3.719 (3H, s), 3.405-3.315 (2H, m), 3.055 (1H, d), 2.772 (1H, t), 2.611 (1H, dd), 2.429 (1 H, m), 2.455 (3H, s), 2.413 (2H, s), 2.22 (1H, dd), 2.077 (1H, td), 2.016 (3H, s), 1.874 (1H, d), 1.608-1.392 (10H, m); ^{13}C NMR (300 MHz, $CDCl_3$): δ 171.9, 170.7, 146.6, 142.2, 130.4, 129.9, 128.3, 126.8, 119.4, 113.1, 88.5, 68.8, 59.1, 56.3, 46.7, 46.1, 43.2, 43.1, 41.7, 40.8, 38.2, 35.6, 34.8, 34.5, 26.2, 23.6, 21.7, 21.6, 20.6; MS (ESI): (M+1) 495 *m/z*.

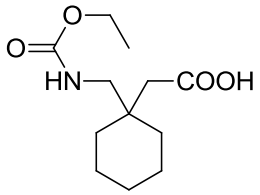

***N*-Ethoxycarbonylgabapentin**

Gabapentin (0.43 g, 2.51 mmol) was added to dry dichloromethane (12 mL) in a round bottom flask, followed by DMAP (0.92 g, 7.53 mmol). Chlorotrimethylsilane (0.64 ml, 5.03 mmol) was added slowly while maintaining the reaction temperature below 15 °C, and the resulting suspension was stirred for 30 min. Ethyl chloroformate (0.327 g, 3.01 mmol) was added slowly while maintaining the temperature below 15 °C. DMAP (0.368 g, 3.01 mmol) was added, and the resulting suspension was stirred at room temperature for 30 min. The resulting silyl ester was converted to the corresponding acid by washing the reaction mixture with water (2 X 15 mL), followed by 1 N HCl (2 X 15 mL) then brine (2 X 15 mL). After drying over anhydrous sodium sulfate and removal of the solvent in vacuo, the crude product (0.513 g, 84%) was obtained as colorless oil and used in the following step without further purification. ^{1}H NMR (500 MHz, $CDCl_3$): δ 6.006 (1H, broad), 5.170 (1H, t), 4.136 (2H, q), 3.225 (2H, d), 2.333 (2H, s), 1.539-1.323 (10H, m), 1.257 (3H, t); ^{13}C NMR (300 MHz, $CDCl_3$): δ 176.6, 157.8, 61.4, 47.8, 41.2, 38.0, 34.2, 26.1, 21.6, 14.9; MS (ESI): (M+1) 244 *m/z*.

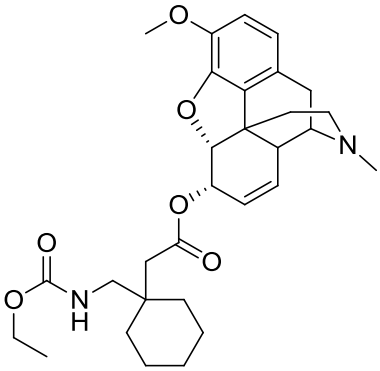

***N*-Ethoxycarbonylgabapentin-codeine ester codrug (CG-4)**

N-ethoxycarbonylgabapentin (0.33 g, 1.36 mmol), codeine (0.487 g, 1.63 mmol), and DMAP (0.066 g, 0.54 mmol) were placed in a round bottom flask and dissolved in 15 mL DCM. The mixture was cooled to 0 °C and then DCC (0.364 g, 1.76 mmol) was

added to the stirred solution. The reaction mixture was allowed to come to room temperature and stirred at room temperature. Progress of the reaction was followed by running TLC. After the reaction was over, reaction mixture was diluted with 50 mL DCM and washed with 50% sodium bicarbonate solution (3 x 20 mL) and brine (20 mL), dried over sodium sulfate and concentrated under reduced pressure to afford a white solid. The crude product was purified using silica gel column chromatography and a methylene chloride-methanol mixture as eluent, to afford the pure product (0.573 g, 67%). ^{1}H NMR (500 MHz, $CDCl_3$): δ 6.664 (1H, d), 6.558 (1H, d), 5.630 (1H, d), 5.450 (1H, dt), 5.311 (1H, t), 5.172 (1H, m), 5.110 (1H, d), 4.106 (2H, q), 3.812 (3H, s), 3.374 (1H, m), 3.16 (2H, d), 3.052 (1H, d), 2.736 (1H, m), 2.586 (1H, dd), 2.445 (3H, s), 2.410 (2H, d), 2.380 (1H, d), 2.322 (1H, td), 2.053 (1H, td), 1.873 (1H, dd), 1.601-1.434 (10H, m), 1.239 (3H, t) ppm; ^{13}C NMR (300 MHz, $CDCl_3$): δ 171.9, 157.4, 146.9, 142.3, 130.6, 130.0, 128.4, 127.1, 119.3, 113.5, 88.3, 69.0, 60.8, 59.2, 56.6, 49.4, 47.6, 46.8, 43.4, 43.2, 41.1, 38.4, 34.4, 34.3, 31.9, 26.3, 25.2, 21.8, 20.6, 15.0; MS (ESI): (M+1) 525 *m/z*.

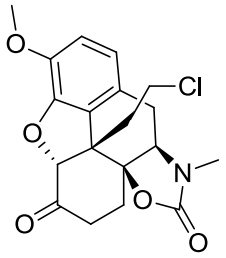

Oxycodone derivative

Oxycodone (0.25 g, 0.79 mmol) and DMAP (0.233 g, 1.91 mmol) were dissolved in 8 mL of anhydrous THF. *para*-Nitrophenylchloroformate (0.367 g, 1.82 mmol), dissolved in 2 mL of dry THF was added to the reaction mixture drop-wise and then the reaction mixture was heated to 170 °C for 4 minutes under microwave irradiation. THF was then evaporated under reduced pressure and the obtained solid was dissolved in 50 mL DCM. The organic layer was washed with 50% sodium bicarbonate solution (5 x 20 mL) and brine (20 mL), dried over sodium sulfate and concentrated under reduced pressure to afford a brown solid. The crude product was purified by recrystallization from ethyl acetate (0.25 g, 84%). ^{1}H NMR (500 MHz, $CDCl_3$): δ 6.786 (1H, d), 6.742 (1H, d), 4.901 (1H, s), 3.07 (3H, s), 6.635 (1H, dd), 3.503 (1H, td), 3.236 (1H, dd), 2.995 (3H, s),

2.938 (2H, m), 2.757 (1H, dd), 2.513 (1H, m), 2.373 (1H, dt), 2.246 (1H, dt), 2.167 (1H, m), 1.611 (1H, td); ^{13}C NMR (300 MHz, $CDCl_3$): δ 204.0, 156.3, 145.8, 143.8, 125.8, 121.5, 121.3, 115.1, 90.4, 90.3, 82.2, 64.4, 56.6, 39.4, 37.4, 36.8, 34.4, 30.9, 29.7; GC-MS M^+ 377 *m/z*.

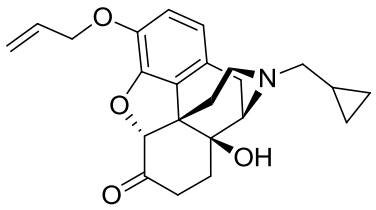

3-*O*-Allylnaltrexone

Naltrexone (0.052 g, 0.15 mmol) was placed in a round bottom flask and dissolved in 6 mL acetone. K_2CO_3 (0.084 g, 0.61 mmol) was added to the solution followed by drop wise addition of ally bromide (0.02 mL, 0.2 mmol). The reaction mixture was refluxed and progress of the reaction was monitored by running TLC. After completion, the reaction mixture was cooled to room temperature and filtered. The organic filtrate was evaporated under reduced pressure and obtained liquid was dissolved in ethyl acetate and washed with water and brine, dried over sodium sulfate and concentrated under reduced pressure to afford a colorless liquid (0.05 g, 87%). ^{1}H NMR (300 MHz, $CDCl_3$): δ 6.720 (1H, d), 6.569 (1H, d), 6.002 (1H, m), 5.350 (1H, d), 5.208 (1H, d), 4.766-4.636 (3H, m), 3.185 (1H, d), 2.991 (2H, m), 2.974-2.560 (2H, m), 2.540-2.225 (4H, m), 2.130 (1H, td), 1.892 (1H, m), 1.689-1.527 (3H, m), 0.869 (1H, m), 0.553 (2H, q), 0.149 (2H, q).

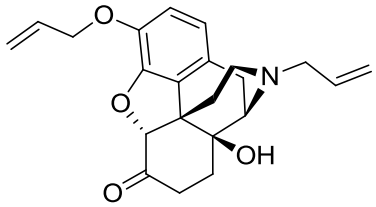

3-*O*-Allylnaloxone

Allyl protection of naloxone was performed by following a procedure same as allyl protection of naltrexone. 90% yield; ^{1}H NMR (500 MHz, $CDCl_3$): δ 6.730 (1H, d), 6.612 (1H, d), 6.076 (1H, m), 5.827 (1H, m), 5.394 (1H, dq), 5.258-5.180 (3H, m), 4.76-

4.662 (3H, m), 3.164 (2H, dd), 3.075-2.992 (3H, m), 2.583 (2H, m), 2.391(1H, td), 2.303 (1H, dt), 2.146 (1H, td), 2.053 (1H, s), 1.872 (1H, ddd), 1.670-1.559 (2H, m); ^{13}C NMR (300 MHz, $CDCl_3$): δ 208.2, 145.2, 141.5, 135.0, 133.8, 129.6, 125.3, 119.4, 118.1, 117.5, 117.5, 90.2, 70.9, 70.2, 62.2, 57.6, 50.7, 43.3, 36.2, 31.4, 30.6, 22.8; GC-MS M^+ 367 *m/z*.

Copyright © Ujjwal Chakraborty 2012

Chapter 3

Analgesic Activities of Codrugs, Parent Drugs and Physical Mixtures of Parent Drugs

3.1 Introduction

Pain has been defined as "an unpleasant sensory and emotional experience associated with actual or potential damage or described in terms of such damage" (Merksey, 1979). Pain is always subjective and each individual learns the application of the word through experiences related to injury in early life. The sensation of pain is primarily a protective mechanism designed to avoid tissue damage (Joshi and Honore, 2006). Unfortunately pain often outlives its usefulness as a warning system and instead becomes chronic and debilitating. Sherrington proposed the existence of the nociceptor, a primary sensory neuron that is activated by stimuli capable of causing tissue damage. According to this theory, nociceptors have characteristic thresholds or sensitivities that distinguish them from other sensory nerve fibers (Sherrington, 1908).

Pain is broadly divided in two categories, nociceptive and neuropathic pain. Nociceptive pain is a normal response to noxious stimuli that elicits tissue injury. This type of pain serves as a warning to protect ourselves from real or impending injury. Nociceptive pain is illustrated by the type of response caused by briefly touching a hot surface or by a pin prick. Such mechanical or thermal stimuli result in the activation of C- and Aδ-fibers in primary afferent nociceptive pathways. Input from these pathways is then integrated in the dorsal horn of the spinal cord and relayed to the brain (Julius and Basbaum, 2001). On the other hand, neuropathic pain is elicited by injury to the peripheral or central nervous system. Injury to the nervous system can be caused by tissue trauma, surgery, limb crush or amputation, infection, autoimmune diseases such as diabetes and arthritis, radiation damage, and by various drug regimens (e.g. chemotherapeutic and anti-HIV agents) (Campbell and Meyer, 2006). The pain can occur even without any physical or chemical stimuli. Unlike nociceptive pain, neuropathic pain

can persist for a long time, even after the initiating injury has been completely healed. This leads to abnormal processing of sensory information by the nervous system. After the nerve injury, changes occurring in the central nervous system can persist indefinitely. The pain is felt in many different ways, such as burning, tingling, prickling, shooting, and spasm (Rotha et al., 1998). Allodynia and hyperalgesia are two hallmarks of neuropathic pain. Allodynia refers to pain due to a stimulus, which does not normally provoke pain, e.g., touch, cold, light pressure can be felt as pain. Hyperalgesia refers to an increased response to a stimulus which is normally painful (Riedel and Neeck, 2001). It has been anticipated that the prevalence of all sorts of neuropathic pain will exceed 75 million worldwide in the next decade (Cavenagh et al., 2006). Qualitatively, pain can further be defined in terms of its severity (mild, moderate and severe pain) and temporality (acute and chronic pain). Acute pain is commonly defined as the normal predicted physiological response to an adverse chemical, thermal or mechanical stimulus associated with surgery, trauma and acute illness (Carr and Goudas, 1999). On the other hand, chronic pain is defined as a pain of greater than six month duration and associated with cancer, AIDS, peripheral nerve disorders and diabetes (Ballantyne and Mao, 2003).

3.2 Animal Models of Pain

Research on the neurobiological bases of nociception and pain and related investigations of potential analgesic therapies require great reliance on animal models of pain. Assessment of clinical pain brings a unique problem compared to other major health conditions, such as heart disease or cancer. The attempts to assess pain in non-human species have involved observations of spontaneous behavioral or physiological reactions to presumed sources of pain. The use of comparable methods in preclinical studies in animals and clinical studies with humans is critical to successful translational research (Rice at al., 2009). Assessment of pain sensitivity should be approached similarly with behavioral observations of humans and laboratory animals. Stimulus response functions for escape from nociceptive stimulation can provide comparable information for laboratory animals (Joshi and Honore, 2006).

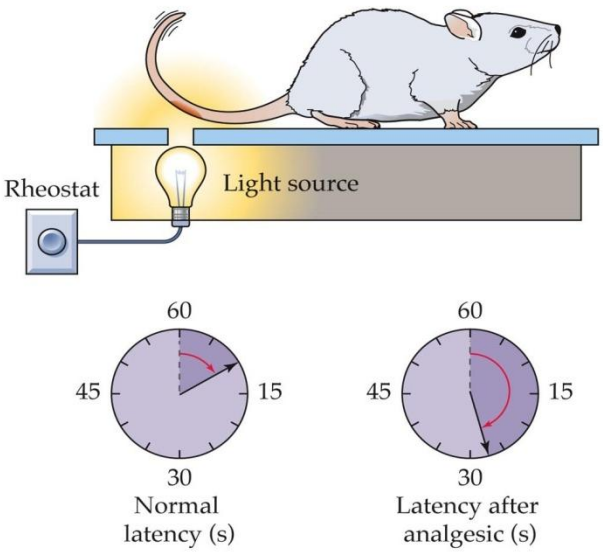

Fig. 3.1: The Tail-Flick test (Reprinted with permission from www.ottoenvironmental.com).

Different animal pain models are used for different kinds of pain. For example models developed to measure responses to acute noxious thermal stimuli use a noxious heat or cold stimulus to the paw or tail of rodents (Mogil, 2009). These models are widely used for testing opioid analgesics. In these methods, latency to behavioral response is recorded and a cut-off time period is set to avoid any tissue damage to the animal. In the tail-flick test, an intense beam of light is applied to the tail of a rat and the latency period is measured until the tail is flicked out of the path of the light beam (Fig. 3.1). One other assay to determine sensitivity to heat in normal animals, as well as in animals under chronic pain conditions, has been described by Hargreaves et al. (Hargreaves et al., 1988) and uses a radiant heat source. In this method, the temperature of the heat source is applied to the hind paw and increases over time until it reaches a painful threshold. Latency of withdrawal of hind paw is recorded and analyzed. One widely used method to test for reactivity to cold is the application of a drop of cold acetone onto the skin of a rat. Acetone produces a distinct kind of sensation when it evaporates. Normal rats do not respond to this stimulus, while nerve-injured rats show an exaggerated response (Vissers and Meert, 2005).

Responses to acute noxious mechanical stimuli are measured by stimulating the paw or the tail of rodents. In the Randall Selitto test, increased pressure is applied to the dorsal surface of the hind paw/tail of a rat via a dome-shaped plastic tip. The threshold (in grams) for either paw or tail withdrawal is then recorded (Randall and Selitto, 1957). Similarly, responses to acute noxious chemical stimuli can be measured by injecting chemical irritants such as capsaicin, formalin or mustard oil. The animal responds by biting or licking the injected paw. These observations are recorded at various time points after administration of the drug to be tested (Rose and Woodbury, 2008).

Fig. 3.2: The Paw-Pressure test (Reprinted with permission from www.ottoenvironmental.com).

Different models are used for pain following injury to the nervous system. One example is the chronic constriction injury pain model (Bennett's model) (Bennett and Xie, 1988). This pain model involves the tying of four loose ligatures around the sciatic nerve of a rat, just tightly enough to touch the nerve. Subsequent swelling of the nerve

constricts the nerve, which develops hyperalgesia and allodynia over 10 to 14 days (Hogan, 2002).

One other most studied neuropathic pain model is L5-L6 spinal nerve ligation (SNL; Chung's model). In this ligation process, the L5 and L6 spinal nerves of the animal are isolated and tightly ligated with silk thread. This induces mechanical allodynia within 7-10 days. Models have also been developed involving cold allodynia and thermal hyperalgesia. Animals exhibit a dynamic mechanical allodynia, which is assessed by gently brushing with a soft brush (Chung, et al., 2004).

In the present chapter, the tail-flick test is used to assess the effect of the codrugs synthesized in Chapter 2 on nociceptive pain, and the chronic constriction injury pain model is used to assess the effect of codrugs on neuropathic pain.

Advantages and disadvantages of animal pain models:

- Animal studies allow controlled investigation of chronic pain conditions that are almost impossible to perform in humans.
- Animal models of pain provide the means to explore basic physiological mechanisms of pain.
- Prediction of analgesic efficacy leading to clinical drug development is moderately accurate based on results from animal studies. No analgesic agent has ever been found in humans that did not have a rodent counterpart.
- One major criticism of animal pain testing is that too much emphasis has been placed on reflexive withdrawal from mechanical or thermal stimuli as a dependent measure.
- In animal models emphasis has been placed on measuring pain itself and not giving importance to the states that accompany pain. Patients suffering from chronic pain experience disability, anxiety, depression, cognitive dysfunction, sleep loss, loss of libido, social withdrawal, and many other symptoms. Most of these symptoms are ignored in animal pain testing.
- Preclinical animal models for chronic pain predominantly measure thermal and mechanical hypersensitivity, whereas symptoms of chronic pain in humans

mainly include spontaneous pain, numbness and dysethesia (unpleasant, abnormal sense of touch).

- Chronic pain sufferers are overwhelmingly female in the case of humans and chronic pain is more prevalent in the middle aged and elderly population than in young adults. On the other hand, animals used in pain models are healthy, young, often genetically identical and overwhelmingly male rodents.
- Some neuropathic pain models have been criticized because of the poor general health of the animals, which may interfere with the outcome of the study. (Mogil et al., 2010; Bennett, 1993; and Vierck et al., 2008)

Codeine and morphine are well known opioid drugs commonly used to control pain, whether alone or in combination with an adjunct drug. Unfortunately, long term use of these opioids results in the development of tolerance and physical dependence (Ballantyne and Mao, 2003). This reduces the analgesic effects necessitating the administration of high and potentially harmful doses to achieve adequate pain control. The efficacies of physical mixtures of opioids and nornicotine enantiomers have previously been characterized in rodent models of nociceptive and neuropathic pain. These models included acute thermal nociception and peripheral neuropathy (chronic constriction nerve injury, CCI). In the present chapter, we have investigated codrug pain therapy where drugs from two different classes (opioids and a nicotinic receptor agonist) are administered as a single chemical entity, whereby the two molecules are covalently linked together via a carbamate linkage. The efficacies of each of the parent drugs as well as a 1:1 physical mixture of the parent drugs were compared with the respective codrug as pain modulators in the above pain models to determine their relative effectiveness.

Analgesic activity study on the codrugs and parent drugs were carried out with the cooperation of Dr. Elzbieta Wala.

3.3 Analgesic Activity of Opioid-*S*-(-)-Nornicotine Codrugs

3.3.1 Animals

Male Sprague-Dawley rats (Harlan, Indianapolis) about 90 days old, weighing 300-350 g were used for all experiments. Rats were housed separately in a transparent

cage; with free access to standard laboratory chow and tap water in a humidity and temperature-controlled facility with lights on between 0600 and 1800 h. Rats were trained in the test situation before initiation of the experimental procedures. Rats were fasted overnight before oral administration of drug. Body weights were determined on the day of experimentation. At the end of the experiment, rats were euthanized with pentobarbital sodium (150 mg/kg, intraperitoneal, IP). A crossover paradigm was used within an experiment (if possible) to minimize the number of rats. All testing was performed in accordance with the guidelines of the National Institute of Health Guide for Care and Use of Laboratory Animals (Publication No. 85-23, revised 1985). The protocol was approved by the University of Kentucky Animal Care and Use Committee.

3.3.2 Drugs

The codeine-*S*-(-)-nornicotine codrug was evaluated using the tail-flick and chronic constriction injury pain models. The individual parent drugs codeine and *S*-(-)-nornicotine were also assessed using the same pain models. A 1:1 physical mixture of codeine and *S*-(-)-nornicotine was also analyzed in tail-flick assay. Similarly, the 3-*O*-acetylmorphine-*S*-(-)-nornicotine codrug, and 3-*O*-acetylmorphine and *S*-(-)-nornicotine parent drugs were evaluated using the tail-flick pain assay. Drugs were dissolved in 15% PEG saline solution and administered by the oral route using a gavage feeding needle after overnight fasting of the animals. A 15% solution of PEG in saline (vehicle) served as the control.

3.3.3 Tail Flick Test (Measure of Analgesia/Antinociception)

The tail-flick test primarily assesses the spinal antinociceptive (pain relief) response to noxious thermal stimuli (D'Amour and Smith, 1941). An intense beam of light is applied to the tail of a Sprague-Dawley rat and the latency period is measured until the tail is flicked out of the path of the light beam (Fig. 3.1). Baseline tail-flick latencies were determined prior to drug administration using the tail-flick latency test.

Tail-flick latencies were also determined at several time points after administration of the analgesic drugs for each individual animal. Time response curve was generated by calculating the average TFL at each time point using 4-6 rats and was plotted as mean ± SEM *versus* time. SEM stands for Standard Error of the Mean and is calculated as [standard deviation / $(N)^{1/2}$], where N is population size. During testing, a cutoff time of 10 s was employed to prevent damage to the tail of the rat.

Initially, rats (6/group) were treated with four different doses (10, 20, 30, and 40 mg/kg) of codeine administered via the oral route. Responsiveness (TFL: Tail Flick Latency) was measured prior to (baseline) and after oral dosing. Time-response and dose-response curves were drawn to calculate ED_{50} value for codeine (Fig. 3.3 and 3.7).

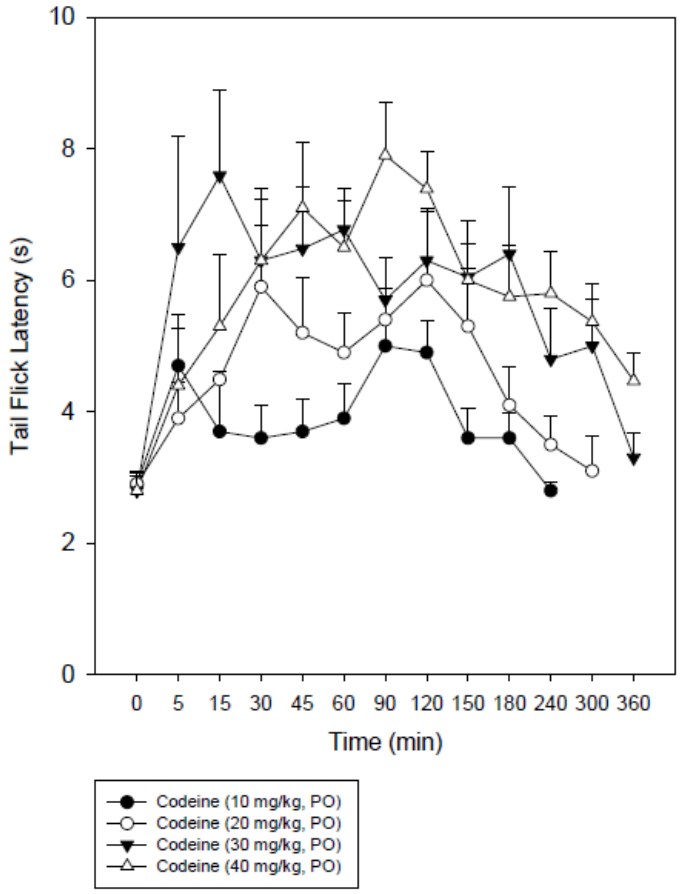

Fig. 3.3: The Tail-Flick latencies of orally administered codeine.

Secondly, rats (6/group) were treated with three increasing doses (20, 40, and 80 mg/kg) of *S*-(-)-nornicotine administered via the oral route. Responsiveness (TFL) was measured prior to (baseline) and after oral dosing. Time-response and dose-response curves were drawn to calculate ED_{50} value for *S*-(-)-nornicotine (Figs. 3.4 and 3.7).

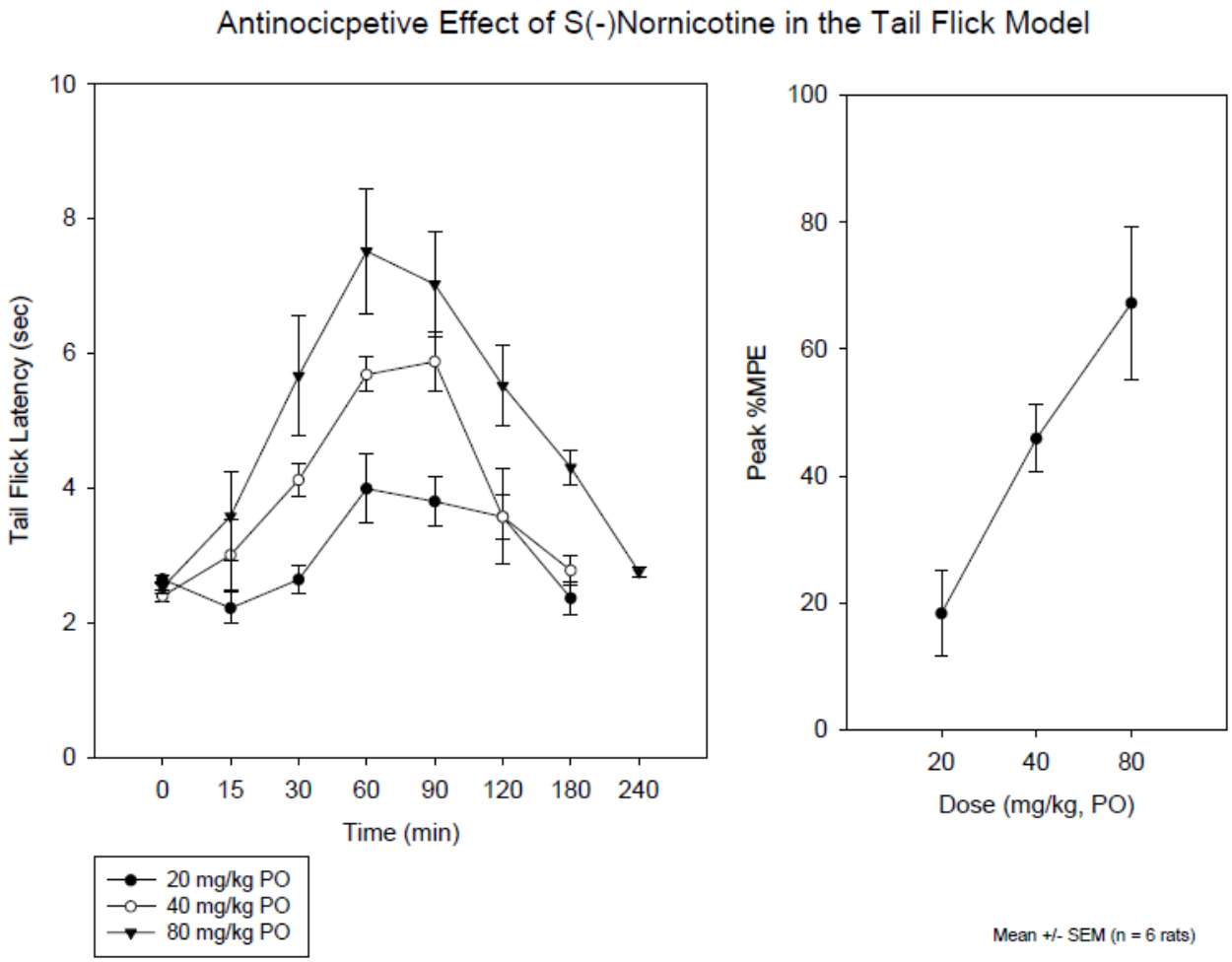

Fig. 3.4: The Tail-Flick latencies and dose response curve of orally administered *S*-(-)-nornicotine.

Thirdly, rats (6/group) were treated with three oral doses (5, 10 and 15 mg/kg) of the codeine-*S*-(-)-nornicotine codrug. In a separate experiment one dose (10 mg/kg codeine + 5 mg/kg *S*-(-)-nornicotine, total of 15 mg/kg, 1:1 molar ratio) of an equimolar physical mixture of the two parent drugs was administered. Drugs were administered via

the oral route. Animals were tested for tail-flick response using the tail-flick apparatus. Intensity of the heat source was adjusted to produce baseline tail-flick latencies of 2 to 3 sec. These baseline tail-flick latencies of the rats were recorded three times (5, 10, 15, 30 min apart). Responsiveness (TFL) was measured again after oral dosing (5, 10, 15, 30 min apart) of the codrug doses and equimolar physical mixture dose of codeine and *S*-(-)-nornicotine. Dose-response curves can be generated if a minimum of three doses of a drug are utilized in this assay. The time-response graphs obtained with the three different doses of codeine-*S*-(-)-nornicotine codrug are illustrated in Fig. 3.5 and are compared with that of an equimolar physical mixture of codeine and *S*-(-)-nornicotine (10 mg/kg codeine + 5 mg/kg *S*-(-)-nornicotine, total of 15 mg/kg of the physical mixture). In Figs. 3.6 and 3.8, efficacy of the codrug is compared with the equivalent dose of physical mixture of the two parent drugs and comparable doses of the individual drugs alone.

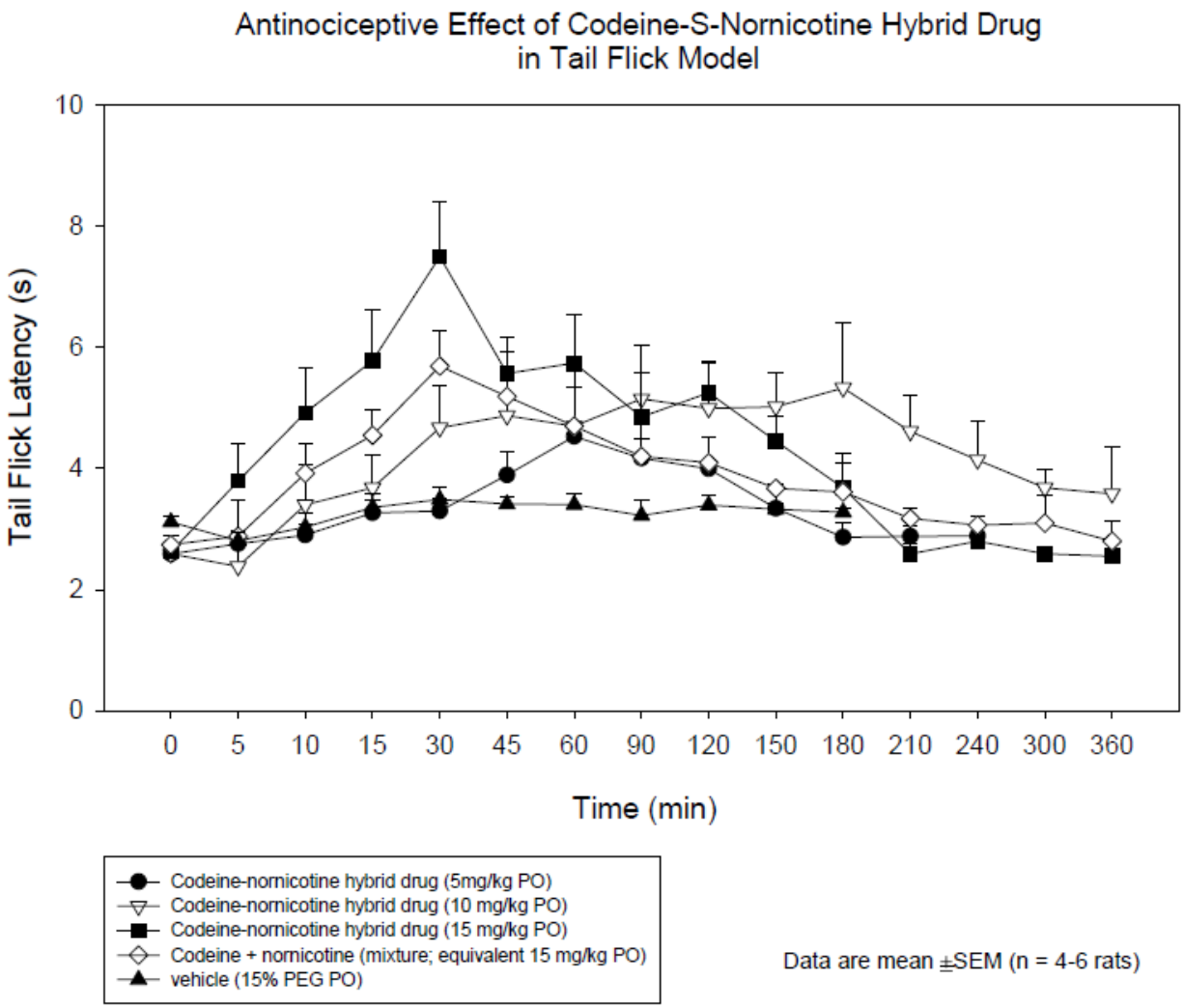

Fig. 3.5: The Tail-Flick latencies of orally administered codeine-*S*-(-)-nornicotine codrug.

In a similar manner, the 3-*O*-acetylmorphine-*S*-(-)-nornicotine codrug and its parent drugs 3-*O*-acetylmorphine and *S*-(-)-nornicotine were also assessed in the tail-flick test. Rats (6/group) were treated with 3-*O*-acetylmorphine alone (3 oral doses: 2.5, 5, and 10 mg/kg), with *S*-(-)-nornicotine alone (3 oral doses: 5, 8, and 30 mg/kg) and with five doses (0.5, 1.25, 2.5, 4 and 8 mg/kg) of 3-*O*-acetylmorphine-*S*-(-)-nornicotine codrug.

3.4 Chronic Constriction Nerve Injury (CCI, Neuropathic Pain Model)

3.4.1 Surgery

The rodent model of peripheral neuropathy (chronic constriction nerve injury, CCI) (Bennett and Xie, 1988) was used to characterize the antihyperalgesic effect of codeine, *S*-(-)-nornicotine and codeine-*S*-(-)-nornicotine codrug. This pain model involves the tying of four loose ligatures around the sciatic nerve, which results in the development of mechanical (tactile) allodynia in the ipsilateral hindpaw of the rat (Bennett and Xie, 1988).

3.4.2 Mechanical Hyperalgesia

Enhanced sensitivity to mechanical noxious stimuli (mechanical hyperalgesia) was evaluated using the paw pressure test (Randall and Selitto, 1957). This was done prior to surgery (pre-CCI baseline) and on the post-surgery day. The hind paw was placed between a blunt pointer and a flat surface and increasing pressure was applied to the dorsal side of the paw. Rats (6/group) were treated with codeine alone (4.9, 10, 20, 40 mg/kg doses), *S*-(-)-nornicotine alone (5, 20, 40, and 60 mg/kg dose) and codeine-*S*-(-)-nornicotine codrug (1, 5 and 10 mg/kg doses). Drugs were administered via the oral route.

3.4.3 Statistical Analysis

Responses were normalized for baseline values. Percent maximum possible effect was calculated at the time of peak response: %MPE = [(TFL-baseline)/ (cut off-baseline)] x 100. ED_{50} values were computed for codeine-*S*-(-)-nornicotine codrug, codeine and *S*-(-)-nornicotine. The overall effects (antihyperalgesia) were presented as areas-under-the-time curves, calculated by the trapezoidal rule for baseline normalized responses. Data were analyzed using regression analysis, analysis of variance (ANOVA), post-hoc

Student Newman Keuls test (SNK) and t-test. Level of significance was $P \leq 0.05$. All data were mean ± SEM (n = number of rats).

3.5 Results

3.5.1 Codeine-*S*-(-)-Nornicotine Codrug Antinociception (Tail Flick Tests)

The antinociceptive effects of codeine alone, *S*-(-)-nornicotine alone, various doses of codeine-*S*-(-)-nornicotine codrug, and an equimolar physical mixture dose of the two parent drugs (codeine and *S*-(-)-nornicotine) were characterized after the oral administration in the tail-flick test. The present data provides evidence (Figs. 3.3, 3.4, 3.5, 3.6, 3.7, and 3.8) that a codrug consisting of codeine (low dose) and *S*-(-)-nornicotine (non-effective dose) significantly enhances effectiveness of the analgesic agent against acute nociception. In preliminary experiments, one dose of codeine-*S*-(-)-nornicotine codrug and one dose of codeine were given to the rats to compare the analgesic effect of the codrug with codeine. A 15 mg/kg dose of codeine-*S*-(-)-nornicotine codrug and a 10 mg/kg codeine dose were chosen for this purpose (Fig. 3.6) (15 mg/kg dose of codrug contains 10 mg/kg dose of codeine). Both codeine and codeine-*S*-(-)-nornicotine codrug tail-flick latency values were above baseline values, which indicates that both drugs exhibit analgesic effects. On comparing the effect of codeine with the codeine-*S*-(-)-nornicotine codrug, it can be observed that the analgesic effect of the codrug is much greater than that of codeine, even though the dose of codeine utilized is one and a half times the weight of the codeine (on a molar equivalent basis) in the codrug molecule. Next, the time-response curve for the three doses of the codeine-*S*-(-)-nornicotine codrug (5, 10, and 15 mg/kg) was generated to obtain a dose-response curve. Figs. 3.5 and 3.7 illustrate the time-response curve and dose response curve for the 5, 10, and 15 mg/kg doses of the codrug. To determine the efficacy of the analgesia produced by the codeine-*S*-(-)-nornicotine codrug as compared to that of a physical mixture of the two parent drugs, an equimolar physical mixture dose (10 mg/kg codeine + 5 mg/kg *S*-(-)-nornicotine, total of 15 mg/kg of the physical mixture) was administered orally and compared with the codrug in terms of dose-response curve.

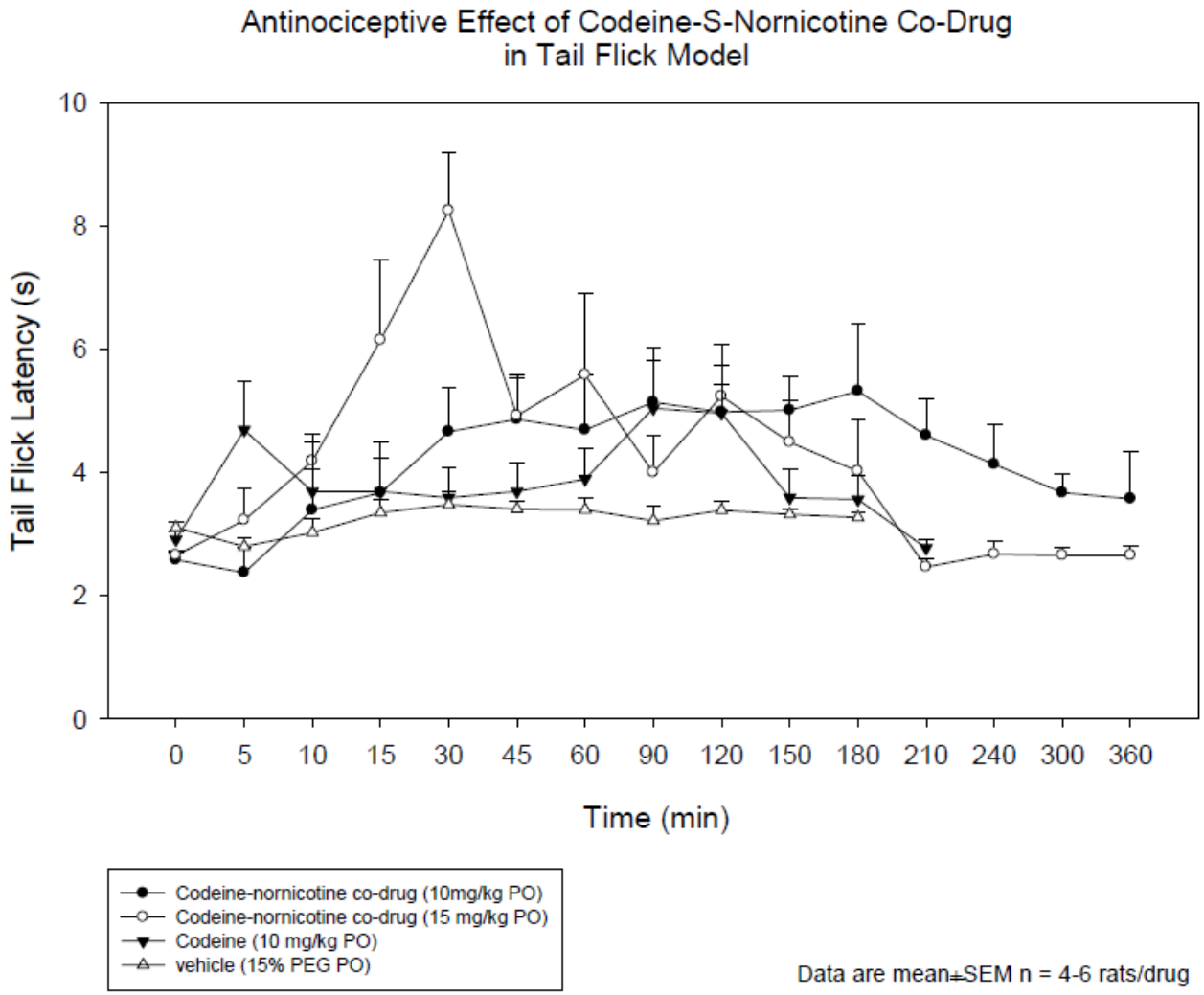

Fig. 3.6: The Tail-Flick latencies codeine-*S*-(-)-nornicotine codrug and codeine.

Fig. 3.7 illustrates the %MPE (Maximum Possible Effect) at the peak of the time response curve for codeine-*S*-(-)-nornicotine codrug, codeine, and *S*-(-)-nornicotine. % MPE can be related to the effectiveness of the drug. The greater the %MPE, the more effective the drug is. The highest %MPE achieved by codeine and the codeine-*S*-(-)-nornicotine codrug is around 80%. Increasing the dose further for codeine does not result in a further increase in the %MPE. The 15 mg/kg dose of the codeine-*S*-(-)-nornicotine codrug produced the highest %MPE among the codrug doses. The equi-effective dose of

codeine was 30 mg/kg compared to a 15 mg/kg dose of the codeine-*S*-(-)-nornicotine codrug. The 15 mg/kg dose of the codeine-*S*-(-)-nornicotine codrug contains 10 mg/kg dose of codeine. Therefore, the analgesic effect shown by 10 mg/kg dose of codeine when given in the form of the codeine-*S*-(-)-nornicotine codrug is equivalent to a 30 mg/kg dose of codeine alone. On the other hand, *S*-(-)-nornicotine does not possess very good analgesic activity on its own. To achieve %MPE similar to codeine or codrug, a very high oral dose of the drug molecule is required. A 60 mg/kg oral dose of *S*-(-)-nornicotine produces %MPE approximately similar to a 15 mg/kg dose of codeine-*S*-(-)-nornicotine codrug. The 15 mg/kg dose of codeine-*S*-(-)-nornicotine codrug contains only a 5 mg/kg dose of *S*-(-)-nornicotine. Fig 3.4 shows that 5 mg/kg dose of *S*-(-)-nornicotine is almost ineffective as an analgesic. It can further be noticed that the dose-response curve for the codrug is shifted to the left compared to the dose response curves of codeine and *S*-(-)-nornicotine. Shifting of the dose response curve to the left signifies that a lesser amount of codrug dose is required to produce analgesic effect similar to the parent drugs.

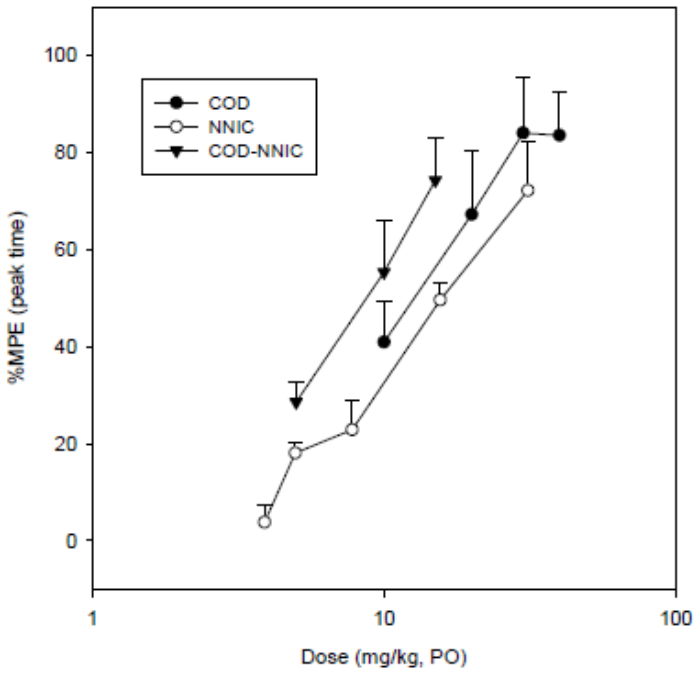

Fig. 3.7: Dose-response curves for codeine, *S*-(-)-nornicotine, and codeine-*S*-(-)-nornicotine codrug in tail-flick test.

Fig. 3.8 illustrates the %MPE (Maximum Possible Effect) at the peak of the time-response curve for the codeine-*S*-(-)-nornicotine codrug (three doses: 5, 10, 15 mg/kg), codeine (one dose: 10 mg/kg), *S*-(-)-nornicotine (one dose: 5 mg/kg), equimolar physical mixture of the two parent drugs (10 mg/kg codeine + 5 mg/kg *S*-(-)-nornicotine, total of 15 mg/kg of the physical mixture), and vehicle. It can be observed that the 15 mg/kg codrug dose is more effective than an equimolar physical mixture dose of codeine and *S*-(-)-nornicotine weighing 15 mg/kg total. It can further be noticed that the 10 mg/kg codrug dose is also more effective than the 15 mg/kg physical mixture dose. The 10 mg/kg codrug dose is also more effective compared to the 10 mg/kg dose of codeine.

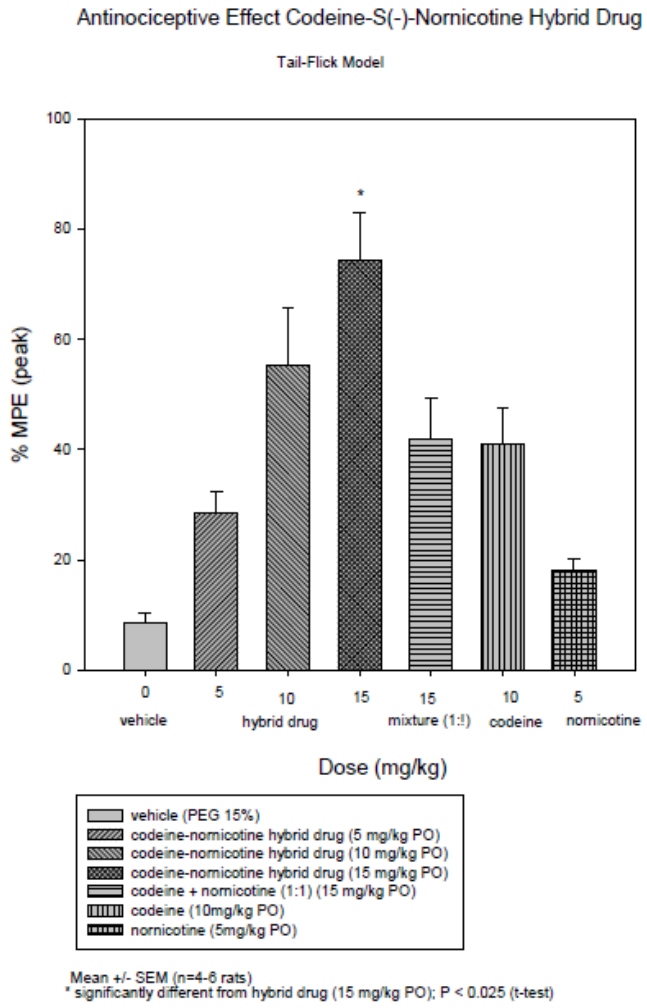

Fig. 3.8: Comparison of %MPE at peak time for codeine-S-(-)-nornicotine codrug, physical mixture, and the individual parent drugs in tail-flick test.

In conclusion, the present data demonstrates that combining codeine with *S*-(-)-nornicotine in the form of a codrug may enhance the effectiveness of both codeine and *S*-(-)-nornicotine against acute nociception. Also side effects associated with higher doses of codeine and *S*-(-)-nornicotine can be avoided by the codrug approach, since lower doses of each parent drug can be utilized.

3.5.2 Codeine-*S*-(-)-Nornicotine Codrug Antihyperalgesic Effect (CCI Model)

Chronic constriction nerve injury (CCI) results in significantly decreased thresholds to mechanical noxious stimuli (hyperalgesia) compared to the pre-surgical threshold. The paw withdrawal threshold (PWT) (pre-CCI) was 225 ± 3.5 g versus a PWT (post-CCI) of 112 ± 4.3 g. The antihyperalgesic effect of codeine alone, *S*-(-)-nornicotine alone and various doses of the codeine-*S*-(-)-nornicotine codrug were characterized after administration via the oral route. The data obtained provides evidence (Figs. 3.9, 3.10, 3.11, and 3.12) that the codeine-*S*-(-)-nornicotine codrug exhibits a synergistic antihyperalgesic effect. Fig. 3.9 demonstrates the time-response and dose-response curves for various doses of codeine alone (4.9, 10, 20, and 40 mg/kg). Dose-response curves for codeine were generated to determine the dose of codeine that was equi-effective as the codeine-*S*-(-)-nornicotine codrug, and to calculate ED_{50} value of codeine. A 65% MPE was exhibited by codeine. Similarly, time-response curves and dose-response curves were generated for *S*-(-)-nornicotine alone after oral dosing of the drug. Four doses (5, 20, 40, and 60 mg/kg) of *S*-(-)-nornicotine were used to generate dose-response curves for the calculation of ED_{50} values. The maximum possible effect shown by *S*-(-)-nornicotine alone was 45%. In a similar manner, time-response and dose-response curves were generated for the codeine-*S*-(-)-nornicotine codrug. Fig. 3.11 shows the time-response curves for various doses (1, 5, and 10 mg/kg) of the codeine-*S*-(-)-nornicotine codrug. Post-hoc Student Newman Keuls (SNK) analysis indicated that the 5 and 10 mg/kg doses of the codrug showed an enhanced antihyperalgesic effect when compared to vehicle alone. The maximum possible effect was achieved around 2 hours

post-dosing with the 15 mg/kg dose of the codeine-*S*-(-)-nornicotine codrug. The enhancement of the analgesic response caused by the codeine-*S*-(-)-nornicotine codrug is evident at several points in the time-response curves.

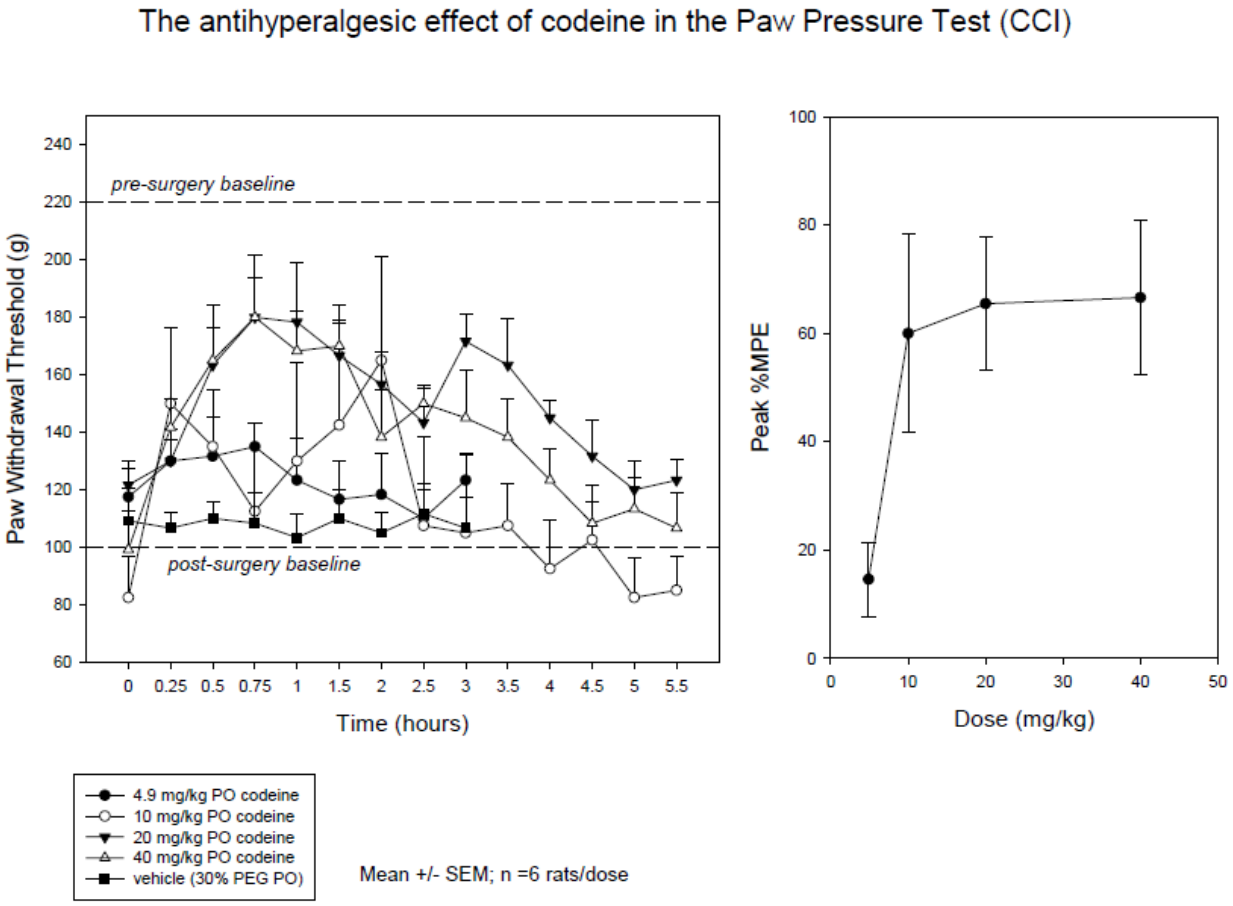

Fig. 3.9: Time-response and dose-response curves for orally administered codeine in the CCI model.

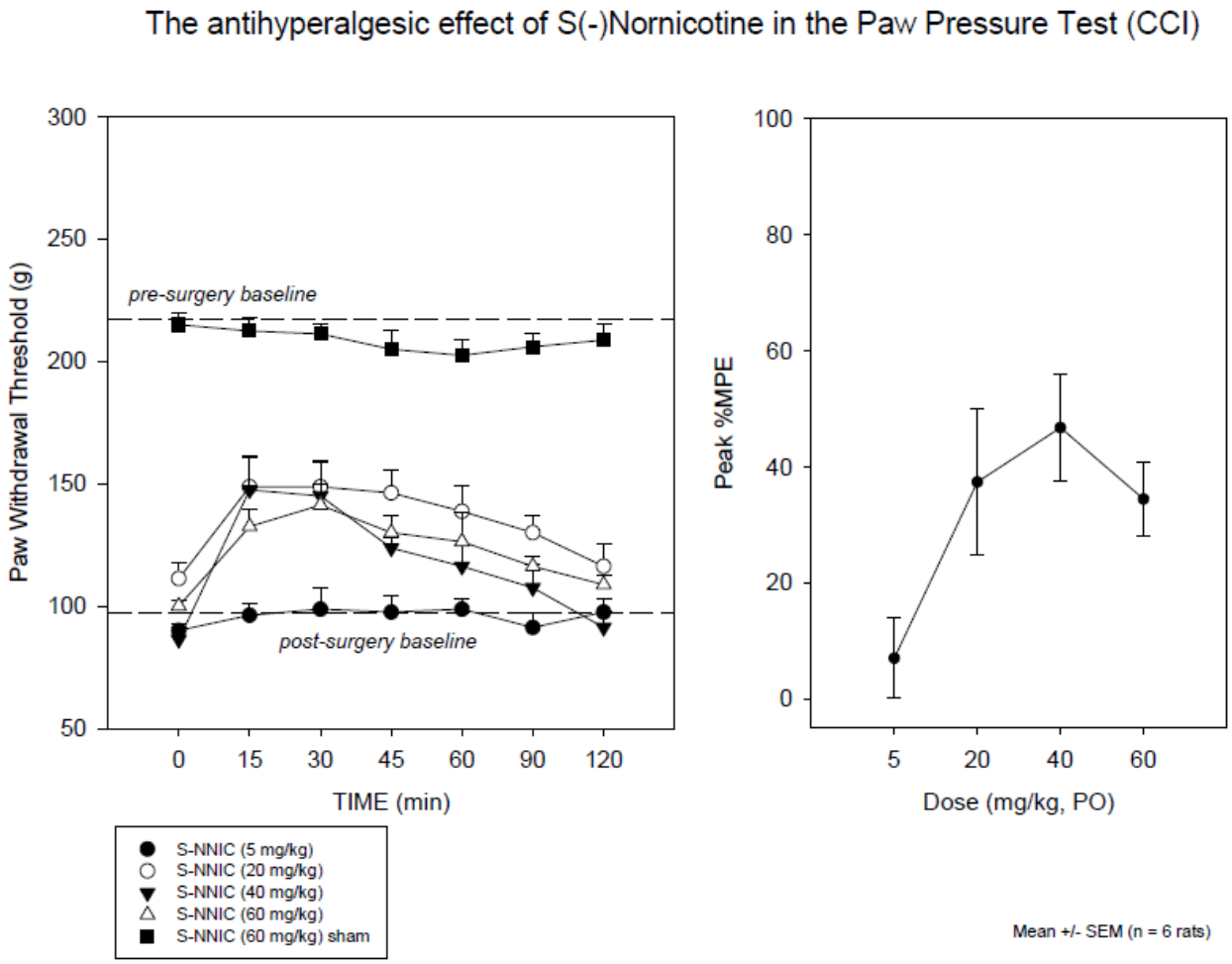

Fig. 3.10: Time-response and dose-response curves for orally administered *S*-(-)-nornicotine in the CCI model

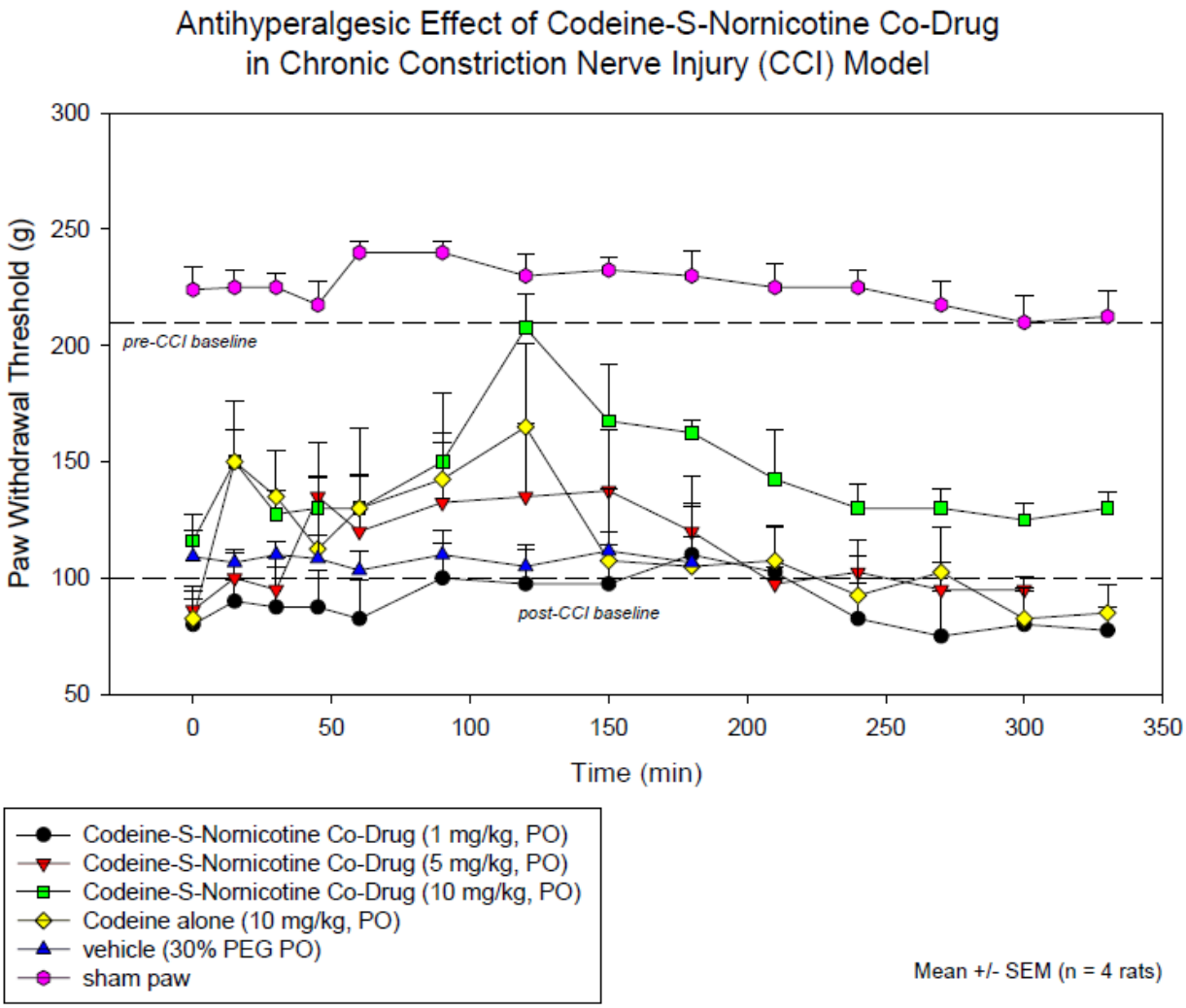

Fig. 3.11: Time-response curves for orally administered codeine-*S*-(-)-nornicotine codrug and codeine in the CCI model.

Fig. 3.12 illustrates the % MPE (Maximum Possible Effect) for the codeine-*S*-(-)-nornicotine codrug and for codeine and *S*-(-)-nornicotine. The highest %MPE achieved by codeine is 65%. Increasing the dose further for codeine does not result in a further increase in the % MPE. The highest % MPE achieved by *S*-(-)-nornicotine is 45% by 40 mg/kg oral dose of *S*-(-)-nornicotine. Increasing the dose from 40 to 60 mg/kg reduces the effectiveness of the drug. The 10 mg/kg dose of the codeine-*S*-(-)-nornicotine codrug produced the highest %MPE (85%). 85% MPE could not be achieved with any dose of codeine or *S*-(-)-nornicotine alone. This clearly demonstrates that codeine-*S*-(-)-

nornicotine is much superior compared to either of the two parent drugs in terms of its antihyperalgesic activity.

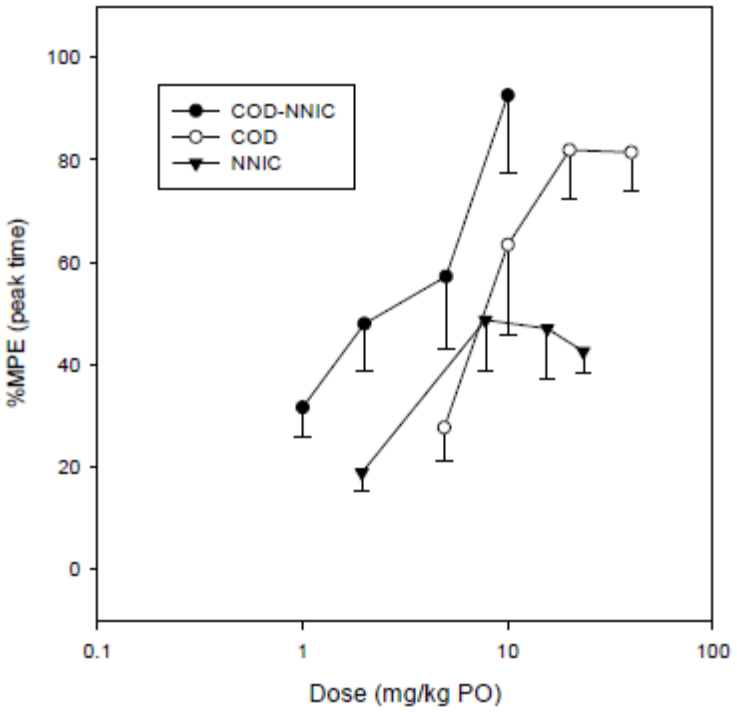

Fig. 3.12: Dose-response curves for orally administered codeine, *S*-(-)-nornicotine, and codeine-*S*-(-)-nornicotine codrug in the CCI animal model.

The 10 mg/kg dose of the codeine-*S*-(-)-nornicotine codrug contains a 6.3 mg/kg dose of codeine and a 3.7 mg/kg dose of *S*-(-)-nornicotine. As is evident from the dose-response curves for codeine and *S*-(-)-nornicotine, a 6.3 mg/kg dose of codeine is considered as a dose producing very low efficacy, and 3.7 mg/kg dose of *S*-(-)-nornicotine is not even considered effective. Therefore, the analgesic effect shown by a 6.3 mg/kg dose of codeine and 3.7 mg/kg dose of *S*-(-)-nornicotine when given in the form of the codeine-*S*-(-)-nornicotine codrug produces profound analgesia which cannot be achieved by the same respective doses of the individual drugs. In conclusion, the present data demonstrates that combining codeine with *S*-(-)-nornicotine in the form of a

codrug may enhance codeine effectiveness against neuropathic pain. Also the accompanying reduction of opioid dose will decrease the adverse effects associated with opioid therapy.

3.5.3 3-*O*-Acetylmorphine-*S*-(-)-Nornicotine Codrug Antinociception (Tail-Flick Test)

The antinociceptive effects of 3-*O*-acetylmorphine alone, *S*-(-)-nornicotine alone and various doses of 3-*O*-acetylmorphine-*S*-(-)-nornicotine codrug were characterized after the oral administration in the tail-flick test. The present data provides evidence (Figs. 3.13, 3.14, 3.15, and 3.16) that a codrug consisting of 3-*O*-acetylmorphine (low dose) and *S*-(-)-nornicotine (non-effective dose) significantly enhances effectiveness of the analgesic agents against acute nociception. In preliminary experiments, three doses of 3-*O*-acetylmorphine (2.5, 5, 10 mg/kg) and four doses of *S*-(-)-nornicotine (5, 8, 15, 30 mg/kg) were administered orally to rats to compare the analgesic effects of the two parent drugs and also to determine the ED_{50} values for the parent drugs. In separate experiments, five doses (0.5, 1.25, 2.5, 4, 8 mg/kg) of the 3-*O*-acetylmorphine-*S*-(-)-nornicotine codrug were administered orally and tail flick latencies were experimentally determined. 3-*O*-Acetylmorphine and 3-*O*-acetylmorphine-*S*-(-)-nornicotine codrug tail-flick latency values were above baseline values, which indicated that both drugs exhibited analgesic effects.

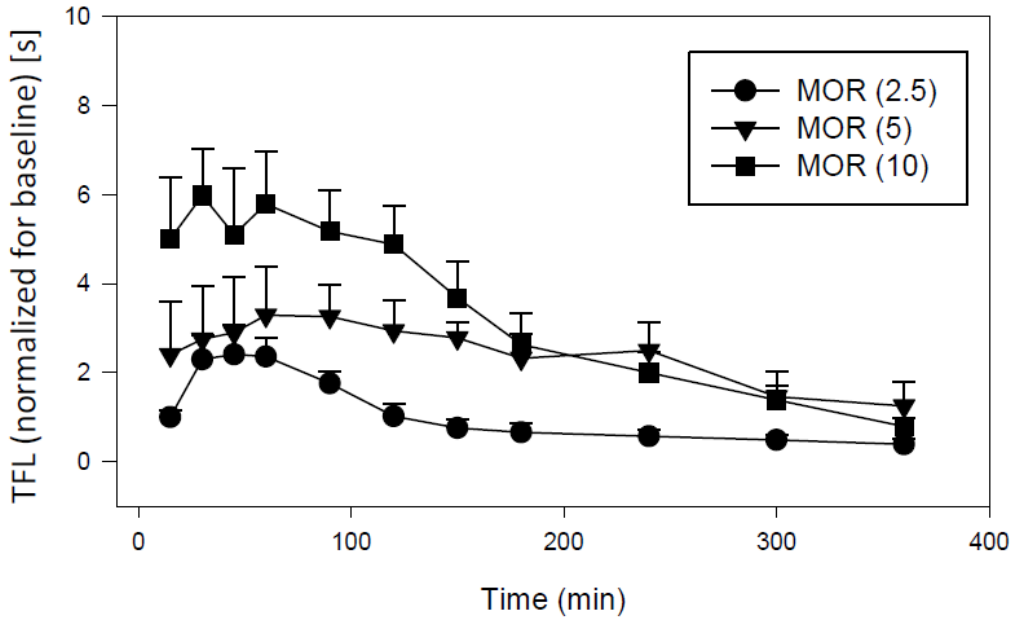

Fig. 3.13: Time-response curves for orally administered 3-*O*-acetylmorphine (MOR) in the tail-flick animal model.

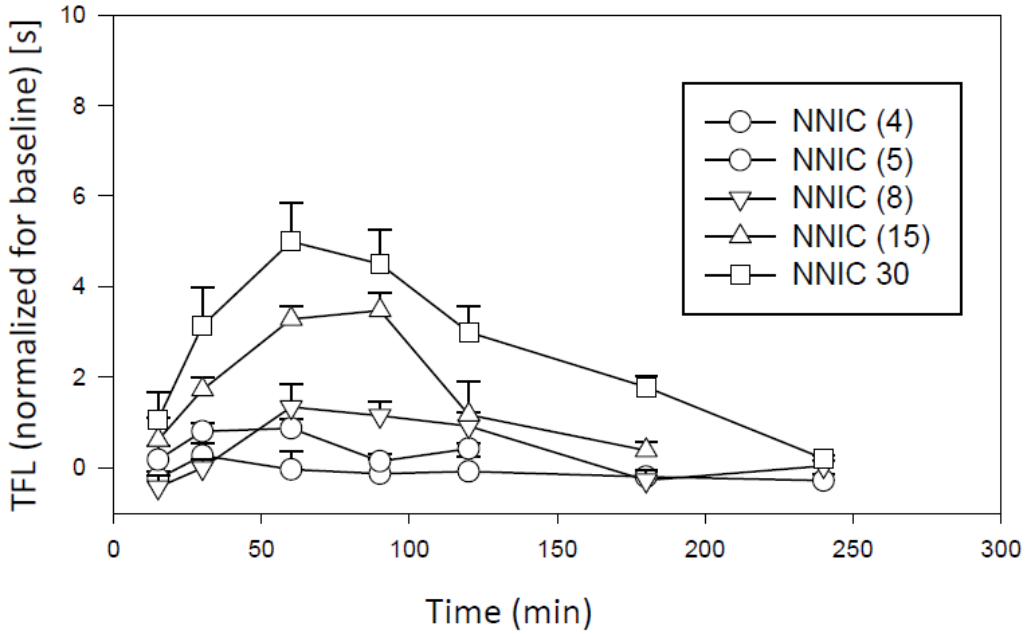

Fig. 3.14: Time-response curves for orally administered *S*-(-)-nornicotine (NNIC) in the tail-flick animal model.

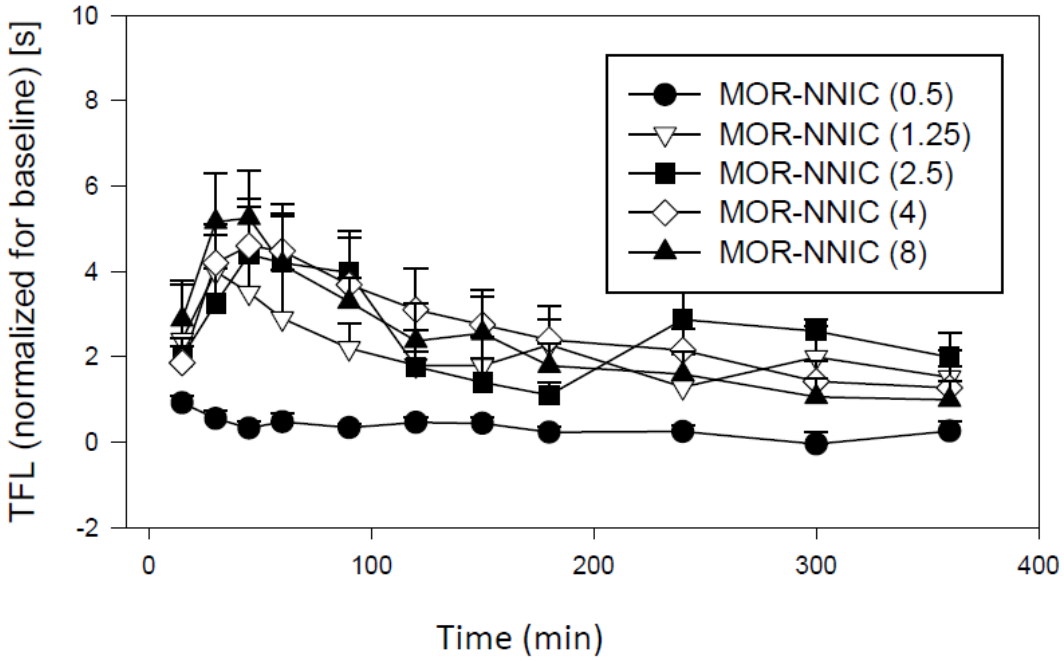

Fig. 3.15: Time-response curves for orally administered 3-*O*-acetylmorphine-*S*-(-)-nornicotine codrug (MOR-NNIC) in the tail-flick animal model.

Fig. 3.16 illustrates the %MPE (Maximum Possible Effect) at the peak of the time response curve for the 3-*O*-acetylmorphine-*S*-(-)-nornicotine codrug, 3-*O*-acetylmorphine, and *S*-(-)-nornicotine. The highest %MPE achieved by 3-*O*-acetylmorphine and the 3-*O*-acetylmorphine-*S*-(-)-nornicotine codrug is around 90%. The 8 mg/kg dose of the 3-*O*-acetylmorphine-*S*-(-)-nornicotine codrug produced the highest %MPE among the codrug doses. The equi-effective dose of 3-*O*-acetylmorphine was 10 mg/kg compared to an 8 mg/kg dose of the 3-*O*-acetylmorphine-*S*-(-)-nornicotine codrug. The 8 mg/kg dose of the 3-*O*-acetylmorphine-*S*-(-)-nornicotine codrug contains a 5.2 mg/kg dose of 3-*O*-acetylmorphine. Therefore, the analgesic effect shown by a 5.2 mg/kg dose of 3-*O*-acetylmorphine when given in the form of the 3-*O*-acetylmorphine-*S*-(-)-nornicotine codrug is equivalent to a 10 mg/kg dose of 3-*O*-acetylmorphine alone. On the other hand, *S*-(-)-nornicotine does not possess very good analgesic activity on its own. To achieve a %MPE similar to 3-*O*-acetylmorphine or codrug, a very high oral dose of *S*-(-)-nornicotine is required, which can cause toxicity in the animal. The 8 mg/kg dose of 3-*O*-

acetylmorphine-*S*-(-)-nornicotine codrug contains only 2.4 mg/kg dose of *S*-(-)-nornicotine. A 2.4 mg/kg dose of *S*-(-)-nornicotine is completely ineffective as an analgesic. It can further be noticed that the dose-response curve for the codrug is shifted to the left compared to the dose response curves of 3-*O*-acetylmorphine and *S*-(-)-nornicotine. Shifting of the dose response curve to the left signifies that a lesser amount of codrug dose is required to produce analgesic effects similar to those produced by the parent drugs.

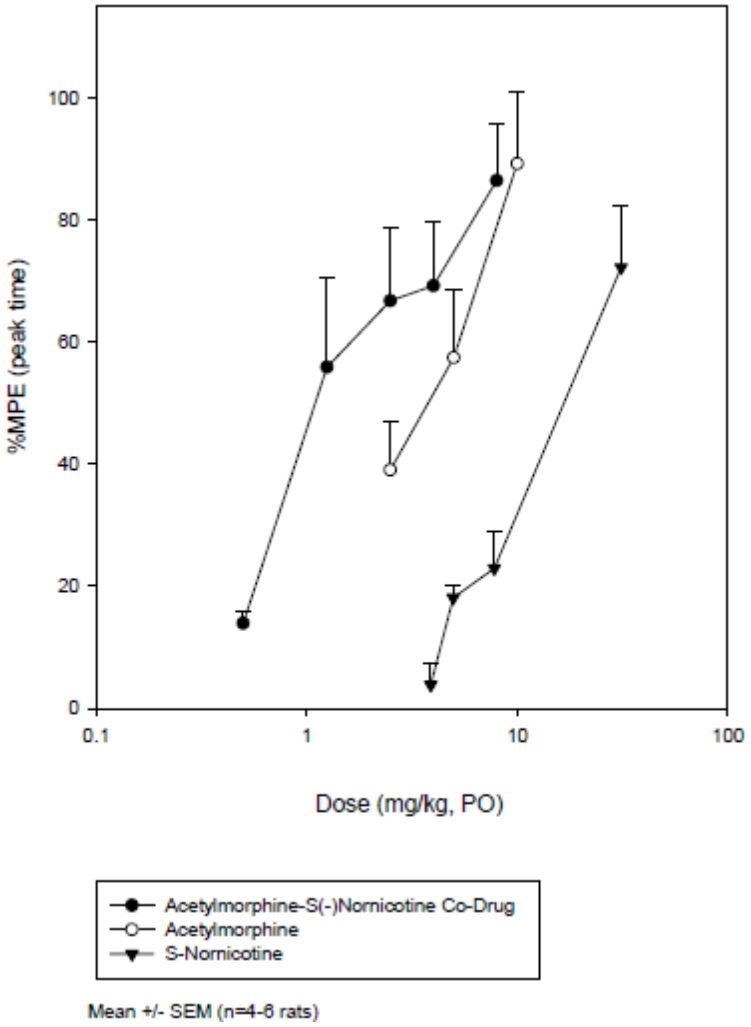

Fig. 3.16: Dose-response curves for 3-*O*-acetylmorphine, *S*-(-)-nornicotine, and 3-*O*-acetylmorphine-*S*-(-)-nornicotine codrug in the tail-flick animal model.

3.5.4 ED_{50} values

The dose of a drug that is pharmacologically effective for 50% of the population exposed to the drug, or that shows a 50% response in a biological system that is exposed to the drug is defined as the ED_{50} value of the drug. To calculate ED_{50}, time-response curve was converted to a dose-response curve. To develop dose-response curve, the maximum TFL for each dose was selected regardless of the time point. The maximum TFL for a dose at any time point was then converted to a %MPE using the formula to calculate %MPE. The %MPE value at the peak of the time-response curve is denoted as %MPE at peak time. Dose-response curve was generated by plotting %MPE (peak time) ± SEM *versus* dose and 4-6 rats were used to obtain each point in the dose-response curve. In the dose-response curve a horizontal line was drawn at 50 %MPE intersecting the dose-response line. From the point of intersection, a vertical line was drawn on the X-axis (Dose). The point of intersection on the X-axis gives the ED_{50} value for the analgesic agent. As the dose-response curve is a line, the obtained ED_{50} value is just a number without any SEM, but it should be kept in mind that 4-6 rats were used to generate each point on the dose-response curve.

As can be seen in Table 3.1, the ED_{50} value for the codeine-*S*-(-)-nornicotine codrug in the tail-flick test, as well as in the CCI pain model is much lower than the ED_{50} value of codeine and *S*-(-)-nornicotine in either test, which suggests that the use of a low dose combination of these two analgesics in a codrug structure is a valid and effective approach for improved treatment of both nociceptive and neuropathic pain.

Table 3.1: ED_{50} values of codrug and parent drugs in tail-flick and CCI models.

	ED_{50} Tail-flick model	ED_{50} C.C.I. model
Codeine	12.4 mg/kg 41.4 µmol/kg	13.5 mg/kg 45.1 µmol/kg
S-(-)-Nornicotine	15.9 mg/kg 107.3 µmol/kg	16.9 mg/kg 114.0 µmol/kg
Codeine-*S*-(-)-Nornicotine Codrug	8.5 mg/kg 18.0 µmol/kg	3.5 mg/kg 7.4 µmol/kg

Table 3.2 lists the ED_{50} values of 3-*O*-acetylmorphine, *S*-(-)-nornicotine, and 3-*O*-acetylmorphine-*S*-(-)-nornicotine codrug in tail-flick model. It can be seen that the codrug is more effective for treating nociceptive pain compared to the parent drugs. Thus, combining an opioid with *S*-(-)-nornicotine in a single chemical entity can increase the efficacy of both the drugs.

Table 3.2: ED_{50} values of morphine, 3-*O*-acetylmorphine, *S*-(-)-nornicotine, and 3-*O*-acetylmorphine-*S*-(-)-nornicotine codrug in tail-flick model.

	ED_{50} Tail-flick model
3-*O*-Acetylmorphine	3.6 mg/kg 11.0 µmol/kg
S-(-)-Nornicotine	15.9 mg/kg 107.3 µmol/kg
3-*O*-Acetylmorphine-*S*-(-)-Nornicotine Codrug	1.5 mg/kg 3.0 µmol/kg

3.6 Analgesic Activity of *N*-Ethoxycarbonylgabapentin-Codeine Codrug (CG-4)

3.6.1 Tail Flick Test (Measure of Analgesia/Antinociception)

Tail flick latencies for several doses of codeine were previously determined and already discussed in this chapter. It has been previously reported in literature that gabapentin alone has no intrinsic effect in the tail flick test (Gilron et al., 2003). Thus, gabapentin was not tested for its efficacy in the tail flick test. The antinociceptive effect of the *N*-ethoxycarbonylgabapentin-codeine codrug (CG-4) was characterized after oral administration in the rat tail-flick test. Three doses (6.25, 12.5, and 25 mg/kg) of *N*-ethoxycarbonylgabapentin-codeine codrug were administered and then tail flick latencies were experimentally determined. CG-4 codrug tail-flick latency values were above baseline values, which indicated that the codrug exhibits an analgesic effect. An equimolar physical mixture dose of codeine and gabapentin (14.3 mg/kg codeine + 8.2 mg/kg gabapentin, total of 22.5 mg/kg physical mixture) equivalent to 25 mg/kg dose of the CG-4 codrug was also administered orally, and then time response curve for tail flick test was generated. The tail flick latency values of the physical mixture dose of gabapentin and codeine (14.3 mg/kg codeine + 8.2 mg/kg gabapentin, total of 22.5 mg/kg physical mixture) were above the baseline, and also the antinociceptive effect of the physical mixture was significantly different from that of the vehicle. Fig 3.17 illustrates the time-response curve for the three doses of the codrug along with the vehicle response. It can be noticed that the 25 mg/kg and 12.5 mg/kg doses of the codrug showed significant antinociceptive effects. It can further be noticed that the codrug showed a prolonged analgesic effect. The analgesic effect of the codrug did not come to baseline even after 24 hours in both the 12.5 and 25 mg/kg doses. To compare the analgesic efficacy of the codrug with an equimolar physical mixture of the two parent drugs a time-response curve was generated for a 25 mg/kg dose of the codrug as well as 22.5 mg/kg dose of an equimolar physical mixture (14.3 mg/kg codeine + 8.2 mg/kg gabapentin, total of 22.5 mg/kg physical mixture. This dose is equivalent to 25 mg/kg dose of CG-4 codrug). By comparing Figs. 3.17 and 3.18, it can be seen that the analgesic effect of the physical mixture reduces to baseline after 8 hours, while the same dose of the codrug remains effective for a much longer time period (30 hours). It can also be noticed that

even the 12.5 mg/kg dose of the codrug shows a much prolonged antinociceptive effect than the equimolar physical mixture dose.

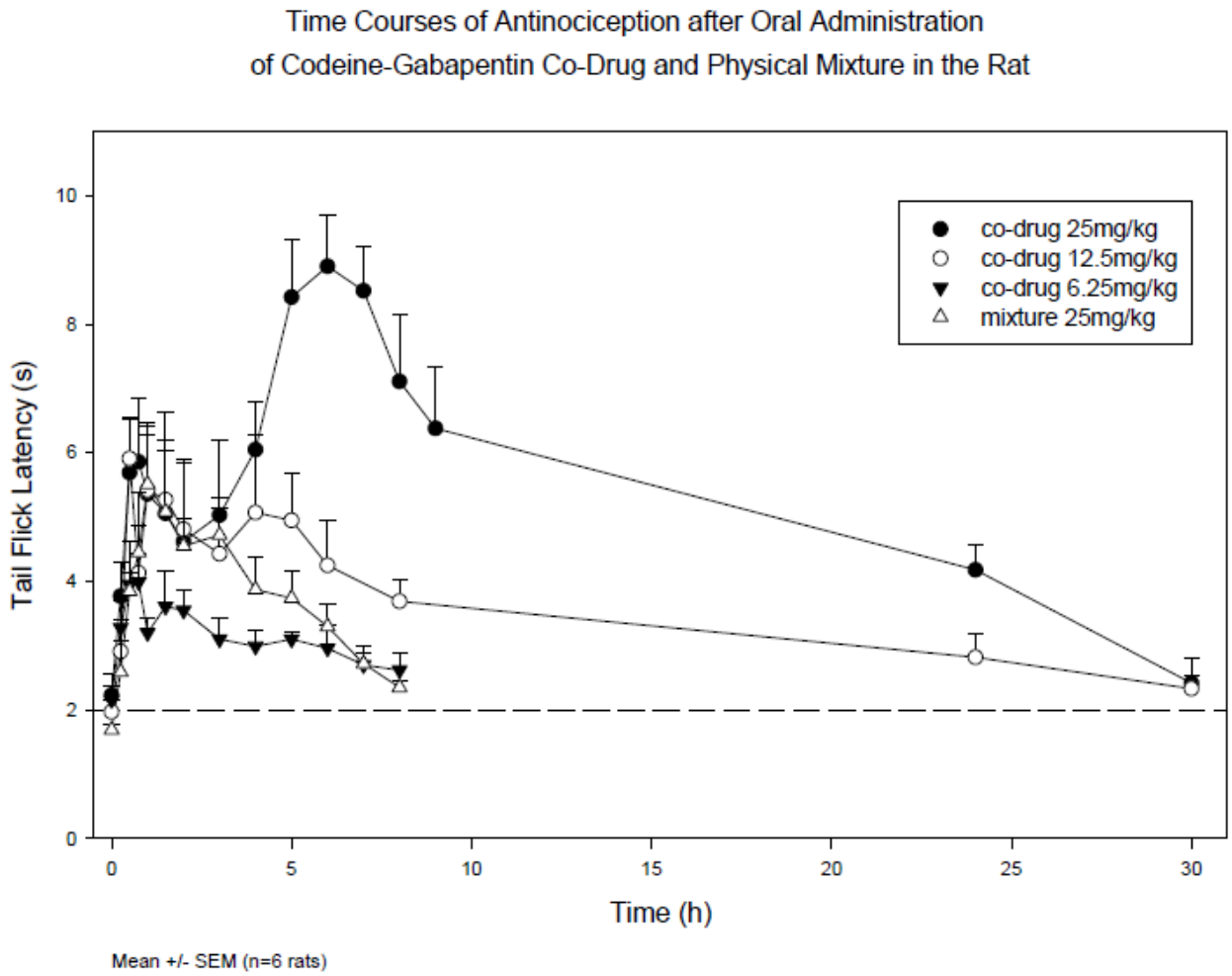

Fig. 3.17: Time-response curves for three oral doses of the *N*-ethoxycarbonylgabapentin-codeine codrug and an equimolar physical mixture dose of codeine and gabapentin in the tail-flick animal model.

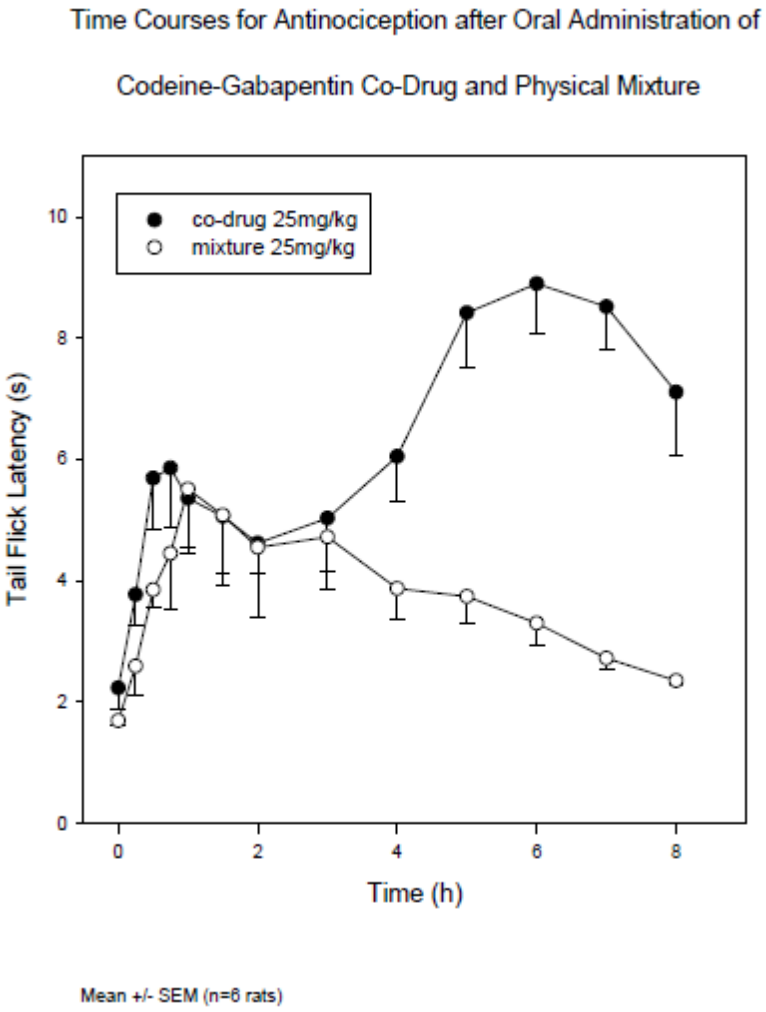

Fig. 3.18: Comparison of time-response curves for *N*-ethoxycarbonylgabapentin-codeine codrug and an equivalent physical mixture dose of the parent drugs.

Fig. 3.19 illustrates the %MPE (Maximum Possible Effect) at the peak of the time response curve for the *N*-ethoxycarbonylgabapentin-codeine codrug and the equimolar physical mixture of codeine and gabapentin. The 25 mg/kg dose of the *N*-ethoxycarbonylgabapentin-codeine codrug produced the highest % MPE among the codrug doses. The highest %MPE achieved by *N*-ethoxycarbonylgabapentin-codeine codrug is around 90%. 90% MPE could not be achieved with any dose of codeine alone. The 25 mg/kg dose of the *N*-ethoxycarbonylgabapentin-codeine codrug contains a 14.3 mg/kg dose of codeine. From the dose response curve of codeine, it can be noticed that a

14.3 mg/kg dose of codeine alone would produce less than 60% MPE. Therefore, the analgesic effect shown by a 14.3 mg/kg dose of codeine when given in the form of the *N*-ethoxycarbonylgabapentin-codeine codrug is much more profound compared to that afforded by the same dose of codeine alone. It can also be noticed from the dose-response curve of the *N*-ethoxycarbonylgabapentin-codeine codrug and an equimolar physical mixture of the two parent drugs, that when the two parent drugs are combined in a single chemical entity as a codrug, this chemical form is much more effective than administering a physical mixture of the two parent drugs.

It can also be proven that the overall analgesic effect of the codrug is greater compared to that produced by the physical mixture by calculating the area under the curve (AUC) of the various doses of the codrug and the physical mixture. Table 3.3 lists the area under the curves until 8 hours ($AUC_{0\text{-}8\ hr}$) after the oral dosing of codrug and an equimolar physical mixture. By comparing the AUCs, it can be concluded that the overall effects of 12.5 and 25 mg/kg doses of the codrug are higher compared to the equimolar dose of the physical mixture. Thus the enhancement of the analgesic response of the two parent drugs when given in the form of a codrug is evident at several points in the time-response curve, as well in the overall effect.

Table 3.3: AUCs for different doses of the *N*-ethoxycarbonylgabapentin-codeine codrug and an equimolar physical mixture dose of codeine and gabapentin.

Codrug and Physical Mixture Dose	$AUC_{0\text{-}8\ hr}$ (s * hr)
6.25 mg/kg codrug	7.50 ± 1.60
12.5 mg/kg codrug	18.50 ± 4.58
25 mg/kg codrug	34.70 ± 5.01
22.5 mg/kg equimolar physical mixture	16.90 ± 1.92

ED_{50} values of the codrug were calculated from dose-response curves and then compared to the ED_{50} values of the parent drugs. It can also be noticed from the ED_{50}

values that the codrug is more efficacious than the parent drugs, and that the opioid dose can be reduced by combining an opioid with gabapentin in a single chemical entity.

Table 3.4: ED_{50} values of codeine, gabapentin, and *N*-ethoxycarbonylgabapentin-codeine codrug in the tail-flick animal model.

	ED_{50} Tail-flick model
Codeine	12.4 mg/kg 41.4 µmol/kg
Gabapentin	Non responsive
N-ethoxycarbonylgabapentin-codeine	10.1 mg/kg 19.2 µmol/kg

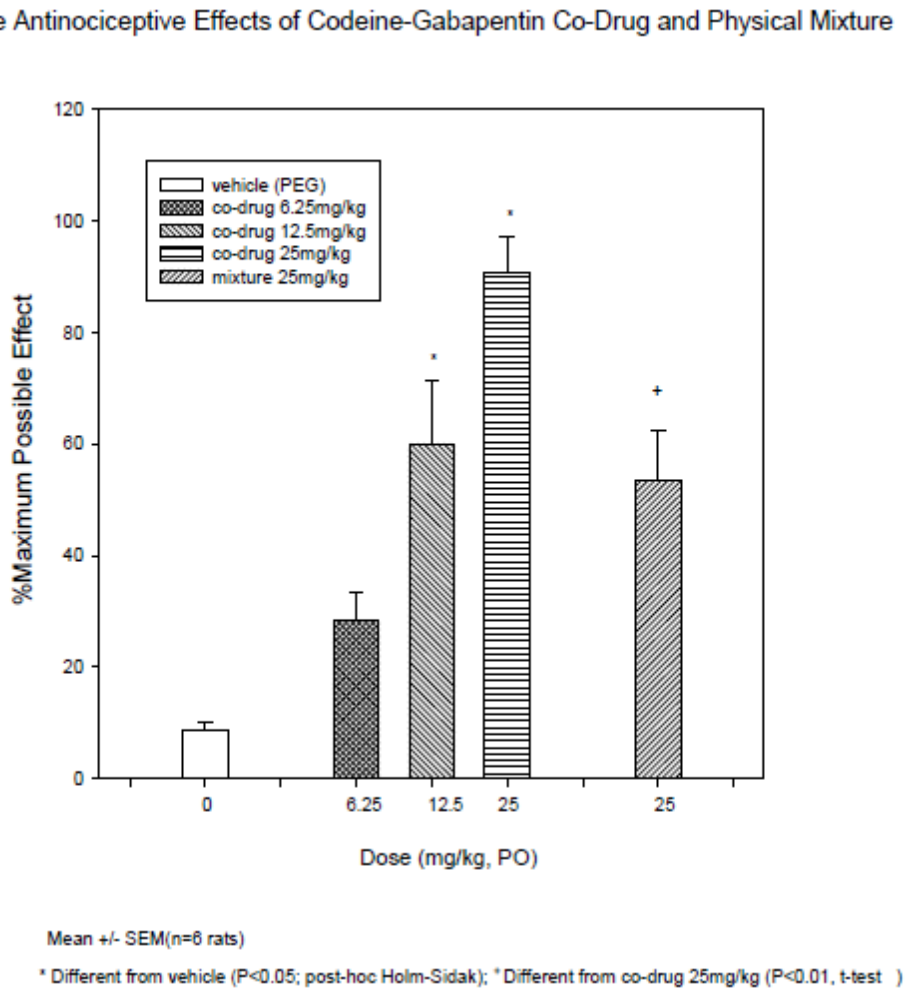

Fig. 3.19: comparison of % MPE at peak time for three different doses of the *N*-ethoxycarbonylgabapentin-codeine codrug and an equimolar physical mixture dose of codeine and gabapentin in tail-flick test.

Thus it can be concluded from the study of several opioid codrugs in different pain assays that combining an opioid with an adjuvant drug in the form of a codrug molecule can increase the analgesic potency of the opioid. This strategy can lead to reduced doses of the opioids for the treatment of pain and can significantly diminish the adverse effects associated with opioid therapy. It can also be noticed from the behavior of the studied codrugs that the codrugs showed longer period of action compared to the parent opioids or physical mixtures. Therefore, codrug strategy can also provide a

prolonged analgesia and can make the dosing regimen less frequent and can also increase the patient compliance. Another important outcome of the study is that, combination of an opioid molecule with an appropriate adjuvant analgesic in the form of a codrug can make the opioid molecule more effective in treating neuropathic pain. Codeine-*S*-(-)-nornicotine codrug showed promising antihaperalgesic effect in the CCI model of neuropathic pain. Thus codrug strategy can be useful for treating a broader range of pain and making opioids more useful for the treatment of both nociceptive and neuropathic pain.

Copyright © Ujjwal Chakraborty 2012

Chapter 4

In Vitro Stability Study of the Codrugs

4.1 Introduction

Orally administered drug molecules experience a wide range of pH in the human body. Harsh acidic conditions are experienced in stomach (pH=1 to 2), mild acidic conditions are experienced at the beginning of small intestine (pH=4 to 5), and basic conditions are experienced in the small intestine and colon (pH=7 to 9). Also, blood plasma has a slightly basic pH of 7.4. Thus, therapeutic molecules need initially to be examined and analyzed *in vitro* at different pH conditions to determine their stabilities. In vitro evaluation of chemical stability is particularly important for prodrugs and codrugs, as they contain labile linkers. Along with the study of chemical stability of codrugs in different aqueous buffers, stability studies in the presence of different enzymatic conditions are also essential. Gastric juice contains hydrolytic enzymes, such as trypsin, pepsin, rennin, and mucin; intestinal fluid also contains hydrolytic enzymes such as pancreatin, and human plasma contains a large number of hydrolytic enzymes such as, cholinesterases, aldolases, lipases, dehydropeptidases, and alkaline and acid phosphatases (Piper et al., 1963; DeBeer et al., 1935). The primary object of performing stability study on a drug molecule in nonenzymatic and enzymatic assays is to predict the stability of the drug in the GI tract after oral dosing. The obtained hydrolytic profile of the drug can guide the structural modification of the drug to improve GI stability and optimize plasma bioavailability (Kern and Di 2008).

In case of codrugs, in vitro stabilities of the molecules need to be studied in depth before starting the more expensive in vivo evaluation experiments. An ideal codrug should not be hydrolyzed to the parent drugs in the GI tract. After the codrug enters systemic circulation, it can behave in two different ways: the codrug may get hydrolyzed in blood to produce the parent drugs. In this scenario, the codrug serves the purpose of a chemical delivery system and provides both parent drugs in systemic circulation, usually

at higher concentrations than administering the parent drugs alone. In a different scenario, the codrug may not get hydrolyzed in the plasma and may target the site of action as a single chemical entity and then be hydrolyzed by tissue-specific enzymes present at site of action to produce the parent drugs concomitantly. In case of opioid codrugs, the site of action is the brain, since opioid receptors are mostly located in the central nervous system (CNS). Thus, to determine the hydrolytic profile of opioid codrugs in the GI tract, stability study should be performed under the following hydrolytic conditions:

- Aqueous buffer of pH 1.3
- Aqueous buffer of pH 5.0
- Aqueous buffer of pH 7.4
- Simulated gastric fluid (containing pepsin) (SGF)
- Simulated intestinal fluid (containing pancreatin) (SIF)

To determine the stability of opioid codrugs in the systemic circulation, stability studies should also be performed in plasma, and to determine the stability at the site of action, stability studies should also be performed in brain homogenate. Thus selected codrugs from each group of synthesized opioid codrugs were examined for the stability under the following hydrolytic conditions to model drug barriers to bioavailability:

- Aqueous buffers (pH 1.3 to 7.4, 37 ºC)
- Simulated gastric fluid (USP, 37 ºC)
- Simulated intestinal fluid (USP, 37 ºC)
- 80% rat plasma (37 ºC)
- Rat brain homogenate (37 ºC)

4.2 Opioid-*S*-(-)-Nornicotine Codrugs

Three of the synthesized opioid-*S*-(-)-nornicotine codrugs were studied under different hydrolytic conditions. The stability of codeine-*S*-(-)-nornicotine, 3-*O*-acetylmorphine-*S*-(-)-nornicotine, and morphine-*S*-(-)-nornicotine codrugs were examined in different nonenzymatic and enzymatic conditions.

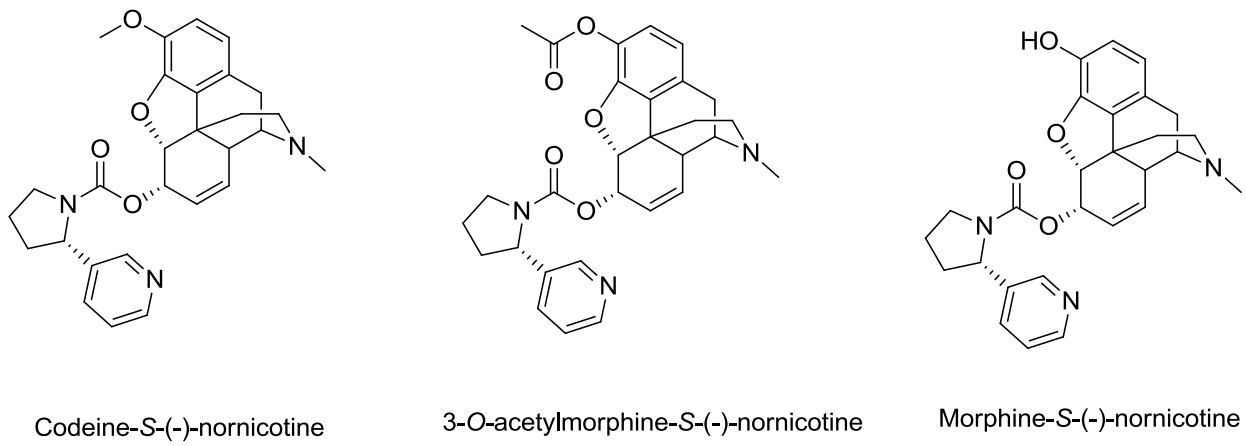

Fig. 4.1: Structures of the opioid-*S*-(-)-nornicotine codrugs used in stability studies.

4.2.1 Standard Curve and Quality Control Validation Solutions

In the stability study of the codeine-*S*-(-)-nornicotine codrug, morphine was used as an internal standard and in the studies involving the 3-*O*-acetylmorphine-*S*-(-)-nornicotine and the morphine-*S*-(-)-nornicotine codrugs, codeine was used as an internal standard. Stock solutions of codrugs, codeine, morphine, 3-*O*-acetylmorphine, and *S*-(-)-nornicotine were prepared in methanol. Standard curves with eight different concentration points were generated and utilized in the quantitative analysis of the unknown samples. Calibration curves were obtained using quadratic least-squares regression of area-under-the-curve (AUC) ratios (analyte peak AUC/internal standard peak AUC) *versus* drug concentration. The amount of codrug, or parent drug, was then determined using the standard curves.

4.2.2 Kinetics of Hydrolysis of the Codrugs in Aqueous Solutions (Non-Enzymatic)

A 0.02 M hydrochloric acid buffer, pH 1.3, was used as a non-enzymatic simulated gastric fluid. A 0.02 M sodium acetate buffer, pH 5.0; and a 0.02 M phosphate buffer, pH 7.4 were also used in this study. The pH 5.0 simulates intestinal fluid present at the beginning of small intestine and the pH 7.4 represents pH of the small intestine and physiological pH (plasma). Reactions were initiated by adding 300 µL of 25 mM stock solution (in methanol) of the codrug to 9 mL of appropriate thermostated (37 ± 0.5 °C) aqueous solutions of the above buffer species. Aliquot-parts (250 µL) were removed from the codrug-buffer solutions at various time intervals, mixed with 50 µL of the 5 mM internal standard solution, and 10 µL of the resulting solution was immediately injected onto the HPLC-DAD analytical system for quantitative analysis. Experiments were run in triplicate (Omar, 1998).

4.2.3 Kinetics of Hydrolysis of the Codrug in Simulated Gastric Fluid (SGF) and Simulated Intestinal Fluid (SIF) (Enzymatic Conditions)

Reactions were initiated by adding 300 µL of a 25 mM stock solution (in methanol) of the codrug to 9 mL of appropriate thermostated (37 ± 0.5 °C) SGF and SIF solutions. Aliquot-parts (250 µL) of the resulting solutions were removed at various time intervals, mixed with 50 µL of the 5 mM internal standard solution and 10 µL of the resulting solution was immediately injected onto the HPLC-DAD analytical system for quantitative analysis. Experiments were run in triplicate.

4.2.4 Kinetics of Hydrolysis of the Codrug in Rat Plasma (*in vitro*):

Plasma from male Sprague-Dawley rats was obtained by centrifugation of blood samples at 12,000 rpm for 10-15 min. The supernatant plasma fractions (2 mL) were diluted with phosphate buffer (pH 7.4) to afford a total volume of 2.5 mL (80% rat plasma). Incubations were performed at 37 ± 0.5 °C in a water-bath with constant stirring. Reactions were initiated by adding 100 µL of the codrug stock solution (5 mM in

methanol) to 2.5 mL of preheated (37 ± 0.5 °C) 80% rat plasma. Aliquot-parts (100 µL) were removed at various times, mixed with 50 µL of the 5 mM internal standard solution, and then deproteinized by mixing with 600 µL of acetonitrile. After centrifugation for 10 minutes at 12,000 rpm, the supernatant was separated, dried under nitrogen gas, the residue reconstituted with 300 µL of methanol, and the resulting solution was analyzed by HPLC-DAD.

4.2.5 Kinetics of Hydrolysis of the Codrug in Rat Brain Homogenate

Brain homogenate obtained from male Sprague-Dawley rats was obtained by homogenizing brain tissues with 3 volumes of 1.15% KCl/g brain tissue for 2 minutes in a tissue homogenizer. Incubations were performed at 37 ± 0.5 °C in a water-bath with constant stirring. The reactions were initiated by adding 100 µL of the codrug stock solution (5 mM in methanol) to 2.5 mL of preheated (37 ± 0.5 °C) brain homogenate. Aliquot-parts (100 µL) were removed at various times, mixed with 50 µL of the 5 mM internal standard solution, and deproteinized by mixing with 600 µL of acetonitrile. After centrifugation for 10 minutes at 12,000 rpm, the supernatant was separated, dried under nitrogen gas, the residue reconstituted with 300 µL of methanol, and the resulting solution analyzed by HPLC-DAD.

4.2.6 HPLC Analysis

HPLC analysis was carried out on an Agilent 1100 series Quatpump, equipped with a photodiode array detector and a computer integrating apparatus. A Waters Symmetry ® C_{18} (5 µm, 3.9 x 150 mm) column protected with guard column (Nova-Pak® C_{18}; 3.9 x 20 mm; 4µ) was used as the stationary phase; a mixture of 0.16% aqueous solution of sodium heptane sulfonate (SHS) adjusted to pH 3.2 with 85% *o*-phosphoric acid (solvent A)/methanol (solvent B)/was used as mobile phase. A 1 mL/min flow rate was used, and UV detection was carried out at 220 nm. This HPLC assay was

used for 3-*O*-acetylmorphine-*S*-(-)-nornicotine and morphine-*S*-(-)-nornicotine codrugs. Naltrexone was used as the internal standard.

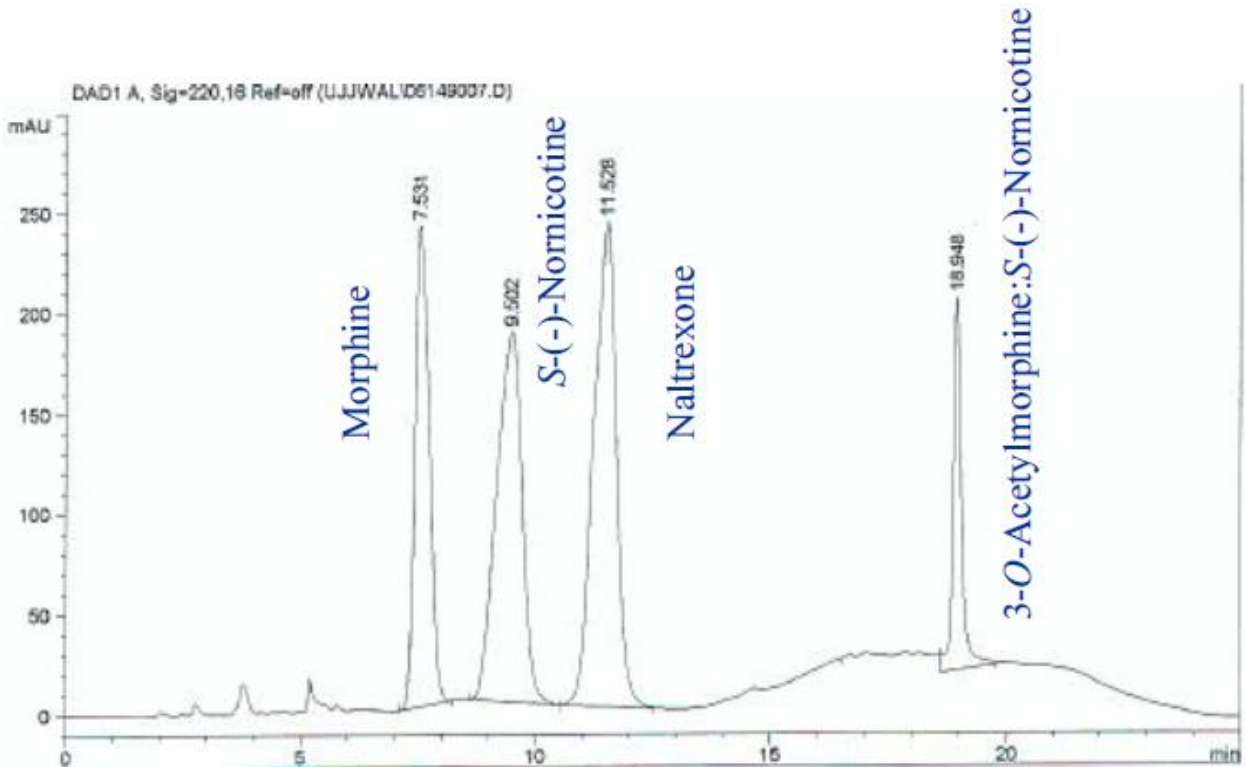

Fig. 4.2: HPLC chromatogram of morphine, *S*-(-)-nornicotine, naltrexone (IS), and 3-*O*-acetylmorphine-*S*-(-)-nornicotine codrug.

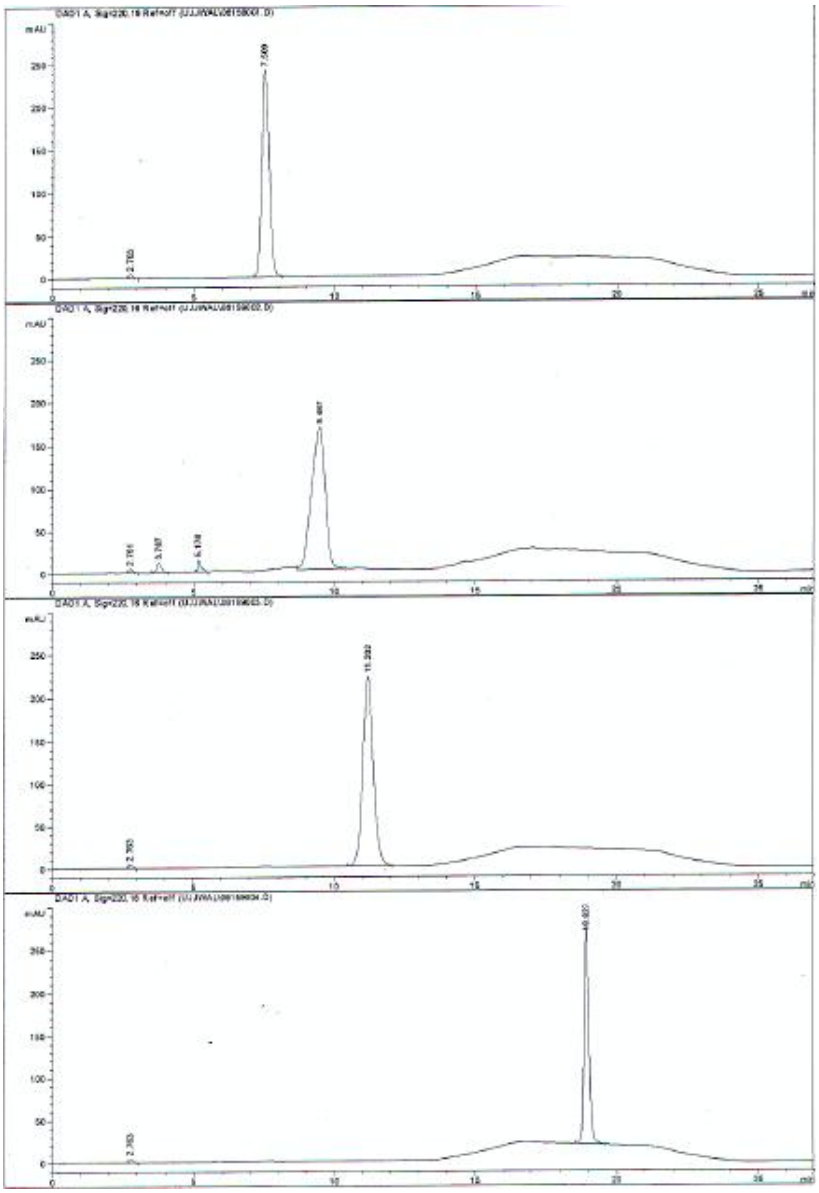

Fig. 4.3: Individual HPLC Chromatograms of morphine, *S*-(-)-nornicotine, naltrexone (IS), and morphine-*S*-(-)-nornicotine codrug (in top to bottom order).

A specific 30 min time gradient program was used for the analysis of 3-*O*-acetylmorphine-*S*-(-)-nornicotine and morphine-*S*-(-)-nornicotine codrugs as follows:

0-11 min: 45% solvent A

11-14 min: 45% to 7% solvent A

14-20 min: 7% solvent A

20-23 min: 7% to solvent A

23-30 min: 45% solvent A

For the codeine-*S*-(-)-nornicotine codrug a different HPLC assay was used. A Waters Symmetry ® C_{18} (5 µm, 3.9 x 150 mm) column protected with an appropriate guard column (Nova-Pak® C_{18}; 3.9 x 20 mm; 4µ) was used as the stationary phase; 0.04% aqueous HFBA solution (solvent A)/0.04% heptafluorobutyric acid (HFBA) solution in methanol (solvent B) was used as mobile phase. A 0.5 mL/min flow rate was used, and UV detection was carried out at 280 nm. Morphine was used as the internal standard.

A specific 20 min time gradient program was used for analysis of the codeine-*S*-(-)-nornicotine codrug as follows:

0-1 min: 76% solvent A

1-17 min: 76% to 28% solvent A

17-17.1 min: 28% to 76% solvent A

17.1-20 min: 76% solvent A

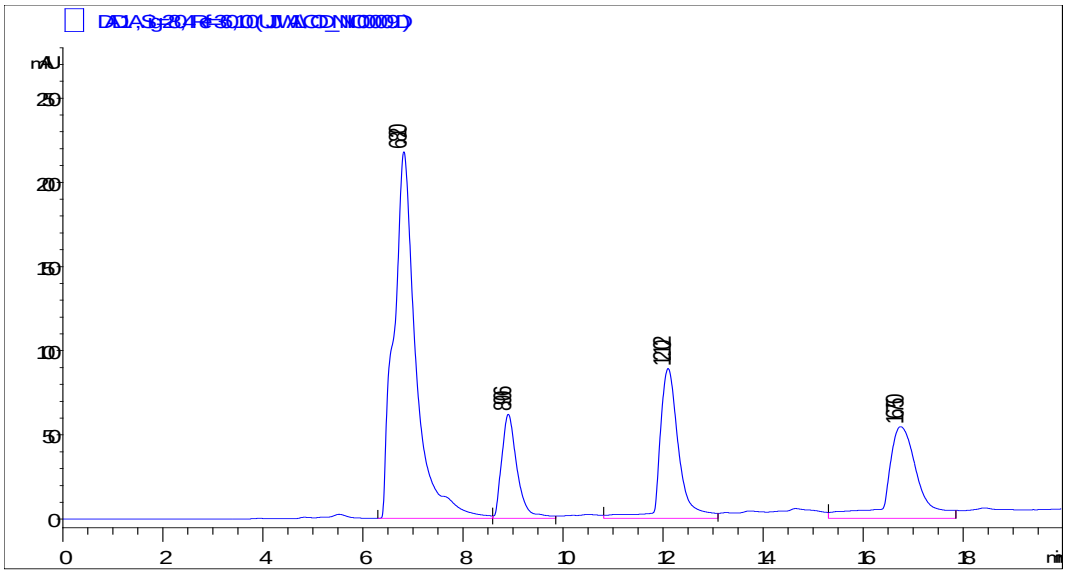

Fig. 4.4: HPLC Chromatogram of *S*-(-)-nornicotine, morphine (IS), codeine, and codeine-*S*-(-)-nornicotine codrug (in order of elution).

4.3 Results

4.3.1 Assay Validation

Calibration curves were generated for each analyte and for each stability study. Table 4.1 summarizes the information regarding the linear range of each analyte.

Table 4.1: Standard curve analysis of the analytes.

Analyte	Linear Range	R^2
Codeine	3.906-1000 µM	0.9994
S-(-)-Nornicotine	31.25-2000 µM	0.9915
Codeine-*S*-(-)-nornicotine	7.813-2000 µM	0.9991
3-*O*-Acetylmorphine-*S*-(-)-nornicotine	23.36-996.9 µM	0.9942
Morphine-*S*-(-)-nornicotine	7.813-2000 µM	0.998
Codeine-Norketamine	31.25-2000 µM	0.992
Morphine-Norketamine	31.25-2000 µM	0.9931
CG-1	7.813-2000 µM	0.9994
CG-2	7.813-2000 µM	0.9978
CG-3	3.906-1000 µM	0.9834
CG-4	2.047-1048 µM	0.9925

4.3.2 Chemical and Enzymatic Stability Study

Chemical and enzymatic stability studies on the codeine-*S*-(-)-nornicotine, 3-*O*-acetylmorphine-*S*-(-)-nornicotine and morphine-*S*-(-)-nornicotine codrugs were carried out *in vitro*. Chemical hydrolysis was examined utilizing buffers at pH 1.3, 5, and 7.4, and enzymatic hydrolysis was examined in simulated gastric fluid (SGF), simulated intestinal fluid (SIF), 80% rat plasma, and brain homogenate. Table 4.2 summarizes the results of the stability studies.

Table 4.2: Results of the stability studies of opioid- *S*-(-)-nornicotine codrugs.

	codeine-*S*-(-)-nornicotine	3-*O*-acetylmorphine-*S*-(-)-nornicotine	morphine-*S*-(-)-nornicotine
pH 1.3	Stable	Deacetylation only	Stable
pH 5.0	Stable	Deacetylation only	Stable
pH 7.4	Stable	Deacetylation only	Stable
SGF	Stable	Deacetylation only	Stable
SIF	Stable	Deacetylation only	Stable
80% Rat Plasma	Stable	Deacetylation only	Stable
Brain Homogenate	Stable	Deacetylation only	Stable

The data from the chemical hydrolysis studies at pH 1.3 and in SGF indicates that the codrugs are stable in these media, and thus are not likely to undergo chemical or enzymatic hydrolysis in the stomach when given orally. In fact, no observable degradation of the codrug occurred in these media over 24 hours. 3-*O*-Acetylmorphine-*S*-(-)-nornicotine codrug underwent hydrolysis of the ester group, as expected, to produce morphine-*S*-(-)-nornicotine codrug, but no carbamate bond hydrolysis was observed. Thus, the codrugs should pass through the stomach after oral administration without any hydrolysis to produce the parent drugs. Additionally, at pHs 5.0 and 7.4, and in SIF, no hydrolysis of the codrugs to produce the parent drugs was observed for 24 hours. Thus, the codeine-*S*-(-)-nornicotine and morphine-*S*-(-)-nornicotine codrugs should be absorbed intact from the intestine and reach the systemic circulation as a single molecular entity, while the 3-*O*-acetylmorphine-*S*-(-)-nornicotine codrug will undergo ester bond hydrolysis to produce morphine-*S*-(-)-nornicotine codrug in the GI tract.

In rat plasma, no significant hydrolysis of the codeine-*S*-(-)-nornicotine and morphine-*S*-(-)-nornicotine codrugs was observed, while 3-*O*-acetylmorphine-*S*-(-)-

nornicotine codrug underwent instantaneous hydrolysis of the O-acetyl moiety to produce morphine-*S*-(-)-nornicotine.

4.3.3 Stability Study in Brain Homogenate

The stability study of the codrugs in brain homogenate was carried out over 8 hrs and samples were analyzed by HPLC–DAD assay. The data from the enzymatic hydrolysis study in brain homogenate indicates that the codrugs are stable in brain with respect to carbamate bond hydrolysis, and thus are not likely to undergo enzymatic hydrolysis in the brain to produce the parent drugs. In fact, no observable generation of the parent drugs occurred over the 8 hours of the study.

4.4 Opioid-Ketamine/Norketamine Codrugs

Three codrugs were synthesized in this series. The structures of the synthesized codrugs are illustrated in Fig 4.5. Codeine-norketamine and morphine-norketamine codrugs were analyzed for their stabilities under the same hydrolytic conditions. Since racemic ketamine and racemic norketamine were used for the synthesis of the codrugs, diasteromeric mixtures of the resultant codrugs were obtained and these diastereomeric mixtures were studied for in vitro stability. The codeine-ketamine codrug was not studied as this codrug contains a secondary carbamate and from the stability study of the opioid-nornicotine codrugs it was found that secondary carbamate linkages are very stable in the studied hydrolytic conditions.

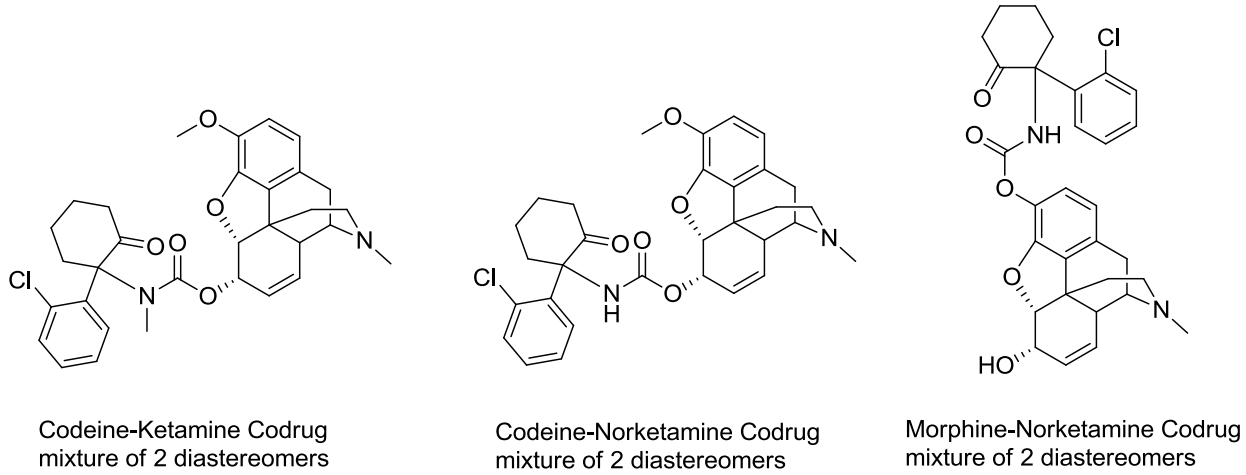

Fig. 4.5: Structures of opioid-norketamine codrugs analyzed for in vitro stability.

4.4.1 HPLC Assay

HPLC assays were developed for the study of the stability of the above codrugs. A Waters Symmetry ® C_{18} (5 µm, 3.9 x 150 mm) column protected with guard column (Nova-Pak® C_{18}; 3.9 x 20 mm; 4µ) was used as the stationary phase; 0.16% aqueous solution of sodium heptane sulfonate (SHS) adjusted to pH 3.2 with 85% *o*-phosphoric acid (solvent A)/methanol (solvent B) was used as mobile phase. A 0.8 mL/min flow rate was used, and UV detection was carried out at 220 nm. Morphine was used as the internal standard in case of the codeine-norketamine codrug, and naltrexol was used as internal standard for the study of the morphine-norketamine codrug.

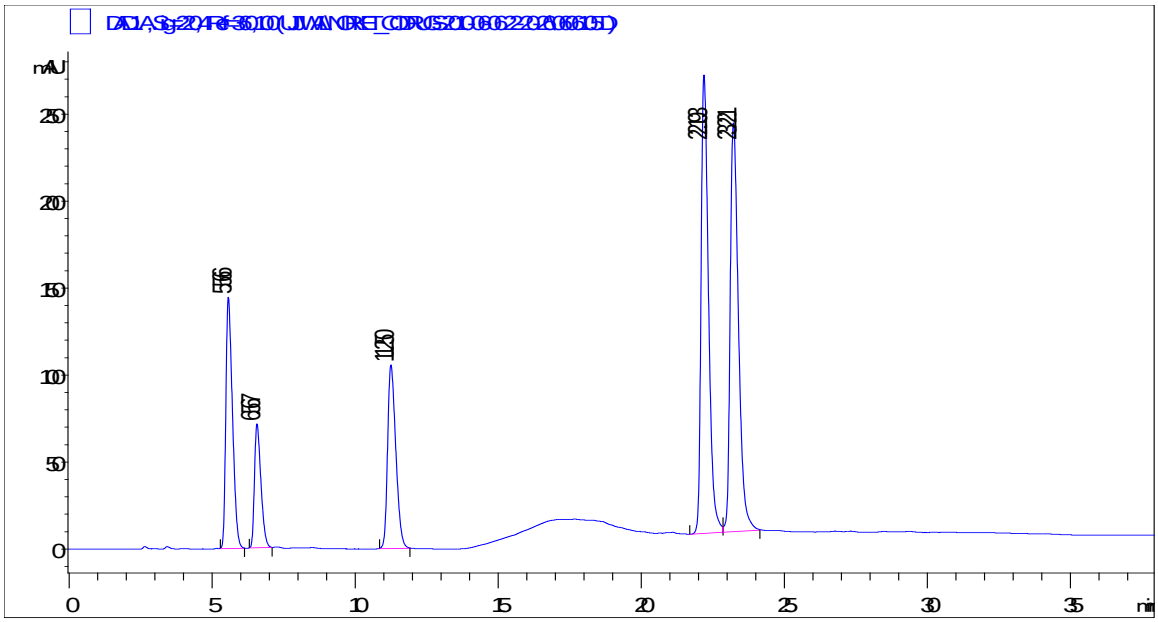

Fig. 4.6: HPLC Chromatogram of Morphine (IS), Codeine, Norketamine, and Norketamine-Codeine codrug (2 peaks for the 2 diastereomers) (in order of elution).

The following gradient program was utilized for the codeine-norketamine codrug stability study:

0-10 min: 46% solvent A

10-13 min: 46% to 30% solvent A

13-35 min: 30% solvent A

35-38 min: 30% to 46% solvent A

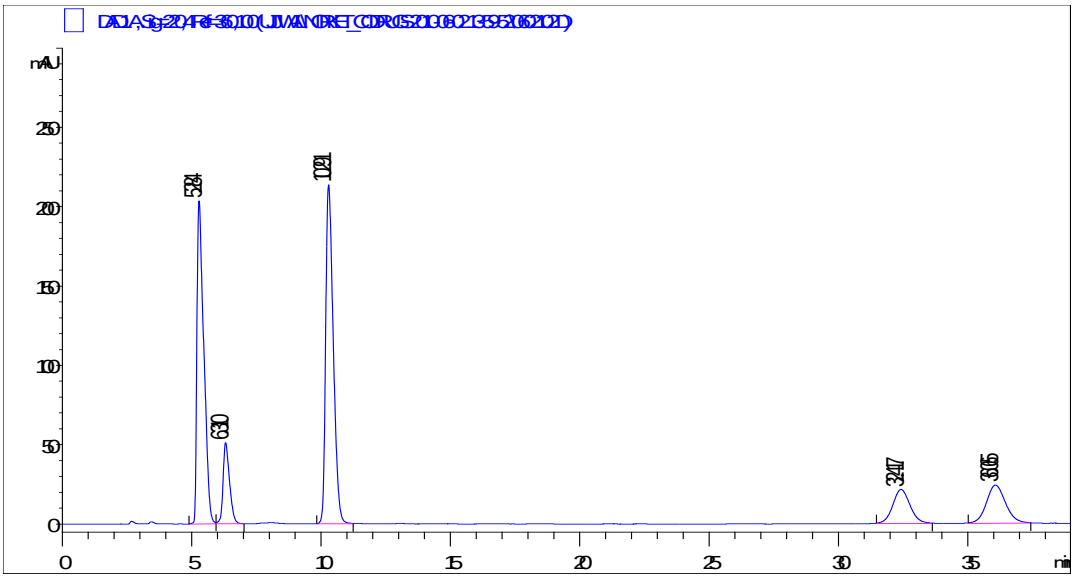

Fig. 4.7: HPLC Chromatogram of Morphine, Naltrexol (IS), Norketamine, and Norketamine-Morphine codrug (2 peaks for the 2 diastereomers) (in order of elution).

A very similar isocratic HPLC assay was utilized for the stability study of the morphine-norketamine codrug utilizing a 0.8 mL/min flow rate and 44.5% composition of solvent A.

4.4.2 Assay Validation

Calibration curves were generated for each analyte and for each stability study. Table 4.2 summarizes the information regarding the linear range of each analyte.

4.4.3 Chemical and Enzymatic Stability Study

Chemical and enzymatic stability studies on the codeine-norketamine and morphine-norketamine codrugs were carried out *in vitro*. Chemical hydrolysis was examined utilizing buffers at pH 1.3, 5.0, and 7.4, and enzymatic hydrolysis was

examined in simulated gastric fluid (SGF), simulated intestinal fluid (SIF), and 80% rat plasma and brain homogenate. Table 4.3 summarizes the results of these stability studies.

Figure 4.3: Results of stability studies of opioid-norketamine codrugs.

	Codeine-Norketamine	Morphine-Norketamine
pH 1.3	Stable	Stable
pH 5.0	Stable	Stable
pH 7.4	Stable	Stable
SGF	Stable	Stable
SIF	Stable	Stable
80% Rat Plasma	Stable	Stable
Brain Homogenate	Stable	Stable

Both the opioid-norketamine codrugs failed to produce the parent drugs in any of the hydrolytic conditions.The codeine-norketamine codrug contains a carbamate linkage between a primary amine and an allylic alcohol moiety. On the other hand, the morphine-norketamine codrug has a carbamate linkage between a primary amine and a phenol. These types of carbamate linkages are expected to be more prone towards hydrolysis, but the two codrugs did not hydrolyze in either the enzymatic or the nonenzymatic conditions. Thus, it can be concluded that these opioid-ketamine/norketamine codrugs will likely not behave as codrugs in vivo; rather, they will act as stable hybrids of two parent analgesic agents (i.e. opioid agonist and NMDA receptor antagonist).

4.5 Codeine-Gabapentin Codrugs

Four different codrugs were synthesized that incorporated codeine and gabapentin or prodrugs of gabapentin. The structures of the 4 codrugs are shown in Fig 4.8. The CG-1 codrug contained an ester linkage between codeine and gabapentin moieties and could only be isolated in the form of the HCl salt. As discussed in Chapter 2, the design of the codrug may be problematic. The pKa of the amino group in CG-1 is expected be about 8 to 8.5. Thus, in slightly basic condition (e.g. small intestine or physiological pH, but not in the stomach), a significant amount of the free amino group of the gabapentin moiety may be generated as a consequence of deprotonation which will lead to the formation of a five-membered cyclic carbamate derivative. The five-membered cyclic carbamate form of gabapentin is expected to be very stable, and will likely not hydrolyze back to gabapentin after cleavage of the inter drug ester linkage, but will form the parent drug codeine and a stable derivative of gabapentin.

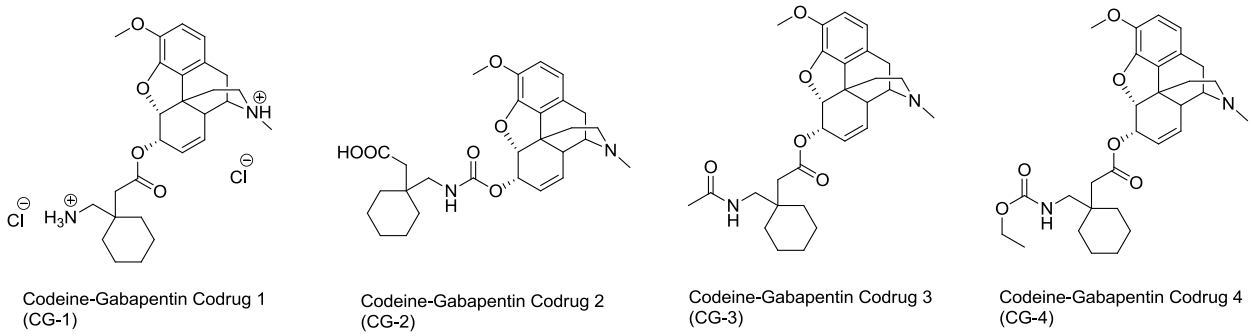

Fig. 4.8: Structures of the codeine-gabapentin codrugs analyzed for their *in vitro* stabilities.

4.5.1 HPLC Assay

To examine the above possibility, codrug CG-1 was synthesized and its stability was studied in pH 7.4 phosphate buffer. An HPLC assay was developed to separate morphine (IS), codeine and CG-1. A Waters Symmetry ® C_{18} (5 µm, 3.9 x 150 mm) column protected with a guard column (Nova-Pak® C_{18}; 3.9 x 20 mm; 4µ) was used as

the stationary phase; 0.04% aqueous HFBA solution (solvent A)/0.04% heptafluorobutyric acid (HFBA) solution in Methanol (solvent B) was used as mobile phase. A 0.5 mL/min flow rate was used, and UV detection was carried out at 280 nm.

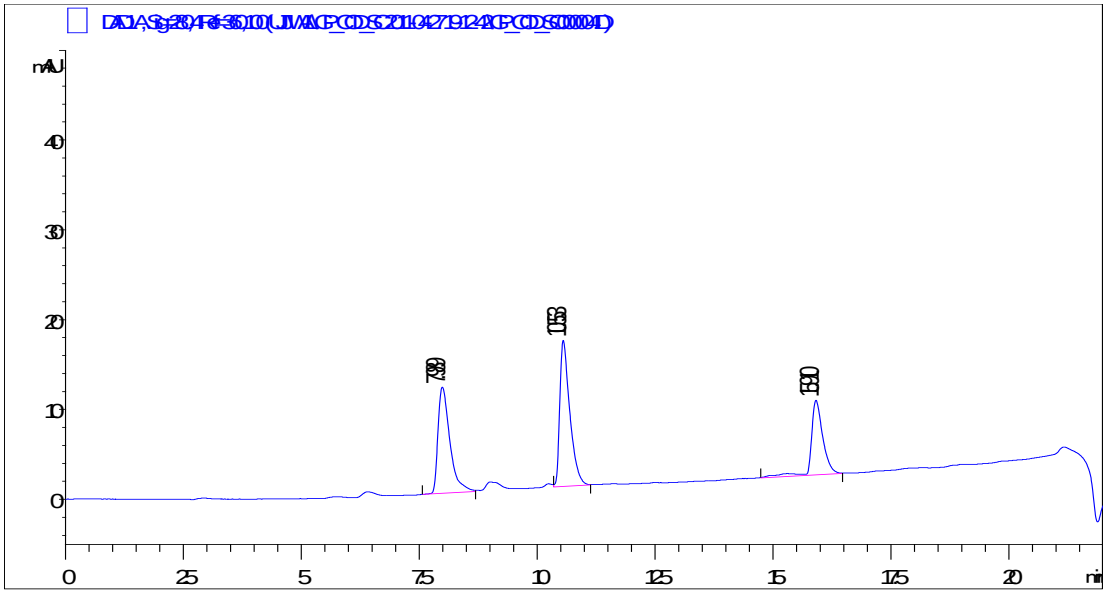

Fig. 4.9: HPLC Chromatogram of Morphine, codeine, and CG-1 codrug.

The 22 min time gradient program used for the analysis of the codeine-*S*-(-)-nornicotine codrug was as follows:

0-1 min: 70% solvent A

1-18 min: 70% to 28% solvent A

18-18.1 min: 28% to 70% solvent A

18.1-22 min: 70% solvent A

4.5.2 Assay Validation

Calibration curves were generated for each analyte and for each stability study. Table 4.1 summarizes the information regarding the linear range of each analyte.

4.5.3 Chemical Stability Study

At physiological pH (7.4), significant hydrolysis of the CG-1 codrug was observed and the kinetics of codrug disappearance with concomitant appearance of codeine was confirmed by HPLC-DAD analysis. The disappearance of the CG-1 codrug was correlated with pseudo first order kinetics. The hydrolytic rate constant and half-life value of the CG-1 codrug were obtained by regression analysis from slopes of semi-logarithmic plots of concentration *versus* time. Thus the codrug is hydrolyzed at a relatively fast rate in the small intestine to produce codeine and the five membered cyclic carbamate analog of gabapentin.

From the previous hydrolytic studies of the carbamate codrugs, it can be predicted that codrug CG-2, which combines codeine and gabapentin via a carbamate linkage, will likely be resistant to hydrolysis. To evaluate this possibility, the CG-2 codrug was analyzed for stability under different hydrolytic conditions. An HPLC assay was developed to study the stability of the codrug. A Waters Symmetry ® C_{18} (5 µm, 3.9 x 150 mm) column protected with a guard column (Nova-Pak® C_{18}; 3.9 x 20 mm; 4µ) was used as the stationary phase; 0.16% aqueous solution of sodium heptane sulfonate (SHS) adjusted to pH 3.2 with 85% *o*-phosphoric acid (solvent A)/ methanol (solvent B) was used as mobile phase. A 0.8 mL/min flow rate was used, and UV detection was carried out at 220 nm. Morphine was used as the internal standard.

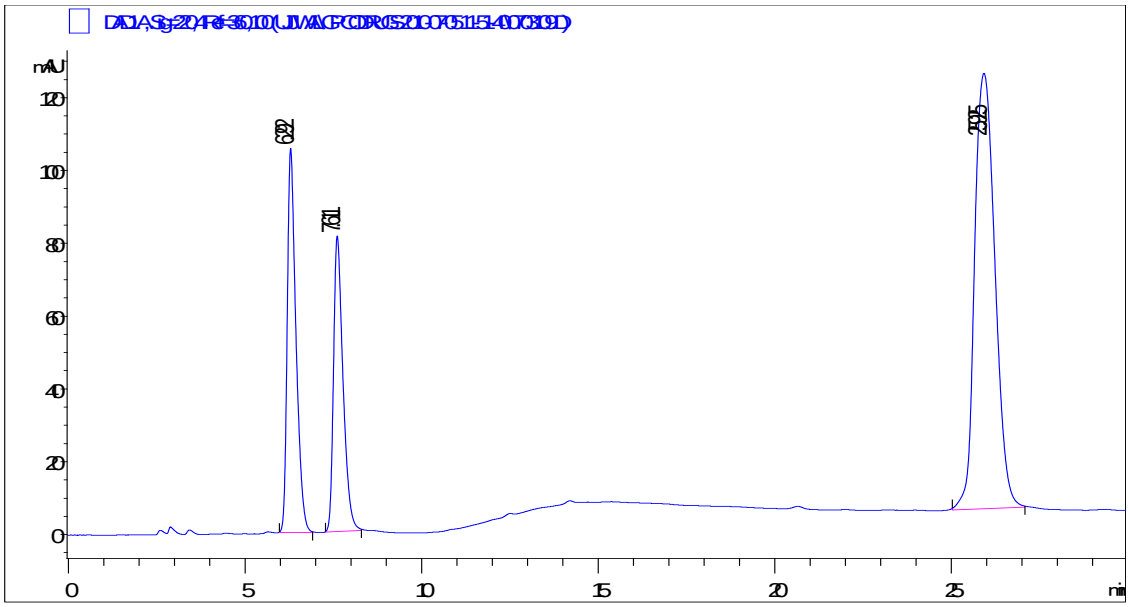

Fig. 4.10: HPLC Chromatogram of morphine, codeine, and CG-2 codrug (in order of elution).

The following gradient program was used for the CG-2 codrug stability study:

0-5.5 min: 47% solvent A

5.5-8.5 min: 47% to 39% solvent A

8.5-27 min: 39% solvent A

27-30 min: 39% to 47% solvent A

As predicted from the results of the previous stability studies the CG-2 carbamate codrug did not hydrolyze to produce the parent drugs codeine and gabapentin in any of the enzymatic or nonenzymatic solutions examined.

Codrugs CG-3 and CG-4 were synthesized by combining amide protected and carbamate protected gabapentin with codeine via a more labile ester linkage. These two codrugs were expected to undergo hydrolysis in several enzymatic and nonenzymatic buffers. It was expected that the more labile ester bond would hydrolyze at the fastest rate to produce codeine and a prodrug of gabapentin, and then the more resilient amide or

carbamate pro-moiety would be hydrolyzed at a slower rate to produce gabapentin. Since gabapentin does not contain a chromophore, it was only possible to follow the initial ester hydrolysis step was by HPLC-DAD assay; the hydrolysis of the pro-moiety of gabapentin could not be followed. [A subsequent *in vivo* study was performed using an LC-MS/MS assay to analyze the complete hydrolytic pattern of the codrugs in the rat (discussed in next chapter)].

4.5.4 HPLC assay

Initially, HPLC assays were developed to study the hydrolytic reactions of the above codrug molecules. The following HPLC assay was used for the stability study of the CG-3 codrug. A Waters Symmetry ® C_{18} (5 µm, 3.9 x 150 mm) column protected with a guard column (Nova-Pak® C_{18}; 3.9 x 20 mm; 4µ) was used as the stationary phase; /0.16% aqueous solution of sodium heptane sulfonate (SHS) adjusted to pH 3.2 with 85% *o*-phosphoric acid (solvent A)/Methanol (solvent B) was used as mobile phase. A 0.8 mL/min flow rate was used, and UV detection was carried out at 220 nm. Morphine was used as the internal standard.

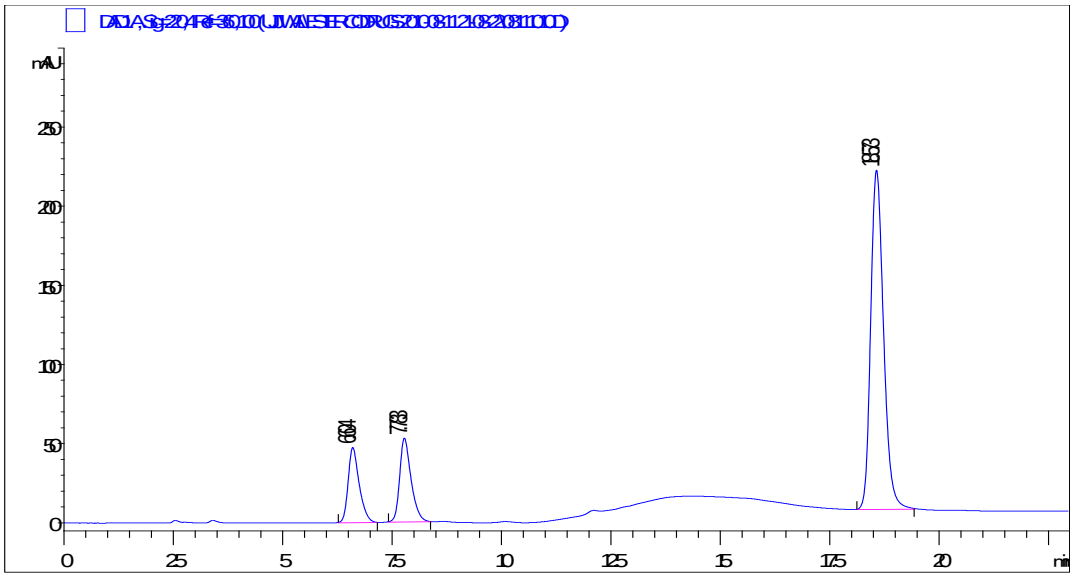

Fig. 4.11: HPLC Chromatogram of morphine (IS), codeine, and CG-3 codrug (in order of elution).

The following gradient program was used for the CG-3 codrug stability study:

0-6 min: 43% solvent A

6-9 min: 43% to 31% solvent A

9-20 min: 31% solvent A

20-23 min: 31% to 43% solvent A

For the hydrolytic study of the CG-4 codrug, the following HPLC assay was used. A Waters Symmetry ® C_{18} (5 µm, 3.9 x 150 mm) column protected with a guard column (Nova-Pak® C_{18}; 3.9 x 20 mm; 4µ) was used as the stationary phase; 0.04% aqueous HFBA solution (solvent A)/ 0.04% heptafluorobutyric acid (HFBA) solution in Methanol (solvent B) was used as mobile phase. A 0.5 mL/min flow rate was used, and UV detection was carried out at 280 nm. Morphine was used as an internal standard.

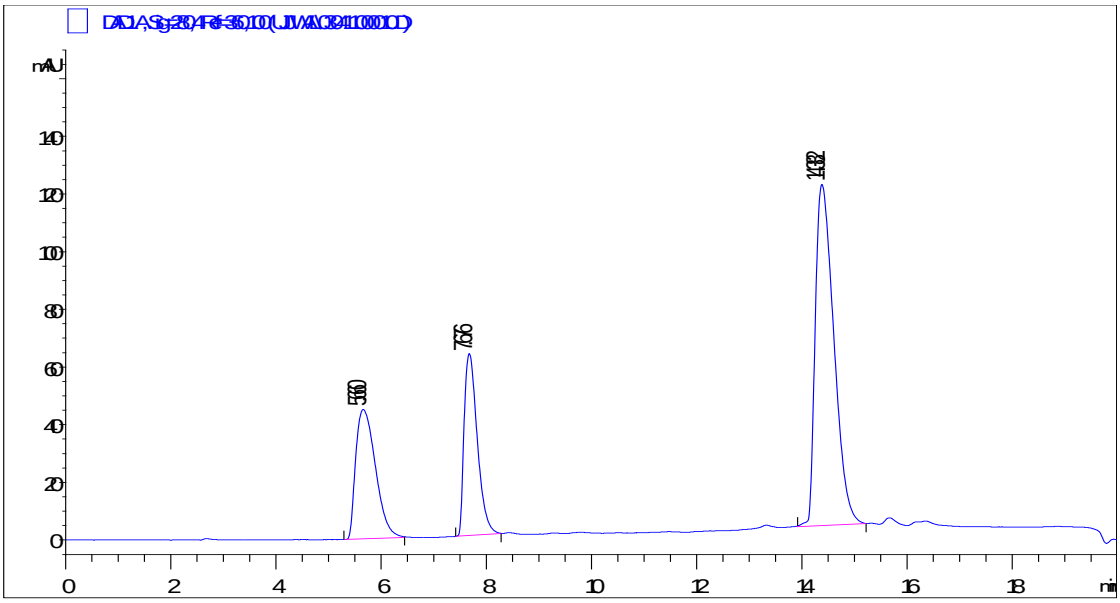

Fig. 4.12: HPLC Chromatogram of morphine (IS), codeine, and CG-4 codrug (in order of elution).

The 20 min time gradient program used for CG-4 codrug was as follows:

0-0.3 min: 65% solvent A

0.3-10 min: 65% to 13% solvent A

10-15 min: 13% solvent A

15-15.1 min: 13% to 65% solvent A

15.1-20 min: 65% solvent A

4.5.5 Assay Validation

Calibration curves were generated for each analyte and for each stability study. Table 4.1 summarizes the information regarding the linear concentration range for each analyte.

Table 4.4: Rate constants for hydrolysis of codeine-gabapentin codrugs.

	CG-1 (hr^{-1})	CG-2	CG-3 (hr^{-1})	CG-4 (hr^{-1})
pH 1.3	Not performed	Stable	0.0018 ± 0.0002	0.0018 ± 0.0002
pH 5.0	Not performed	Stable	0	0
pH 7.4	0.2220 ± 0.0003	Stable	0.0018 ± 0.0001	0.0012 ± 0.0002
SGF	Not performed	Stable	0.0020 ± 0.0003	0.0022 ± 0.0001
SIF	Not performed	Stable	0.0041 ± 0.0004	0.0048 ± 0.0002
80% Rat Plasma	Not performed	Stable	0.0123 ± 0.0025	0.0134 ± 0.0021
Brain Homogenate	Not performed	Stable	0.0052 ± 0.0019	0.0060 ± 0.0011

4.5.6 Results

Results from stability studies performed on the codeine-gabapentin codrugs are summarized in Table 4.4. Both CG-3 and CG-4 codrugs showed improved hydrolytic profiles compared to any of the other synthesized codrugs. Both codrugs underwent ester bond hydrolysis in 80% rat plasma to produce codeine and a prodrug of gabapentin. This data signifies that in the systemic circulation these codrugs will be cleaved to produce either parent drugs or parent drugs attached to a pro-moiety. The rates of hydrolysis in 80% rat plasma were comparatively slow, which may result in CG-3 and CG-4 having prolonged effects (sustained release). In addition to hydrolysis in 80% rat plasma, CG-3 and CG-4 were also hydrolyzed in pH 1.3 and pH 7.4 buffers and in SGF and SIF. These observations are not ideal for codrugs as it is not desirable to have significant hydrolysis of the codrugs in GI tract. It can be seen that these rates of hydrolysis in the above mentioned enzymatic and nonenzymatic conditions are very slow and the half-lives range from 144.38 hr to 577.5 hr. Since the mean residence time of a drug in the stomach is

roughly 30 min to 1 hr, it can be concluded that codrugs CG-3 and CG-4 will practically remain unhydrolyzed in stomach before being absorbed into systemic circulation. The same conclusion can be drawn in the case of probable hydrolysis of the codrugs in intestine, by observing the large half-life values of the codrugs at pH 7.4 and in SIF. It can also be seen that the CG-3 and CG-4 codrugs are hydrolyzed by brain homogenate at a relatively slow rate. This observation indicates that if the codrug molecules enter brain as a single chemical entity, they will be slowly hydrolyzed over time by enzymes present in brain to produce the parent drugs.

Results of the comprehensive stability study of the synthesized codrugs in different nonenzymatic aqueous buffers and biological media demonstrate that carbamate linkages are not always ideal in codrug design. In literature codrugs and prodrugs containing carbamate linkage have been reported, but most of them are either a type of activated carbamate linkage, or a very simple carbamate of a primary amine and a primary alcohol (Das et al., 2010). Since the carbamate linked codrugs did not show any sign of hydrolysis in enzymatic and nonenzymatic media, it can be concluded that these codrugs will not cleave to the respective parent drugs inside the body, but will rather behave as stable hybrids of the two parent analgesic drug molecules. On the other hand, ester-linked codrugs showed promising hydrolytic behavior. Ester linkages were cleaved in the plasma to produce parent drugs at a slow rate, which allows these codrugs to act as a chemical reservoir of the parent drugs for a sustained period of time. Though the ester linked codrugs were hydrolyzed in both acidic and basic pH conditions, the rates of hydrolysis were relatively too slow to be significant. Thus, ester linked codrugs CG-3 and CG-4 are predicted to be stable enough in the GI tract when administered orally to be absorbed from GI tract as a single chemical entity. Hydrolysis of the ester linkages in 80% rat plasma showed that such codrugs would hydrolyze in systemic circulation to produce codeine and a prodrug of gabapentin.

Copyright © Ujjwal Chakraborty 2012

Chapter 5

Pharmacokinetic Analysis of the Codrugs

5.1 Introduction

Pharmacokinetics is the study of the time course of drug concentration in different body compartments, such as plasma, blood, urine, cerebrospinal fluid, and tissues, and incorporates the processes of absorption, distribution, metabolism and excretion (ADME) after a specific route of administration of a drug (Smith et al., 2001).

The drug can enter the body in a variety of ways. Drugs are mostly given orally for reasons of convenience and patient compliance. If the drug has been administered orally, then it first enters the gastrointestinal tract, and gets absorbed through the gastrointestinal mucosal wall into the bloodstream. It is then shunted via the portal vein through the liver, where the "first pass effect" takes place, and it then reaches the blood circulation. The first-pass effect is a phenomenon of drug metabolism whereby the concentration of a drug is immensely reduced before it reaches the systemic circulation. It is a fraction of the administered drug that gets absorbed, which mainly takes place in liver and gut wall. Therefore, the oral delivery of a drug involves an additional absorption step. The percentage of the administered dose reaching the circulation as the free drug is called the bioavailability of the drug. The drug then gets distributed to various tissues and organs in the body. The extent of this drug distribution depends on the structural and physicochemical properties of the drug. Some drugs might enter the brain and the central nervous system by crossing the blood–brain barrier. Finally, the drug will bind to its molecular target, for example, a receptor or an ion channel, and exert its anticipated action. If the drug is injected directly into the bloodstream (e.g. by the intravenous route), then it is totally available for distribution to the tissues. But if it is administered orally, then its bioavailability will usually be less than 100% (Smith et al., 2001).

Once the drug is in the systemic circulation, a portion of it is available to illicit its pharmacodynamic effect; the rest may bind to plasma proteins in an inactive reversible protein-drug complex. Binding to plasma proteins is sometimes advantageous since the drug is continuously freed from the protein-drug complex and this can result in a

extended drug action (Smith et al., 2001). The unbound drug follows the concentration gradient and gets distributed into the peripheral tissues. These tissues may contain specific or non-specific binding sites. The non-specific binding sites can act as reservoirs for the drug molecule. This "total volume of distribution" determines the equilibrium concentration of a drug after administration of a specific dose (van de Waterbeemd and Gifford, 2003).

Pharmacokinetic parameters are derived from the measurement of drug concentrations in bloodstream or plasma after administration. The key pharmacokinetic parameters are Volume of Distribution (V_d), Clearance (Cl), Half-life ($t_{1/2}$) and Oral Bioavailability (F).

Volume of Distribution (V_d) -- Volume of Distribution is defined as the apparent space or volume into which a drug distributes itself. It is a theoretical concept that relates the administered dose with the actual initial concentration (C_0) present in the systemic circulation. If a drug is highly lipophilic in nature, then the drug will have a very high volume of distribution, because the drug specifically or non-specifically binds to tissues and stays there (Mehvar, 2004).

$$V_d = \text{Dose}/C_0$$

Clearance (Cl) --Clearance of a drug from the body mainly takes place via the liver (hepatic clearance or metabolism, and biliary excretion) and the kidney (renal excretion).

By plotting the plasma concentration against time, the area under the curve (AUC) relates to dose, bioavailability (F) and clearance.

$$\text{AUC} = F \times \text{Dose}/\text{Cl}$$

Half-life ($t_{1/2}$) --Half-life is the time taken for the drug concentration in the plasma to be reduced by 50%. It is a function of the clearance and volume of distribution, and determines how often a drug needs to be administered.

$$t_{1/2} = 0.693\ V_d/Cl$$

Intravenous (IV) bolus dosing (i.e, the entire drug dose is given as a rapid injection) captures the pure distribution and elimination processes.

In the "first pass effect" the liver bio-transforms the drug into active or inactive metabolites, which can then be more easily excreted. Prodrugs are inactive chemical entities that get activated only after they are metabolized to an active drug. This is often a strategy utilized to improve pharmacokinetic properties and drug-likeness. Some drugs are excreted in the bile and eventually may pass out of the body in the feces, while some are filtered by kidney, where a portion undergoes reabsorption, with the remainder being excreted in the urine. Smaller amounts of drug are excreted in the tears, breast milk and sweat (Dingemanse and Dingemanse, 2007).

5.2 Pharmacokinetic Profile of Codeine and Gabapentin

Codeine is mostly metabolized in liver to seven metabolites: codeine-6-*O*-glucuronide, norcodeine, norcodeine-glucuronide (6-*O*-), morphine, morphine-3-*O*-glucuronide, morphine-6-*O*-glucuronide, and normorphine. It has been hypothesized that codeine exerts its moderate analgesic potency through partial biotransformation to morphine via oxidative *N*-demethylation. Apart from morphine, two other metabolites of codeine, morphine-6-*O*-glucuronide and normorphine were found to be analgesic. Morphine-6-*O*-glucuronide was found to be a much stronger analgesic than morphine (Thorn, 2009).

Orally administered gabapentin is absorbed slowly with maximum plasma concentration attained within 3-4 hours (Bockbrader et al., 2010). Plasma concentrations of gabapentin do not increase proportionally with increasing oral dose. The bioavailability of gabapentin is dose-dependent and the absolute bioavailability drops from 60% to 33% as the dosage increases from 900 to 3600 mg/day in humans (Eckhardt et al., 2000). Gabapentin does not bind to plasma proteins, and is excreted renally. Gabapentin is metabolized to *N*-methyl gabapentin in dogs. In mice, rats and humans it undergoes negligible metabolism, and the metabolites account for less than 1% of the administered dose (Rose and Cam, 2002).

Pharmacokinetic studies on selected codrugs were performed in cooperation with Dr. Zaineb Albayati, Dr. Manjula Sunkara, and Mr. John May.

5.3 Materials and Methods

5.3.1 Chemicals and Reagents

S-(-)-Nornicotine, 3-*O*-acetylmorphine-*S*-(-)-nornicotine codrug, morphine-*S*-(-)-nornicotine codrug, CG-3 (amide protected gabapentin-codeine codrug) and CG-4 (carbamate protected gabapentin-codeine codrug) were synthesized in the laboratory (see Chapter 2 for details). The reagents and buffer salts used in this study were of HPLC grade or equivalent quality. Acetonitrile and potassium chloride were obtained from Thermo Fisher Scientific (Pittsburgh, PA). Heparin sodium injection, 10,000 USP units/ml, was purchased from Baxter Healthcare Corporation (Deerfield, IL). Nembutal sodium (pentobarbital sodium injection, USP) was obtained from Abbott Laboratories (North Chicago, IL).

5.3.2 Animals

All procedures involving animals were performed in compliance with the guidelines of the University of Kentucky Institutional Animal Care and Use Committee established by the National Institutes of Health's *Guide for the Care and Use of Laboratory Animals* (1996). Male Sprague-Dawley rats (200–250 g) were obtained from Harlan (Indianapolis, IN) and housed two per cage with *ad libitum* access to food and water in the Division of Laboratory Animal Resources at the University of Kentucky

College of Pharmacy. Body weights at the time of dosing were 280-360 g. Rats were anesthetized with pentobarbital (40 mg/kg i.p.) and surgically implanted with jugular and femoral vein cannulas for *i.v.* drug dosing and blood sampling, respectively. For the first 3 to 4 days after surgery, the rats were observed for signs of infection at the surgical sites, yellowing of hair and hair texture, presence of blood around the eyes or nose, indications of loss of appetite, and decreased or absent fecal activity before the start of *i.v.* dosing.

5.4 *In vivo* Pharmacokinetic Study of 3-*O*-Acetylmorphine-*S*-(-)-Nornicotine Codrug

5.4.1 Instrumentation

Samples were analyzed for analyte-specific (149 m/z to 130 m/z, *S*-(-)-nornicotine; 328 m/z to 211 m/z, 3-*O*-acetylmorphine; 460 m/z to 268 m/z, morphine-*S*-(-)-nornicotine; 286 m/z to 201 m/z morphine; and 502 m/z to 310 m/z, 3-*O*-acetylmorphine-*S*-(-)-nornicotine) and internal standard-specific (342 m/z to 324 m/z, naltrexone) transitions by LC/MS/MS utilizing reverse-phase chromatography and positive-mode ionization. The instrumentation consisted of a Varian LC system (ProStar 210 pumps, Prostar 410 autoinjector) connected through an ESI source to a Varian 1200L triple quadrupole mass spectrometer with all components controlled by a Varian MS Workstation version 6.42. Individual analyte-dependent ESI-(+)-MS/MS parameters were optimized for signal intensity.

5.4.2 HPLC and Mass Spectrometric Conditions

Individual analyte-dependent ESI-(+)-MS/MS parameters were optimized for signal intensity. These optimized parameters were subsequently used in the analysis of biological samples (CE = 11 V for *S*-(-)-nornicotine, 16.5 V for morphine, 22 V for 3-*O*-acetylmorphine, 15.5 V for naltrexone, 19.5 V for morphine-*S*-(-)-nornicotine, and 20 V for 3-*O*-acetylmorphine-*S*-(-)-nornicotine). Briefly, 10 µL of the biological sample was injected onto a guard column protected (Nova-Pak® C_{18}; 3.9 x 20 mm; 4µ) Nova-Pak® C_{18} analytical column (3.9 x 150 mm; 4 um). Analytes were eluted at 11.12 min (morphine), 13.36 min (*S*-(-)-nornicotine), 13.77 min (naltrexone, internal standard), 14.38 min (3-*O*-acetylmorphine), 15.12 min (morphine-*S*-(-)-nornicotine), and 16.24 min (3-*O*-acetylmorphine-*S*-(-)-nornicotine) using water containing 0.04% HFBA (solvent A)

and methanol containing 0.04 % HFBA (solvent B), using a gradient program and a 0.3 mL/min flow rate. The 36 min gradient program began with 75:25 solvents A: B for 0.5 min followed by a 21.5 min linear ramp to 10:90 solvents A: B. This percentage was held constant for 4 min, and then returned to 75:25 solvents A:B over a 3 min linear ramp; and then held at 75:25 solvents A:B for an additional 9 min. Argon was used as a collision gas at 2.0 m Torr, and nitrogen was used as a drying gas at 300 °C. The needle voltage was 5000 V, the shield voltage was 600 V, and the capillary voltage was 40 V.

5.4.3 Plasma Pharmacokinetics

It was observed in *in vitro* stability studies performed on the 3-*O*-acetylmorphine-*S*-(-)-nornicotine codrug, that the carbamate linkage joining the two parent drugs did not cleave under any enzymatic or non-enzymatic conditions. Thus, the 3-*O*-acetylmorphine-*S*-(-)-nornicotine codrug was predicted to be quite stable in the GI tract as well as in systemic circulation, and would likely not hydrolyze to the parent drugs. This prediction was proven in a quick pharmacokinetic study. 3-*O*-Acetylmorphine-*S*-(-)-nornicotine codrug solution was prepared in 15% PEG-400 solution in saline and filtered through a 0.2-µm filter. The animal was administered with 8 mg/kg oral dose of the codrug. Dose and route of administration were chosen on the basis of studies that evaluated the analgesic effect of 3-*O*-acetylmorphine-*S*-(-)-nornicotine codrug (Chapter 3). Blood samples (0.2 mL) were obtained at 5, 15, 35, 45 min, 1, 2, 4, 7, 10, and 26 hrs after oral dosing. The withdrawn blood was replaced with heparinized saline (0.2 mL). Blood samples were centrifuged at 1200 g for 15 min, and the plasma was separated. The separated plasma was frozen immediately on dry-ice and stored at −80 °C prior to analysis.

5.4.4 Extraction Procedure

To isolate the analytes from rat plasma, 50 µL of plasma was transferred to polypropylene tubes to which 10 µl of working internal standard solution was added followed by vortexing for 1 min. 300 µL of acetonitrile was then added for deproteinization. The samples were then centrifuged for 15 min at 8000 rpm. The supernatant was transferred into silylated micro-serts and evaporated to dryness under

nitrogen gas at 37 °C. Following drying, the residue was dissolved in 80 µl of mobile phase by vortexing for 1min; 10 µl of the sample was then injected into the LC-MS/MS unit.

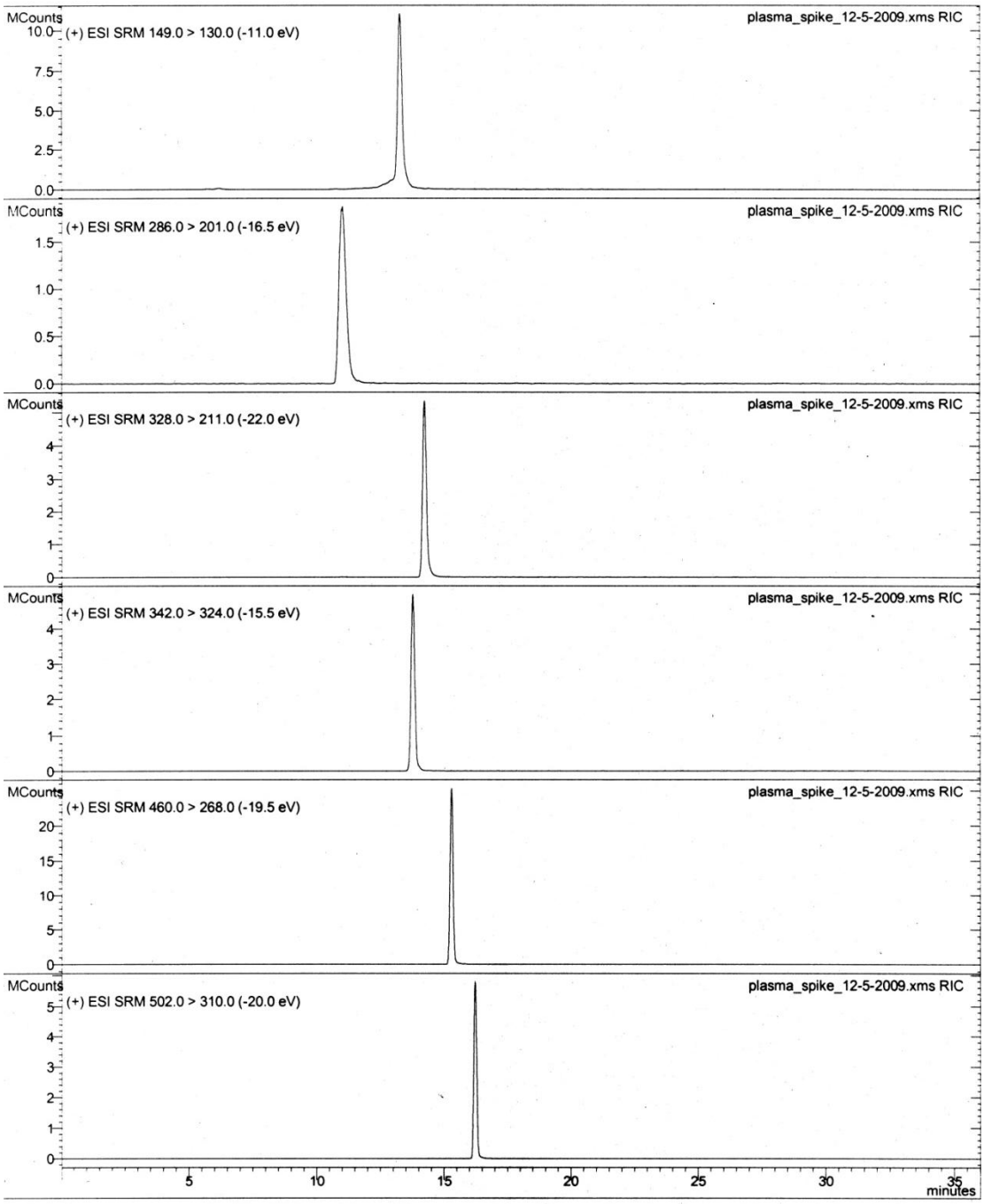

Fig. 5.1: Chromatograms of *S*-(-)-nornicotine, morphine, 3-*O*-acetylmorphine, naltrexone (IS), morphine-*S*-(-)-nornicotine, and 3-*O*-acetylmorphine-*S*-(-)-nornicotine (top to bottom order).

The *in vivo* study of 3-*O*-acetylmorphine-*S*-(-)-nornicotine codrug indicated that the carbamate linkage of the codrug did not undergo hydrolysis. The only analyte that was observed in the collected blood samples was the morphine-*S*-(-)-nornicotine hybrid resulting from *O*-deacetylation of the administered codrug. Thus, the predictions regarding *in vivo* stability of the 3-*O*-acetylmorphine-*S*-(-)-nornicotine codrug were correct. Under *in vivo* hydrolytic conditions, 3-*O*-acetylmorphine-*S*-(-)-nornicotine codrug exhibited only ester hydrolysis of the *O*-acetyl moiety and no evidence of carbamate bond hydrolysis was demonstrated.

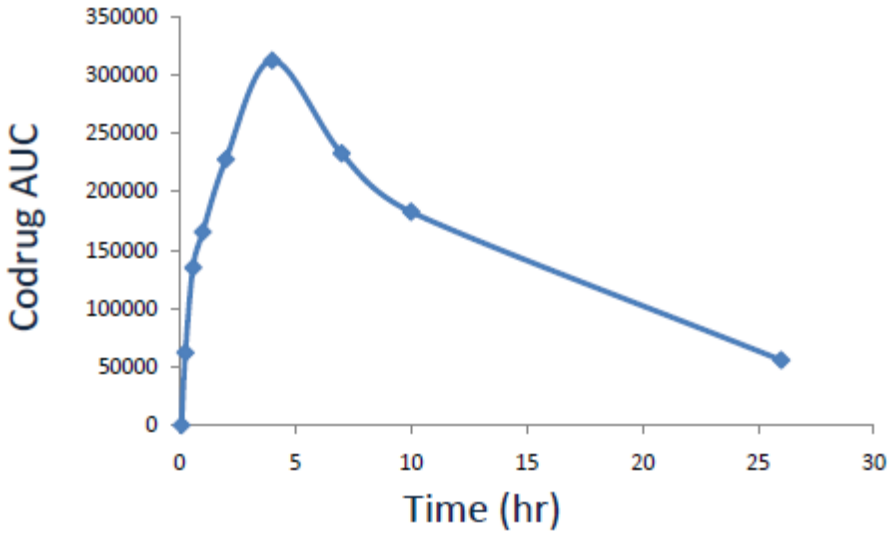

Fig. 5.2: AUC for the morphine-*S*-(-)-nornicotine codrug *versus* time plot after oral administration of *O*-acetylmorphine-*S*-(-)-nornicotine codrug.

5.5 *In vivo* Pharmacokinetic Study *N*-Acetamidogabapentin-Codeine (CG-3) Codrug

5.5.1 Instrumentation

Samples were analyzed for analyte-specific (172 m/z to 154 m/z, gabapentin; 214 m/z to 154 m/z, *N*-acetamidogabapentin; 300 m/z to 215 m/z, codeine; 286 m/z to 201 m/z morphine, and 495 m/z to 282 m/z *N*-acetamidogabapentin-codeine (CG-3) codrug and internal standard-specific (342 m/z to 324 m/z, naltrexone) transitions by LC/MS/MS utilizing reverse-phase chromatography and positive-mode ionization. The instrumentation consisted of a Varian LC system (ProStar 210 pumps, Prostar 410

autoinjector) connected through an ESI source to a Varian 1200L triple quadrupole mass spectrometer with all components controlled by a Varian MS Workstation version 6.42. Individual analyte-dependent ESI-(+)-MS/MS parameters were optimized for signal intensity.

5.5.2 HPLC and Mass Spectrometric Conditions

Individual analyte-dependent ESI-(+)-MS/MS parameters were optimized for signal intensity. These optimized parameters were subsequently used in the analysis of biological samples (CE = 7.5 V for gabapentin, 9.5 V for codeine, 7 V for *N*-acetamidogabapentin, 8 V for naltrexone, 7.5 V for morphine, and 18.5 V for CG-3. Briefly, 10 µL of the biological sample was injected onto a guard column protected (Nova-Pak® C_{18}; 3.9 x 20 mm; 4µ) Nova-Pak® C_{18} analytical column (3.9 x 150 mm; 4 um). Analytes were eluted at 6.55 min (morphine), 9.87 min (codeine), 10.49 min (naltrexone, internal standard), 13.59 min (gabapentin), 19.52 min (*N*-acetamidogabapentin), and 20.12 min (CG-3). 10 mM aqueous ammonium formate solution adjusted to pH 3.3 with formic acid (solvent A) and methanol containing 10 mM ammonium formate and formic acid (solvent B) were used as the mobile phases. A gradient program with 0.3 mL/min flow rate was used for the LC-MS/MS assay. The 36 min gradient program began with 75:25 solvents A: B for 0.5 min followed by a 21.5 min linear ramp to 10:90 solvents A: B. This percentage was held constant for 4 min, and then returned to 75:25 solvents A:B over a 3 min linear ramp; and then held at 75:25 solvents A:B for an additional 9 min. Argon was used as a collision gas at 2.0 m Torr, and nitrogen used as a drying gas at 300 °C. The needle voltage was 5000 V, the shield voltage was 600 V, and the capillary voltage was 40 V.

5.5.3 Plasma Pharmacokinetics

CG-3 codrug was dissolved in a saline solution containing 15% concentration of PEG-400 and filtered through a 0.2-µm filter. A 10 mg/kg oral dose was administered to the animals. Blood samples (0.2 mL) were obtained at 5, 15, 30 min, 1, 2, 4, 6, 10, 11, and 29 hrs after oral dosing. The withdrawn blood was replaced with heparinized saline (0.2 mL). Blood samples were centrifuged at 1200 g for 15 min, and the plasma was

separated. The separated plasma was frozen immediately on dry-ice and stored at −80 °C prior to analysis.

5.5.4 Standard Curves and Quality Control Validation Solutions

Stock solutions of the analytes and internal standard (naltrexone) were prepared in methanol. Two stock solutions were prepared; one for generating the standard curve, and a second one for quality control (QC) and method validation. A standard curve with eight different concentration points was prepared for the analysis of unknown samples. Standard curve samples were prepared by spiking blank plasma with working solutions of all the different analytes. Calibration curves were obtained using quadratic least-squares regression of AUC ratio (analyte peak AUC/internal standard peak AUC) *versus* drug concentrations. The amounts of codrug, or parent drugs, were then determined. Three quality control samples with different concentrations were prepared to check the sensitivity of the instrument. The three concentrations chosen were: one towards the higher end of the standard curve concentrations, one towards the middle, and the third one towards the lower end of the standard curve concentrations.

5.5.5 Extraction Procedure

To isolate the analytes from plasma, 50 µL of plasma was transferred to polypropylene tubes to which had been added 10 µl of working internal standard solution followed by vortexing for 1 min. 300 µL of acetonitrile were then added for deproteinization. The samples were then centrifuged for 15 min at 8000 rpm. The supernatant was transferred into silylated micro-serts and evaporated to dryness under nitrogen gas at 37 °C. Following drying, the residue was dissolved in 80 µl of mobile phase by vortexing for 1 min; 10 µl of the sample was then injected onto the LC-MS/MS unit.

5.5.6 Assay Validation

Blank plasma samples were extracted and analyzed by reverse phase HPLC for potential interfering peaks within the range of the retention time for analytes and the internal standard, naltrexone. An 8-point calibration curve for each analyte was generated. Table 6.1 summarizes the information regarding the standard curves.

Table 5.1: Linear ranges of analytes in the LC-MS/MS assay.

Analyte	Linear Range	R^2
Morphine	20-500 ng/mL	0.9999
Codeine	2-500 ng/mL	0.9997
Gabapentin	2-500 ng/mL	0.9992
N-acetylgabapentin	0.5-500 ng/mL	0.9986
CG-3	0.5-500 ng/mL	0.9992

5.5.7 Results

Mean concentration versus time profile of the codrug and parent drugs is plotted in Fig. 6.3. It can be noticed from the concentration versus time profile that the ester linkage in the codrug undergoes hydrolysis to produce codeine and *N*-acetylgabapentin, but the amide pro-moiety is not cleaved from the gabapentin derivative to produce gabapentin. The codrug hydrolysis profile was studied for a time period of 29 hrs, but no gabapentin formation was observed over that time period. It can also be noticed that at any time point in the concentration profile, codrug is present at a higher concentration than codeine or *N*-acetylgabapentin. Thus, the ester bond hydrolysis is likely being very slow in both plasma and GI tract, and the *N*-acetylgabapentin product is stable to hydrolytic cleavage.

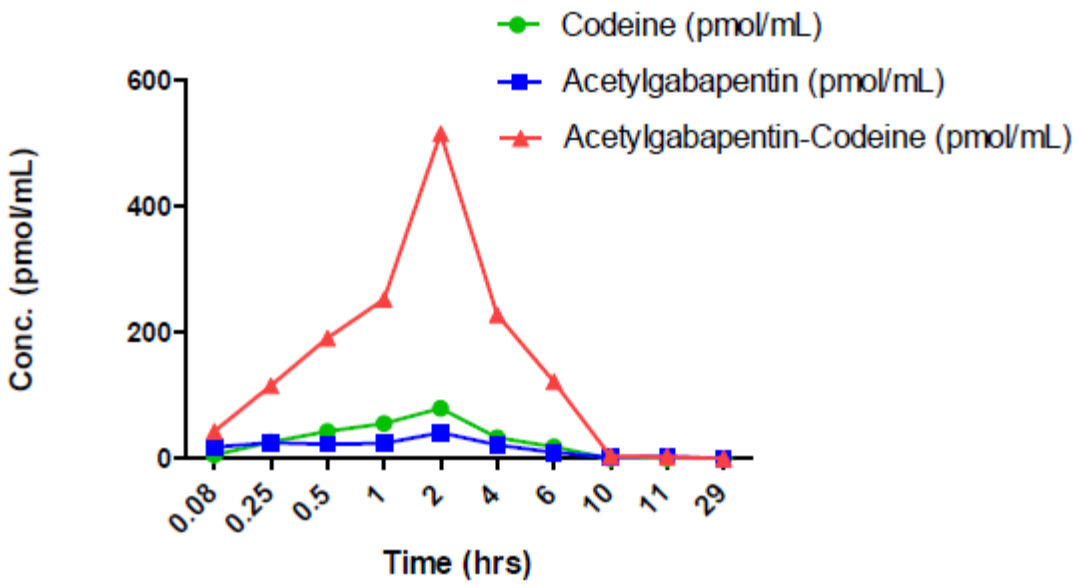

Fig. 5.3: Mean concentrations of the analytes versus time plot after oral dosing of CG-3 codrug.

5.6 *In vivo* Pharmacokinetic Study of *N*-Ethoxycarbonylgabapentin-Codeine (CG-4) Codrug

5.6.1 Instrumentation

Samples were analyzed for analyte-specific (172 m/z to 154 m/z, gabapentin; 244 m/z to 154 m/z, *N*-ethoxycarbonylgabapentin; 300 m/z to 152 m/z, codeine; 286 m/z to 152 m/z morphine, and 525 m/z to 282 m/z *N*-ethoxycarbonylgabapentin-codeine (CG-4) codrug and internal standard-specific (342 m/z to 324 m/z, naltrexone) transitions by LC/MS/MS utilizing reverse-phase chromatography and positive-mode ionization. The instrumentation consisted of a Varian LC system (ProStar 210 pumps, Prostar 410 autoinjector) connected through an ESI source to a Varian 1200L triple quadrupole mass spectrometer with all components controlled by a Varian MS Workstation version 6.42. Individual analyte-dependent ESI-(+)-MS/MS parameters were optimized for signal intensity.

5.6.2 HPLC and Mass Spectrometric Conditions

Analysis of codeine, *N*-ethoxycarbonylgabapentin, gabapentin, CG-4 codrug, morphine and naltrexone was carried out using a Shimadzu UFLC coupled with an AB

Sciex 4000-Qtrap hybrid linear ion trap triple quadrupole mass spectrometer in multiple reaction monitoring (MRM) mode. Naltrexone was used as an internal standard. Codeine, *N*-ethoxycarbonyl- gabapentin, gabapentin, CG-4 codrug, morphine and naltrexone were separated using a Zorbax Eclipse XDB C18 column, 5 µM, 4.6 X 150 mm column (Agilent). The mobile phase consisted of water containing 0.1% TFA (solvent A) and acetonitrile containing 0.1% TFA (solvent B). Analysis of these compounds was achieved by starting with 10 % solvent B for an initial 1 min, changing from 10% B to 100 % B over the next 7 min, and maintained at 100% B for the last 4 min. The HPLC column was equilibrated back to the initial conditions over 3 min. The flow rate was 0.5 mL/min with a column temperature of 30 °C. The sample injection volume was 10 µL. The mass spectrometer was operated in the positive electrospray ionization mode with optimal ion source settings determined by synthetic standards of codeine, *N*-ethoxycarbonylgabapentin, gabapentin, CG-4 codrug, morphine and naltrexone with a curtain gas of 20 psi, ion spray voltage of 5500 V, ion source gas1/gas2 of 40 psi and temperature of 550 °C.

Table 5.2: Optimal ion source settings for each MRM transition monitored.

	Q1	Q3	DP (volts)	CE (volts)	CXP (volts)
Codeine	300.197	152.2	56	87	8
	300.197	165.2	56	59	8
N-ethoxycarbonylgabapentin	244.081	154.1	46	27	8
	244.081	226.1	46	13	14
Gabapentin	172.118	154.1	51	21	8
	172.118	137.1	51	25	6
Gabapentin-Codeine Codrug (CG-4)	525.298	282	151	45	18
	525.298	154.1	151	65	8
Morphine	286.152	152.2	116	85	8
	286.152	201	116	37	12
Naltrexone	342.123	324.1	96	31	16
	342.123	270.1	96	37	16
N-ethoxycarbonylgabapentin	244.081	180.1	46	21	10
	244.081	198.1	46	19	10

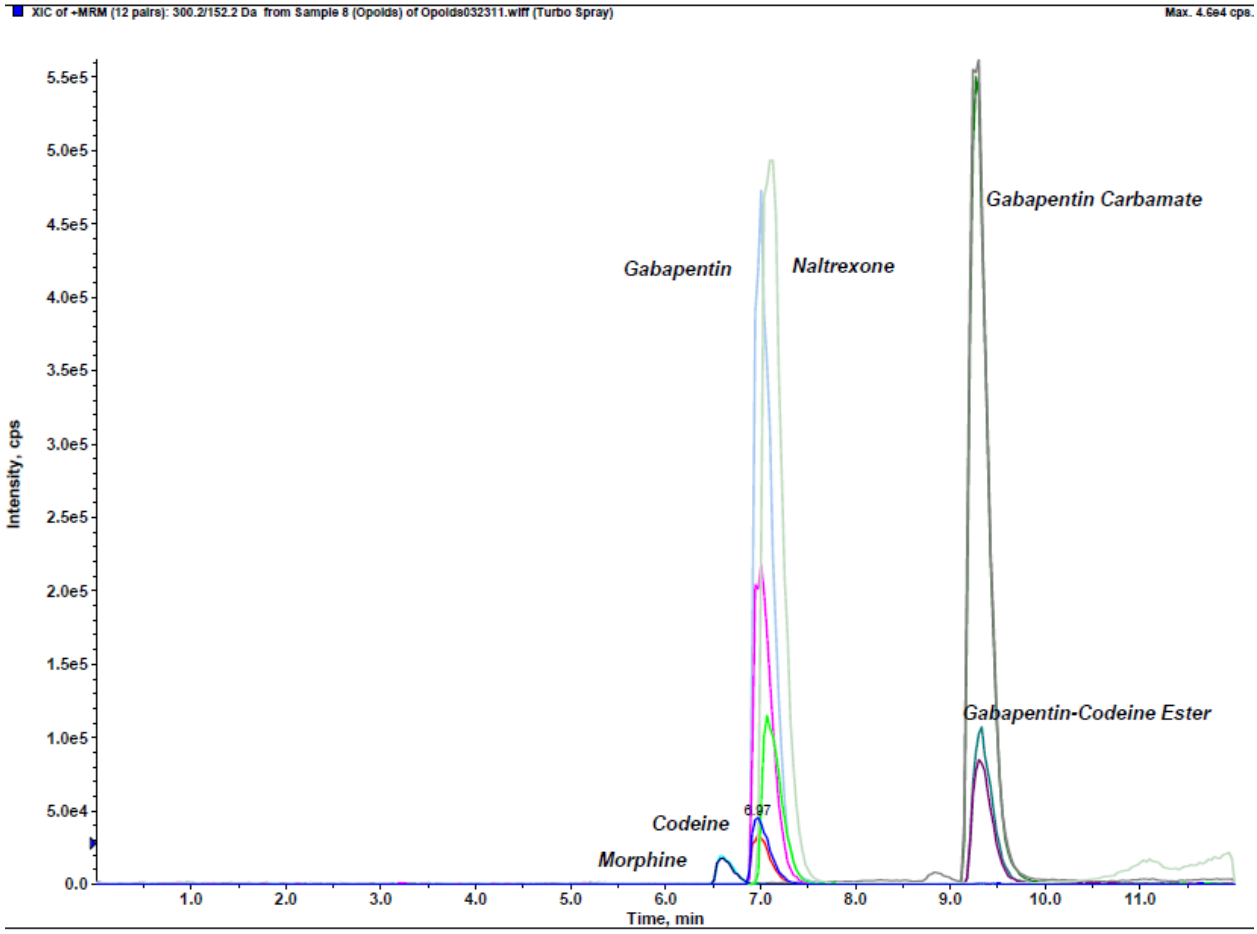

Fig. 5.4: LC-MS/MS chromatograms of morphine, codeine, naltrexone, gabapentin, *N*-ethoxycarbonylgabapentin (gabapentin carbamate), and CG-4 codrug.

5.6.3 Plasma Pharmacokinetics

15% solution of PEG-400 in saline was used as the vehicle. The CG-4 codrug was dissolved in the vehicle and filtered through a 0.2-µm filter. The animals were administered with 12.5 and 25 mg/kg oral doses and 1 mg/kg iv dose. Blood samples (0.2 mL) were obtained at 5, 15, 30 min, 1, 2, 4, 6, 9, 10, and 24 hrs after oral dosing and at 5, 15, 30 min, 1, 2, 3, 5, 7, and 9 hrs after iv dosing. The withdrawn blood was replaced with heparinized saline (0.2 mL). Blood samples were centrifuged at 1200 g for 15 min, and the plasma was separated. The separated plasma was frozen immediately on dry-ice and stored at −80 °C prior to analysis.

5.6.4 Standard Curve and Quality Control Validation Solutions

Stock solutions of the analytes and internal standard (naltrexone) were prepared in methanol. Two stock solutions were prepared; one for generating the standard curve, and a second one for quality control (QC) and method validation. A standard curve with eight points was prepared for the analysis of unknown samples. Standard curve samples were prepared by spiking blank plasma with working solutions of all the different analytes. Calibration curves were obtained using quadratic least-squares regression of AUC ratio (analyte peak AUC/internal standard peak AUC) *versus* drug concentrations. The amounts of codrug, or parent drugs, were then determined. Three quality control samples with different concentrations were prepared to check the sensitivity of the instrument. The three concentrations chosen were: one towards the higher end of the standard curve concentrations, one towards the middle, and the third one towards the lower end of the standard curve concentrations.

Table 5.3: Linear ranges of the analytes in standard curves.

Analyte	Linear Range	R^2
Morphine	0.02-10 µM	0.9998
Codeine	0.005-10 µM	0.9998
Gabapentin	0.1-10 µM	0.9961
N-ethoxycarbonylgabapentin	0.01-10 µM	0.9970
CG-4	0.005-10 µM	0.9971

5.6.5 Extraction Procedure

To isolate the analytes from plasma, 125 µL of plasma was transferred to polypropylene tubes to which 50 µL of working internal standard solution was added followed by vortexing for 1 min. 700 µL of acetonitrile was added for deproteinization. The samples were then centrifuged for 15 min at 8000 rpm. The supernatant was transferred into silylated micro-serts and evaporated to dryness under nitrogen gas at 37 °C. Following drying, the residue was dissolved in 50 µl of mobile phase by vortexing for 1min; 10 µl of the sample was then injected onto the LC-MS/MS unit.

5.6.6 Assay Validation

Blank plasma samples were extracted and analyzed by reverse phase HPLC for potential interfering peaks within the range of the retention time for analytes and the internal standard, naltrexone.

5.6.7 Results

The mean concentration versus time profiles for 12.5 and 25 mg/kg oral doses and 1 mg/kg iv dose of the codrug are shown in Figs. 6.5, 6.6, and 6.7. It can be noticed that in all of the oral and iv doses, the *N*-ethoxycarbonylgabapentin-codeine codrug (CG-4) is hydrolysed to codeine and *N*-ethoxycarbonylgabapentin (a prodrug of gabapentin). The rate of hydrolysis of the ester linkage joining the two parent drugs is slow, and the hydrolysis is not complete, as it can be noticed that at all time points CG-4 codrug is present in the plasma. These data also show a prolonged release of the parent drugs from the codrug over time. It can further be observed that the hydrolysis of the pro-moiety in the *N*-ethoxycarbonylgabapentin product is very slow and the concentration of gabapentin observed in the plasma is low. Along with the codrug, codeine, *N*-ethoxycarbonylgabapentin, and gabapentin, presence of morphine can also be observed in the plasma samples from orally dosed rats. It has already been reported in literature that in the liver codeine is metabolized to morphine to some extent (Thorn, 2009). Morphine was not observed in the plasma samples of the rats that had been administered codrug via the iv route since the codrug and codeine do not get exposed to the liver enzymes.

The pharmacokinetic parameters for codeine, *N*-ethoxycarbonylgabapentin, gabapentin, CG-4 codrug, and morphine are listed in Table 6.4. Following the oral administration of 25 and 12.5 mg/kg doses of codrug CG-4, plasma concentration of the codrug reached a maximum within 3 hours for both oral doses. Plasma concentrations of codeine, *N*-ethoxycarbonylgabapentin, gabapentin, and morphine reached the maxima at a later time, due to slow hydrolysis of the ester and the even slower hydrolysis of the carbamate moiety. The data clearly show a dose-dependent relationship, since the AUC for the codrug, as well as for the parent drugs, increases with increasing doses of codrug.

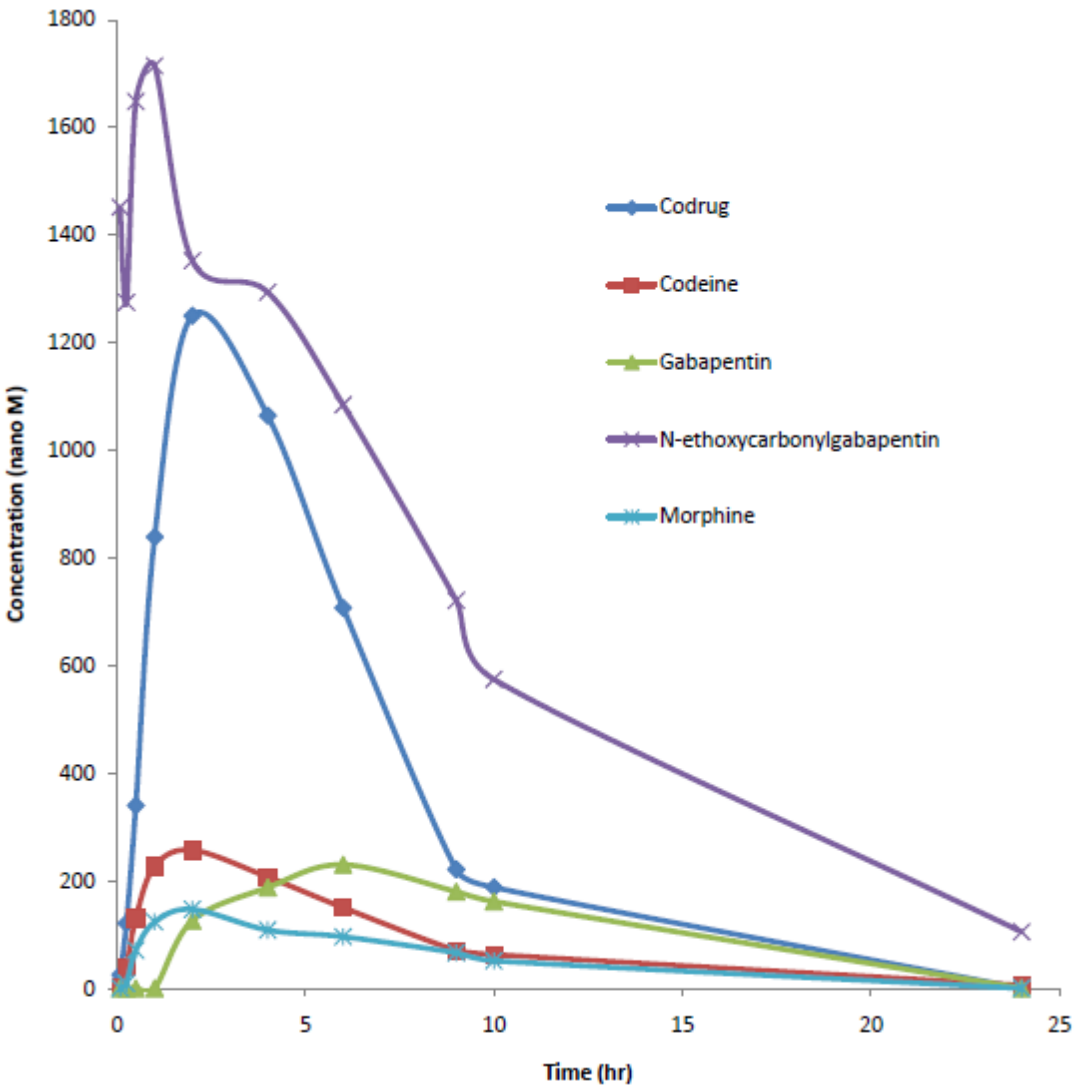

Fig. 5.5: Mean concentrations of the analytes versus time plot after administration of 25 mg/kg oral dose of CG-4 codrug.

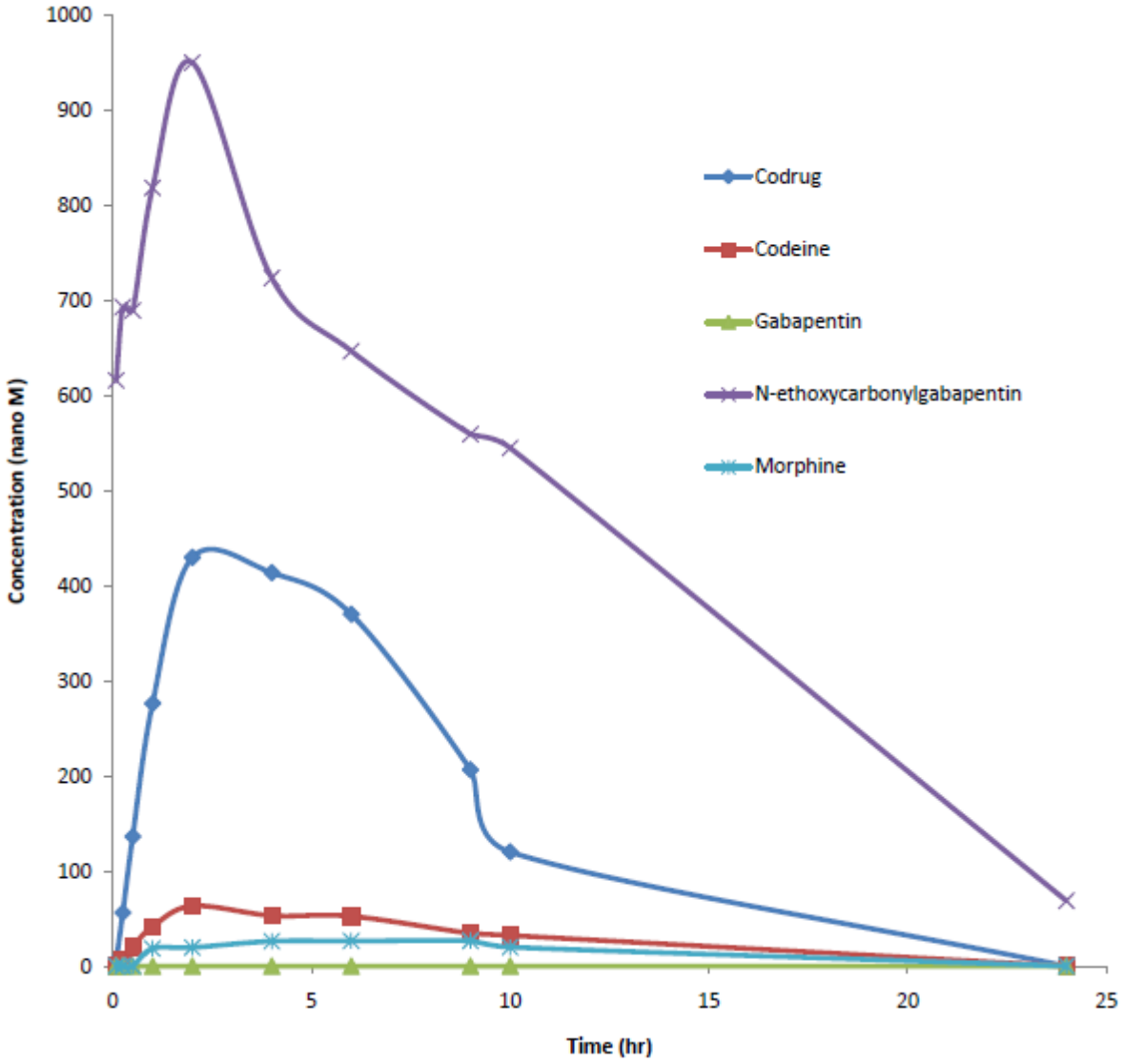

Fig. 5.6: Mean concentrations of the analytes versus time plot after administration of 12.5 mg/kg oral dose of CG-4 codrug.

Table 5.4: Pharmacokinetic parameters of the codrug and parent drugs.

Analyte	Dose (mg/kg)	AUC (hr*mg/mL)	T_{max} (hr)	C_{max} (mg/mL)	$T_{1/2}$ (hr)
CG-4 Codrug	25	3.72 ± 1.15	2.67 ± 0.94	0.71 ± 0.09	1.88 ± 0.86
	12.5	1.65 ± 0.14	3.00 ± 2.16	0.24 ± 0.02	3.62 ± 2.50
Codeine	25	0.58 ± 0.09	2.67 ± 0.94	0.08 ± 0.01	3.85 ± 1.11
	12.5	0.14 ± 0.02	3.33 ± 1.89	0.020 ± 0.003	8.88 ± 7.08
N-ethoxycarbonylgabapentin	25	3.93 ± 0.64	2.98 ± 1.76	0.67 ± 0.26	5.40 ± 0.71
	12.5	2.47 ± 0.83	4.08 ± 2.44	0.26 ± 0.04	5.75 ± 0.48
Gabapentin	25	0.28 ± 0.06	7.00 ± 1.41	0.04 ± 0.01	4.65 ± 2.67
	12.5				
Morphine	25	0.27 ± 0.03	2.67 ± 0.94	0.04 ± 0.01	3.73 ± 0.82
	12.5	0.07 ± 0.01	8.33 ± 1.70	0.0102 ± 0.0004	4.48 ± 2.91

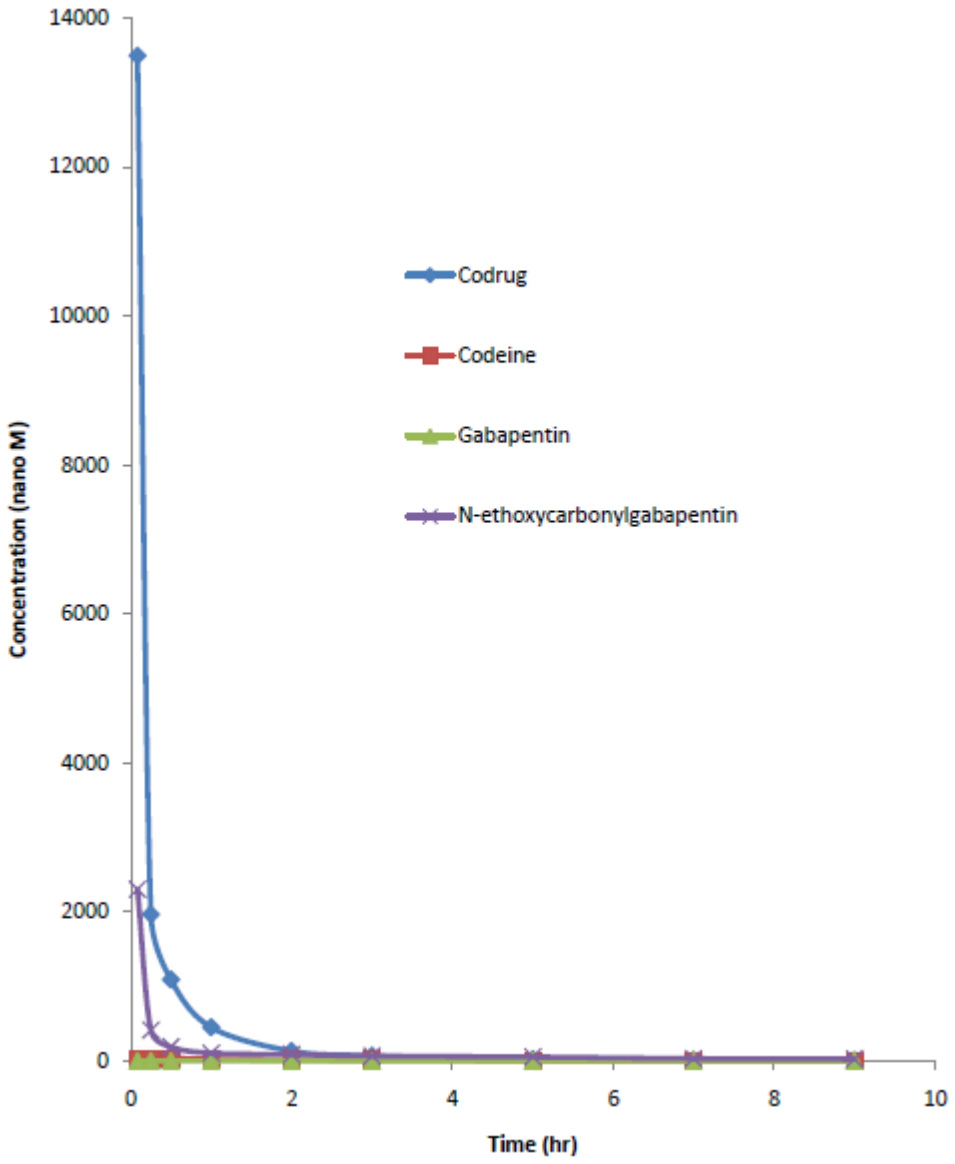

Fig. 5.7: Mean concentrations of the analytes versus time plot after administration of 1 mg/kg i.v. dose of CG-4 codrug.

5.6.8 Bioavailability

Bioavailabilities of codeine and gabapentin in rats are already reported in literature. Codeine has an oral bioavailability of 2.9 ± 1.4% (Holtman et al., 2006) and gabapentin has a dose-dependent oral bioavailability (Bockbrader et al., 2010). The oral bioavailability in rats after administration of gabapentin HCl salt was determined (Cundy et al., 2004) to be 83.8 ± 10.1 % at low dose (25 mg/kg) but decreased significantly to

47.5 ± 7.72 % at 200 mg/kg dose. This is explained by the saturation of the active transport pathway responsible for the absorption of gabapentin (Cundy et al., 2004). The clinical pharmacokinetics of gabapentin has also been studied in healthy volunteers and patients with epilepsy. Gabapentin oral bioavailability was found to be dose-dependent in humans and decreases from an average of 60% at a 300 mg dose to about 35% or less at doses used to treat neuropathic pain (Eckhardt et al., 2000). The reason for the decrease in oral bioavailability with increasing dose is believed to be the same as observed in rats, i.e. saturation of absorption pathways. The absorption pathway for gabapentin apparently achieves saturation at doses normally used to treat neuropathic pain. As a consequence, the plasma concentration of gabapentin in patients receiving Neurontin (brand name of gabapentin in the United States) is not dose-proportional and thus might not reach therapeutically useful levels in many patients. After oral absorption, gabapentin is excreted in the urine without significant metabolism. The plasma half-life of gabapentin in humans is relatively short, necessitating three to four times administration of gabapentin per day (Eckhardt et al., 2000). It has been shown that dosing regimens requiring three to four doses per day may lead to significant noncompliance in patients with epilepsy (Eckhardt et al., 2000). Thus a more prolonged, stable exposure to gabapentin will provide several clinical benefits, including greater efficacy and prolonged duration of action.

The half-life of gabapentin in rats after oral dosing varies from 1.9 hrs for a dose of 25 mg/kg to 2.6 hrs for a dose of 200 mg/kg (Cundy et al., 2004). The half-life of gabapentin was found to be 4.7 hrs after orally administering the CG-4 codrug at a dose of 25 mg/kg (8.2 mg equivalent gabapentin/kg). Thus delivering gabapentin in the form of the CG-4 codrug significantly increases the half-life of gabapentin. Therefore, the codrug strategy appears to be a way to achieve a more prolonged exposure of gabapentin to patients and consequently a less frequent dosing regimen. Calculation of the oral bioavailability of the CG-4 codrug is not straight-forward because of the time-dependent hydrolysis of the codrug to the parent compounds in the plasma. Thus, two bioavailability values for the codrug can be calculated, i.e. the “actual” codrug bioavailability, and the “total” codrug bioavailability. The actual codrug bioavailability is based on the amount of actual codrug present in the plasma; whereas the total codrug bioavailability is calculated

assuming no hydrolysis of the codrug has taken place in the plasma. The total bioavailability value represents an approximation of the total amount of the codrug entering the systemic circulation after oral dosing. The actual codrug bioavailability was calculated to be 5.37 ± 1.45 %, and the total codrug bioavailability was found to be 16.32 ± 3.85 %. It should be noted that the total codrug bioavailabilty value may be underestimated, since the clearance parameters are not taken into account for the parent drugs. Since the actual and total codrug bioavailability is higher than the bioavailability of codeine after oral administration, this shows that a greater amount of codeine can be delivered orally in the form of the CG-4 codrug than codeine itself. The bioavailability of CG-4 codrug does not exceed the oral bioavailability of gabapentin. Thus more gabapentin cannot be delivered by utilizing this codrug strategy. By administering gabapentin in the form of the CG-4 codrug will increase the half-life of gabapentin. Thus the codrug strategy will cause prolong release of gabapentin and patients will need less frequent dosing of the codrug to maintain therapeutic level of gabapentin in plasma. Thus the frequent dosing regimen of gabapenting might be made simpler and patient compliance can be improved via a codrug strategy.

Copyright © Ujjwal Chakraborty 2012

Chapter 6

Summary

6.1 Introduction

There is an ongoing need for analgesic medications that are able to provide high efficacy pain relief and covering broader ranges of pain while providing more favorable pharmacokinetics and reducing the possibility of undesirable side effects. Enhancement of the analgesic effect of opioids when administered with *S*-(-)-nornicotine /ketamine or norketamine/gabapentin has been previously described and is well known in literature (see Chapter 1 for references). However, appropriate dosing of these analgesic agents to the site of action, e.g., the brain or spinal column, can be difficult because of their differential pharmacokinetics. Therefore, in the present dissertation, a codrug strategy is presented for orally administering opioids concomitantly with either nicotinic receptor agonists, NMDA receptor antagonists, or anticonvulsants, to provide a more favorable pharmacokinetic and analgesic profile than would be attainable by administering equimolar amounts of the parent drugs as a physical mixture.

Codrugs are designed to overcome various barriers to drug formulation and delivery, such as poor or extreme aqueous solubility, chemical instability, insufficient absorption after oral administration, rapid pre-systemic metabolism, inadequate brain penetration, and toxicity and local irritation. The first chapter in this dissertation demonstrates the usefulness of the codrug strategy by discussing several reported examples. The codrug strategy is very useful when the physicochemical and/or pharmacokinetic properties of two synergistic drugs are not favorable for delivery as a physical mixture, but can be improved by chemical combination of the two drugs (Crooks et al., 2010).

6.2 Opioid-*S*-(-)-Nornicotine Codrugs

A series of codrugs were synthesized by conjugating an opioid molecule with the nicotinic receptor agonist, *S*-(-)-nornicotine. Codeine, morphine and 3-*O*-acetylmorphine, a prodrug of morphine, were used as the opioid and were conjugated to *S*-(-)-nornicotine via a carbamate linkage moiety. The structures of the five synthesized codrugs in this

series are shown in Fig. 6.1. The codrugs were synthesized by either converting the opioid molecule into an *O*-*p*-nitrophenoxy ester and then reacting the ester with *S*-(-)-nornicotine; or by converting *S*-(-)-nornicotine into its *p*-nitrophenoxy derivative and then reacting this intermediate with the opioid molecule.

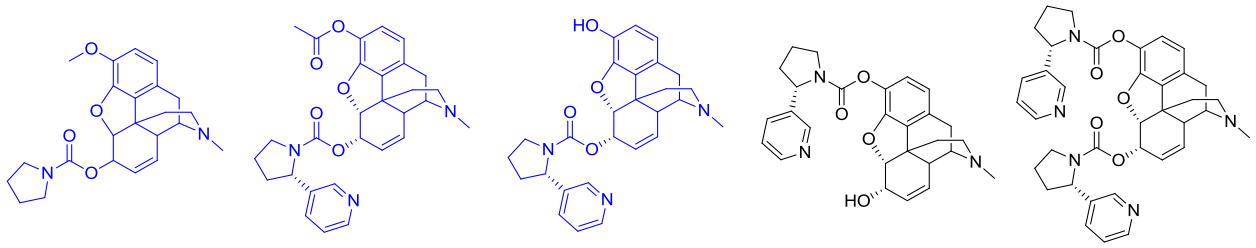

Fig. 6.1: Structures of synthesized opioid-*S*-(-)-nornicotine codrugs.

After their synthesis, some of the codrugs and parent drugs were analyzed for their analgesic actions in different pain models. The codeine-*S*-(-)-nornicotine codrug, codeine, and *S*-(-)-nornicotine were evaluated in the rat tail-flick pain model for their efficacy for treating nociceptive pain, and in the rat paw-pressure (CCI) pain model for their efficacy for treating neuropathic pain. The codrug and the parent drugs were administered orally in separate experiments. All three drug molecules showed analgesic activity to some extent in both pain models. Codeine is known to be effective in treating nociceptive pain (Loeser and Melzack, 1999) and the observed ED_{50} value for this opiate was 41.42 µmol/kg in tail-flick assay. *S*-(-)-Nornicotine was found to have very little efficacy in the tail-flick pain model and showed an ED_{50} of 107.29 µmol/kg in this assay. The codrug of codeine and *S*-(-)-nornicotine was found to be much more effective than either of the parent drugs in tail-flick pain model. The codrug had an ED_{50} of 17.95 µmol/kg. The same trend was observed in CCI pain model. The codrug (ED_{50} = 7.39 µmol/kg) was much more effective compared to either of the parent drugs (codeine, ED_{50} = 45.10 µmol/kg, and *S*-(-)-nornicotine, ED_{50} = 114.04 µmol/kg).

Another codrug of 3-*O*-acetylmorphine and *S*-(-)-nornicotine was also evaluated in the tail-flick pain model and its activity was also compared with the parent drugs. This codrug was found to be very effective in the pain model for nociceptive pain. ED_{50} values of the codrug and parent drugs were determined from their dose-response curves. The

ED_{50} value of the codrug was found to be 2.99 µmol/kg, which is much lower compared to the parent drugs (3-*O*-acetylmorphine, ED_{50} = 11.00 µmol/kg, and *S*-(-)-nornicotine, ED_{50} = 107.29 µmol/kg).

Thus it was observed that combing an opioid molecule with the nicotinic receptor agonist, *S*-(-)-nornicotine, in a single molecular entity enhanced the analgesic efficacy of both the opioid molecule and *S*-(-)-nornicotine. By utilizing the codrug strategy, the opioid dose can be reduced and the adverse side effects related to opioid therapy may be avoided. Also, the codeine-*S*-(-)-nornicotine codrug was found to be effective in the treatment of neuropathic pain. Opioids are known to have little or no effect in treating neuropathic pain (Woolf and Mannion, 1999). Thus, administering an opioid with *S*-(-)-nornicotine in the form of a codrug may be useful in treating neuropathic pain.

After synthesis and assay in the pain models, the stabilities of the codrugs were analyzed under different enzymatic and nonenzymatic conditions. In the different pain assays discussed in Chapter 3, the oral route was used as the route of administration, and the codrugs showed significant analgesic activity. Orally administered drug molecules experience the harsh conditions of GI tract, encountering encounter strongly acidic, mildly acidic, and basic conditions in different parts of the GI tract (Kern and Di, 2008). Within addition to experiencing acidic and basic environments, orally administered drug molecules also experience a variety of enzymes in GI tract. After the drug molecule is absorbed into systemic circulation (pH 7.4) a variety of hydrolytic enzymes in the plasma can interact with the therapeutic agents. Depending on the molecular weight and polarity of the drug molecule, permeation of the blood-brain barrier may occur and the drug will be taken up into brain, where it can also interact with different CNS enzymes. An ideal codrug should not undergo hydrolysis in the GI tract, and should get absorbed into systemic circulation as a single chemical entity (i.e. the original codrug molecule). In the plasma, the codrug may or may not undergo hydrolysis to produce the parent drugs. If the codrug does not undergo hydrolysis in the plasma to produce the parent drugs, it must undergo hydrolysis at the site of action (i.e. brain, in the case of opioid codrugs), otherwise, it will not have any pharmacological effect. To examine the stability of the codrug molecules, and to determine if the codrug possesses the desired stability

characteristics as described above, the codrug was exposed to the following hydrolytic conditions:

- Aqueous buffers (pH 1.3 to 7.4, 37 ºC)
- Simulated gastric fluid (USP, 37 ºC)
- Simulated intestinal fluid (USP, 37 ºC)
- 80% rat plasma (37 ºC)
- Rat brain homogenate (37 ºC)

Three of the opioid-*S*-(-)-nornicotine codrugs (drawn in the color blue in Fig. 6.1) were analyzed in all of the above hydrolytic conditions. All of the three codrugs showed lack of hydrolysis in buffers at pH 1.3, 5.0, 7.4, and in SGF, and SIF, with the exception of the 3-*O*-acetylmorphine-*S*-(-)-nornicotine codrug. The 3-*O*-acetylmorphine-*S*-(-)-nornicotine codrug underwent fast *O*-deacetylation to produce the morphine-*S*-(-)-nornicotine codrug, however, no carbamate bond cleavage was observed. Thus, it can be predicted that all the analyzed codrugs will be absorbed into the systemic circulation without any hydrolysis to the parent drugs. The stability of the carbamate codrugs in 80% rat plasma and brain homogenate showed that the carbamate linkage was difficult to cleave in plasma, and thus, the codrugs in this series were not substrates for rat plasma esterases, and would likely not cleave hydrolytically to afford the parent drugs. To examine this likelihood, a quick pharmacokinetic study was performed with the 3-*O*-acetylmorphine-*S*-(-)-nornicotine codrug. The codrug was administered orally to rat and blood samples were collected over a 24 hr time period. Plasma samples were analyzed by LC-MS/MS for both codrug and parent drugs. The only analyte observed in the blood samples was the morphine-*S*-(-)-nornicotine codrug; no parent drugs were detected. Thus, it was concluded from both the *in vitro* and *in vivo* studies on the opioid-*S*-(-)-nornicotine codrugs that a carbamate linkage between a secondary amine and an alcohol moiety is too stable and will not be effective in liberating the parent drugs in the plasma. The enzymes present in GI tract, plasma, and brain are not capable of cleaving such a carbamate linkage; thus, even if the codrug entered the CNS it likely would not convert to the parent drugs via carbamate bond hydrolysis. Since the codrug molecules that incorporated an opioid molecule and *S*-(-)-nornicotine did not cleave to produce the respective parent drugs, these drug molecules are better termed drug hybrids rather than codrugs. The

analgesic activity exhibited by two of these “hybrid” drugs can only be explained by the hybrid molecules having significant analgesic activity of their own. Further experiments beyond the scope of this project are required to determine the mechanism of action of these hybrid drugs.

6.3 Opioid-Ketamine and Opioid-Norketamine Codrugs

Three codrugs were synthesized in this series following a similar synthetic strategy. Most pharmaceutical preparations of ketamine utilize the racemic form of the drug. Thus, racemic ketamine and racemic norketamine were used in the synthesis of the codrugs. Consequently, a mixture of diastereomeric codrugs was obtained in each case. *In vitro* stability studies were performed on the codrugs prior to analyzing the codrugs in the different pain models. Since the codeine-ketamine codrug contains a carbamate linkage between a secondary amine and an alcohol, as in the opioid-*S*-(-)-nornicotine codrug structures, a stability study under the different hydrolytic conditions was not performed. From the previous stability studies, it was shown that a carbamate linkage between a secondary amine and an alcohol is not readily hydrolysable in the plasma. Thus, the codeine-ketamine conjugate is an example of a drug hybrid between codeine and ketamine rather than a codrug.

The codeine-norketamine conjugate contains a carbamate linkage between a *primary* amine and a secondary allylic alcohol, whereas the morphine-norketamine codrug contains a carbamate linkage between a primary amine and a phenolic hydroxyl group. These two codrugs were thought to be more likely to behave as classical codrugs, since they contain a more labile carbamate linker. A comprehensive stability study was performed on each of these codrugs to determine their hydrolytic profile. Both codrugs were resistant to hydrolysis under both enzymatic and nonenzymatic conditions, as well as in plasma and brain homogenate incubates, and did not afford any detectable amounts of the parent drugs in these *in vitro* stability studies. The reason for this might be the sterically hindered nature of the carbamate moiety as a consequence of the norketamine structure. Thus, it was predicted that in the *in vivo* experiments, the codeine-norketamine and morphine-norketamine conjugates would likely not undergo hydrolytic cleavage to produce the parent drugs. Since the codrugs will not be able generate the parent drugs, as

with the previous series of drug conjugates they are more correctly termed drug hybrids. *In vivo* pain model studies were not performed on the hybrid drugs from this series.

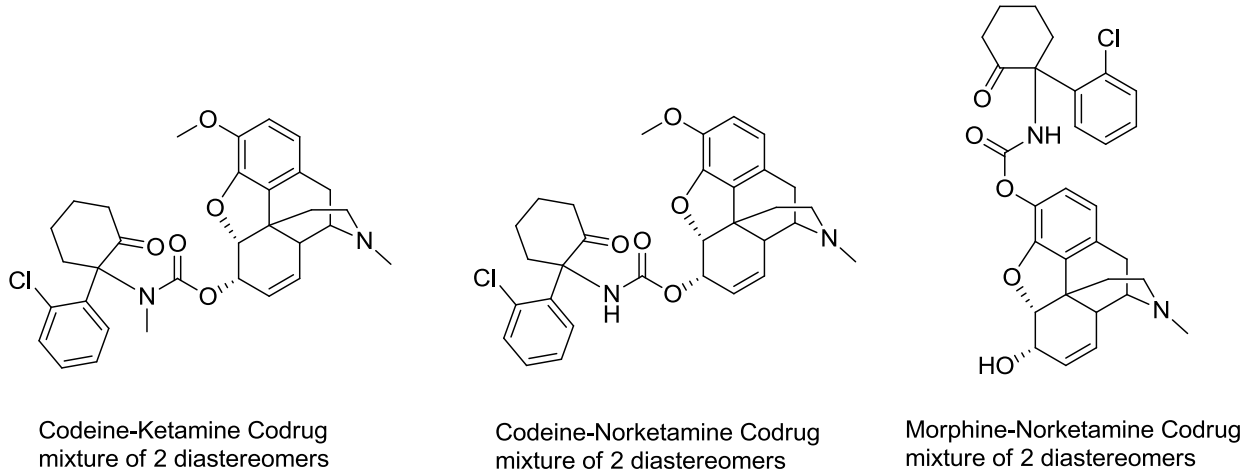

Fig. 6.2: Structures of synthesized opioid-ketamine and opioid-norketamine codrugs.

6.4 Codeine-Gabapentin Codrugs

Four different codrugs were synthesized in this series (Fig. 6.3). Three of the codrugs contained ester linkers, which are known to be more prone to hydrolytic cleavage than carbamate linkers. The CG-1codrug was predicted to be very labile under neutral or slightly basic physiological condition and afford codeine and the cyclic carbamate of gabapentin in the small intestine or plasma, where the pH is 7.4. The stability of the CG-1 codrug was studied in aqueous buffer at physiological (pH 7.4). The codrug was found to be cleaved hydrolytically at physiological pH; the rate constant for hydrolysis was determined to be 0.222 hr^{-1}. Thus, the CG-1 codrug is not an ideal codrug, since it will be partly hydrolyzed in GI tract before being absorbed into systemic circulation. Also, it will not produce gabapentin, but rather the five-membered cyclic carbamate of gabapentin, which might be difficult to hydrolyze to gabapentin by plasma esterases.

CG-2, CG-3, and CG-4 codrugs were studied extensively in different enzymatic and nonenzymatic buffers. Codrugs CG-3 and CG-4 are ester-linked codrugs, while CG-2 is a carbamate- linked codrug. The CG-2 codrug did not cleave under any of the studied hydrolytic conditions. Thus, it can be predicted that the CG-2 codrug will not hydrolyze in plasma to produce the parent drugs, and thus is a hybrid drug.

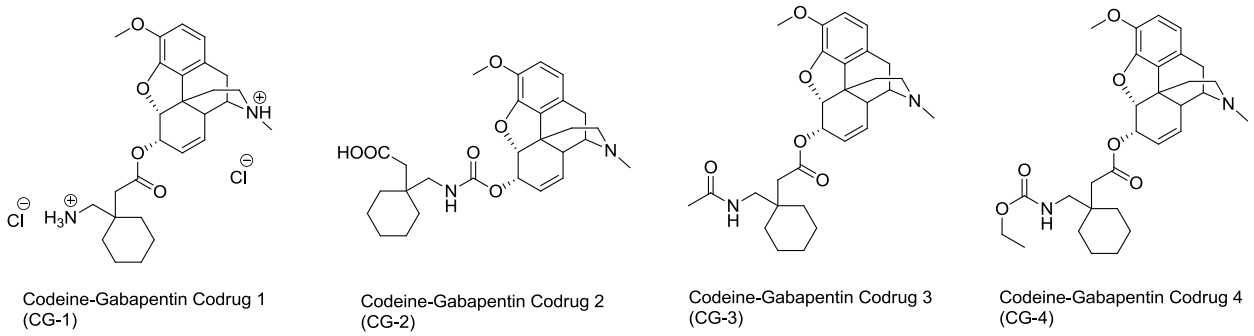

Fig. 6.3: Structures of codeine-gabapentin codrugs.

In the CG-3 and CG-4 codrugs, codeine is linked through an ester moiety with either an amide protected gabapentin molecule or a carbamate protected gabapentin molecule. Stability studies on these two codrugs were performed under the different enzymatic and nonenzymatic conditions previously described. The hydrolytic reactions were monitored by HPLC-DAD assay. Since gabapentin and gabapentin-protected hydrolytic products do not contain a chromophore, only the ester bond cleavage could be followed by HPLC assay. Amide bond hydrolysis in the amide-protected and carbamate-protected gabapentin products could not be followed by HPLC assay. Both the CG-3 and CG-4 codrugs underwent ester bond hydrolysis at pH 1.3 and 7.4, and in SGF and SIF at a very slow rate to produce codeine and gabapentin or protected gabapentin. This is not an ideal rate of hydrolysis for codrugs, but since the rate of hydrolysis was very slow, it can be predicted that most of the codrug will be absorbed through the epithelial lining of the GI tract into the systemic circulation as a single chemical entity. The rates of hydrolysis of the ester linkages were comparatively faster in plasma and brain homogenate compared to the rates in simulated GI fluids. Thus, it can be predicted that after the codrugs are absorbed into the systemic circulation, they will be hydrolyzed in the plasma as well as in brain, to afford codeine and gabapentin or protected gabapentin.

After the *in vitro* stability study was performed, the CG-3 codrug was evaluated *in vivo* in the rat to determine whether the codrug is hydrolyzed to the parent drugs codeine and gabapentin in the plasma. Codrug CG-3 was administered orally to rats and blood samples were collected over a time period of 24 hrs. The blood samples were analyzed by LC-MS/MS assay. The only analytes detected in plasma samples of the rats were

codeine, CG-3 codrug and *N*-acetylgabapentin; no gabapentin parent drug was detected. It was concluded that the ester linkages are labile enough to be hydrolyzed in the plasma, however, amide bonds that incorporate the primary amino group of gabapentin do not get hydrolyzed to gabapentin. Thus CG-3 codrug was not studied in relevant rat pain models.

The pharmacokinetic profile of the CG-4 codrug was evaluated in the rat after oral administration. Rat plasma concentrations of the CG-4 codrug were determined after oral and i.v. administration utilizing an LC-MS/MS analytical methodology. Several groups have reported the low bioavailability of codeine (4 to 8%) after oral administration in rats, due to poor absorption from the gastrointestinal tract (Shah and Mason, 1990; Holtman et al., 2006). The oral bioavailability of gabapentin varies from 83.8% to 47.5% (Eckhardt et al., 2000), and the bioavailability decreases with increasing dose. Gabapentin has a shorter half-life ranging from 1.9 to 2.6 hours (Cundy et al., 2004). Because of shorter half-life value, repeated dosing is required to maintain therapeutically significant concentrations of gabapentin in the plasma.

The CG-4 codrug, codeine, *N*-ethoxycarbonylgabapentin, gabapentin, and morphine were detected in the plasma of rats that had been administered with the CG-4 codrug via the oral route. The codrug was detected in plasma samples at all time points up to and including 24 hrs. Thus, it can be concluded that ester bond hydrolysis occurs at a slow rate and that the codrug slowly releases codeine and *N*-ethoxycarbonylgabapentin. The *N*-ethoxycarbonylgabapentin product is then slowly hydrolyzed to afford gabapentin. Due to the relatively slow hydrolysis of the ester linkage of the codrug, and the even slower hydrolysis of the carbamate bond of the *N*-ethoxycarbonylgabapentin product, the parent drugs were generated at a slow rate, and were present in plasma for a long period of time. The actual codrug bioavailability was calculated to be 5.37%, and the total codrug bioavailability was found to be 16.32%. The bioavailability of the codrug was much higher compared to the parent drug codeine. Thus, a codrug strategy can be used to effectively improve the bioavailability of codeine. Also, due to the sustained release of codeine from the codrug, the dosing regimen of codeine or another structurally related opioid molecule can be made simpler by having a less frequent dosing of the codrug. However, this codrug strategy did not increase the oral bioavailability of gabapentin. Nevertheless, due to very slow release of gabapentin from the codrug, its half-life was

increased to 4.7 hrs. Thus, the codrug is effectively acting as a sustained release chemical delivery system for gabapentin, and the dosing regimen of gabapentin may be made less frequent by utilizing a codrug strategy. Interestingly, a significant amount of morphine was also detected in the plasma samples of rats after oral administration of the CG-4 codrug. It is reported in literature that codeine is metabolized to morphine in liver. Some investigators believe that the analgesic activity of codeine is mainly due to its bioconversion to morphine, since codeine itself has little or no analgesic action when administered by iv injection to rats (Trescot et al., 2008). Generation of morphine in the plasma after oral administration of the CG-4 codrug would definitely contribute towards the analgesic efficacy of this codrug.

Finally, the analgesic action of the CG-4 codrug was determined in the rat tail-flick model after oral administration of the codrug. Tail-flick latencies of codeine were determined, and from the dose response curve ED_{50} value of codeine was calculated to be 41.42 µmol/kg. It has been previously reported in literature that gabapentin alone has no intrinsic effect in the rat tail flick test. Thus, gabapentin was not tested for its efficacy in this pain model. Three doses (6.25, 12.5, and 25 mg/kg) of codeine-*N*-ethoxycarbonylgabapentin codrug (CG-4) were administered orally and tail flick latencies were experimentally determined. A dose of an equimolar physical mixture of codeine and gabapentin equivalent to 25 mg/kg dose of the CG-4 codrug was also administered orally, and the time response curve for rat tail flick test was determined. The CG-4 codrug was found to be more effective than codeine in the tail-flick pain model with ED_{50} value of 19.17 µmol/kg. Thus, it can be concluded that the efficacy of codeine or another structurally related opioid can be improved by combining it with gabapentin in a single codrug molecule. This strategy can be utilized to reduce the opioid dose while treating pain, and the adverse side effects of opioids may be avoided. It was also found that a 25 mg/kg oral dose of the CG-4 codrug was more effective than the equivalent oral dose of a physical mixture of codeine and gabapentin. Thus the codrug strategy is more effective in treating pain than a drug combination strategy.

Copyright © Ujjwal Chakraborty 2012

References:

Abdel-Azeem AZ, Abdel-Hafez AA, El-Karamany GS, Farag HH (2009) Chlorzoxazone esters of some non-steroidal anti-inflammatory (NSAI) carboxylic acids as mutual prodrugs: design, synthesis, pharmacological investigations and docking studies. Bio Med Chem 17: 3665-3670.

Aggarwal SK, Gogu SR, Rangan SRS, Agrawal KC (1990) Sunthesis and biological evaluation of prodrugs of Zidovudine. J Med Chem 33: 1505-1510.

Algvere P, Bill A (1981) Effects of vitrectomy and phakectomy on the drainage of the vitreous compartment. Albrecht von Graefe's. Arch Clin Exp Ophthalmol 216: 253–260.

Anderson GW, McGregor AC (1957) *t*-Butyloxycarbonylamino acids and their use in peptide synthesis. J Am Chem Soc 79:6180-6183.

Armstrong SC, Cozza KL (2003) Pharmacokinetic drug interactions of morphine, codeine and their derivatives: theory and clinical reality. Psychosomatics 44: 515-520.

Arneric SP, Holladay M, Williams M (2007) Neuronal nicotinic receptors: a perspective on two decades of drug discovery research. Biochem Pharmacol 74: 1092-1101.

Ascher JA, Cole JO, Colin JN, Feighner JP, Ferris RM, Fibiger HC, Golden RN, Martin P, Potter WZ, Richelson E (1995) Bupropion: a review of its mechanism of antidepressant activity. J Clin Psychiatry 56: 395–401.

Ashton P, Crooks PA, Cynkowski T, Cynkowska G, Riggs RM, Guo H (2000) Means to Achieve Sustained Release of Synergistic Drugs By Conjugation. U.S. Patent No. 6,051,576, April 18th, 2000.

Azad Khan AK, Guthrie G, Johnson HH, Truelove SC, Williamson D (1983) Tissue and bacterial splitting of sulphasalazine. Clin Sci 64: 349-354.

Ballantyne JC (2006) Opioids for chronic nonterminal pain. Southern Med J 99: 1245-1253.

Ballantyne JC, Mao J (2003) Opioid therapy for chronic pain. N Eng J Med 349: 1943-1953.

Baltzer B, Binderup E, von Daehne W, Godtfredsen WO, Hansen K, Nielsen B, Sørensen H, Vangedal S. (1980) Mutual pro-drugs of beta-lactam antibiotics and beta-lactamase inhibitors. J Antibiot 10: 1183–1192.

Balzarini J, De Clercq E (1999) Nucleoside and nonnucleoside reverse transcriptase inhibitors active against HIV. Textbook of AIDS Medicine; Merigan, T. C., Bartlett, J. G., Bolognesi, D., Eds. Williams and Wilkings, Baltimore, 815-847.

Bardo MT, Green TA, Crooks PA, Dwoskin LP (1999) Nornicotine is self administered intravenously by rats. Psychophrmacology 146: 290-296.

Beales DL, Burry HC, Graham R (1972) Comparison of aspirin and benorylate in the treatment of rheumatoid disease. Brit Med J 2: 483-485.

Bennett GJ (1993) An animal model of neuropathic pain: a review. Muscle and Nerve 16: 1040-1048.

Bennett GJ, Xie YK (1988) A peripheral neuropathy in rat that produces disorders of pain sensation like those seen in man. Pain 33:87-107.

Bennett MI, Simpson KH (2004) Gabapentin in treatment of neuropathic pain. Pallitative Med 18: 5-11.

Benyamin R, Trescot AM, Datta S, Buenaventura R, Adlaka R, Sehgal N, Glaser SE, Vallejo R (2008) Opioid complications and side effects. Pain Physician 11: S105-S120.

Berde C, Nurko M (2008) Opioids side effects-mechanism-based therapy. N Eng J Med 358: 2400-2402.

Berger AS; Cheng CK; Pearson PA, Ashton P, Crooks PA, Cynkowski T, Cynkowska G, Jaffe GJ (1996) Intravitreal sustained release corticosteroid-5-fluorouracil conjugate in

the treatment of experimental proliferative vitreoretinopathy. Invest Ophthalmol Vis Sci 37: 2318–2325.

Berlan J, Giboreau P, Lefeuvre S, Marchand C (1991) Synthese organique sous champ microondes: premier exemple d'activation specifique en phase homogene. Tetrahedron Lett 32: 2363-2366.

Besson JM (1999) The neurobiology of pain. Lancet 353: 1610-1614.

Bidaut-Russell M, Howlett A (1988) Opioid and cannabinoid analgetics both inhibits cyclic AMP production in the rat striatum, in Advances in the biosciences. Pergamom Press, Oxford.

Biewenga GP, Haenen G, Bast A (1997) The pharmacology of the antioxidant lipoic acid. Gen Pharmacol 29: 315–331.

Bloom AS, Dewey WL (1978) A comparison of some pharmacological actions of morphine and Δ^9-Tetrahydrocannabinol in the mouse. Psychopharmacology 57: 1432-2072.

Blumenkranz M, Ophir A, Claflin A (1981). A pharmacological approach to non-neoplastic intraocular proliferation. ARVO Abstracts. Invest Ophthalmol Vis Sci, 200.

Bockbrader HN, Wesche D, Miller R, Chapel S, Janiczek N, Burger P (2010) A comparison of the pharmacokinetics and pharmacodynamics of pregabalin and gabapentin. Clin Pharmacokinet 49: 661-669.

Bolla M, Almirante N, Benedini F (2005) Therapeutic potential of nitrate esters of commonly used drugs. Curr Top in Med Chem 5: 707-720.

Burk RM, Roof MB (1993) Safe and efficient method for conversion of 1,2- and 1,3-diols to cyclic carbonates using triphosgene. Tetrahedron Lett 34:395-398.

Burne K (1986) Comparative pharmacology of non-opioid analgesics. Med Toxicol Suppl 1: 1–9.

Cami-Kobeci G, Neal AP, Bradbury FA, Purington LC, Aceto MD, Harris LS, Lewis JW, Traynor JR, Husbands SR (2009) Mixed κ/μ opioid receptor agonists: the 6β-naltrexamines. J Med Chem 52: 1546-1552.

Campbell JN, Meyer RA (2006) Mechanisms of neuropathic pain. Neuron 52: 77-92

Carr DB, Goudas LC (1999) Acute pain. Lancet 353: 2051-2058.

Cavenagh J, Good P, Ravenscroft P (2006) Neuropathic pain: are we out of the woods yet? Internal Medicine Journal 36: 251-255.

Cheng CK, Berger AS, Pearson PA, Ashton P, Jaffe GJ (1995) Intravitreal sustained-release dexamethasone device in the treatment of experimental uveitis. Invest Ophthalmol Vis Sci 36: 442-453.

Cheng YC, Dutschman GE, Bastow KF, Sarngadharan MG, Ting RYC (1987) HIV reverse transcriptase. General properties and its interactions with nucleoside triphosphate analogues. J Biol Chem 262: 2187-2189.

Chiang CN and Barnett G (1984) Marijuana effect and delta-9-tetrahydrocannabinol plasma level. Clin Pharmacol Ther 6: 234-238.

Chung JM, Kim HK, Chung K (2004) Segmental spinal nerve ligation model of neuropathic pain. Pain Res 99: 35-45.

Cichewicz DL, Martin ZL, Smith FL, Welch SP (1999) Enhancement of μ opioid antinociception by oral Δ^9-Tetrahydrocannabinol: dose-response analysis and receptor identification. J Pharmacol Exp Ther 289: 859–867.

Cichewicz LD, McCarthy EA (2002) Antinociceptive synergy between delta(9)-tetrahydrocannabinol and opioids after oral administration. J Pharmacol Exp Ther 304: 1010-1015.

Coller JK, Christrup LL, Somogyi A (2009) Role of active metabolites in the use of opioids. Eur J Clin Pharmacol 65: 121-139.

Cooper BR, Wang CM, Cox RF, Norton R, Shea V, Ferris RM (1994) Evidence that the acute behavioral and electrophysiological effects of bupropion (Wellbutrin) are mediated by a noradrenergic mechanism. Neuropsychopharmacology 11: 133–141.

Crooks PA, Rivera M (2004) Analgesic uses of *S*-(-)-norketamine. PCT/US2003/036789.

Crooks PA, Dhooper HK, Chakraborty U (2010) Improving the use of Drug Combinations through the Codrug Approach. 'Prodrugs and Targeted Delivery: Towards Better ADME Properties'. Copyright © 2010 WILEY-VCH, ISBN: 978-527-32603-7.

Cundy KC, Branch R, Chernov-Rogan T, Dias T, Estrada T, Hold K, Koller K, Liu X, Mann A, Panuwat M, et al. (2004) XP13512, a novel gabapentin prodrug: I. design, synthesis, enzymatic conversion to gabapentin, and transport by intestinal solute transporters. J Pharmacol Exp Ther 311: 315–323 [1].

Cundy KC, Annamalai T, Bu L, Vera JD, Estrela J, Luo W, Shirsat P, Torneros T, Yao F, Zou J, Barrett RW, Gallop MA (2004) XP13512 [(±)-1-([(α-Isobutanoyloxyethoxy)carbonyl] aminomethyl)-1-cyclohexane acetic acid], a novel gabapentin prodrug: II. improved oral bioavailability, dose proportionality, and colonic absorption compared with gabapentin in rats and monkeys. J Pharmacol Exp Ther 311: 324-333 [2].

D'Amour FE, Smith DL (1941) A method for determining loss of pain sensation. J Pharmacol Exp Ther 72:74-79.

Das N, Dhanawat M, Dash B, Nagarwal RC, Srivastava SK (2010) Codrug: an efficient approach for drug optimization. Euro J Pharm Sci 41: 571-588.

Das KM, Eastwood MA, McManus JPA, Sircus W (1973) Adverse reactions during salicylazosulfapyridine therapy and the relation with drug metabolism and acetylater phenotype. New Engl J Med 289: 491-495.

DeBeer EJ, Johnston CH, Wilson DW (1935) The composition of intestinal secretions. J Biol Chem 108:113-120.

Decker MW, Meyer MD (1999) Therapeutic potential of neuronal nicotinic acetylcholine receptor agonists as novel analgesics. Biochem Pharmacol 58: 917-923.

De Clercq E (1995) Toward improved anti-HIV chemotherapy: therapeutic strategies for intervention with HIV infections. J Med Chem 38: 2491-2517.

De Clercq E (1997) In search of a selective antiviral chemotherapy. Clin Microbiol Rev 10: 674-693.

Dhooper HK, Holtman J, Crooks PA (2008) Preparation of a Synergistic Codrug of Codeine and Δ^9-THC as a Potent Antinociceptive Agent. Twenty Second Annual Meeting and Exposition of the American Association of Pharmaceutical Scientists, November, 2008, Atlanta, GA.

Dingemanse J, Dingemanse SA (2007) Integrated pharmacokinetics and Pharmacodynamics in drug development. Clin Pharmacokinet 46: 713-737.

Eckhardt K, Ammon S, Hofman U, Riebe A, Gugeler N, Mikus G (2000) Gabapentin enhances the analgesic effect of morphine in healthy volunteers. Anesth Analg 91: 185-191.

Epstein DI, Roberts BC, Skinner LL (1997) Nonsulfhydryl-reactive Phenoxyacetic Acids Increase Aqueous Humor Outflow Facility. Invest Ophthalmol Vis Sci 38: 1526-1534.

Fadl TA, Omar FA (1998) Paracetamol (Acetaminophen) esters of some non-steroidal anti-inflammatory carboxylic acids as mutual prodrugs with improved therapeutic index. Inflammopharmacology 6: 143-157.

Fischl MA, Richman DD, Grieco MH, Gottlieb MS, Volberding PA, Laskin OL, Leedom JM, Groopman JE, Mildvan D, Schooley RT, Jackson GG, Durack DT, King D (1987) The efficacy of azidothymidine (AZT) in the treatment of patients with AIDS and AIDS-related complex. A double blind, placebo-controlled trial. N Engl J Med 317: 185-191.

Flores CM (2000) The promise and pitfalls of a nicotinic cholinergic approach to pain management. Pain 88: 1-6.

Flower RD (2003) The development of COX2 inhibitors. Nature Rev 2: 179-189.

Foley KM (2003) Opioids and chronic neuropathic pain. New Eng J Med 384: 1279-1281.

Furman PA, Fyfe JA, St. Clair MH, Weinhold K, Rideout JL, Freeman GA, Nusinoff-Lehrman S, Bolognesi DP, Broder S, Mitsuya H, Barry DW (1986) Phosphorylation of 3'-azido-3'-deoxythymidine and selective interaction of the 5'-triphosphate with HIV reverse transcriptase. Proc Natl Acad Sci U.S.A. 83: 8333-8337.

Gabriel C, Gabriel S, Grant EH, Halstead BSJ, Mingos DMP (1998) Dielectric parameters relevant to microwave dielectric heating. Chem Soc Rev 27: 213-223.

Gairola N, Nagpal D, Dhaneshwar SS, Dhaneshwar SR, Chaturvedi SC (2005) Synthesis, hydrolysis kinetics and pharmacodynamic profile of novel prodrugs of Flurbiprofen. Indian J Pharm Sci 369-373.

Gensler HL, Aickin M, Peng YM, Xu M (1996) Importance of the form of topical vitamin E for prevention of photocarcinogenesis. Nutr Cancer 26: 183– 191.

Ghosheh O, Dwoskin LP, Li WK, Crooks PA (1999) Residence times and half lives of nicotine metabolites in rat brain after acute peripheral administration of [2'-^{14}C]Nicotine. Drug Metab Dispos 27: 1448-1455.

Ghosheh O, Dwoskin LP, Miller DK, Crooks PA (2001) Accumulation of nicotine and its metabolites in rat brain after intermittent or continuous peripheral administration of [2'-^{14}C]Nicotine. Drug Metab Dispos 29: 645-651.

Gilron I, Biederman J, Jhamandas K, Hong M (2003) Gabapentin blocks and reverses antinociceptive morphine tolerance in the rat paw-pressure and tail-flick tests. Anaesthesiology 98: 1288-1292.

Gilron I, Max MB (2005) Combination pharmacotherapy for neuropathic pain: current evidence and future directions. Expert Rev Neurotherapeutics 5:823-830.

Goromaru T, Matsura H, Furuta T, Baba S (1984) Identification of isopropylantipyrine metabolites in rat and man by using stable isotope tracer techniques. Chem Pharm Bull 32: 3179–3186.

Grinberg L, Fibach E, Amer J, Atlas D (2005) *N*-Acetylcysteine amide, a novel cell-permeating thiol, restores cellular glutathione and protects human red blood cells from oxidative stress. Free Radical Biol Med 38: 136–145.

Gulin PO, Rabanal F, Giralt E (2006) Efficient preparation of proline N-carboxyanhydride using polymer supported bases. Org Lett 8; 5385-5388.

Gupta SK, Mahajan A, Tandon V (2004) Gabapentin for the treatment of neuropathic pain. JK Science 6: 113-114.

Haenen G, Bast A (1991) Scavenging of hypochlorous acid by lipoic acid. Biochem Pharmacol 42: 2244–2246.

Hamad, M.O., Kiptoo, P.K., Stinchcomb, A.L., Crooks, P.A. (2006) Synthesis and hydrolytic behavior of two novel tripartate codrugs of naltrexone and 6β-naltrexol with hydroxybupropion as potential alcohol abuse and smoking cessation agents. Bioorgan Med Chem 14: 7051-7061.

Hammell DC, Hamad M, Vaddi HK, Crooks PA, Stinchcomb AL (2004) A duplex "Gemini" prodrug of naltrexone for transdermal delivery. J Control Release 97: 283-90.

Hammond CL, Lee TK, Ballatori N (2001) Novel roles for glutathione in gene expression, cell death, and membrane transport of organic solutes. J Hepatol 34: 946–954.

Hao Z, Cooney DA, Hartman NR, Perno CF, Fridland A, De Vico AL, Sarngadharan MG, Broder S, Johns DG (1988) Factors determining the activity of 2',3'-dideoxynucleosides in suppressing human immunodeficiency virus *in vitro*. Mol Pharmacol 34: 431-435.

Hargreaves K, Dubner R, Brown F, Flores C, Joris J (1988) A new and sensitive method for measuring thermal nociception in cutaneous hyperalgesia. Pain 32: 77-88.

Hartley S, Wise R. (1982) A three-way crossover study to compare the pharmacokinetics and acceptability of sultamicillin at two dose levels with that of ampicillin. J Antimicrob Chemother 10: 49-55.

Hocking G, Cousins MJ (2003) Ketamine in chronic pain management: an evidence based review. Anesth Analg 97: 1730-1739.

Hogan Q (2002) Animal Pain Models. Region Anesth and Pain M 27:385-401.

Hohmann AG, Briley EM, Miles H (1999) Pre- and postsynaptic distribution of cannabinoid and mu opioid receptors in rat spinal cord. Brain Res 822:17-25.

Holladay MW, Dart MJ, Lynch JK (1997) Neuronal nicotinic acetycholine receptors as targets for drug discovery. J Med Chem 40: 4169-4190.

Horwitz LD (2003) Bucillamine: a potent thiol donor with multiple clinical applications. Cardiovasc Drug Rev 21: 77–90.

Holtman JR, Crooks PA, Dhooper HK (2006) Novel synergistic opioid-cannabinoid codrug for pain management. US Patent 2008/0176885A1.

Holtman JR, Crooks PA, Johnson-Hardy JK, Hojomat M, Kleven M, Wala EP (2008) Effects of norketamine enantiomers in rodent models of persistent pain. Pharmacol Biochem and Behav 90: 676-685 [1].

Holtman JR, Crooks PA, Johnson-Hardy JK, Wala EP (2008) Interaction between morphine and norketamine enantiomers in rodent models of nociception. Pharmacol Biochem and Behav 90: 769-777 [2].

Holtman JR, Crooks PA, Johnson-Hardy JK, Wala EP (2010) The analgesic and toxic effects of nornicotine enantiomers alone and in interaction with morphine in rodent models of acute and persistent pain. Pharmacol, Biochem and Behav 94:352-362.

Howard M, Al-Ghananeem A, Crooks PA (2007) A novel chemical delivery system comprising an ocular sustained release formulation of a 3α, 17α, 21-trihydroxy-5β-pregnan-20-one-BIS-5-Flouroucil codrug. Drug Dev Ind Pharm 33: 677-682.

Howard M, Al-Ghananeem A, Crooks PA (2007) A novel chemical delivery system comprising an ocular sustained release formulation of a 3α, 17α, 21-trihydroxy-5β-pregnan-20-one-BIS-5-Fluoroucil codrug. Drug Dev Ind Pharm 33: 677-682.

Howard-Sparks M, Al-Ghananeem AM, Pearson AP, Crooks PA (2005) Evaluation of $O^{3\alpha}$-, O^{21}-Di-(N^{1}-methyloxycarbonyl-2,4-dioxo-5-fluoropyrimidinyl)17α-hydroxy-5β-pregnan-20-one as a novel potential antiangiogenic codrug. J Enzym Inhib Med Ch 20: 417–428.

Hoz ADL, Ortiz AD, Moreno A (2005) Microwave in organic synthesis. Thermal and non-thermal microwave effects. Chem Soc Rev 34: 164-178.

Hughes J, Smith T, Kosterlitz H, Fothergill L, Morgan B, Morris H (1975) Identification of two related pentapeptides from the brain with potent opiate agonist activity. Nature 258: 577-580.

Jacob J, Chia LHL, Boey FYC (1995) Thermal and non-thermal interaction of microwave radiation with materials. J Mat Sci 30: 5321-5327.

Joshi KS, Honore P (2006) Animal models of pain for drug discovery. Expert Opin Drug Dis 14:323-334.

Julius D, Basbaum AI (2001) Molecular mechanisms of nociception. Nature 413: 203-210.

Kalso E (2005) Improving opioid effectiveness: from ideas to evidence. Euro J of Pain 9: 131-135.

Kern EH, Di L (2008) Drug-like properties: concepts, structure design and methods. Elsevier, Oxford.

Kiptoo PK, Hamad MO, Crooks PA, Stinchcomb AL (2006) Enhancement of transdermal delivery of 6-beta-naltrexol via a codrug linked to hydroxybupropion. J Control Release 113: 137–145.

Kiptoo PK, Paudel KS, Hammell DC, Hamad MO, Crooks PA, Stinchcomb AL (2008) *In vivo* evaluation of a transdermal codrug of 6-β-naltrexol linked to hydroxybupropion in hairless guinea pigs. J Pharm Sci 33: 371–379.

Klecker RW, Collins JM, Yarchoan R, Thomas R, Jenkins JF, Broder S, Meyers CE (1987) Plasma and cerebrospinal fluid pharmacokinetics of 3'-azido-3'-deoxythymidine: A Novel pyrimidine analog with potential application for the treatment of patients with AIDS and related diseases. Clin Pharmacol Ther 41: 407-412.

Kurz A, Sessler DI (2003) Opioid-induced bowel dysfunction: pathophysiology and potential new therapies. Drugs 63: 649-671.

Lampen P, Pittermann W, Heise HM, Schmitt M, Jungmann H, Kietzmann M (2003) Penetration studies of vitamin E acetate applied from cosmetic formulations to the stratum corneum of an in vitro model using quantification by tape stripping, UV spectroscopy, and HPLC. J Cosmet Sci 54: 119– 131.

Leppanen J, Huuskonen J, Nevalainen T, Gynther J, Taipale H, Jarvinen T (2002) Design and synthesis of a novel L-Dopa–entacapone codrug. J Med Chem 45: 1379-1382.

Lew A, Krutzik PO, Hart ME, Chamberlin AR (2002) Increasing rates of reactions: microwave assisted organic synthesis for combinatorial chemistry. J Comb Chem 4: 95-105.

Lipinski CA, Lombardo F, Dominy BW, Feeney PJ (2001) Experimental and computational approaches to estimate solubility and permeability in drug discovery and development settings. Adv Drug Deliver Rev 46: 3–26.

Lippiello PM, Bencherif M, Hauser TA, Jordan KG, Letchworth SR, Mazurov AA (2007) Nicotinic receptors as targets for therapeutic discovery. Expert Opin Drug Discov 2: 1185-1203.

Loeser JD, Melzack R (1999) Pain: an overview. Lancet 353: 1607-1609.

Loh TP, Zhou JR, Li XR, Sim KY (1999) A novel reductive aminocyclization for the syntheses of chiral pyrrolidines: stereoselective syntheses of (*S*)-nornicotine and 2-(2'-pyrrolidyl)-pyridines. Tetrahedron Lett 40: 7847-7850.

Lussier D, Huskey AG, Portenoy RK (2004) Adjuvant analgesics in cancer pain management. The Oncologist 9:571-591.

Machemer R (1988) Proliferative vitreoretinopathy (PVR): a personal account of its pathogenesis and treatment. Invest Ophthalmol Vis Sci 29: 1771-1783.

Mao J (1999) NMDA and opioid receptors: their interactions in antinociception, tolerance and neuroplasticity. Brain Res Rev 30: 289-304.

Mao J, Chen LL (2006) Gabapentin in pain management. Anesth Analg 91: 680-687.

Martin MW, Newcomb J, Nunes JJ, McGowan DC, Armistead DM, Boucher C, Buchanan JL, Buckner W, Chai L, Elbaum D, Epstein LF, Faust T, Flynn S, Gallant P, Gore A, Gu Y, Hsieh F, Huang X, Lee JH, Metz D, Middleton D, Mohn D, Morgenstern K, Morrison MJ, Novak PM, Oliveira-dos-Santos A, Powers D, Rose P, Schneider S, Sell S, Tudor Y, Turci SM, Welcher AA, White RD, Zack D, Zhao H, Zhu L, Napier XS, Power E (2006) Novel 2-aminopyrimidine carbamates as potent and orally active inhibitors of Lck: synthesis, SAR, and in vivo anti-inflammatory activity. J Med Chem 49:4981-4991.

Martı´nez M, Martı´nez N, Herna´ndez AI, Ferra´ndiz ML (1999) Hypothesis: Can *N*-acetylcysteine be beneficial in Parkinson's disease? Life Sci 64: 1253–1257.

McCamley K, Ripper JA, Singer RD, Scammells PJ (2003) Efficient N-demethylation of opiate alkaloids using modified nonclassical Polonovski reaction. J Org Chem 68: 9847-9850.

McCartney CJL, Sinha A, Katz J (2004) A qualitative systematic review of the role of N-methyl-D-aspartate receptor antagonists in preventive analgesia. Anesth Analg 98: 1385-1400.

McQuay H (1999) Opioids in pain management. Lancet 353: 2229-2232.

Mehvar R (2004) The relation among pharmacokinetic parameters: effect of altered kinetics on drug plasma concentration-time profile. Am J Pharm Educ 68: 1-9.

Melamed S, Kotas-Neumann R, Barak A, Epstein DL (1992) The affect of intracamerally injected ethacrynic acid on intraocular pressure in patients with glucoma. Am J Ophthalmol 113: 508-512.

Melnikova I (2010) Pain market. Nature Rev 9: 589-590.

Melzack R, Wall PD (1965) Pain mechanisms: a new theory. Science Wash 50: 971-979.

Merksey H (1979) Pain terms: a list with definitions and notes on usage; recommended by the IASP subcommittee on taxonomy. Pain 6: 249-252.

Meyers BE, Moonka DK, Davis RH (1979) the effect of selected amino acids on gelatin-induced inflammation in adult male mice. Inflammation 3: 225-233.

Meymandi MS, Sepehri GR, Mobasher M (2006) gabapentin enhances the analgesic response to morphine in acute model of pain in male rats. Pharmacol, Biochem and Behav 85: 185-189.

Mitsuya H, Broder S (1986) Inhibition of the in vitro infectivity and cytopathic effect of human T-lymphotropic virus, type III/lymphadenopathy-associated virus (HTLV III/LAV) by 2’,3’- dideoxynucleosides. Proc Natl Acad Sci U.S.A. 83: 1911-1915.

Mitsuya H, Weinhold KJ, Furman PA, St. Clair MH, Nusinoff-Lehrman S, Gallo RC, Bolognesi DP, Barry DW, Broder S (1985) 3’-azido-3’-deoxythymidine (BWA509U): an antiviral agent that inhibits the infectivity and cytopathic effect of human T-cell lymphotropic virus type III/lymphadenopathy-associated virus *in vitro*. Proc Natl Acad Sci U.S.A. 82: 7096-7100.

Mizuno T, Takahashi J, Ogawa A (2002) Non-phosgene synthesis of benzyl chloroformate (CbzCl). Tetrahedron Lett 43: 7765-7767.

Mogil JS (2009) Animal models of pain: progress and challenges. Nature Rev 10: 283-293.

Mogil JS, Davis KD, Derbyshire SW (2010) The necessity of animal models in pain research. Pain 151: 12-17.

Morganti P Mandassi E, Touitou E (1999) Skin hydration in novel cosmetic delivery systems, Marcel Dekker, New York, 71– 97.

Moulin DE, Iezzi A, Amireh R, Sharpe WK, Boyd D, Merskey H (1996) Randomised trial of oral morphine for chronic noncancer pain. *Lancet* 347:143-147.

Moynihan H, Jales AR, Greedy BM, Rennison D, Broadbear JH, Purington L, Traynor JR, Woods JH, Lewis JW, Husbands SM (2009) 14*β*-*O*-Cinnamoylnaltrexone and related dihydrocodeinones are mu opioid receptor partial agonists with predominant antagonist activity. J Med Chem 52: 1553-1557.

Nehru K, Seo MS, Kim J, Nam W (2007) Oxidative N-dealkylation reactions by oxoiron(IV) complexes of nonheme and heme ligands. Inorg Chem 46: 293-298.

Neugebauer M, Khedr A, El-Rabbat N, El-Kommes M, Saleh G (1997) Stereoselective metabolic study of Famprofazone. Biomed Chromatogr 11: 356–361.

Neumeyer JL, Shagoury RA (2006) Chemistry and pharmacology of marijuana. J Pharm Sci 60: 1433-1457.

Nicholson B (2000) Gabapentin use in neuropathic pain syndromes. Acta Neurol Scand 101: 359-371.

O-Arciniega MDL, Reval MRD, Arroyo ARC, Ramirez AMD, Munoz FJL (2009) Antinociceptive synergism of morphine and gabapentin in neuropathic pain induced by chronic constriction injury. Pharmacol, Biochem and Behav 92: 457-464.

Offen D, Ziv I, Sternin H, Melamed E, Hochman A (1996) Prevention of dopamine-induced cell death by thiol antioxidants: possible implications for treatment of Parkinson's disease. Exp Neurol 141: 32–39.

Okie S (2010) A flood of opioids, a rising tide of deaths. New Eng J Med 363: 1981-1985.

Olofson RA, Bauman BA, Wancowicz DJ (1978) Synthesis of enol chloroformates. J Org Chem 43: 752-754.

Omar FA (1998) Cyclic amide derivatives as potential prodrugs. Synthesis and evaluation of N-hydroxymethylphthalimide esters of some non-steroidal anti-inflammatory carboxylic acid drugs. Eur J Med Chem 33:123-131.

Ostacolo C, Marra F, Laneri S, Sacchi A, Nicoli S, Padula C, Santi P (2004). α-Tocopherol pro-vitamins: synthesis, hydrolysis and accumulation in rabbit ear skin. J Control Release 99: 403-413.

Otagiri M, Fukuhara TI (1999) Improving the pharmacokinetic and pharmacodynamic properties of a drug by chemical conversion to a chimera drug. J Control Release 62: 223-229.

Papke RL, Dwoskin LP, Crooks PA (2007) The pharmacological activity of nicotine and nornicotine on nAChRs subtypes: relevance to nicotine dependence and drug discovery. J Neurochem 101: 160-167.

Parsons CG (2001) NMDA receptors as targets for drug action in neuropathic pain. Euro J Pharmacol 429: 71-78.

PDR Generics, 2nd ed., Medical Economics, Montvale, New Jersey, 1996, 2229–2233.

Peczon JD, Grant WM (1968) Diuretic drugs in glaucoma. Am J Ophthalmol 66: 680-683.

Pelissier T, Laurido C, Kramer V, Harnandez A, Paeile C (2003) Antinociceptive interaction of ketamine with morphine or methadone in mononeuropathic rats. Euro J Pharmacol 477: 23-28.

Peppercorn MA and Goldman P (1972) The role of intestinal bacteria in the metabolism of salicylazosulphapyridine. J Pharmac Exp Ther 181: 555-562.

Pert CB, Snyder SH (1973) Opiate receptor: its demonstration in nervous tissue. Science 179: 1011-1014.

Petrenko AB, Yamakura T, Baba H, Shimoji K (2003) The role of N-methyl-D-aspartate receptors in pain: a review. Anesth Analg 97: 1108-1116.

Piera S, Iannitelli A, Cerasa SL, Cacciatore I, Cornacchia C, Giorgioni G, Ricciutelli, M, Nasuti C, Cantalamessa F, Stefano DA (2008) New L-dopa codrugs as potential antiparkinson agents. Arch Pharm Chem Life Sci 341:412-417.

Pinnen F, Cacciatore I, Cornacchia C, Sozio P, Cerasa SL, Iannitelli A, Nasuti C, Cantalamessa F, Sekar D, Gabbianelli R, Falcioni LM, Stefano DA (2009) Codrugs linking L-dopa and sulfur-containing antioxidants: new pharmacological tools against Parkinson's disease. J Med Chem 52: 559-563.

Poyhia R, Seppala T, Olkkola KT, Kalso E (1992) The pharmacokinetics and metabolism of oxycodone after intramuscular and oral administration to healthy subjects. Br J Clin Pharmacol 33: 617-621.

Price DD, Mayer DJ, Mao J (2000) NMDA receptor antagonists and opioid receptor interactions as related to analgesia and tolerance. J Pain and Sympt Manage 19: S7-S12.

Pud D, Cohen D, Lawental E, Eisenberg E (2006) Opioids and abnormal pain perception: New evidence from a study of chronic opioid addicts and healthy subjects. Drug Alcohol Depend 82:218-223.

Raffa RB (2001) Pharmacology of oral combination analgesics: rational therapy for pain. J Clin Pharmacy and Therapeutics 26: 157-264.

Raffa RB, Clark-Vetri R, Tallarida RJ, Wertheimer AI (2003) Combination strategies for pain management. Expert Opin Pharmacother 4:1697-1708.

Raja SN, Haythornthwaite JA (2005) Combination therapy for neuropathic pain-which drugs, which combinations, which patients? N Engl J Med 352: 1373-1375.

Randall LO, Selitto JJ (1957) A method for measurement of analgesic activity on inflamed tissue. Arch Int Pharmacodyn 61:409–419.

Ravard A, Crooks PA (1996) Chiral purity determination of tobacco alkaloids and nicotine-like compounds by ^{1}H NMR spectroscopy in the presence of 1,1'-binaphthyl-2,2'-diylphosphoric acid. Chirality 8: 295-299.

Reche I, Fuentes AJ, Ruiz-Gayo M (1996) Potentiation of Δ^{9}-tetrahydrocannabinol induced analgesia by morphine in mice: involvement of μ- and κ-opioid receptors. Eur J Pharmacol 318:11-16.

Renfrey S, Downton C, Featherstone J (2003) The painful reality. Nature Rev 2: 175-176.

Rice ASC, Brown DC, Eisenach JC, Kontinen VK, Fralish MLL, Machin I, Mogil JS, Stohr T (2009) Animal models and prediction of efficacy in clinical trials of analgesic drugs: a critical appraisal and call for uniform reporting standards. Pain 139: 243-247.

Richman DD, Fischl MA, Grieco MH, Gottlieb MS, Volberding PA, Laskin OL, Leedom JM, Groopman JE, Mildvan D, Hirsch MS, Jackson GG, Durack DT, Nusinoff-Lehrman S (1987) The toxicity of azidothymidine (AZT) in the treatment of patients with AIDS and AIDS-related complex. A double blind, placebo-controlled trial. N Engl J Med 317: 192-197.

Riedel W, Neeck G (2001) Nociception, pain and antinociception: current concepts. Z Rheumatol 60: 404-415.

Roberts BA, Strauss CR (2005) Toward rapid, green, predictable microwave-assisted synthesis. Acc Chem Res 38: 653-661.

Robertson A, Glynn JP, Watson AK (1972) The absorption and metabolism in man of 4-acetamidophenyl-2-acetoxybenzoate (benorylate). Xenobiotica 2: 339-347.

Rose MA, Kam PCA (2002) Gabapentin: pharmacology and its use in pain management. Anaesthesia 57: 451-462.

Rose JD, Woodbury (2008) Animal models of nociception and pain. Source book of models for biomedical research. Humana Press Inc., Totowa, NJ.

Rosenau T, Hofinger A, Potthast A, Kosma P (2004) A general, selective, high yield N-demethylation procedure for tertiary amines by solid reagents in a convenient column chromatography-like setup. Org Lett 6: 541-544.

Rotha LB, Willinsa LD, Kroezec KW (1998) G protein-coupled receptor-GPCR trafficking in the central nervous system: relevance for drugs of abuse. Drug Alcohol Depen 51:73-85.

Rukstalis MR, Stromberg MF, O'Brien CP, Volpicelli JR (2000) 6-β-Naltrexol reduces alcohol consumption in rats. Alcohol Clin Exp Res 24: 1593–1596.

Safran AB, Simona F, Sansonetti A, Pometta D, James R (1993) Topical timolol maleate might adversely affect serum lipoproteins. Int Ophthalmol 17: 109-110.

Sanchez C, Hyttel J (1999) Comparison of the effects of antidepressants and their metabolites on reuptake of biogenic amines and on receptor binding. Cell Mol Neurobiol 19: 467–489.

Scholz J, Woolf CJ (2002) Can we conquer pain? Nature Neurosci 5: 1062-1067.

Shah J, Mason DW (1990) Pharmacokinetics of codeine after parenteral and oral dosing in the rat. Drug Metab Dispos 18: 670-673.

Shanbhag VR, Crider AM, Gokhale R, Harpalani A, Dick RM (1992) Esters and amide prodrugs of ibuprofen and naproxen: synthesis, antiinflammatory activity, and gastrointestinal toxicity. J Pharm Sci 81: 149–154.

Shargel L, Mutnick A, Souney P, Swanson L, Block L, Comprehensive Pharmacy Review: Baltimore: Maryland, 1997.

Shehaa M, Khedr A, Elsherief H (2002) Biological and metabolic study of naproxen–propyphenazone mutual prodrug. Eur J Pharm Sci 17: 121–130.

Sherrington CS (1908) The interactive actions of nervous system. Archibald Constable, London.

Shimoyama M, Shimoyama N, Inturrisi CE, Elliott KJ (1997) Gabapentin enhances the antinociceptive effects of spinal morphine in the rat tail-flick test. Pain 72: 375-382.

Silverman, R.B. (2004) The organic chemistry of drug design and drug action, 2nd edn, Elsevier, Oxford.

Slemmer JE, Martin BR, Damaj MI (2000) Bupropion is a nicotinic antagonist. J Pharmocol Exp Ther 295: 321-327.

Smith DA, van de Waterbeemd H, Walker DK, Mannhold R, Kubinyi H, Timmerman H (2001) Pharmacokinetics and Metabolism in Drug Design. Wiley-VCH Verlag GmbH.

Stefano DA, Sozio P, Iannitelli A, Cocco A, Orlando G, Ricciutelli M (2006) Synthesis and preliminary evaluation of L-dopa/benserazide conjugates as dual acting codrugs. Letters in Drug Design and Discovery 3: 747-752 [1].

Stefano DA, Sozio P, Cocco A, Iannitelli A, Santucci E, Costa M, Pecci L, Nasuti C, Cantalamessa F, Pinnen F (2006) L-Dopa and dopamine-(R)-α-lipoic acid conjugates as multifunctional codrugs with antioxidant properties. J Med Chem 49: 1486-1493 [2].

Stefano DA, Sozio P, Cocco A, Iannitelli A, Santucci E, Costa M, Pecci L, Nasuti C, Cantalamessa F, Pinnen F (2007) Synthesis and study of L-dopa-glutathione codrugs as new anti-parkinson agents with free radical scavenging properties. J Med Chem 50: 2506-2515.

Stefano DA, Sozio P, Iannitelli A, Cocco A, Orlando G, Ricciutelli M (2006) Synthesis and preliminary evaluation of L-dopa/benserazide conjugates as dual acting codrugs. Letters in Drug Design and Discovery 3: 747-752 [3].

Stern WH, Guerin CJ, Erickson PA, Lewis GP, Anderson DH, Fisher SK (1983) Ocular toxicity of fluorouracil after vitrectomy. Am J Ophthalmol 96: 43-51.

Subramaniam K, Subramaniam B, Steinbrook RA (2004) Ketamine as adjuvant analgesic to opioids: a qualitative and quantitative systematic review. Anesth Analg 99: 482-495.

Svartz N. (1942) Salazopyrin, a new sulfanilimide preparation. Acta Med Scand 110: 577-598.

Swango JH, Bhatti B, Qureshi MM, Crooks PA (1999) A novel enantioselective synthesis of (S)-(-)- and (R)-(+)-nornicotine via alkylation of a chiral 2-hydroxy-3-pinanone ketimine template. Chirality 11: 316-318.

Tano Y, Chandler D, Machemer R (1980) Treatment of intraocular proliferation with intravitreal injection of triamcinolone acetonide. Am J Ophthalmol 90: 810-816.

Tano Y, Sugita G, Abrams G, Machemer R (1980) Inhibition of intraocular proliferations with intravitreal corticosteroids. Am J Ophthalmol 89: 131-136.

Terasaki T, Pardridge WM (1988) Restricted transport of 3'-azido-3'-deoxythymidine and dideoxynucleosides through the blood-brain barrier. J Infect Dis 158: 630-632.

Thiele JJ, Dreher F, Packer L, Elsner P, Maibach H (2000) Antioxidant defense system in skin: Cosmeceuticals, Marcel Dekker, New York, 145– 177.

Thorn CF (2009) Codeine and morphine pathway. Pharmacogenet Genomics 19:556-558.

Tingey DP, Schroeder A, Epstein MPM, Epstein DL (1992) Effects of Topical Ethacrynic Acid Adducts on Intraocular Pressure in Rabbits and Monkeys. Arch Ophthalmol 110: 699-702.

van de Waterbeemd H, Gifford E (2003) ADMET in silico modelling: Towards prediction paradise? Nature Rev Drug Discov 2:192–204.

van Henegouwen B, Junginger HE, de Vries H (1995) Hydrolysis of RRR-α-tocopheryl acetate (vitamin E acetate) in the skin and its UV protecting activity (an in vivo study with the rat). J Photochem Photobiol 29: 45–51.

Venuti MC, Young JM, Maloney PJ, Johnson D, McGreevy K (1989) Synthesis and biological evaluation of omega-(N,N,N-tri-alkylammonium)alkyl esters and thioesters of carboxylic acid non-steroidal antiinflammatory agents. Pharm Res 6: 867–873.

Vierck CJ, Hansson PT, Yezierski (2008) Clinical and pre-clinical pain assessment: are we measuring the same thing? Pain 135: 7-10.

Vigroux A, Bergon M (1995) Synthesis of prodrugs and mutual prodrug of Chlorzoxazone and Acetaminophen based on masked Benzoxazolone. Bioorg Med Chem Lett 5: 427-430.

Vincler M (2005) Neuronal nicotinic receptors as targets for novel analgesics. Expert Opin Investig Drugs 14: 1191-1198.

Vissers K, Meert T (2005) A behavioral and pharmacological validation of the acetone spray test in Gerbils with a chronic constriction injury. Anest Analg 101: 457-464.

Volpicelli JR, Alterman AI, Hayashida M, O'Brien CP (1992) Naltrexone in the treatment of alcohol dependence. Arch Gen Psychiatry 49: 876–880.

Volpicelli JR, Rhines KC, Rhines JS (1997) Naltrexone and alcohol dependence. Role of subject compliance. Arch Gen Psychiatry 54: 737–743.

Vree TB, van Dongen RT, Koopman-Ki-menai PM (2000) Codeine analgesia is due to codeine-6-glucuronide, not morphine. Int J Clin Pract 54: 395-398.

Wang D, Raehal KM, Bilsky EJ, Sadee W (2001) Inverse agonists and neutral antagonists at mu opioid receptor (MOR): possible role of basal receptor signaling in narcotic dependence. J Neurochem 77: 1590–6000.

Williams J, Edwards S, Rubo A, Haller VL, Stevens DL, Welch SP (2006) Time course of the enhancement and restoration of the analgesic efficacy of codeine and morphine by Δ^9-tetrahydrocannabinol. Eur J Pharmacol 539: 57–63.

Woolf CJ, Mannion RJ (1999) Neuropathic pain: aetiology, symptoms, mechanisms, and management. Lancet 353: 1959-1964.

Vita

Born in Kolkata, India on June 27th, 1981

Education

Ph. D. in Chemistry, University of Kentucky, Lexington, KY
GPA: 3.66 / 4 Expected Graduation: Spring, 2012

Master of Science in Chemistry, Indian Institute of Technology, Kanpur, India
CPI: 9.1 / 10 Graduation: May, 2005

Bachelor of Science in Chemistry, University of Calcutta, Calcutta, India
Score: 1st class in Chemistry Graduation: May, 2003

Presentation

"A Novel Drug Hybrid of Codeine and *S*-(-)-Nornicotine as a Potent Analgesic". Ujjwal Chakraborty, Joseph R. Holtman, Elzbieta P. Wala and Peter A. Crooks. Twenty Second Annual Meeting and Exposition of the American Association of Pharmaceutical Scientists, November, 2008, Atlanta, GA.

"A Novel Drug Hybrid of 3-*O*-Acetylmorphine and *S*-(-)-Nornicotine as a Potent Analgesic". Ujjwal Chakraborty, Elzbieta Wala, Joseph Holtman, and Peter A. Crooks. Twenty Third Annual Meeting and Exposition of the American Association of Pharmaceutical Scientists, November, 2009, Los Angeles, CA.

"Novel Drug Hybrids of Morphine and *S*-(-)-Nornicotine as Potent Analgesics". Ujjwal Chakraborty, Elzbieta Wala, Jaime J. Hardy, Joseph Holtman, and Peter A. Crooks. Twenty Fourth Annual Meeting and Exposition of the American Association of Pharmaceutical Scientists, November, 2010, New Orleans, LA.

Publication

"Opioid-Nornicotine Codrugs for Pain Management". Joseph R. Holtman, Peter A. Crooks, and Ujjwal Chakraborty, International Patent No. WO2009/121018, October 1st, 2009.

"Opioid-Ketamine and Norketamine Codrug Combinations for Pain Management". Joseph R. Holtman, Peter A. Crooks, and Ujjwal Chakraborty, International Patent Application No. WO 2009/131794 A1, October 29th, 2009.

"Improving the use of Drug Combinations through the Codrug Approach". Peter A. Crooks, Harpreet K. Dhooper, and Ujjwal Chakraborty. '*Prodrugs and Targeted Delivery: Towards Better ADME Properties'.* Copyright © 2010 WILEY-VCH, ISBN: 978-527-32603-7.

Professional Affiliations

AAPS American Association of Pharmaceutical Scientists